Leaf Senescence

Induction, Signalling and Its Impact on Nutrient Remobilisation

Dissertation

der Mathematisch-Naturwissenschaftlichen Fakultät
der Eberhard Karls Universität Tübingen

zur Erlangung des Grades eines
Doktors der Naturwissenschaften
(Dr. rer. nat.)

vorgelegt von

Dipl. Biol. Stefan Bieker
aus Kassel

Tübingen
2019

Gedruckt mit Genehmigung der Mathematisch-Naturwissenschaftlichen Fakultät der Eberhard Karls Universität Tübingen.

Tag der mündlichen Qualifikation	28.05.2019
Dekan:	Prof. Dr. Wolfgang Rosenstiel
1. Berichterstatter	Prof. Dr. Ulrike Zentgraf
2. Berichterstatter	Prof. Dr. Klaus Harter

Contents

List of Abbreviations

A. thaliana	*Arabidopsis thaliana*
AAP	Amino acid permease
ABA	Abscisic acid
ACA	Automated colorimetric assay
AGI	Arabidopsis Genome Initiative
AHK5	*Arabidopsis* histidine kinase 5
APX	Ascorbate peroxidase
AS	Asparagine synthetase
ASC	Ascorbic acid
ATG	Autophagy-related
B. napus	*Brassica napus*
BR	Brassinosteroid
C	Carbon
CaM4	Calmodulin 4
Ca^{2+}	Calcium
CAB	Chlorophyll a/b binding protein
CAT	Catalase
CIRP	Calcium induced ROS production
CO_2	Carbon dioxide
Col-0	*Columbia 0*
cpYFP	Circularly permuted YFP
DAS	Days after sowing
Dh-Asc	Dehydroascorbate
DCMU	3-(3,4-Dichlorophenyl)-1,1-dimethylurea
DNA	Deoxyribonucleic acid
DPI	Di-phenylene-iodonium chloride
DREB2A	Dehydration-responsive element-binding protein 2A
E. coli	*Escherichia coli*
esl	*Early-senescence-leaf*

EIN3	Ethylene insensitive3
EMR	Emission maximum ratio
ER	Endoplasmatic reticulum
EREBP	Ethylene-responsive element binding protein
ETR1	Ethylene response 1
FRET-FLIM	Förster resonance energy transfer-fluorescence lifetime imaging microscopy
GA	Gibberellic acid
GBF-1	G-Box binding factor 1
GFP	Green fluorescent protein
GOGAT	Glutamine oxoglutarate aminotransferase
GR	Glutathione reductase
GS	Glutamine synthetase
GSH	Glutathione
GSSG	Glutathione disulphide
H_2DCFDA	Di-Hydro-Di-Carboxy-Hydro-Fluorescein-Di-Acetate
H_2O_2	Hydrogen peroxide
ha	Hectare
H. annuus	*Helianthus annuus*
HL	High light
IMS	Inter-membrane space
JA	Jasmonic acid
JUB1	Jungbrunnen 1
kg	Kilogram
MA	Microarray
MeJA	Methyl-jasmonate
MSH1	MutS HOMOLOG1

N	Nitrogen
N_L	Low nitrogen
N_O	Optimal nitrogen
NAC	NAM/ATAF and CUC
NADH	Nicotinamide adenine dinucleotide
NADPH	Nicotinamide adenine dinucleotide phosphate
NAP	NAC-like, activated by apetala3/pistillata
NH_3	Ammonia
N. benthamiana	*Nicotiana benthamiana*
nm	Nanometer
NO_3^-	Nitrate
NOX	NADPH oxidase
NTL4	NAC with trans-membrane motif 1-like 4
O_2^{*-}	Superoxide
$^1O_2$	Singlet oxygen
OH^{*-}	Hydroxyl radical
ORE1	Oresara 1
Orp1	Oxidant receptor peroxidase 1
ORS1	Oresara sister 1
O. sativa	*Oryza sativa*
OSR	Oilseed rape
PDF	Plant defensin
pETC	Photosynthetic electron transfer chain
POX	Peroxidase
PP2C	Protein phosphatase 2C
ppm	Parts per million
PRX	Peroxiredoxin
PS	Photosystem
PTM	Posttranslational modification
Rboh	Respiratory burst oxidase homologue
RICR	ROS induced calcium release

RNA	Ribonuleic acid
RNAseq	RNA sequencing
RNS	Reactive nitrogen species
roGFP	Reduction-oxidation sensitive green fluorescent protein
ROS	Reactive oxygen species
Rpk1	Receptor protein kinase 1
RUBISCO	Ribulose-1,5-bisphosphate carboxylase/oxygenase
SA	Salicylic acid
SAG	Senescence associated gene
SDG	Senescence down-regulated gene
SIRK	Senescence-induced receptor like kinase
SOD	Superoxide dismutase
SPAD	Soil plant analysis development
SSP	Seed storage protein
TF	Transcription factor
UmamiT	Usually multiple amino acids move in and out transporter
V. radiata	*Vigna radiata*
VPE	Vacuolar processing enzyme
VSP	Vegetative storage protein
WGR1	WRKY generating ROS 1

The idea is to die young as late as possible.

Ashley Montagu

Eidesstattliche Versicherung
Statement of Authorship

Ich versichere hiermit, dass ich

- die vorliegende Arbeit selbstständig verfasst habe,
- keine anderen als die angegebenen Quellen benutzt und alle wörtlich oder sinngemäß aus anderen Werken übernommenen Aussagen als solche gekennzeichnet habe,
- und dass die eingereichte Arbeit weder vollständig noch in wesentlichen Teilen Gegenstand eines anderen Prüfungsverfahrens gewesen ist.

I hereby certify that

- I have composed this Ph.D. thesis by myself,
- all references and verbatim extracts have been quoted, and all sources of information have been specifically acknowledged
- this Ph.D. thesis has not been accepted in any previous application for a degree, neither in total nor in substantial parts.

Ort, Datum/Place, Date

Unterschrift/Signature

1 Abstract

In *Arabidopsis thaliana* (*A. thaliana*), induction of leaf senescence is accompanied by a reduction of the transcription and activity of central hydrogen peroxide (H_2O_2) scavenging enzymes, which prompts the accumulation of intracellular H_2O_2 (Zimmermann et al., 2006; Smykowski, 2010). The expression of multiple early senescence associated genes (SAGs) is H_2O_2 inducible, and the role of H_2O_2 as a signalling molecule during senescence has often been demonstrated and is widely accepted. However, a central question of reactive oxygen species (ROS) mediated signal transmission is, how a specific response can arise from signalling cascades, which rely on rather simple and commonly occurring ROS. Within this work, this question has been addressed with respect to senescence inducing signalling.
Besides the type of ROS, the only information directly carried by H_2O_2 is its concentration, rate of production, and its location. To precisely monitor these properties, we intended to use the fluorescent H_2O_2 sensor protein *HyPer* (Belousov et al., 2006). However, during the initial establishment of required measurement protocols (Wierer et al., 2011), its H_2O_2 scavenging and thus senescence delaying properties in *A. thaliana* became clear (Bieker et al., 2012). Nonetheless, because the *HyPer* constructs were targeted to different subcellular compartments, their respective expression lead to clearly distinguishable effects on intracellular H_2O_2 contents and the induced senescence phenotype (Bieker et al., 2012). In the following, I developed a new technique for the analysis of senescence induction and progression on the basis of leaf colouration (Bresson et al., 2017). This allowed me to harness *HyPers'* H_2O_2 scavenging properties for the closer analysis of the impact the subcellular location of H_2O_2 signals has on the downstream triggered signalling events. I was able to demonstrate that the reduction of peroxisomal (data not shown) or cytoplasmic H_2O_2 contents provokes a delay of senescence induction, whereas chloroplastic scavenging has a disturbed senescence progression as consequence (unpublished, see Section 6.1). Thus, I could show, that the site of ROS generation and perception is of importance for the elicitation of specific downstream signalling cascades.

Biotic and abiotic stress responses very often entail the generation of ROS, including H_2O_2. Moreover, most of these stress responses also can provoke the induction of leaf senescence. This indicates an intricate connection between stress elicited and senescence inducing signalling. For example, expression of the early SAG *WRKY53* is responsive to H_2O_2. But furthermore, we demonstrated an additional regulatory mechanism of *WRKY53* expression via WRKY18, a factor also known to be involved in diverse plant stress responses (Potschin et al., 2014; Chen et al., 2010). During

pre-senescent plant growth, WRKY18 acts as a homo-dimer and represses *WRKY53*. However, upon senescence induction, *WRKY53* expression is induced and the resulting WRKY53 protein can form hetero-dimers with WRKY18. This withdraws WRKY18 proteins from the homo-dimer and reduces the transcriptional suppression of *WRKY53*. Moreover, the formed W53/W18 hetero-dimers now enhance *WRKY53* expression (Potschin et al., 2014).

Leaf senescence also is an integral element of nutrient remobilization from leaves to developing reproductive organs and seeds. For this reason, H_2O_2 dependent senescence induction was analysed in the agronomically relevant species *Brassica napus* (*B. napus*). As both, *B. napus* and *A. thaliana* are members of the *Brassicaceae* family, similarities in senescence inducing mechanisms were expected. Indeed, the induction of *SAG* expression and the beginning decline of chlorophyll contents were also here accompanied by the reduction of anti-oxidative capacities and an increase of intracellular H_2O_2 contents. To investigate a possible influence on senescence induction exerted via the plants' nutritional status, plants were grown under different nitrogen (N) and carbon dioxide (CO_2) regimes. When *B. napus* plants were supplied with low N combined with high CO_2 levels, senescence induction took place slightly earlier than in control plants (Bieker et al., 2012). Moreover, the reduction of N supply to a minimum (N starvation) provoked the induction of leaf senescence. However, despite the measured reduction of anti-oxidative capacities during this, leaf H_2O_2 contents decreased severely in N starved *B. napus* and *A. thaliana* plants. This indicates a different mechanism of senescence induction during N-starvation in comparison to age-dependent leaf senescence (Bieker et al., 2019). To further elucidate the impact of the plants' nutritional status on leaf senescence, transcriptome profiling was conducted of leaf material also analysed in Bieker et al. (2012) (380 ppm CO_2, N_L & N_O; see Franzaring et al., 2011; Bieker et al., 2012; Safavi-Rizi et al., 2018).

I processed and screened the raw data for genes displaying expression profiles (anti-) correlated to the previously measured H_2O_2 contents. Surprisingly, I found seed storage proteins (SSPs) to be expressed in vegetative tissue, and also to be correlating with respective H_2O_2 contents. Further investigation of this revealed a progressive accumulation pattern of SSPs during senescence. Starting in the oldest leaves at senescence induction, the proteins accumulated and then seemingly ascended to the next younger leaf-position, shortly before the former was shed. Moreover, the expressed SSP type varied with the nitrogen supply of the plant. Smaller 2S-SSPs were expressed under low N, bigger 12S variants under optimal N supply and none of both under N starvation conditions. Taken together, this indicates a possible mechanism supporting senescence associated nutrient (esp. N) remobilisation, which also adapts to different N supply conditions (Bieker et al., 2019).

Zusammenfassung

In *A. thaliana* wird die Induktion der Blattseneszenz begleitet von einer Reduktion der Transkription und der Aktivität zentraler H_2O_2 detoxifizierender Enzyme, was eine Erhöhung der intrazellulären H_2O_2 Konzentrationen nach sich zieht (Zimmermann et al., 2006; Smykowski, 2010). Die Expression vieler SAGs ist durch H_2O_2 induzierbar und die Rolle des H_2O_2 als Signalmolekül während der Seneszenzinduktion wurde oft gezeigt und ist allgemein anerkannt. Eine jedoch noch immer offene Frage ROS basierter Signaltransduktion ist, wie eine spezifische Antwort auf eine Signalkaskade erfolgen kann, die auf einem sehr einfachen und häufig in der Zelle anzutreffendem Molekül wie H_2O_2 basiert. Im Rahmen der vorliegenden Arbeit wurde unter anderem eben diese Frage mit Bezug auf die Seneszenzinduktion adressiert.
Neben der Art des ROS Moleküls sind die einzigen weiteren Information, die direkt durch H_2O_2 übermittelt werden, die Konzentration, die Produktionsrate und der Ort des Vorkommens. Um diese Details genau erheben zu können, sollte das fluoreszente H_2O_2 Sensor Protein *HyPer* eingesetzt werden (Belousov et al., 2006). Jedoch stellte sich während der initialen Etablierung geeigneter Messmethoden heraus (Wierer et al., 2011), dass *HyPer* H_2O_2 reduzierende Eigenschaften aufweist und somit in *A. thaliana* eine Seneszenzverzögerung induziert (Bieker et al., 2012). Nichtsdestotrotz zeigten aufgrund der unterschiedlichen subzellulären Lokalisation der *HyPer* Konstrukte, die verschiedenen Linien klar voneinander abgrenzbare Seneszenzphänotypen (Bieker et al., 2012). Im Folgenden entwickelte ich eine Methode zur genaueren Analyse der Seneszenzinduktion und -progression anhand der Blattfärbung (Bresson et al., 2017). Diese erlaubte es mir, die verschiedenen, durch *HyPer* induzierten Phänotypen zu nutzen, um die Relevanz des subzellulären Bildungs- bzw. Wirkortes des H_2O_2 näher zu untersuchen. Ich konnte zeigen, dass die Reduktion des peroxisomalen (Daten nicht gezeigt) und auch des cytoplasmatischen H_2O_2 zu einer verzögerten Seneszenzinduktion führen, während eine Reduktion des chloroplastidären H_2O_2 eine gestörte Seneszenzprogression bei normalem Induktionszeitpunkt zur Folge hat (nicht publiziert, siehe Abschnitt 6.1). Daraus ließ sich auch schlussfolgern, dass die subzelluläre Lokalisation von ROS für die Spezifizität der induzierten Signalkaskaden von Relevanz ist.

Auch die pflanzliche Antwort auf (a)biotische Stressfaktoren beinhaltet in den meisten Fällen die Produktion von ROS wie H_2O_2. Des Weiteren können die meisten dieser Stressantworten auch zum Auslösen der Blattseneszenz führen. Das weist auf eine komplexe Verbindung zwischen den Signalkaskaden vieler Stressantworten

und der Seneszenzinduktion hin. Dies kann am Beispiel von *WRKY53* illustriert werden. Die Expression des frühen SAG ist durch H_2O_2 induzierbar. Des Weiteren ist *WRKY53* auch durch WRKY18 reguliert, einem Transkriptionsfaktor, der auch während vielen Stressreaktion eine Rolle spielt (Potschin et al., 2014; Chen et al., 2010). Während des vegetativen Wachstums bildet WRKY18 Homodimere, welche *WRKY53* reprimieren. Wird nun bei Seneszenzinduktion die Expression von *WRKY53* induziert (durch H_2O_2), kann WRKY53 mit WRKY18 Heterodimere bilden. Dieser Vorgang verringert zum einen WRKY18 Homodimere und damit auch die Repression von *WRKY53*, zum anderen aber hat das gebildete W53/W18 Heterodimer eine aktivierende Wirkung auf die *WRKY53* Transkription (Potschin et al., 2014).

Da Blattseneszenz ein integraler Bestandteil der Nährstoffremoblisierung aus dem Blatt während der Blüte und Fruchtentwicklung ist, kann eine zu frühe Induktion, etwa hervorgerufen durch Stresssituationen, zu einer starken Minderung der Fruchtqualität führen. Dies ist vor allem beim Anbau von landwirtschaftlich genutzen Pflanzen von großer Bedeutung. Aus diesem Grund wurde die H_2O_2 abhängige Seneszenzinduktion auch in der agronomisch relevanten Pflanze *B. napus* untersucht. Sowohl *A. thaliana* als auch *B. napus* gehören der Familie der *Brassicaea* an, daher wurden auch Überlappungen der Seneszenzinduktionsmechanismen erwartet. Tatsächlich konnte auch hier eine Reduktion der anti-oxidativen Kapazität und eine Zunahme des intrazellulären H_2O_2 mit der Induktion von SAGs und der Abnahme des Chlorophyllgehalts zeitlich in Verbindung gebracht werden.
Im Weiteren sollte eine mögliche Beeinflussung der Seneszenzinduktion durch den Ernährungszustand der Pflanze geprüft werden. Die Nährstoffversorgung von im Feld kultivierten Pflanzen lässt sich relativ umfassend kontrollieren und würde somit ein einfach zugängliches Mittel zur Effizienzsteigerung bieten. Hierfür wurden *B. napus* und *A. thaliana* Pflanzen unter verschiedenen N und CO_2 Bedingungen kultiviert. *B. napus* Pflanzen, die eine niedrige N Düngung kombiniert mit hoher CO_2 Versorgung erhielten, zeigten eine leicht verfrühte Seneszenzinduktion (Bieker et al., 2012).Zusätzlich konnte auch gezeigt werden, dass eine Reduktion der N Gabe auf ein Minimum die Seneszenzinduktion provoziert. Jedoch war trotz der gemessenen Reduktion der anti-oxidativen Kapazitäten in den entsprechenden *B. napus* und *A. thaliana* Pflanzen, eine starke Verringerung des Blatt-H_2O_2 Gehalts zu verzeichnen. Dies deutet im Vergleich zur altersbedingten Seneszenzinduktion auf einen anderen Induktionsmechanismus oder aber einen Mechanismus zur Verzögerung der Blattseneszenz unter N-Entzug hin (Bieker et al., 2019).
Um den durch den Ernährungszustand der Pflanze ausgeübten Einfluss auf die Blattseneszenz weiter aufzuklären, wurden Blattproben der schon in Bieker et al.

(2012) analysierten Pflanzen einer Transkiptomanalyse zugeführt (380 ppm CO_2 und N_L & N_O; siehe Franzaring et al., 2011; Bieker et al., 2012; Safavi-Rizi et al., 2018). Die erhaltenen Rohdaten wurden prozessiert und nach Genen gefiltert, die ein Expressionsprofil entsprechend oder gegensätzlich dem Verlauf der schon gemessenen H_2O_2 Konzentrationen aufwiesen. Überraschender Weise wurden hier auch Transkripte von eigentlich exklusiv in Samengewebe exprimierten SSPs identifiziert. Folgende Untersuchungen ergaben, dass diese Proteine währen der Blattseneszenz ein progressives Akkumulationsmuster aufweisen, dass scheinbar die Pflanze hinauf wandert. Beginnend am ältesten Blatt akkumulieren SSPs, bis sie kurz vor dem Abwerfen des Blattes abgebaut werden. Daraufhin ist die Akkumulation im nächst jüngeren Blatt zu beobachten. Zusätzlich ist die transiente Bildung von SSPs in Sprossgewebe nahe der ersten sich entwickelnden Blüten zu beobachten. Auch die verschiedenen N Düngungen zeigten einen Effekt auf die SSP Expression. Bei geringer Düngung wurden kleinere 2S-SSPs gebildet, bei stärkerer Düngung größere 12S-Varianten. Unter Stickstoffentzug hingegen war keine der Formen nachzuweisen. Zusammenfassend deutet dies auf einen Mechanismus zur Unterstützung der seneszenzassozierten Nährstoffremobilisierung hin, der sich der verfügbaren N Menge anpasst (Bieker et al., 2019).

2 Publications

Research articles

1 **Determination of the *in vivo* redox potential using roGFP and fluorescence spectra obtained from one-wavelength excitation**
S. Wierer, K. Elgass, S. Bieker, U. Zentgraf, A. J. Meixner, F. Schleifenbaum
Proceedings of SPIE - The International Society for Optical Engineering; February 2011

2 **Senescence-specific Alteration of Hydrogen Peroxide Levels in *Arabidopsis thaliana* and Oilseed Rape Spring Variety *Brassica napus* L. cv. Mozart**
S. Bieker, L. Riester, M. Stahl, J. Franzaring, U. Zentgraf
Journal of Integrative Plant Biology; July 2012

3 **Senescence Networking: WRKY18 is an Upstream Regulator, a Downstream Target Gene, and a Protein Interaction Partner of WRKY53**
M. Potschin, S. Schlienger, S. Bieker and U. Zentgraf
Journal of Plant Growth and Regulation; March 2014

4 **Nitrogen Supply Drives Senescence-Related Seed Storage Protein Expression in Rapeseed Leaves**
S. Bieker, L. Riester, J. Doll, J. Franzaring, A. Fangmeier and U. Zentgraf
Genes 2019, 10(2), 72; January 2019

Review articles

1 **Plant Senescence and Nitrogen Mobilization and Signalling**
S. Bieker and U. Zentgraf
Senescence and Senescence-Related Disorders; Intech Open; February 2013

2 **A guideline for leaf senescence analyses: from quantification to physiological and molecular investigations**
J. Bresson, S. Bieker, L. Riester, J. Doll and U. Zentgraf
Journal of Experimental Botany; August 2017

3 Personal Contributions

Research Articles

Determination of the *in vivo* redox potential using roGFP and fluorescence spectra obtained from one-wavelength excitation; Wierer et al., 2011

This article demonstrates the ability to use a *one-wavelength* technique to measure reduction-oxidation sensitive green fluorescent protein (roGFP).
I cloned expression constructs of *roGFP(2)* and took part in the purification. Furthermore, I grew plants for the analysis and assisted some measurements.

Senescence-specific Alteration of Hydrogen Peroxide Levels in *Arabidopsis thaliana* and Oilseed Rape Spring Variety *Brassica napus* L. cv. Mozart; Bieker et al., 2012

In this article we investigated senescence processes in *B. napus* (cv. *Mozart*) and demonstrated the impact of *HyPer* expression in *A. thaliana*.
For the latter I grew the plants and conducted the phenotyping experiments of the *HyPer* expressing *A. thaliana* plants. This included analysis and photographic documentation of leaf colouration, measurement of leaf H_2O_2 and chlorophyll contents, as well as the protein extractions, western blots and protein detection to examine the expression strength of *HyPer* in the analysed lines. Also, I conducted the statistical analysis of the data and assisted preparation of the figures (Figure 1 and 2). During the first *B. napus* experiment, I planned and conducted the senescence analysis, including H_2O_2, chlorophyll fluorescence measurements and catalase & ascorbate peroxidase activity gels. Also, I conducted the catalase (CAT) isoform identification (Figures 3 A,C and 4). In the second senescence analysis of *B. napus*, I contributed to initial planning, helped with plant growth and preparation and I took part in sampling as well as sample preparation/extraction and measurements. I supervised and assisted conduction of all shown experiments, respective data analysis and figure preparation (Figures 5 & 6). Furthermore, I conducted sample preparation for CNS measurements and following data analysis. During the third *B. napus* phenotyping experiment, I assisted documentation, conducted sampling of the *B. napus* leaves for the H_2O_2 measurements as well as for the transcriptome analysis conducted by R. Kunze (FU Berlin, Safavi-Rizi et al., 2018). I conducted H_2O_2 and chlorophyll fluorescence measurements as well as following statistical analysis of the data (Figure 7).

Senescence Networking: WRKY18 is an Upstream Regulator, a Downstream Target Gene, and a Protein Interaction Partner of WRKY53; Potschin et al., 2014

In this article, the impact of WRKY18 on *WRKY53* expression and its role during leaf senescence is demonstrated.

I conducted the Förster resonance energy transfer-fluorescence lifetime imaging microscopy (FRET-FLIM) measurements, the following data analysis and contributed to the figure preparation (Figure 5 B and C).

Nitrogen Supply Drives Senescence-Related Seed Storage Protein Expression in Rapeseed Leaves; Bieker,et al., 2019

This research article demonstrates the expression of SSPs in vegetative tissue during senescence of *B. napus*. This process was found to be dependent of N supplied to the plants and seemingly (anti-)correlated with intracellular H_2O_2 contents.

The initial finding is based on the transcriptome data generated from the samples I took in Bieker et al. (2012). Sample preparation and conduction of the microarray (MA) was conducted by Safavi-Rizi et al. (2018). I received raw data for analysis, conducted the bioinformatic processing and evaluation and identified SSP expression to be (anti-)correlated with H_2O_2 contents. I grew and sampled all plants of all the follow up experiments with *B. napus* and *A. thaliana* under full N, low N and N starvation conditions (with exception of the *B. napus* N starvation experiment on hydroponics). Moreover, I conducted the H_2O_2, chlorophyll fluorescence and CAT activity measurements and respective data analysis. I chose the peptide sequences for antibody generation and conducted the protein extraction, blotting, detection and quantification as well as the statistical data analysis and figure preparation (Figures 2, 3, 5 and 6; Supplemental Figures S2 and S5). I prepared the samples for the data shown in Figure S1. I conducted the transcription factor (TF) binding site identification, further promoter analysis and the respective data and Figure preparation (Supplemental Tables S3, S4 and S5 and Figures S4 and S5). I wrote the initial manuscript and took part in the revision process.

Review Articles

Plant Senescence and Nitrogen Mobilization and Signalling; Bieker and Zentgraf, 2013

Here, an overview of nitrogen remobilisation processes during leaf senescence is given and the connection of this process to ROS and reactive nitrogen species (RNS) signalling.

I wrote the manuscript and implemented the required revisions.

A guideline for leaf senescence analyses: from quantification to physiological and molecular investigations; Bresson, Bieker, Riester, Doll and Zentgraf, 2017

In this manuscript a guideline for leaf senescence analysis is provided together with respective protocols and example data.

I took part in initial manuscript structuring, planning and the writing. I reviewed the manuscript during preparation, including overall proofreading and input, with special focus and contributions to ROS and redox related parts. I developed and tested the automated colorimetric assay (ACA) and wrote the respective protocol (Supplemental Protocol S3). I contributed data to Figure 5, and processed the data and prepared the figure elements shown in Figure 4. Also, I wrote Supplemental Protocol S4, S5 & S8, and established the calibration method shown in S4.

4 Introduction

Since the development of aerobic metabolism, the evolution of reactive oxygen species (ROS) became an inevitable element of cellular metabolism. For long, ROS were regarded only as harmful by-product which needs to be detoxified as fast as possible. However, to date their function as major regulatory molecules and their role in early signalling events initiated by environmental stimuli has become established.

4.1 Reactive Oxygen Species in Plant Signalling

In plant cells ROS can be generated by multiple processes in mainly four subcellular locations: chloroplasts, peroxisomes, mitochondria and the apoplast. ROS produced here entail superoxide (O_2^{*-}), H_2O_2 and hydroxyl radical (OH^{*-}). Generation of the highly reactive singlet oxygen ($^1O_2$) is a feature unique to chloroplasts (Waszczak et al., 2018).

Production and Scavenging One of the most prevalent, actively ROS producing enzymatic systems in plants is the RESPIRATORY BURST OXIDASE HOMOLOGUE (RBOH) family. With its ten members, this set of enzymes catalyses the generation of apoplastic O_2^{*-} by one electron transfer to O_2, where nicotinamide adenine dinucleotide phosphate (NADPH) serves as electron donor (Alscher et al., 2002). In peroxisomes O_2^{*-} is generated by xanthine oxidase during purine catabolism (Corpas et al., 2001). Also, complexes I and III of the mitochondrial electron transport chain can produce O_2^{*-} into the inter-membrane space (IMS). No enzymatic ROS scavenging systems are known to be located to the IMS, additionally, the permeability of the outer membrane might allow leaking into the cytoplasm (Waszczak et al., 2018). Otherwise, plant mitochondrial contribution to ROS production is very limited due to activity of alternative oxidase (Purvis, 1997; Maxwell et al., 1999; Apel and Hirt, 2004). Another main O_2^{*-} source in plants are the chloroplasts. Especially in situations of excess light energy and/or limited CO_2, large amounts of ROS are produced here. Besides the generation of singlet oxygen under high light and overload of the photosynthetic electron transfer chain (pETC), direct photoreduction of O_2 to O_2^{*-} via reduced components of photosystem I occurs (Mehler reaction). In summary, these processes render O_2^{*-} as the most commonly occurring ROS in plants, together with H_2O_2, which evolves from the dismutation of O_2^{*-}.

As a result of the ever-present generation of O_2^{*-}, enzymes of the superoxide dismutase (SOD) family play a major role in ROS defence. Seven SODs have been identified in *A. thaliana*, of which three are iron (FeSODs), three copper zinc (CuZnSODs) and one manganese dependent (MnSOD) (Kliebenstein et al., 1998). The almost omnipresent generation of O_2^{*-} is reflected in the also ubiquitous localization of SODs. CuZnSODs can be found in chloroplasts, the cytoplasm, peroxisomes and the apoplast (Asada et al., 1973; Ogawa et al., 1996; Sandalio and Rio, 1987). FeSODs are localized to the chloroplast, MnSODs occur in peroxisomes and mitochondria (Alscher et al., 2002; del Rio et al., 1992). Although dismutation of O_2^{*-} to hydrogen peroxide is considered as detoxification, H_2O_2 itself is often integrating in many signalling pathways, thus activating downstream responses to the initial O_2^{*-} production.

Moreover, direct generation of H_2O_2 takes place in the peroxisomes. Under CO_2 limitation the oxygenation of ribulose-1,5-bisphosphate via RIBULOSE-1,5-BISPHOSPHATE CARBOXYLASE/OXYGENASE (RUBISCO) yields glycolate, which then translocates to the peroxisomes. Here, H_2O_2 is formed during glycolate conversion to glyoxylate. Additionally, during peroxisomal β-oxidation of fatty acids H_2O_2 is produced.
Peroxidases (POXs) are the predominant H_2O_2 detoxification system in peroxisomes. Plant POX enzymes can be subdivided into two groups, heme-containing and non-heme peroxidases. Heme containing, class I POXs are separated into three subgroups: the CATs, ascorbate peroxidases (APXs) and CYTOCHROME PEROXIDASEs (Cosio and Dunand, 2009). CATs and APXs are the most prevalent.

Subcellular localization of CATs is thought to be restricted to the peroxisomes. However, cytosolic CAT activity has been observed, but it is unclear whether the activity resulted from pre-assembled tetramers awaiting peroxisomal import or from organelles, which ruptured during preparation of organelle free cytosolic fractions (Mhamdi et al., 2010). In contrast to catalases, APXs require ascorbate as a co-factor. Ascorbate serves as electron donor during reduction of H_2O_2, forming 2 H_2O and dehydroascorbate (Dh-Asc). Regeneration of ascorbate is achieved by a series of reactions comprising the ascorbate-glutathione cycle, which has a net consumption of 1 NADPH per H_2O_2. (Noctor and Foyer, 1998). Membrane bound APXs are located at the peroxisomes and chloroplast thylakoids. Soluble isoforms are found in the cytosol and also in chloroplasts (Teixeira et al., 2004).

The lifetime of all ROS largely depends on the abundance and activity of scavenging systems in proximity to the site of generation. Superoxide has a lifetime in the range of milliseconds. OH^{*-} is highly reactive, thus its lifetime ranges only up to nanoseconds. Therefore, when considering signalling function, a focus may be put on H_2O_2. It has a comparably long lifetime (up to seconds) (Waszczak et al.,

2018), in that way it can diffuse away from its site of production to fulfil a signalling function. Furthermore, its reactivity is only moderate in comparison to other ROS, thus enabling it to act on specific targets, rather than oxidizing everything available in close proximity.

ROS and Redox Signalling Key questions in ROS research are *'How can a destructive agent like oxygen radicals act in a directed way, without simply damaging all surrounding molecules?*' and *'How can specific responses arise from the rather general event of ROS production?*'. A simple and ubiquitous molecule as H_2O_2 does not carry any information.

In contrast to ROS signalling, redox signalling does not necessarily depend on the involvement of unspecific ROS. Despite its at least indirect dependence on ROS, the redox status of ROS scavenging enzymes, or electron donors as NADPH, ferredoxin, glutathione (GSH), or ascorbic acid (ASC) also can be influenced by metabolic changes, changes in activity of re-reducing enzymes, etc. Thus, redox-systems can be pushed to a more oxidized or reduced state without the direct need of ROS generation. Based on measurements indicating equal GSH concentrations in the chloroplast and the cytosol (Krueger et al., 2009), Dietz and Hell (2015) suggested a possible GSH equilibrium between the compartments and with that, also the possibility to channel redox-disturbances from the chloroplast into the cytosol. This would allow retrograde signalling without the need for ROS molecules traversing the cytoplasm (*redox based signalling*).

Nevertheless, most of the ROS sensing mechanism are believed to rely on the oxidative properties of ROS (Waszczak et al., 2018). This includes the oxidation of metabolites and oxidative posttranslational modification (PTM) of target proteins or sensors. Especially the sulfhydryl groups of cysteines and its derivative seleno-cysteine are considered to be main access points for protein redox regulation as so-called thiol switches. The reaction of H_2O_2 with the cysteine thiolate anion ($-S^-$) forms cysteine sulfenic acid (-SOH). If not stabilized, this residue can react with GSH, thus forming a S-gluthathionylated protein (-SSG), or with other thiol groups from within the same or other proteins, thus forming disulphide bonds (-S-S-) (Waszczak et al., 2018). Thiol switches enable the oxidation or reduction of proteins at these residues, in that way adjusting protein conformation and function. Not only the reactivity of certain residues, but multiple layers of control can influence the outcome of *oxidative signalling/PTM*.

Both systems, ROS and redox-based signalling, are intertwined and depend on each other. Also, redox signalling elements can induce ROS based signalling. Wu et al.

(2015) showed involvement of plastidic fatty acid synthesis in triggering cell death by modulating mitochondrial ROS production (Wu et al., 2015). Moreover, ROS based, inter-compartmental signalling is possible. While membranes represent natural barriers to ROS, plant aquaporins have been demonstrated to allow H_2O_2 to cross membranes. This allows ROS to move between compartments for signalling purposes (Tian et al., 2016; Choudhury et al., 2017). So far, aquaporins have been verified to be present in the plasma- and the vacuolar membrane, chloroplasts and mitochondria (Bienert and Chaumont, 2014). Regarding inter-organellar signalling, multiple studies have demonstrated that chloroplasts, peroxisomes and mitochondria either move into close proximity to the nucleus to allow transmission of (ROS based) signals and/or can extend membrane structures which contact the nuclear envelope (stromules, peroxules and matrixules, respectively) (Caplan et al., 2015; Rodriguez-Serrano et al., 2016; Noctor and Foyer, 2016). This illustrates the possibility of inter-compartmental signalling within one cell. Moreover, despite their high reactivity and thus in most cases very limited diffusion distance, ROS based signals have been demonstrated to be able to be transmitted over long distances.

Long Distance Signalling Although H_2O_2 is relatively stable and can diffuse over comparably long distances, POX distribution in plants basically is ubiquitous and would prevent a long range communication via ROS. However, experiments entailing the local application of different abiotic stresses demonstrated initial local ROS bursts as well as systemic, auto-propagating waves of ROS (Miller et al., 2009; Mittler et al., 2011; Suzuki et al., 2013). This mechanism of ROS wave propagation is intricately connected to calcium (Ca^{2+}) dependent signalling. ROS spreading from one cell to another induce Ca^{2+} release from the vacuole into the cytoplasm (ROS induced calcium release (RICR), Gilroy et al., 2014), as well as an additional Ca^{2+} influx via ROS activated calcium channels in the plasma membrane. The cytoplasmic accumulation of Ca^{2+} now can activate RBOHD dependent O_2^{*-} production into the apoplast (calcium induced ROS production (CIRP)), which is then converted to H_2O_2 via SODs. The generated H_2O_2 can then propagate to the next cell, again eliciting Ca^{2+} accumulation in the cytoplasm and further ROS production. These waves of Ca^{2+} and ROS propagation have been shown to travel across the plant with a velocity of ~8.4 cm/min (Gilroy et al., 2014). Besides symplastic and vasculature based signalling mechanisms via hormones and metabolites, this form of apoplastic signalling allows the plant to systemically communicate information about potential challenges to the whole plant, which might initially only be sensed by a few local cells (Gilroy et al., 2014).

***In-Vivo* H_2O_2 Measuring Techniques** To date, many H_2O_2 sensitive dyes are available (e.g. Di-Hydro-Di-Carboxy-Hydro-Fluorescein-Di-Acetate (H_2DCFDA) (Cathcart et al., 1983), Amplex Red (Mohanty et al., 1997), PeroxyCrimson 1 and PeroxyGreen 1 (Miller et al., 2007)). Here, either a non-fluorescent reagent is applied to the investigated tissue, which is then oxidised and thus made fluorescent by ROS from the tissue, or the dye needs to be applied to a cell extract and the detection is coupled to an enzymatic reaction. Thus, measuring techniques employing the use of such dyes bear some essential problems. The dye application in many cases is difficult, only some dyes are able to penetrate into living cells. The application requires detachment or destruction of the tissue for incubation in the dye solution or even methods as vacuum infiltration. This, especially when working with ROS, distorts the outcome of the experiment. Moreover, neither a direct application to a specific subcellular compartment is feasible with these dyes, nor is clear how deep and evenly distributed sample penetration is. Next, most of the dyes do not only react with one specific ROS and in some cases even tend to auto-oxidation (e.g. for H_2DCFDA see Wiederschain, 2011). Lastly, dye oxidation is irreversible. This makes it impossible to monitor dynamics in ROS signalling processes.

This makes the use of genetically encoded redox sensors superior to the application of fluorescent dyes. These sensors are fluorescent protein molecules, which can be expressed as any other protein: inducible, constitutively, tissue specific or even with subcellular targeting. Most of the sensors are selective to certain ROS, and their monitoring does not require lengthy incubation processes or extractions. This provides the opportunity to monitor redox-processes and dynamics in living systems in real-time (Bilan and Belousov, 2018).

To investigate the dynamics specifically of H_2O_2, there are two families of genetically encoded sensor proteins available. The family of roGFPs is based on a redox-sensitive green fluorescent protein (GFP) which, in difference to GFP, contains two surface-exposed cysteines capable of forming an intra-molecular disulphide bond (Hanson et al., 2004). In consequence, roGFP can be involved in intra-cellular thiol-disulphide exchanges. This reversible reaction provokes a conformational change of the roGFP, which has a change in its fluorescent properties as consequence (Hanson et al., 2004; Bilan and Belousov, 2018). To gain (more) specificity towards single ROS, it can be fused to ROS specific redox sensors. For example, roGFP2 was fused to the yeast protein oxidant receptor peroxidase 1 (Orp1), which is specific to H_2O_2. These chimeric proteins construct so-called *redox-relays*. As they are in such close proximity to each other, Orp1 can relay the electron gained from the redox reaction with H_2O_2 onto roGFP, thus inducing the aforementioned formation of a disulphide bond and conformational change. But still, roGFPs' inherent sensitivity towards

thiol-disulphide exchanges is not lost, leaving it susceptible to also reflect the status of the GSH system.

Another, more direct variant of H_2O_2 sensors is the family of *HyPer* proteins. Instead of constructing a redox-relay, *HyPer* utilizes the sensor domain of *OxyR*, an H_2O_2 responsive TF from *Escherichia coli* (*E. coli*). In this case, a circularly permuted YFP (cpYFP) has been inserted into OxyR at a region providing high flexibility (Belousov et al., 2006). Upon oxidation via H_2O_2, a conformational change within the OxyR domain is induced, which transfers onto the cpYFP. This in turn induces a change in the fluorescent properties of the cpYFP part, eliciting a measurable change in the emission spectrum from ~420 nanometer (nm) (reduced) to ~500 nm (oxidized).

The ratio-metric character of both types of H_2O_2 detection has the advantage that these sensors are robust to variation in expression strength, photo-bleaching as well as variability in tissue depth/light penetration (Hanson et al., 2004). A significant downside of *HyPer* is the inherent sensitivity of GFP-like proteins to pH changes in physiological range (Belousov et al., 2006). As with roGFPs, also here the problem of dependency to another system arises. However, by now, appropriate controls have been developed. For example, a redox insensitive version of *HyPer*, which otherwise retains its fluorescent properties (*SypHer*). It can be implemented as pH control in parallel experiments (Poburko et al., 2011).

In summary, both methods, dye application as well as the use of genetically encoded sensors, bear inherent problems. Nevertheless, while fluorescent dyes are very limited in their specificity and targeted application, genetically encoded protein sensors have significant advantages over these. However, also the use of fluorescent protein sensors is not by any means trivial and requires appropriate controls.

4.2 Leaf senescence

The term *plant senescence* entails the orderly deconstruction and degeneration of single cells, tissues, organs or even the whole organism. This process is of utmost importance to the plants' fitness. It enables the plant to restructure itself and reallocate nutrients from one organ to another. As plants are sessile and can only cope with their environment physiologically, senescence is their major strategy to mitigate many adverse circumstances (Woo et al., 2016).

But also during unstressed growth, senescence optimizes nutrient usage and thereby enhances the chances of survival of the plant itself and especially its progeny. This

is reflected in particular during *leaf* senescence, where at the end of its life-cycle the plant frees up the majority of available resources and reallocates them to its developing flowers and fruits. The resulting developmental benefit for the progeny translates into such a considerable evolutionary advantage, that the concept of ageing and senescence, or the so-called *'unilateral maternal gift economy'*, is prevalent in all evolutionary kingdoms and seems to be a fundamental aspect of living organisms (Arking, 2019). However, substantial differences between the plant and animal kingdoms have been revealed in their respective ageing processes. In plants, ageing advances with tight temporal and inter-organellar coordination to maximize nutrient recycling, whereas ageing in animals is a degenerative process leading to the end of the organisms lifespan (Woo et al., 2016).

Leaves are the plants' main energy generating organ. They are the essential structure for photosynthesis and carbon accumulation and represent the primary organ for plant growth and development (Kim et al., 2018). Almost all of the nutrients plants acquire during their life-cycle are deposited here, mostly incorporated into the photosynthetic machinery, the major source of nitrogen and carbon during remobilisation processes (Woo et al., 2016). Upon flower induction and seed setting, the leaves undergo leaf senescence, a form of organ-level senescence, and begin to remobilise nutrients to the developing reproductive organs and seeds. The leaves' metabolism shifts from an anabolic to a catabolic state. Macromolecules, such as proteins, carbohydrates, chlorophylls, etc., are degraded and the liberated nutrients are mobilised to newly developing sink organs. For this, a large number of genes is differentially regulated. Very early, autophagy related as well as ROS responsive genes are induced. Genes involved in abscisic acid (ABA) and jasmonic acid (JA) signalling are also induced during early stages of leaf senescence. A little further into the process, transcription of genes related to deoxyribonucleic acid (DNA), protein and metal ion binding is increased. Down-regulated genes include transcripts related to amino acid metabolism, protein and chlorophyll synthesis, carbon utilization and photosynthesis. While at first the down-regulation of synthesis pathways is predominant, during mid and later stages of senescence, genes encoding for degradative enzymes (for example pectinesterases, caspases, etc.) are induced. At very late stages, transcription of cytoskeletal elements is induced and the remaining structures as the nucleus and mitochondria are disassembled (Breeze et al., 2011). Until then, these were excluded from degradation to ensure energy supply and genetic control of the whole process.

To achieve these transcriptomic changes, many TFs need to be differentially regulated in the first place. The largest families of senescence involved TFs are the NAM/ATAF and CUC (NAC), WRKY, C2H2-type zinc finger, ethylene-responsive element binding protein (EREBP) and MYB proteins (Lim et al., 2007).

Age Dependent Leaf Senescence and ROS ROS related gene-expression is one of the earliest events during the induction of developmental senescence. Consequently, one of the early events that also can be observed, is a transient increase in intracellular ROS levels.

There are two major classifications of ROS sources in plants. First, metabolic pathways can be disturbed or disrupted and thus elicit ROS production (*metabolic ROS*). This is often the case during abiotic stress (e.g. high light, toxic compounds, nutrient deficiencies, etc.) but also during developmental processes and signalling cascades. For example when the activity or availability of anti-oxidative enzymes are altered, in that way disturbing the cellular balance between the unavoidable generation of (metabolic) ROS and the respective detoxification of these. Second, ROS can be intentionally produced for the purpose of signalling, for example as an early part of a stress response (*signalling ROS*) (Choudhury et al., 2017). This is often the case during biotic stress, e.g. during pathogen attacks. Both ROS sources are intertwined, overlap and impact each other. Metabolic ROS are produced in compartments like the chloroplast, mitochondria or the peroxisomes, where metabolism takes place. In contrast, the main source of signalling ROS is the apoplast, where dedicated enzymes as RBOHs generate reactive oxygen species (see above, Choudhury et al., 2017).

In the case of age dependent induction of leaf senescence in *A. thaliana*, an initial reduction of CAT activity can be observed. Additionally, this is followed by the partial shutdown of APXs, another component of the cell, specialized on H_2O_2 detoxification. This is then followed by H_2O_2 accumulation (Zimmermann et al., 2006). Earlier publications have already demonstrated the connection between H_2O_2 and senescence induction. In 2004, Miao et al. described the positive role of WRKY53 during senescence induction and additionally demonstrated the responsiveness of its expression to H_2O_2. Smykowski (2010) demonstrated the repressive function of G-BOX BINDING FACTOR 1 (GBF-1) on *CAT2* gene expression during senescence induction. In *B. napus* the WRKY-type TF WRKY GENERATING ROS 1 (WGR1) has been identified to be involved in senescence initiation via ROS. It induces transcription of *Rboh D* and *F*, thus enhancing ROS accumulation and promoting leaf senescence (Yang et al., 2018). This indicates, that during induction of leaf senescence, both, *signalling* and *metabolic ROS*, are involved.

WRKY TFs are not the only ones responsive to H_2O_2 and are involved in senescence induction. Several transcriptome studies indicated a large number of NAC family TFs to be associated with (H_2O_2 dependent) senescence induction (see e.g. Breeze et al., 2011). *NAC-like, activated by apetala3/pistillata (NAP)* and *Oresara 1 (ORE1)* have been shown to be involved in senescence regulation (Guo and Gan, 2006; Kim et al., 2009). Moreover, Balazadeh et al. (2011) demonstrated the senescence inducing

function as well as the H_2O_2 dependency of *Oresara sister 1 (ORS1)* expression. Another ROS responsive NAC family TF involved in senescence induction is *Jungbrunnen 1 (JUB1)*. Its transcription is induced by H_2O_2 and in turn it reduces ROS levels, presumably by direct transcription activation of *dehydration-responsive element-binding protein 2A (DREB2A)*, a stress related TF which induces expression of several anti-oxidative enzymes (Wu et al., 2012). *NAP*, *ORE1* and *ORS1* have positive functions during senescence induction. In accordance with its ROS reducing effect, *JUB1* expression has a senescence delaying effect (Podzimska-Sroka et al., 2015).

In addition to ROS dependency, the induction of leaf senescence is heavily impacted by external influences. Environmental stresses that can elicit senescence induction include nutrient deficiencies, salinity, radiation, drought, pathogen infection, toxic compounds, and extremes of light and temperature (Podzimska-Sroka et al., 2015). Consequently, as many possible senescence promoting influences there are, as many different pathways of induction are present, too. However, despite being elicited by multiple different possible factors, all stress dependent pathways of senescence induction tend to converge with the pathway of age dependent induction of leaf senescence at some point (Guo and Gan, 2012).

4.3 Connecting Age- and Stress-Induced Leaf Senescence

Plants are not able to evade or flee from impacting stresses as nutrient or water limitation or pathogen infestations. This is why their 'ultima ratio' under stressful circumstances is the induction of senescence, attempting to at least ensure the survival of their progeny. Plant hormones represent a pivotal point of convergence between senescence induction and the adaptation to external biotic and abiotic stresses. In general, a positive involvement in senescence induction has been shown for ABA, JA, ethylene, methyl-jasmonate (MeJA) and salicylic acid (SA), whereas a delaying effect was demonstrated for auxin, cytokinin and gibberellic acid (GA).

Plant Hormones Leaf ABA contents increase with leaf-age and promote senescence (Gepstein and Thimann, 1980; Thomas and Stoddart, 1980; Zeevaart and Creelman, 1988). Exogenously applied ABA elicits expression of several SAGs. Additionally, ABA is a key hormone in many stress signalling pathways, including stomatal closure (Zhang et al., 2006). *AtNAP* enhances ABA biosynthesis by directly activating transcription of a key ABA biosynthetic gene, *Abscisic aldehyde oxidase 3*, and

thus enhances senescence induction (Yang et al., 2014; Guo and Gan, 2006; Zhang and Gan, 2012). During water stress, ABA accumulates in leaves and roots. In leaves, ABA induces the closing of guard cells, thus reducing leaf water evaporation. Surprisingly, during senescence induction, stomatal conductance and water loss stay at high levels in spite of increasing leaf ABA contents (Jordan et al., 1975; Thimann and Satler, 1979; Gepstein and Thimann, 1980). Zhang et al. (2012) have shown that instead of limiting, during leaf senescence ABA actually promotes leaf water-loss. The increasing leaf ABA contents induce SAG113 expression, a protein phosphatase 2C (PP2C) protein which in turn suppresses stomatal closure (Zhang et al., 2012; Zhang and Gan, 2012). The now enhanced water-loss supports senescence progression. Another connection of age-induced senescence and ABA dependent regulation is made by ABA inducible *Receptor protein kinase 1 (Rpk1)*. In mature leaves, its expression provokes senescence induction. In young leaves, no such effect is observable (Lee et al., 2011). This indicates, that similar to the ABA dependent suppression of stomatal closure, other factors dependent on the age of the leaf are required to support ABA in exerting its senescence inducing functions (Koo et al., 2017; Miret et al., 2018).
ORE1 is a direct target of ETHYLENE INSENSITIVE3 (EIN3) and has been shown to accelerate de-greening during ethylene mediated induction of leaf senescence (Qiu et al., 2015). JUB1 can be induced by GA and brassinosteroid (BR) treatment and inhibits GA synthesis in a negative feedback loop by inhibition of *Gibberellin 3-oxidase 1*. The reduction of GA-levels has an increase in DELLA-proteins as consequence, which again results in a reduction of cellular ROS levels (Shahnejat-Bushehri et al., 2016b). Thus, JUB1 seems to balance senescence induction and pathogen responses (Wu et al., 2012; Shahnejat-Bushehri et al., 2016a).

Transcriptional Interconnection Most TF families involved in age dependent induction of leaf senescence have also been demonstrated to have functions during stress responses. Especially the NAC TF family often shows a direct connection between stress responses and senescence induction via modulation of ROS contents. The drought responsive TF *NAC with trans-membrane motif 1-like 4 (NTL4)* promotes ROS production and senescence induction by activating transcription of *RbohC* and *E* (Lee et al., 2012). The H_2O_2 responsive ORE1 is induced in response to salinity and has senescence promoting function (Balazadeh et al., 2010a,b).

Also WRKY TFs form a connection between senescence induction and stress responses. When overexpressed in *A. thaliana*, the *Oryza sativa* (*O. sativa*) TF WRKY23 enhances expression of pathogenesis related genes and thus also enhances

resistance to bacterial pathogens. Additionally, it has been demonstrated to have a senescence promoting function during dark induced leaf senescence (Jing et al., 2009). Besides its induction via H_2O_2 during senescence, *WRKY53* is also expressed upon SA mediated stimuli during systemic acquired resistance. *WRKY18* is induced during pathogen response (together with *WRKY40*). It represses SA-mediated signalling and induces JA-dependent pathways as response necrotrophic pathogens (Xu et al., 2006; Chen et al., 2010). Its influence on leaf senescence is exerted via a repressive impact on *WRKY53* expression as homo-dimer, whereas the WRKY18/53 hetero-dimer induces *WRKY53* expression (Potschin et al., 2014). Thus, while WRKY18 assists JA and ABA facilitated signalling and connects these pathways to senescence induction via the interaction with WRKY53, WRKY53 itself on the other hand is able to link SA induced pathogen responses with the route of senescence induction (Wang et al., 2006; Potschin et al., 2014).

Nutrient Signalling Plant nutrient supply severely impacts plant development and determines leaf senescence. Nutrient deficiencies of any kind can elicit premature senescence induction. For example, upon phosphate limitation senescence induction promotes the remobilisation of phosphate via the degradation of DNA and ribonuleic acid (RNA) molecules (Himelblau and Amasino, 2001). A big influence is also exerted by N and carbon (C). Both, general availability as well as associated internal factors (e.g. C/N ratio) highly influence plant growth, development and senescence processes (Wingler and Roitsch, 2008).

Elevated CO_2 concentrations have been shown to have a fertilizing effect, especially under adequate water and nutrient supply, leading to more biomass and higher photosynthetic rates (Franzaring et al., 2011; De la Mata et al., 2013). However, this has an accumulation of sugars as consequence as well as a reduced nitrate (NO_3^-) assimilation. Elevated CO_2 concentrations reduce the rate of photorespiration, thus it is thought to reduce the amount of cytosolic nicotinamide adenine dinucleotide (NADH) and limit nitrate reduction (Bloom et al., 2010; Peterhansel and Maurino, 2011). This also might be the cause of reduced glutamine synthetase (GS) activity, observed in plants exposed to high CO_2 concentrations (Buchner et al., 2015). In summary, elevated CO_2 is able to alter C and N metabolism. Reduced nitrate assimilation and higher sugar accumulation leads to an increased C/N ratio, which in turn can provoke premature induction of leaf senescence (Pourtau et al., 2006; Wingler and Roitsch, 2008).

Limitation of N supply limits plant growth due to reduced chlorophyll and protein contents (Agüera and De la Haba, 2018). During development under limited N

supply, leaf chlorophyll contents start to drop earlier, thus suggesting an earlier senescence induction (Agüera et al., 2010). In addition, it causes sugar accumulation in *A. thaliana* (Pourtau et al., 2006). When treatments of elevated CO_2 and reduced N availability are combined, both have an amplifying effect on each other and anthocyanin accumulation, chlorosis and increased expression of SAGs occur. The decrease in anti-oxidative activity in early senescent leaves, which leads to the accumulation of H_2O_2, is observed earlier in N deficient plants (Agüera et al., 2010). A high sugar to nitrogen ration could act as a signal to release N from old leaves (induce senescence), making it available for the incorporation into excess carbon skeletons (Agüera and De la Haba, 2018).

4.4 Plant Nitrogen Management and Remobilisation

Especially N, a key component for plant growth and fertilization, usually is applied in cropping systems in huge amounts. However, the production of nitrogenous fertilizers is very cost and resource intensive. Moreover, its often excessive and continuous application in agricultural cropping systems leads to severe pollution of the surrounding ecosystems. Depending on the soil and the type of applied N, up to 65 % of the N fertilizers can be lost from cropping systems due to volatilization processes alone, not including N leaching into nearby water systems, N immobilisation in the soil and other processes (Cameron et al., 2013). To reduce these losses, various techniques to decrease the required amounts of applied fertilizers have been implemented. This includes optimized timing and application rates, new application techniques and others. However, besides all that, another central leverage point to reduce the required fertilizer input, is to optimize plant nutrient use efficiencies. Along with uptake and allocation, this also includes remobilisation to the developing grain. A process, severely impacted by leaf senescence. By enhancing use of already acquired nutrients, it can limit residual nutrients within the plants' remains to a minimum. Thus, also reducing the needed fertilizer input, which translates into enormous economical and ecological benefits.

In the following, a short overview about N acquisition, storage and remobilisation processes during leaf senescence will be given.

Assimilation Acquisition of N in most cases is facilitated via the roots. A variety of transporters for organic and inorganic N with different substrate affinities and specificities have been identified in roots. Accordingly, substrates can range from

NO_3^- and ammonia (NH_3) to organic N sources as amino acids and even small peptides (Tegeder and Masclaux-Daubresse, 2018). After root uptake, acquired NO_3^- needs to be reduced to NH_3. This is carried out by nitrate and nitrite reductases. The assimilation of NH_3 into amino acids is then accomplished via GSs, glutamine oxoglutarate aminotransferase (GOGAT) and asparagine synthetase (AS) (Masclaux-Daubresse et al., 2010). Transport from root to shoot (source) takes place via the xylem. As this is driven by transpiration of aboveground tissues, compounds are usually transported to photosynthetically active leaves (Tyree, 2003). In the roots, after export into the apoplast, xylem loading is thought to be a passive process. Aspartate, glutamate, asparagine and glutamine are the most abundant amino acids in the xylem. Xylem unloading is an active process, facilitated via proton symporters into the xylem paranchyma cells. Further transfer then to the phloem requires symplastic movement and apoplastic loading into the phloem. Not much is known about the following import into mesophyll cells. Besides ammonium and nitrate transporters, lysine/histidine-like transporters are known to be involved (for detailed review see Tegeder and Masclaux-Daubresse, 2018).

Storage Nitrate is stored in the vacuoles of root and leaf cells, but exported upon demand by cytosolic N assimilation (Miller and Smith, 1996). Leaf free amino acid contents and compositions are highly variable, depending on leaf age, developmental stage and exposure to (a-)biotic stress. Amino acids are also mainly stored in the vacuole, export is adapted to the current amino acid turnover of cellular processes. Proteins are considered to be the largest N stock in all plant tissues. Especially, abundant RUBISCO has been suggested to not only serve carbon fixation, but also function as a protein storage element, as it easily represents 50 % of total leaf protein content (Ishida et al., 1997; Tegeder and Masclaux-Daubresse, 2018; Staswick, 1997). Vegetative storage proteins (VSPs) are dedicated to N storage in vegetative tissue and represent a large portion of leaf N reserves. Additionally, their transcription is activated in response to wounding and methyl jasmonate, and they have been demonstrated to have acid phosphatase activity, thus also exhibiting insecticidial effect (Liu et al., 2005; Berger et al., 1995). Hence, a function in herbivore defence is assumed. Furthermore, in soybean VSP accumulation has been shown to increase to up to 50 % of total leaf protein contents but then to decline again during senescence and seed filling (Staswick, 1994). However, such function as interim storage has not been established for *A. thaliana*, yet.

Salvage Remobilisation of organic N during senescence strongly depends on autophagy and vacuolar proteases. Autophagy is a vesicular pathway that secludes (defective) cellular cytosolic proteins and delivers them to the vacuole, where they are degraded to amino acids, thus keeping protein homeostasis in balance (Tegeder and Masclaux-Daubresse, 2018). It is mainly activated upon nutrient starvation and similar stresses as well as during developmental senescence. Overexpression of *Autophagy-related (ATG) 8*, an essential gene for autophagsome formation, has been shown to increase 12S-SSP accumulation in *A. thaliana* seeds, therefore also to increase N remobilisation during senescence. Under full N supply, total seed N contents of *ATG8* overexpression lines increased and remaining N contents in leaves decreased significantly. During low N treatment, no significant increases were observed, suggesting that due to N limitation autophagy is already contributing to nutrient remobilisation, thus rendering the possible effect of *ATG8* overexpression negligible (Chen et al., 2018).

Transport The increase of phloem glutamine and asparagine contents as well as the induction of *GS1* and AS genes in phloem companion cells during senescence indicates, that the amino acids released by protein degradation for the most are transaminated to the transport forms glutamine and asparagine before phloem loading (Tegeder and Masclaux-Daubresse, 2018). In general, the transport of N to sinks occurs in form of amino acids, whereas the nitrate portion is relatively low (Peuke, 2009).

The mechanisms of the transport out of the leaf to the phloem are not fully clarified yet and several possibilities are given, including symplastic and apoplastic routes as well as passive and active mechanisms (Rennie and Turgeon, 2009). Phloem loading from leaf/phloem apoplast primarily involves amino acid permeases (AAPs), AAP8 in particular (Tegeder and Ward, 2012; Santiago and Tegeder, 2016). Amino acid phloem unloading at the end of the funiculus' vasculature is facilitated via Usually multiple amino acids move in and out transporters (UmamiTs), as well as import and following release from the seed coat. AAPs and the Cationic amino acid transporter 6 probably facilitate amino acid import into the embryo (see Tegeder and Masclaux-Daubresse, 2018 and references within). Following the import into the embryo, the majority of nutrients moves to the cotyledon parenchyma cells, either for incorporation into storage structures or for the use in seed metabolism (Tegeder and Rentsch, 2010).

Contribution to seed filling of remobilised N versus newly assimilated N strongly depends on plant species, the genotype and soil nutrient conditions (Masclaux-Daubresse et al., 2010). As mentioned earlier, also the general mechanisms of N remobilisation might vary, as for example VSP accumulation upon senescence has been observed in soybean, while it has not been described e.g. for *A. thaliana*, yet (Staswick, 1994). This makes it very demanding, to investigate these processes in different plant species. Nevertheless, more profound knowledge would enable agricultural systems to be managed much more efficient and less resource and cost intensive.

5 Objectives

Expression and activity of components of central anti-oxidative systems have been shown to be reduced during induction of leaf senescence in *A. thaliana* (Zimmermann et al., 2006). Following research has demonstrated, that the GBF-1 mediated suppression of CAT2 expression is pivotal for the induction of leaf senescence (Smykowski, 2010). A consequence of GBF-1 mediated CAT2 suppresion is the accumulation of large amounts of H_2O_2 (Smykowski, 2010; Giri et al., 2017). The central objective of this thesis was to scrutinize and further establish the role of H_2O_2 accumulation during induction of developmental leaf senescence.

ROS production in plant cells is a commonly observed event. Most (a)biotic stresses as well as many developmental processes elicit the production of ROS. It is unclear how the rather unspecific incident of ROS generation can result in the induction of specific signalling cascades. One central hypothesis is, that the subcellular location of ROS accumulation serves the generation of a specific response. To investigate this theory, I intended to use the genetically encoded, fluorescent H_2O_2 sensor protein *HyPer* (Belousov et al., 2006). When targeted to different organlles, this sensor protein enables monitoring of the dynamics of H_2O_2 production specifically within these compartments.

Furthermore, senescence is a crucial element of nutrient remobilisation. It represents a possible key mechanism to improve nutrient use efficiencies, and consequently also yield of annual plants. For this reason, another goal of this thesis was to analyse the mechanisms of senescence induction in the agronomical relevant species *B. napus*. I aimed to analyse senescence induction and progression by monitoring the activity of central anti-oxidative systems, leaf H_2O_2 and chlorophyll contents and expression of genetic senescence markers.

Lastly, I intended to investigate senescence behaviour in response to different stresses in *A. thaliana* and *B. napus*. I investigated a WRKY TF that is involved in stress responses but also shows expression patterns related to senescence. Moreover, general responses to stresses commonly occurring under field conditions and their connection to senescence induction were scrutinized. The goal was to further clarify the mechanisms linking stress responses and leaf senescence, and thus possibly to uncover points of leverage for the improvement of nutrient remobilisation processes under stress conditions.

6 Results and Discussion

Senescence is a very versatile process. Virtually every influence impacting the plant in any imaginable way is integrated into the decision of senescence induction or delay, progression and termination. Thousands of genes are differentially regulated during senescence induction, progression and termination (Breeze et al., 2011). This reflects the importance of this process for the fitness of the plant and especially its offspring. Failure of plant senescence would consequently lead to the failure of the plants' progeny in the following generation and thus possibly to the eradication of the plant. But leaf senescence is not only essential for the plants survival itself, this process also offers multiple ways to adapt plant growth and development to the needs of a modern, agronomic industry.
Within this thesis, multiple aspects especially of the regulation associated to senescence induction have been addressed. A focus was put on the involvement of reactive oxygen species. In particular the possible locations of ROS generation and sensing and the impact of H_2O_2 during senescence signalling was investigated.

6.1 Hydrogen Peroxide as Signalling Molecule during Age-Dependent Senescence Induction and the Influence of the Expression of *HyPer*

Former research of our group has shown a transient increase of H_2O_2 contents during senescence induction in *A. thaliana* (e.g. Miao et al., 2004; Zimmermann et al., 2006). It is argued, that mainly CAT2 and cytoplasmic APX are deactivated, thus leading to the accumulation of H_2O_2. After that, anti-oxidative capacity is restored again by higher CAT1/3 and recovered APX activity (Zimmermann et al., 2006). CAT1 & 3, however, usually have a different tissue localisation than CAT2. While CAT2 (Class I) is mainly associated with photosynthetic tissue, CAT1 (Class III) is predominantly localized to reproductive tissue and seeds, and CAT3 (Class II) to the vasculature (Mhamdi et al., 2010). Nevertheless, all isoforms (in *Arabidopsis*) contain a carboxy-terminal peroxisomal targeting sequence, thus subcellular localization to the peroxisome should be the same for all three isoforms and activity of all has clearly been recognized in *whole leaf* extracts of *A. thaliana* during and after senescence induction (Zimmermann et al., 2006). But at least for CAT3 it cannot be fully excluded that the detected enzymatic activity stems from the vasculature of the sampled leaf tissue rather than from parenchymatic cells.

In *B. napus* we were able to detect an increase of H_2O_2 levels in leaves together with the reduction of anti-oxidative capacities at senescence induction. Here, CAT as well as APX activity decreased (Bieker et al., 2012). However, in contrast to the restoration of anti-oxidative capacity via activation of different CAT isoforms as in *A. thaliana*, in *B. napus* CAT activity was by far not restored to the initial levels observed before its reduction. Moreover, total contents of ascorbic acid and dehydroascorbate as well as concentrations of GSH and glutathione disulphide (GSSG) steadily declined during development of the oilseed rape plants. Still, in contrast to this and albeit the steadily increasing lack of APX substrates, activity of APX rose again, even above initially measured activity levels (see Bieker et al., 2012, Figures 4 A and 5 B-E). In summary, overall anti-oxidative capacities in *B. napus* as well as in *A. thaliana* rather decrease after senescence induction.
As anti-oxidative capacities do not seem to increase again to initial levels for at least the bigger part of the different anti-oxidative systems in *A. thaliana* as well as in *B. napus*, the observed *transient character* of H_2O_2 accumulation is unlikely to be achieved only by the reduction and following restoration of ROS scavenging enzymes. This hints to a mechanism to be in place, which includes a temporary increase of ROS production. Still, *where* and *how* senescence inducing ROS are potentially produced, is unknown so far.

The Use of Genetically Encoded Redox Sensors We envisaged to determine the subcellular origin of senescence associated H_2O_2 and to analyse the contribution of respective compartments to this H_2O_2 production. For this, we aimed to implement genetically encoded fluorescent sensors. This required to first test, adapt and establish a technique for the *in-planta* use of fluorescent ratio-metric sensors.
Although we intended to use the H_2O_2 specific probe *HyPer*, we started with the measurements of *roGFP*(2) expressing *A. thaliana* plants. The lines were readily available to us and most importantly, *roGFP* requires the same measuring technique as *HyPer* does, thus providing the opportunity to encounter possibly upcoming technical difficulties of ratio-metric measurements *in-planta* also with this system.

When measuring roGFP(2) fluorescence ratios in *A. thaliana* plants, it became clear that a two- wavelength excitation measurement would be too lengthy and stressful for the samples to reliably draw conclusions on intracellular ROS contents based on the obtained results. With the employed imaging system, a two-wavelength excitation measurement required the sample to endure irradiation with laser light for several minutes. This can severely overload the pETC. Irradiation of plant material with high light intensities has been shown to provoke a high light (HL) stress reaction. This

involves ROS production (photo-oxidative stress) as well as signalling cascades leading to downstream genetic reprogramming and adaptation to the HL situation (see for example Foyer et al., 1994). If measured in that way, the light stress response would modulate other developmental features and disrupt *unstressed* plant development, especially including age-dependent induction of leaf senescence. Additionally, a two wavelength measurement with this system did not allow measurements of moving organelles within the cells. While, due to the ratio-metric readout, measurements are stable against variation in sample depth, structure and expression levels differing between samples, movement of sensor containing organelles between the excitation with one or the other laser distorts the results (Hanson et al., 2004).

Nonetheless, high resolution spectral analysis of purified roGFP protein solutions with either fully reduced or oxidized roGFP was conducted to acquire an emission spectrum of both (see Wierer et al., 2011, Fig. 1). Proteins of both states emit fluorescence in the same spectral range. But if fully reduced, the emission maximum of the protein shifts to a wavelength 7 nm higher than if oxidized (516 and 509 nm, respectively). An in the following recorded calibration curve displaying the emission maximum ratio (EMR) revealed a linear relationship between the chemically adjusted redox potential of the protein solution and the 509/516 nm ratio (Wierer et al., 2011, Fig. 3). This allowed to conduct measurements with only one laser, thus also in half the time and in that way to draw more reliable conclusions on the roGFP redox-state *in planta*, because of a much lower risk of manipulating the outcome of the experiment only by measuring the sample.

In an initial experiment to verify the function of this technique, the redox-state of different positions within a single chloroplast was analysed. These organelles are most prone to changes in the redox-state by applied high light. The results indicated a more negative redox-potential in the stroma than in the grana stacks (Wierer et al., 2011, Fig. 4). More importantly, this result demonstrates that measuring with only one wavelength is mild enough to analyse organelles highly responsive to light irradiation.

If also applicable to *HyPer*, this technique would eliminate a central problem of *HyPer in-vivo* measurements. However, an initial phenotypic analysis of the plants expressing differently localized *HyPer* constructs indicated a delayed senescence induction and reduced H_2O_2 contents in all analysed *HyPer* lines. Because plant development as well as H_2O_2 contents were affected by expression of the constructs, the microscopic study of the plants was deferred.

Such pronounced scavenging of hydrogen peroxide was an unexpected effect of *HyPer* expression. *HyPer* has been successfully implemented in many experiments, including animal, plant and bacterial studies (see Bilan and Belousov (2018) and references

within). Experiments in animal systems seem to be prevalent. Multiple publications investigating *inflammation*, *development and ageing*, and *tissue regeneration* are available. In many studies controls were implemented to show that the observed effects rest on the *natural* alteration of H_2O_2 levels. This entails application of several different antioxidants and/or NADPH oxidase (NOX) inhibitors to suppress or enhance the corresponding effect observed. But expression of *HyPer* alone has not been shown to have an impact on the results of any of these studies (e.g. see Love et al., 2013).

Also in plants *HyPer* was successfully used. Most recently, Exposito-Rodriguez et al. (2017) could show with different *HyPer* constructs and other fluorescent indicators, that after HL treatment of *Nicotiana benthamiana* (*N. benthamiana*) leaf discs, H_2O_2 generated in chloroplasts residing near the nucleus accumulates inside these nuclei. In this study, *HyPer2* and the H_2O_2 insensitive variant *SypHer2* were used. After 1 hour of HL treatment, expression of *N. benthamiana APXa* was induced. While application of the pETC inhibitor 3-(3,4-Dichlorophenyl)-1,1-dimethylurea (DCMU) as well as expression of a stromal APX reduced the expression induction, expression of a cytoplasmic *APX* did not. Additionally, nuclear localized *HyPer* indicated a lower oxidation when DCMU was applied or stromal *APX* was expressed. In conclusion, plastidic H_2O_2 can directly transfer to the nucleus without passing through the cytosol.
However, also here no appropriate controls were implemented to test for an H_2O_2 scavenging effect of *HyPer*, and it cannot be excluded that elevation of H_2O_2 contents and the induced expression of *APXa* would have been more pronounced in a *HyPer* free context. Still, expression of stromal *APX* was able to suppress the related induction of gene expression, while *HyPer* was not. Thus, it can be concluded that *HyPer* does not scavenge with the same or higher efficiency as a component of the anti-oxidative system.

Although no study available at the moment has either genuinely taken it into account or demonstrated it, a potential anti-oxidative effect of *HyPer* seems to be obvious, considering that besides fluorescence the only function of *HyPer* is the specific oxidation by H_2O_2 (in that way consuming H_2O_2). Also, it has to be considered that all available studies from the plant field employing *HyPer* in their experimental procedures investigated stress conditions. The here associated ROS production is not comparable to senescence associated H_2O_2 production. Stress reactions elicit rapid production of ROS within minutes, whereas senescence associated increases of cellular H_2O_2 contents occur slowly over several days to weeks. It is very likely, that the in these experiments elicited generation of H_2O_2 exceeds the scavenging capabilities of *HyPer*, while the slow rise during plant development does not. However, a direct proof

of the H_2O_2 scavenging effects of *HyPer* is still pending. Nevertheless, the observed reduction of H_2O_2 contents occurred in several independent *HyPer* expressing plant lines, irrelevant of subcellular localization. Thus, an explanation other than *HyPer* mediated H_2O_2 scavenging seems highly unlikely.

Although the effects induced by its expression rendered the implementation of *HyPer* pointless to the intended use, the induced phenotypes, especially regarding the localization dependency, still provided insight into senescence associated H_2O_2 production.

The Origin of Senescence Inducing Hydrogen Peroxide In Bieker et al. (2012), we could show that the effects triggered by reduction of intracellular H_2O_2 contents largely depend on the subcellular localisation of scavenging and thus presumably also the site of production. When hydrogen peroxide contents were lowered in the cytoplasm, the delay of leaf senescence induction was much more pronounced than if scavenged in the peroxisomes (Bieker et al., 2012, Figure 2). Still, regarding the observed phenotype, the connection between peroxisomal H_2O_2 production and the induction of leaf senescence cannot be dismissed.

Peroxisomes Peroxisomal H_2O_2 is generated during photorespiration (glycolate cycle) and β-oxidation of fatty acids. Both processes can evolve large amounts of H_2O_2 (Wang et al., 2015). Peroxisomal ROS detoxification systems include peroxiredoxins (PRXs), CATs, SODs, APXs (membrane bound, facing the cytosol) and an almost complete set of enzymes for the ascorbate glutathione cycle, with the exception of a glutathione reductase (GR) (Schrader and Fahimi, 2006; Wang et al., 2015).

Fatty acid turnover via β-oxidation seems to take place to the same extent in old and in young *A. thaliana* leaves (Bonaventure et al., 2004; Yang and Ohlrogge, 2009). In consequence, the associated generation of H_2O_2 also is constant over plant development. *Arabidopsis* GBF-1 can repress CAT2 expression during senescence induction and in response to pathogens (Smykowski, 2010; Giri et al., 2017). In that way, peroxisomal H_2O_2 accumulation can be triggered, which in turn can contribute to the senescence inducing H_2O_2 peak. Despite the presence of multiple other ROS detoxification systems, considerable amounts of H_2O_2 accumulate upon the deactivation of CAT2 (Giri et al., 2017). This indicates, that CATs are the central H_2O_2 detoxification system in peroxisomes. Moreover, their transcriptional deactivation represents an efficient mechanism to induce H_2O_2 accumulation here.

However, native membranes represent significant barriers for H_2O_2 (Dynowski et al.,

2008). A possible pathway of H_2O_2 efflux and downstream signalling originating from peroxisomes still needs to be elucidated. Approaches to proof the presence of plant aquaporins in peroxisomes have not been successful yet (Reumann et al., 2007; Eubel et al., 2008; Wudick et al., 2009; Corpas et al., 2017). Still, for signalling purposes, H_2O_2 itself would not necessarily need to leave the peroxisomes. In theory, also other peroxisome localized messenger molecules may be oxidized and leave the peroxisome for signal transmission to other components of theoretical signalling cascades within the cell. However, such components of a possible signalling cascade still await discovery.

Conclusively, while the connection between peroxisomal ROS production and induction of leaf senescence has been demonstrated, the exact underlying mechanisms remain to be elucidated. Still, two possible pathways for efficient H_2O_2 production as well as a mechanism to provoke the rapid accumulation of H_2O_2 are given in peroxisomes. Furthermore, Giri et al. (2017) and Smykowski (2010) were able to link peroxisomal H_2O_2 production to the induction of a plant stress response as well as a developmental program, respectively. This demonstrates that peroxisomal ROS can act as components of cellular responses, even though the mechanisms of efflux and signal transmission are unclear.
However, under the assumption that *HyPer* scavenges H_2O_2 with comparable efficiencies in the cytosol and in the peroxisomes, the results also indicate that H_2O_2 produced in the peroxisomes has less impact on leaf senescence induction than H_2O_2 localized in the cytosol (see Bieker et al. (2012), Fig. 2C).

Cytoplasm Although ROS production directly in the cytoplasm is very uncommon if not completely unknown, the observed effect of cytosolic *HyPer* on the measured H_2O_2 contents was much more pronounced than that of peroxisomal *HyPer*. Known sources of cytoplasmic ROS include either production in and subsequent release from subcellular compartments as for example the mitochondria, or apoplastic evolution of O_2^{*-} via RBOHs followed by conversion to H_2O_2 and subsequent influx into the cell. But, as the cytoplasm (the symplast) is considered to be a very reductive milieu, incoming H_2O_2 should be rapidly scavenged by cytoplasmic ROS detoxification systems (e.g. via cytoplasmic APX and other antioxidants) (Foyer and Noctor, 2016; Noctor et al., 2016). However, cytoplasmic APXs are deactivated at the time of leaf senescence induction via an unknown mechanism (see section 4.2). In that way, the probability for accumulation of cytoplasmic ROS increases.

RBOHs (NOXs) are integral plasma membrane proteins. They utilize cytoplasmic NADPH as substrate to be oxidized and transfer one electron to molecular oxygen

residing in the apoplastic space. The generated O_2^{*-} can then be dismutated to hydrogen peroxide, either spontaneously or by apoplast localized SODs. H_2O_2 has been shown to be able to pass the plasma membrane back into the cytoplasm via aquaporins (Tian et al., 2016; Dynowski et al., 2008).

Endogenous ABA contents have been shown to increase during leaf senescence in multiple species, including for example tobacco, rice, maize and *Arabidopsis* (Even-Chen and Itai, 1975; Philosoph-Hadas et al., 1993; He et al., 2005; Zhao et al., 2010), and to have a supportive function in age dependent senescence induction (Gepstein and Thimann, 1980; Thomas and Stoddart, 1980; Zeevaart and Creelman, 1988). Li et al. (2018) suggested an involvement of ABA induced, NOX mediated O_2^{*-} production during leaf senescence induction of *O. sativa*. The *O. sativa* mutant line *early-senescence-leaf* (*esl*) displays early senescence as well as higher superoxide and ABA contents in leaves combined with higher activity of several NOX isoforms (Li et al., 2018).

Also in *Arabidopsis*, an RBOH dependent signalling pathway involved in senescence induction was revealed. Here, *Receptor protein kinase 1 (Rpk1)* was identified to take part in ABA dependent senescence signalling. The kinase is age- as well as ABA-inducible and *Arabidopsis rpk1* plants show a significant delay in age dependent senescence induction (Lee et al., 2011). Interestingly, artificially induced *Rpk1* expression is able to provoke senescence symptoms in old leaves, but not in young, what implies yet another layer of control (Lee et al., 2011; Koo et al., 2017). More recently, Koo et al. (2017) identified parts of the regulation network involving RPK1 during induction of age-dependent cell death. They found the usually observed transient increase of apoplastic O_2^{*-} preceding the senescence associated H_2O_2 accumulation to be almost completely absent in *A. thaliana rpk1* plants. The then following increase of H_2O_2 was less pronounced in these plants and in comparison to the wild-type also delayed by three days. *Rpk1* expression as well as RPK1 mediated signalling is induced by O_2^{*-}, but is unresponsive to H_2O_2. Koo et al. (2017) demonstrated, that RPK1 initially perceives an incoming O_2^{*-} signal, upon which it activates RBOHF via phospho-transfer from RPK1 to CALMODULIN 4 (CaM4). CaM4 in turn phosphorylates and activates RBOHF. In that way, the initially perceived O_2^{*-} signal is amplified by further RBOHF mediated O_2^{*-} production.

Following RBOHF activation, the expression of genes as for example *Senescence-induced receptor like kinase (SIRK)* is induced. *SIRK* expression activation via RPK1 still is possible also in *cam4* plants, but it is significantly reduced and a Ca^{2+} conferred enhancement of expression then is not possible any more (Koo et al., 2017).

In conclusion, RPK1 induces downstream SAGs and amplifies incoming O_2^{*-} signalling events. This in turn has an influx of apoplastic H_2O_2 as consequence, which

might mediate senescence induction.

However, despite the seemingly obvious involvement of NADPH oxidases in senescence induction, no senescence phenotype has been described for various *NOX/Rboh* mutant plants, yet. This most probably rests on their indispensability for multiple developmental processes, making it virtually impossible to obtain viable *NOX* null mutants. Additionally, the redundancy of the *NOX* gene families makes it very problematic to analyse their function. In many cases when using single mutant lines, the remaining NOX isoforms can compensate at least in part for the loss of other homologues. Nonetheless, the aforementioned results clearly indicate that apoplast derived/NOX generated superoxide and thus H_2O_2 are most likely involved in ABA and age-dependent senescence induction. Thus, the effect of the observed H_2O_2 scavenging in the cytoplasm might, at least in part, rest on the reduction of apoplast derived H_2O_2 in the cytosol.

A supportive role of cytoplasmic H_2O_2 is further backed by recently emerging results showing chloroplast-nuclear communication inducible by cytoplasmic H_2O_2. In leaves, the chloroplast is the main sites of ROS production (Rogers and Munné-Bosch, 2016). Interestingly, Caplan et al. (2015) have shown that chloroplasts form stromules upon external treatment with H_2O_2 or SA. They observed chloroplast-chloroplast as well as chloroplast-nuclear connections. Most importantly, they demonstrated that chloroplast localized proteins as well as chloroplast produced H_2O_2 can pass through the stromules directly into the nucleus, similar to the above mentioned observations made by Exposito-Rodriguez et al. (2017).

This indicates that cytoplasmic H_2O_2 may induce stromule formation and further chloroplast facilitated ROS signalling during senescence induction. Thus, underlining the importance of cytoplasmic ROS for senescence induction and propagation. Furthermore, this is supported by the observation of altered stromule formation in also senescence delayed, chloroplastic *HyPer* lines, which will be discussed in the following.

Chloroplasts Considering that leaf yellowing is the earliest *visible* symptom of leaf senescence, chlorophyll degradation and the in that way elicited photo-oxidative stress would provide a central important pathway of ROS production for the induction of leaf senescence (Rogers and Munné-Bosch, 2016). Furthermore, retrograde signalling from the chloroplast could easily give direct feedback on senescence regulatory mechanisms, status of photosynthetic capacity and activity, as well as the progression of protein degradation and nutrient remobilisation from the chloroplast. By using chloroplast localized *HyPer*, we were also able to demonstrate the importance of

chloroplastic H_2O_2 for senescence inducing signalling.

The cytoplasmic as well as the chloroplastic *HyPer* expressing lines display a severe reduction of leaf H_2O_2 contents, which is most pronounced in the chloroplastic *HyPer* line. Here, the expected senescence associated increases of H_2O_2 contents are only barely observable (see Figure 1, left graph). Considering leaf colouration, the delayed senescence phenotype of both *HyPer* expressing lines seems very similar to each other. The leaf colouration of both show a severely delayed senescence phenotype compared to the wild type, which is even more pronounced in the chloroplastic *HyPer* line, comparable to the also lower leaf H_2O_2 contents in this line (see Figure 1, right graph).

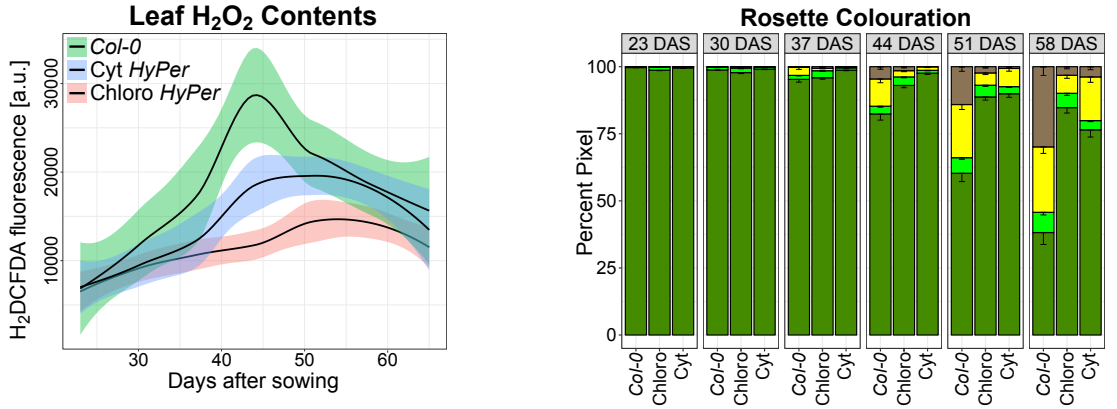

Figure 1: H_2O_2 and ACA results of plastid and cytoplasmic *HyPer* and *Columbia 0* (*Col-0*). **Left:** H_2O_2 content of chloroplastic and cytoplasmic *HyPer* line and *Col-0* (leaf 7). The line displays a local regression of the data. Coloured areas reflect value distribution. Six biological replicates were sampled per harvest and line. **Right:** Whole rosette ACA analysis of cytoplasmic and chloroplastic *HyPer* plants. Errorbars reflect standard deviation. Here, twelve biological replicates were sampled per harvest for *Col-0* and cytoplasmic *HyPer*, for chloroplastic *HyPer* twenty-four per harvest. *Unpublished data.*

However, when closely inspecting the recorded leaf colouration in Figure 1, it becomes obvious, that in the chloroplastic *HyPer* line the observed changes in leaf colouration have to be distinguished from the changes in the cytoplasmic line. In the chloroplastic *HyPer* plants the green proportion of the leaf begins to decrease already at 23-30 days after sowing (DAS), which is even slightly earlier than for *Col-0* plants (here discolouration begins at 30 DAS). In contrast, the cytoplasmic *HyPer* line displays first recognizable changes in leaf-colouration as late as 44-51 DAS. The leaf colouration data was acquired with a pixel-wise analysis of leaf images (ACA, Bresson et al., 2017), this allows for a very detailed inspection of leaf-colouration data. For example, by switching ACA data display from *whole rosette* to *single colours* (Figure 2). Here it is easily recognizable, that the data-points of *Columbia-0* and chloroplastic *HyPer*

plants start spreading already at ~23-30 DAS, while the plants expressing cytoplasmic *HyPer* begin to show comparable increases in data dispersion only from 44-51 DAS on. Moreover, the increase in *non-green* leaf tissue then is much faster in cytoplasmic than in chloroplastic *HyPer* and wildtype *Arabidopsis* plants.

Taken together, this indicates a delay in senescence induction to be present in cytoplasmic *HyPer* plants, while if localized to the chloroplast, *HyPer* appears not to influence senescence induction but to slow its progression. This assumption is further supported by the timing and achievement of developmental hallmarks like shoot induction and flower development. As here no significant differences were recognised, a general developmental delay or acceleration can be excluded (data not shown).

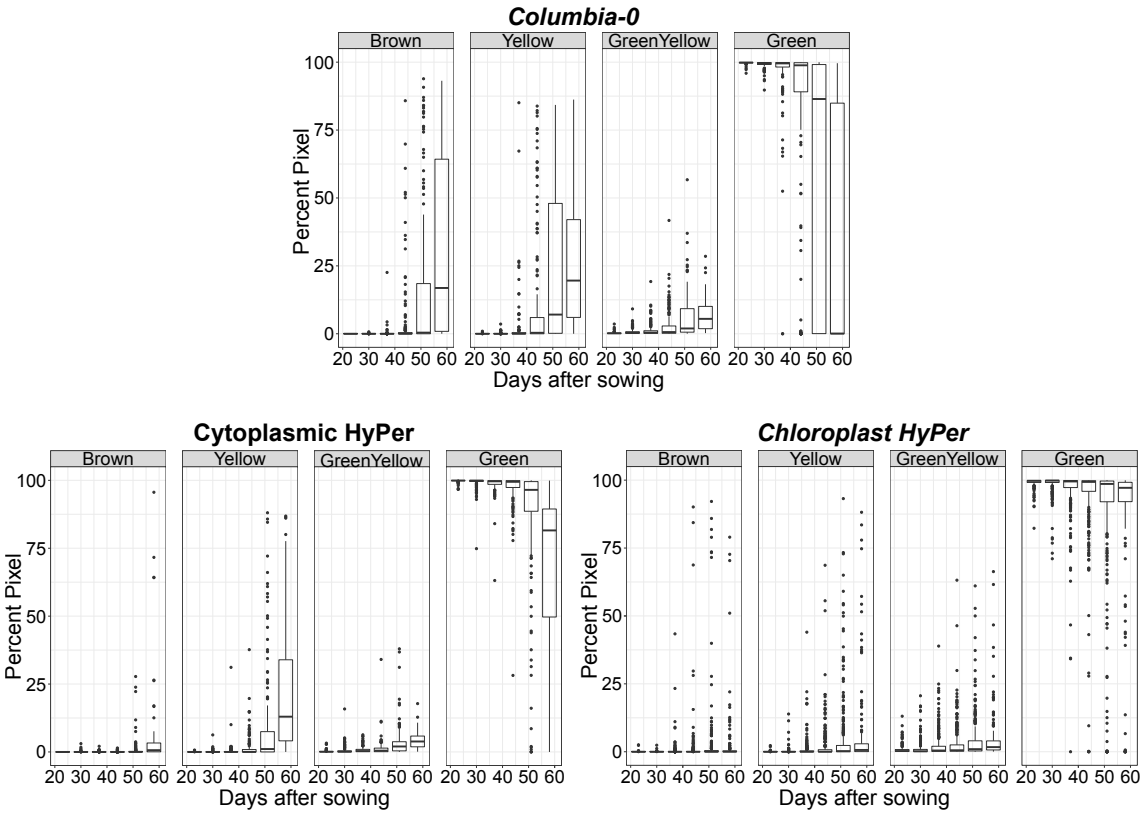

Figure 2: ACA single colour quantification of *Colunbia-0* (**top**), cytoplasmic and plastid *HyPer* plants (**bottom left & right**). Twelve biological replicates were sampled per harvest for *Col-0* and cytoplasmic *HyPer*, twenty-four for chloroplastic *HyPer*. Quantification of colours reflecting either other cellular processes or errors in data acquisition (purple and unknown, respectively) did not contain any data and graphs were excluded. Lower and upper hinges of the boxplots correspond to the 25 % & 75 % quartiles. The horizontal line reflects the median, the whiskers indicate 1.5xIQR range. Outliers are represented as black dots. *Unpublished data.*

According to the mechanism of senescence induction already proposed above, chloroplastic H_2O_2 production is elicited via cytoplasmic H_2O_2, produced upstream of chloroplast signalling. In combination with the phenotypical observations made, this hypothesis can be extended as follows. Initial cytoplasmic H_2O_2 accumulates inside the cell and *induces* leaf senescence. This would lead to chloroplastic *HyPer* plants showing a normal timing of induction, whereas cytoplasmic *HyPer* plants exhibit a delayed senescence induction. The slower progression of senescence in chloroplastic *HyPer* plants indicates a central position of chloroplast derived ROS then during execution of induced senescence, with an in consequence slowed *progression* in chloroplast *HyPer* expressing plants. Inhibited processes of senescence may include for example RUBISCO degradation. Its initial degradation has been shown to occur in the chloroplast via ROS. The oxidation facilitates fragmentation of RUBISCO subunits, leaving them prone to further degradation by peptide hydrolases. The resulting fragments then show an increased tendency to bind to the chloroplast envelope, making it available for transport out of the chloroplast via *Rubisco containing bodies*, followed by further degradation (Desimone et al., 1996; Chiba et al., 2003). But not only RUBISCO degradation might be affected. Assuming that cytoplasmic ROS elicit production of chloroplastic ROS, which then significantly mediate senescence progression, many other downstream signalling and other senescence related processes are most probably misregulated, too.

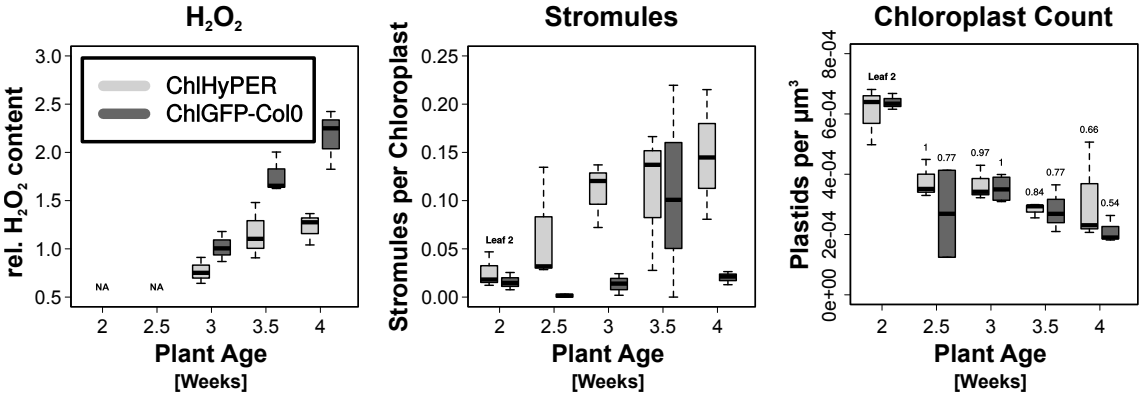

Figure 3: Stromule development in plastidic *HyPer* and *Col-0* plants. **Left:** H_2O_2 contents measured in leaf 4. Values are normalized to corresponding oxidized dye solution. **Middle:** Stromules counted in 3-6 regions of leaf 3. **Right;** Average chloroplasts per μm^3 cell volume of 3-6 regions per leaf. Numbers above boxplots indicate percentage of respective maximal counts (2 weeks after sowing not included as it was sampled from leaf position 2). Statistical tests were not conducted as only three biological replicates per line and harvest were sampled. NA: leaf was not available. Whiskers indicate 1.5xIQR, bar represents median. *Unpublished data.*

A possible signalling mechanism that might be affected was observed microscopically in chloroplastic *HyPer* plants. Here, formation of stromules was altered in comparison to non *HyPer* expressing control plants. While the control plants induced stromule formation only at H_2O_2 peak levels, plants expressing chloroplast *HyPer* induced stromule formation already during early leaf development (see Figure 3). Caplan et al. (2015) reported stromule formation upon external application of H_2O_2 to chloroplasts. Accordingly, stromule formation in wildtype plants takes place preferably at (*cytoplasmic*) H_2O_2 peak levels (see Figure 3). However, plastidic *HyPer* plants display a much earlier induction of stromule formation, independent of H_2O_2 accumulation (see Figure 3, middle).
This indicates that not only the external application of H_2O_2 to plastids induces stromule outgrowth, but rather a high ratio of oxidative levels between cytoplasm and the chloroplasts may be decisive (Ox_{Cyt}/Ox_{Chloro}). As chloroplastic *HyPer* supposedly acts as H_2O_2 specific anti-oxidant and reduces plastidic H_2O_2 contents, this ratio would be higher than in wildtype already during early leaf development. Furthermore, the still occurring cytoplasmic H_2O_2 accumulation in plastidic *HyPer* plants would then increase Ox_{Cyt}/Ox_{Chloro} even more, possibly leading to a stromule count even higher than in wildtype plants during H_2O_2 peak values (see Figure 3, middle). Lastly, this mechanism would also provide an explanation for the only transient presence of stromules in wildtypic plants. After initial stromule induction, further cytoplasmic ROS accumulation also elicits chloroplastic ROS production (see Figure 6). This then lowers the value of Ox_{Cyt}/Ox_{Chloro}, thus again reducing stromule development (Figure 3, middle).

The importance of chloroplastic signalling during senescence progression is supported by examples from the literature. Caplan et al. (2015) and Exposito-Rodriguez et al. (2017) proposed a mechanism of stromule mediated chloroplast-nuclear contact and signal transmission. This is further underlined by the stromules shown in Figure 4. Seemingly, these extrude from chloroplasts and establish connections with the *neighbouring cell* and its nucleus. Interestingly, the stromules as well as the chloroplast they are extruding from appear to be fluorescing much brighter than the other chloroplasts.
An explanation for this rests on the image acquisition. Images were recorded using only the 480 nm laser line, as the objective was only to record stromule formation, not *HyPer* fluorescence ratios. This laser predominantly excites the oxidized variant of *HyPer*. Thus the image indicates a very oxidized milieu around the stromule extrusion sites as well as *inside* of the stromules (Figure 4, bottom). This might reflect their possible function as a chloroplast-nucleus ROS transmitting structure. Also, Caplan et al. (2015) demonstrated the transfer of ROS from chloroplasts to

the nucleus. On the other hand, this may only be a side-effect of the necessity for an oxidative situation for stromule formation. Still, when closely inspecting Figure 4, one might conclude that the stromule itself becomes only oxidized when a connection to a nucleus has been established (compare Figure 4 top row: no visible nuclear connection and lower brightness; bottom row nuclear connection established, high brightness). Unfortunately, observations as in Figure 4 bottom were made only very rarely and the shown pictures are the best available concerning quality and *visibility* of a chloroplast-nuclear connection. Thus, drawing conclusions from that at this point may be considered quite far fetched.

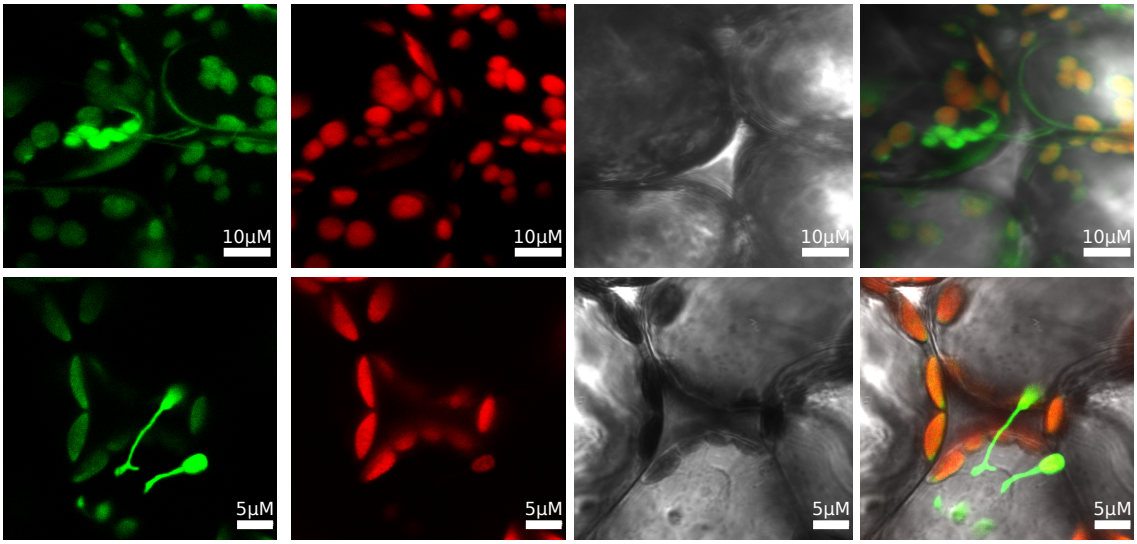

Figure 4: Cell-cell connections via stromules, observed in leaf mesophyll cells of *A. thaliana* plants expressing plastid localized *HyPer*. From left to right: *HyPer*-fluorescence, auto-fluorescence, transmitted light and overlay of all three. **Top row:** Mesophyll cells with several stromules connecting the top-left with the top-right cell. Also noteworthy is the cytoplasmic fluorescence in the right cell. **Bottom row:** Cell-cell connection from the top right cell to the nucleus of the bottom middle cell. Both pictures are 3D reconstructions of multiple stacked images. To prevent oversaturation of the transmitted image, *HyPer* and auto-fluorescence are *brightest point* 3D-reconstructions, transmitted and overlay *nearest point* 3D-reconstruction. *Unpublished data.*

Further support for the importance of the Ox_{Cyt}/Ox_{Chloro} ratio is provided by specific changes in gene expression profiles of the different *HyPer* lines. We conducted an RNA sequencing (RNAseq) experiment analysing expression profiles at different developmental stages of cytoplasmic and chloroplastic *HyPer* plants and the wildtype (*data not shown; unpublished*). Both *HyPer* lines exhibit common as well as line specific changes in gene expression. Here, one example is highlighted, demonstrating the importance of the *origin* of H_2O_2 involved in signalling cascades and possibly of the Ox_{Cyt}/Ox_{Chloro} ratio as well.

Only in chloroplastic *HyPer* plants, a whole cluster of *plant defensin (PDF)* genes was highly induced. *PDFs* are known to be a part of the plant innate immunity. During plant pathogen defence responses, the cell surface localized production of ROS (via RBOHs) is one of the earliest detectable events. A flow of H_2O_2 back inside the cell via aquaporins is conceivable. Thus, the pathogen triggered, apoplastic oxidative burst may elicit an increase in cytoplasmic ROS contents, which, if pronounced enough, in turn would result in an increase of the Ox_{Cyt}/Ox_{Chloro} ratio. Again, this also may be mimicked by the lowering of the chloroplastic ROS levels via *HyPer*, what then also might provoke *PDF* expression.
However, whether this effect relies on the ratio increase or another effect mediated by the reduction of chloroplastic H_2O_2 contents is still unclear. Moreover, it has to be mentioned that a ROS burst during plant pathogen response is very common and not limited to specific pathogens. The identified *PDFs* however are all known to be responsive only to fungal pathogens. Such a specific response hints at a more elaborated mechanism. Additionally, one of the identified PDFs (*PDF1.2A*, At5G44420) was shown to be responsive to paraquat treatment (Manners et al., 1998). While this reflects a connection to chloroplastic ROS in general, paraquat is known to be a non-selective herbicide that induces O_2^{*-} accumulation in chloroplasts (Farrington et al., 1973). This contradicts the hypothesis of lowered chloroplastic H_2O_2 contents or an increased ratio Ox_{Cyt}/Ox_{Chloro} inducing *PDF* expression.
Nevertheless, H_2O_2 contents were monitored throughout the RNAseq experiment and no unusual accumulation of H_2O_2 was detected during or prior to the induction of these genes (see Figure 1, left). Also, no fungal infestation of any of the plants was observed during the experiment (*unpublished results*). A more detailed analysis of the RNAseq data and especially of plant-pathogen responses in the different *HyPer* lines will shed further light on this.

Conclusively, the in the chloroplastic line apparent accumulation of H_2O_2 originating from the cytoplasm/apoplast and the following, timely induction of senescence implies that cytoplasmic H_2O_2 production is independent and most likely upstream of plastidic ROS production, and a necessity for the induction leaf senescence, whereas the following increase in chloroplastic H_2O_2 contents is of pivotal relevance for senescence progression and signalling.

Systemic Signalling Systemic propagation of the senescence inducing signal via cell-, tissue- and organ-level communication is major prerequisite for an efficient performance of leaf senescence. An indication for the involvement of chloroplastic H_2O_2 in senescence propagation can be seen in the senescence pattern of chloroplast

HyPer plants. A wildtypic senescence progression pattern primarily originates from the tip and progresses to the leaf base (see Figure 5, left). A different pattern of senescence progression can be observed in chloroplastic *HyPer* plants (Figure 5, right). In early stages, leaves tend to develop yellow spots distributed over the whole leaf. Then especially the left and right margins start senescing, while the leaf tip remains green.

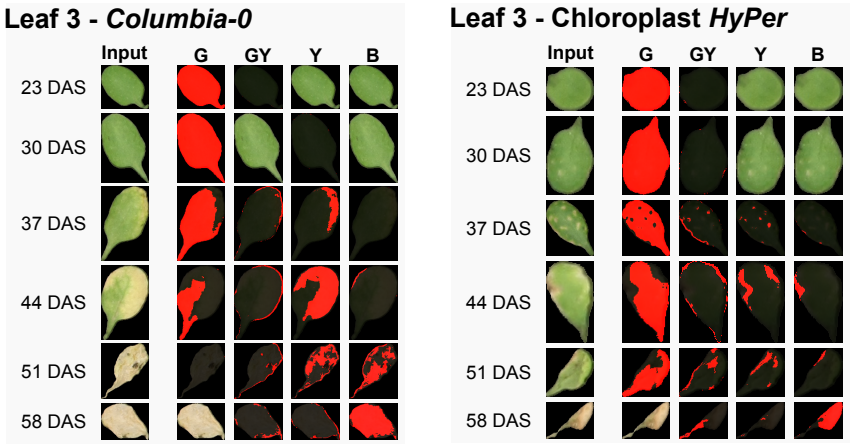

Figure 5: Exemplary pictures of leaf 3 over the development of *Columbia-0* (**left**) and chloroplast *HyPer* plants (**right**). Pictures do not necessarily reflect pace of senescence progression, but were chosen to depict complete as possible senescence progression. Colours were detected and pictures generated with ACA. Red regions indicate identified corresponding colour. *Unpublished data.*

In Figure 4, cell-cell connections via stromules can be seen. The top row displays cell-cell connections via multiple stromules, the bottom row shows two stromules expanding from one cell directly to the nucleus of a second cell. So far this was only observed by us in plants expressing plastidic *HyPer*. However, despite the lack of other, already published supporting evidence, this represents a very enticing possible signalling mechanism. This connection could provide a way to spread senescence induction to surrounding cells. Clearly, it could only serve as short distance signalling, and thus it most probably is more relevant to *inter-organellar* signalling within one cell. Also peroxisomes and mitochondria have been shown to develop peroxules and matrixules, respectively. Although a direct connection from these organelles to the nucleus has not been observed, yet, the aggregation of mitochondria and peroxisomes upon oxidative stress as well as the gathering of these aggregates around chloroplasts has been (Sinclair et al., 2009; Noctor and Foyer, 2016).

Long distance signalling might be facilitated via the in Gilroy et al. (2014) presented mechanism. They proposed that long distance signalling of ROS is mediated via RICR and CIRP. Incoming ROS from neighbouring cells may activate ROS dependent Ca^{2+}

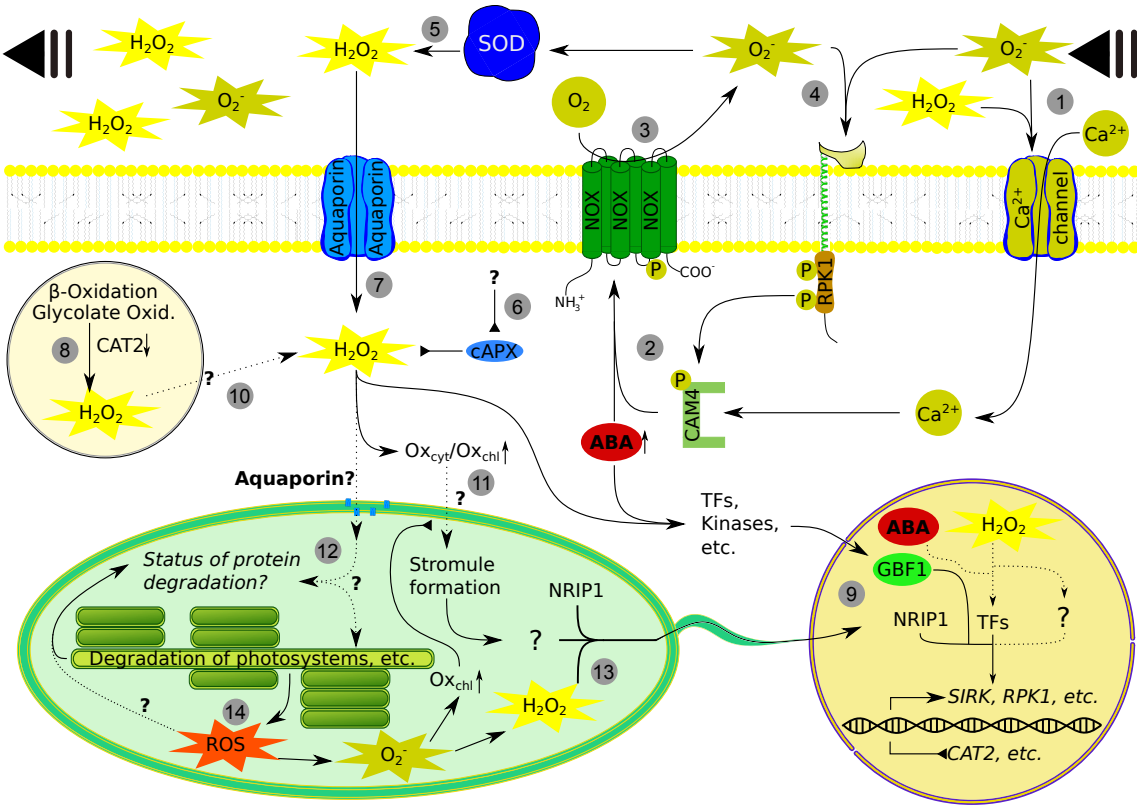

Figure 6: *Model for possible pathway of ROS mediated senescence induction.* Expression of *Rpk1* and *CaM4* increases with leaf age, hence the leafs' susceptibility to induce either age dependent or stress-provoked leaf senescence also increases. As soon as one or the other takes place, for example via Ca^{2+} assisted systemic O_2^{*-} signalling (1), NOXs are activated via ABA and Rpk1 mediated by phosphotransfer via CaM4 (2). NOX/RBOH generates superoxide (3), which amplifies the aforementioned Rpk1 signalling (4), but also increases generation of apoplastic H_2O_2 (5). If cytoplasmic ROS scavenging is reduced, e.g. through deactivation of APX (6), apoplastic H_2O_2 may influx and accumulate inside the cell (7). Peroxisomal H_2O_2 may accumulate (8) only if CAT2 activity is reduced due to the activity of GBF-1 (9). Although unknown how, peroxisomal H_2O_2 assists in ROS mediated senescence induction (10). H_2O_2 accumulated in the cytosol induces stromule formation (11) and retrograde signalling, maybe even oxidative degradation of RUBISCO (12). ROS accumulating in the chloroplast are taking part in chloroplast-nuclear communication (13), maybe are involved in feedback on protein degradation status and presumably again suppress stromule formation by the increase of chloroplastic oxidative status and thus the reduction of the oxidative ratio *Cyt/Chloro* (14). Possible peroxule- and matrixule-chloroplast connections, as well as chloroplast mediated cell-cell signalling as described above are not included. Model is based on Dynowski et al., 2008; Yang and Ohlrogge, 2009; Zhao et al., 2010; Lee et al., 2011; Bieker et al., 2012; Gilroy et al., 2014; Caplan et al., 2015; Tian et al., 2016; Exposito-Rodriguez et al., 2017; Giri et al., 2017; Koo et al., 2017; Li et al., 2018 and *unpublished data*.

channels. Ca^{2+} entering the cell then initiates ROS production (for example via Rpk1, CaM4 and RBOHF). ROS generated in the apoplast can then induce downstream pathways after entering the cell. But also they might diffuse to neighbouring cells, where again the signal can be perceived, amplified and transmitted further. Putting all information together, the in Figure 6 displayed model can be proposed.

Obviously, only a small excerpt of *possible* senescence inducing signalling events can be depicted here. Besides a development or age dependent pathway of senescence induction, many other responses as for example nutrient starvation, low light/shading or pathogen infestation may lead to senescence induction eventually. Still, the connection of the depicted mechanism to ABA mediated signalling already combines aspects of age- as well as stress-dependent induction of leaf senescence. As already mentioned above, all the elicited cascades of the aforementioned stimuli may converge at the pathway of age dependent senescence induction, although all fed into separate signalling cascades at first.

While many stresses involve initial H_2O_2/ROS dependent signalling, some stresses do not. For example, N starvation does seem to repress H_2O_2 dependent senescence induction (Bieker et al., 2019). Thus, it appears even more necessary to further elucidate the various pathways and elements of senescence induction and to reveal the elements facilitating interconnection of senescence inducing and other pathways.

6.2 The Integration of Stress Elicited Pathways into Senescence Induction

Plants are exposed to biotic and abiotic stresses on a regular basis. Commonly, multiple stresses occur at the same time. For example, during high temperatures usually also high light stress arises. In most cases, this is accompanied by drought stress, which again can lead to salt stress. All impacting physiological pressures feed into their own signalling cascades, which also do overlap in parts. And as mentioned above, if the exerted pressure of an individual or of multiple stresses becomes too high, these signalling cascades converge into the fallback program of leaf senescence induction. This *fail-safe mode* does not serve to secure the survival of the plant itself but rather to push forward the support of reproductive organs with the goal to ensure the survival of the plants' offspring. The connection between stress responses and senescence induction becomes even more obvious, when considering the dual functions of many TF families. For example, *WRKY* TFs take a central role in responses to biotic and abiotic stress as well as senescence induction.

Regulation of *WRKY* expression and activity takes place on multiple levels. WRKY proteins can interact with each other and form homo- and hetero-dimers, thus modifying activity and target sites binding affinities. WRKYs bind to W-boxes (TGACC (A/T)), a DNA motif also present in the promoter region of all *WRKYs*. Moreover, in multiple cases they have been shown to interact with downstream targets or upstream regulators on protein level. Thus, feed-forward and feed-back loops are often observed. A common feature of the processes WRKY factors are predominantly involved in is a prominent association with ROS signalling. In *A. thaliana* expression of *WRKY6, WRKY8, WRKY22, WRKY30, WRKY39, WRKY48, WRKY53*, and *WRKY75* has been demonstrated to be responsive to H_2O_2 treatment (Jiang et al., 2017). The redox regulation of *WRKY* expression and function was further underlined by *A. thaliana apx1* lines. Here, expression of *WRKY6, 18, 25, 33, 40, 46, 54, 60* and *WRKY70* was induced (Li et al., 2014). In summary, the family of *WRKY* TFs forms a highly complex transcription factor network with multiple layers of control on DNA and protein level and involvement in a multitude of plant developmental and stress related regulatory processes (Potschin et al., 2014; Banerjee and Roychoudhury, 2015; Jiang et al., 2017).
The structurally related Arabidopsis WRKY18, WRKY40, and WRKY60 are pathogen-induced TFs. All three factors are involved in plant biotic and abiotic stress responses (see section 4.3 and Chen et al., 2010). In Potschin et al. (2014), we could show that WRKY18, a factor known for its involvement in pathogen response and

ABA dependent regulation (see e.g. Liu et al., 2012), also takes part in expression control of *WRKY53*, which has been demonstrated to play a central role in the initiation of age dependent leaf senescence (Miao et al., 2004). Like most of the WRKY factors, also the WRKY18 protein can form homo- and hetero-dimers with itself as well as with other WRKY factors, respectively. If present as a homo-dimer, it represses *WRKY53* expression. However, as soon as WRKY53 protein is present and WRKY18/WRKY53 hetero-dimers are formed, expression of *WRKY53* is induced by the hetero-dimers of these factors (Potschin et al., 2014). *WRKY18* knock down plants show an early senescence phenotype as well as earlier and more pronounced expression of *WRKY53* and other SAGs. Accordingly, *WRKY18* overexpression plants display a delayed senescence phenotype with delayed *WRKY53* expression.

Also WRKY53 serves a dual role by acting in plant defence as well as senescence induction. Besides its already mentioned central function during age dependent senescence induction, *WRKY53* expression is up-regulated in response to SA treatment and *wrky53* plants exhibit higher susceptibility to pathogen infection (Murray et al., 2007). Another factor, WRKY70, has also been shown to be involved in SA mediated defence responses as well as senescence regulation. Also, it has a SA responsive expression pattern and the senescence associated expression of *WRKY53* and *WRKY70* is reduced in SA deficient mutant plants (Besseau et al., 2012). However, in contrast to WRKY53, WRKY70 has a negative impact on senescence induction. In conclusion, expression of both *WRKY53* and *WRKY70* is SA inducible, both are involved in SA mediated defence responses, their senescence associated expression is reduced in SA mutants and they have *opposing* effects regarding senescence regulation (Murray et al., 2007; Besseau et al., 2012). However, while expression of *WRKY53* is H_2O_2 responsive, *WRKY70* is not. Moreover, its expression is even reduced upon senescence induction (Besseau et al., 2012). Thus, WRKY70 opposes WRKY53 mediated senescence induction during pathogen responses and early development, but as soon, as senescence induction will be elicited, its expression is reduced and thus it cannot exert any longer its WRKY53 opposing function.

NAC transcription factors are also known to act as an interface between stress induced signalling and senescence. The NAC TF *ANAC092* has been shown to be involved in salt induced senescence. Comparable to senescence induction, this mechanism also has been demonstrated to be reliant on H_2O_2 dependent signalling (Balazadeh et al., 2010a,b). Thus, also in this case ROS mediated signalling may be the overlapping element of stress and developmentally induced senescence.
The drought inducible NAC TF NTL4 promotes ROS production by directly activating the promoters of *RbohC* and *E*. Knock-out plants display lower ROS levels, higher tolerance to salt and a delayed age dependent senescence phenotype (Lee

et al., 2012). This again not only reflects the importance of ROS/H_2O_2 during senescence induction as well as stress responses, but also supports the above discussed possible involvement of NOXs in senescence induction (see chapter 6.1 and Figure 6). Moreover, as with *ANAC092*, the NTL4 dependent salt response also is ABA dependent. Induction of *NTL4* transcription is induced by ABA (Lee et al., 2012).

Conclusively, many major transcription factor families involved in senescence induction are also involved in stress responses. Not only are ROS a common denominator in all related signalling cascades, but also a strong interaction of the different signalling pathways via the involved transcription factors is obvious. Moreover, plant hormones, especially ABA and SA, play a central role in connecting these signalling cascades.

Especially this entanglement of stress and senescence pathways can make it difficult to distinguish the different processes when analysing plants with respect to their senescence behaviour. Parameters usually used for rough assessment of senescence progression can be easily misleading under stress conditions. For example, leaf discolouration due to nutrient deficiencies, pathogen infection, or other stress responses in some cases may be of similar appearance as discolouration caused by senescence induction. Moreover, also widely used molecular markers are prone to false interpretation. For example ROS accumulation, as it is a central feature of senescence induction as well as many (a-)biotic stress responses. Lastly, as outlined above, also the analysis of (isolated) genetic markers for senescence can be misconstrued due to the involvement of many TFs in multiple processes. For this reason, we established a guideline on how senescence experiments can be constructed to yield reproducible and comparable results. With the aim to enable the reader to reliably characterize a senescence program, we provided advice on basic experimental design (light and soil composition, day-length etc.) as well as sets of techniques to assess senescence progression on macroscopic and molecular level. The recommended methods include assessment of developmental hallmarks, evaluation of photosynthetic capacities and composition of the photosystems, automated quantification of leaf-colouration, redox-profiling, monitoring membrane integrity and sets of genetic markers (Bresson et al., 2017).

However, stress programs eventually leading to the *fail-safe* mechanism of senescence induction have a potentially adverse impact on the plants' overall performance in respect to agricultural use. In crop plants, the early induction of leaf senescence also leads to lower yield and crop loss. Therefore, especially here it is pivotal to understand the mechanisms of age and stress dependent senescence induction. This may give the opportunity to fine tune either the integration of stress-responses into senescence induction or to modify the process of leaf and plant senescence itself.

Thus possibly gaining the ability to genetically modify crop plants in a way that would allow the plants to handle stressful circumstances more efficiently and with lower associated losses regarding yield and nutrient use efficiencies.

6.3 Senescence Processes in *Brassica napus*

As nutrient remobilisation is an integral component of leaf senescence processes, we investigated senescence induction and propagation in the *agronomical relevant* species *B. napus*. First, a more general analysis of parameters associated with leaf senescence induction and propagation was conducted.

General Senescence Parameters We were able to observe the accumulation of H_2O_2, and prior to that the reduction of anti-oxidative capacities via the reduction of CAT and APX activity. Additionally, a decrease of GSH and ASC cycle substrates was measured (see Figures 4 and 5 in Bieker et al., 2012). Peak values of H_2O_2 and the reduction of anti-oxidative capacity coincided with induction of flowering and the beginning degradation of chlorophyll in leaves, which was assessed via soil plant analysis development (SPAD) measurements (see Bieker et al., 2012, Figure 5).

While the expression of the early senescence markers *WRKY53* and *SAG13* was enhanced, expression of senescence down-regulated genes (SDGs) for example *CAT2*, *chlorophyll a/b binding protein (CAB)* and *RUBISCO* decreased at the same time (Fig. 6, Bieker et al., 2012). In *A. thaliana*, expression of the SAG *WRKY53* was shown to be H_2O_2 responsive (Miao et al., 2004). In *B. napus* we also observed increasing *WRKY53* expression coinciding with the accumulation of intracellular H_2O_2 (Figures 5 E and 6 C in Bieker et al., 2012). Thus, the down-regulation of anti-oxidative capacities and a following increase of H_2O_2 contents appear to be an indicator for senescence induction not only in *A. thaliana* but also in *B. napus*.

Indeed, the reduction of anti-oxidative capacities and the accumulation of ROS, H_2O_2 in particular, concurring with senescence induction are by far not restricted to the family of *Brassicaceae*. Experiments conducted by Agüera et al. (2010) have demonstrated similar mechanisms in sunflower (*Helianthus annuus*, *Asteraceae*). In mung bean (*Vigna radiata*, *Fabaceae*), H_2O_2 but not O_2^{*-} has been proposed to play a role during induction of cotyledon senescence. Here, H_2O_2 accumulates at the outer regions of the cotyledon where storage protein remobilisation is initialized, while O_2^{*-} contents increase around the vasculature and even show a *positive* correlation with total chlorophyll contents (Pal and Kar, 2018). Although it is questionable how

comparable age-dependent leaf senescence and cotyledon senescence in mung bean are, Brown and Hudson (2015) have shown a significant overlap of gene expression profiles of both. Still, ~10 % of differentially regulated genes are being exclusively expressed during cotyledon senescence.

Even more remarkably, Yang et al. (2018) found that the expression of the oilseed rape (OSR) TF *WRKY generating ROS 1 (WGR1)* can promote senescence symptoms not only in *B. napus* and *A. thaliana* but also in *N. benthamiana*. Also here, ROS signalling is involved in senescence induction. They could demonstrate the binding of WGR1 to the W-Boxes contained in the promoter regions of *RbohD* and *RbohF* of *B. napus* and *A. thaliana*. The factor activates transcription of the ROS generating enzymes and thus promotes leaf senescence. *WGR1* overexpression in stable *A. thaliana* lines provokes early senescence induction and transient expression in *N. benthamiana* results in senescence symptoms and H_2O_2 accumulation at the sites of infiltration (Yang et al., 2018). Unfortunately, these experiments have not been combined with the application of RBOH blocking agents as di-phenylene-iodonium chloride (DPI). This would have allowed to distinguish effects directly based on ROS production from effects possibly exerted by (yet unknown) targets of WGR1.

In conclusion, the down-regulation of anti-oxidative capacities, the induction of oxidative enzymes and the thus inevitable, following accumulation of ROS seems to be a central component of senescence induction not only in the model plant *A. thaliana* but also in plants of other genera, as *B. napus*, and even plants of other orders, as *H. annuus* and *V. radiata* (*Asteraceae* and *Fabaceae*, respectively).

The Influence of Different C and N Supplies on Senescence Induction After the analysis of more general senescence features, we focussed on the influence of the plants nitrogen and CO_2 supply. In the following experiment, treatments with normal and enriched atmospheric carbon dioxide contents (380 parts per million (ppm) and 550 ppm, respectively) were applied to *B. napus* plants in combination with available soil nitrogen adjusted to either *minimal* (75 kilogram (kg) per hectare (ha)), *optimal* (150 kg $* ha^{-1}$) or *surplus* (225 kg $* ha^{-1}$). Nitrogen was provided to the plants in three N gifts distributed over plant development (0, 72 and 80 DAS). This again was combined with ^{15}N labelling. Within the minimal, optimal and surplus N groups, three subgroups were set up. These were then supplied with ^{15}N labelled fertilizer at either 0, 72 or 80 DAS (Franzaring et al., 2011; Bieker et al., 2012; Safavi-Rizi et al., 2018; Bieker et al., 2019).

High CO_2 Supply and Elevated C/N-Ratio While under normal CO_2 concentrations none of the N supplies induced any change of the timing of senescence induction, plants subjected to elevated atmospheric CO_2 contents and low nitrogen (N_L) or optimal nitrogen (N_O) supply exhibited an earlier peak in leaf intracellular H_2O_2 contents and an earlier beginning of chlorophyll degradation (Bieker et al., 2012, Figure 7 B and C).
Elevated CO_2 concentrations alone have been shown to have a fertilizing effect. Especially under sufficient water and nutrient supply, elevated CO_2 is able to increase photosynthetic rates and thus biomass and yield (e.g. Högy and Fangmeier, 2008). The *in-planta* C to nitrogen (N) ratio has long been hypothesized to be a possible element of the age dependent senescence inducing signal cascade (Pourtau et al., 2006; Wingler and Roitsch, 2008). In our experiment, enriching the supplied atmosphere with CO_2 and simultaneously limiting the availability of nitrogen, might have induced a rise of the C/N ratio above a critical threshold, thus eliciting senescence at an earlier time than in the other treatments. Unfortunately, C and N contents have not been analysed in this experiment, but only in another rapeseed senescence experiment also conducted by us (in the following termed '*Exp.2*').

However, in *Exp.2*, C and N regimes were not adjusted to different levels as they were before, but rather senescence progression was analysed under normal/optimal conditions. Still, an increase in C/N ratio was observed shortly before senescence induction. Though, C/N ratio then markedly increased during, rather than before senescence induction (see Bieker et al., 2012, Fig. 5 F). What has to be considered here, is that the measured carbon contents also include structural C. Plant C/N ratios usually describe the relation of *soluble* sugars to nitrogen. Thus, interpretation of the measured C and N contents with respect to plant C/N ratios is rather speculative.

Still, a regulatory role of the C/N ratio during senescence has also been described for example in *Sorghum bicolor* exposed to drought stress (Chen et al., 2015). Albeit contents of soluble sugars and soluble N sources (e.g. amino acids or proteins) decreased already 5–8 days after beginning of the drought treatment, after 10–12 days of continued treatment, the plants exhibited a further, significant increase in C/N ratio. Only then, this coincided with peak levels in *WRKY53* expression, which can serve as marker gene for senescence induction. In conclusion, drought may induce a slow increase of C/N ratio, which in turn then elicits senescence induction after reaching a certain threshold. Additionally, in this study it was shown that treatment of detached leaves with high sugar contents in combination with low nitrogen availability promoted leaf senescence symptoms. This was even more pronounced when the respective treatments were combined with osmotic stress. This indicates that an increasing C/N ratio may function as a general senescence inducing parameter that

is deliberately provoked upon certain stresses (in this case drought).

Moreover, the authors were able to show that drought induced elevation of C/N ratio started in lower/older leaf positions while the younger leaves maintained lower C/N ratios and showed less severe senescence symptoms as well. Still, other senescence symptoms as for example a reduced photosynthetic capacity were observable in all leaf positions at the same time (Chen et al., 2015). While the progression from older to younger leaves reflects the order of events during sequential leaf senescence, the decrease of photosynthetic activity in all leaf positions at the same time appears more like a systemic stress response. Again, this indicates the C/N ratio to play a role primarily during stress mediated senescence induction.
An increased C/N ratio can also be induced by nitrogen deprivation. Not only does a low N regime reduce the amount of N that can be acquired by the plant, it also increases sugar contents, as plant growth in general is limited and because C skeletons designated for amino acid synthesis are not utilized.

N Starvation To further scrutinize the influence of N availability on the induction and progression of leaf senescence, two different N starvation experiments were conducted. During the first experiment, short term N starvation was analysed in hydroponically cultivated *A. thaliana* and *B. napus* plants. First, plants were pre-cultivated on N containing media to ensure proper germination and early development. At around 3–4 weeks of plant age, *A. thaliana* plants were then transferred to a *completely* N free medium, *B. napus* plants to a medium containing only 0.1 millimolar N. After a few days of habituation, harvests were conducted. Leaves of different ages were sampled for H_2O_2 measurements and chlorophyll contents were monitored. Of the *B. napus* plants additional samples to determine CAT activity were taken.

N *starvation* seemingly elicited a premature senescence program, most likely as a part of stress-induced N remobilisation. The induction of a premature senescence program was concluded from the reduction of CAT activity in N starved plants and the starting decrease of chlorophyll contents in older, but not younger leaves. Surprisingly, despite a severe reduction of CAT activity, no increase in intracellular H_2O_2 contents could be measured. Instead, a decline of H_2O_2 was observable in comparison to the control plants (see Bieker et al., 2019, Figure 5 A&B, 6 A&B and S5).

The rapid accumulation of anthocyanins in the leaves indicated an additional underlying stress program. This was observed in *A. thaliana* as well as *B. napus* (see Bieker et al., 2019; Figure 5 C&D, 6 C&D). Usually, anthocyanin synthesis is part

of a general stress response. The phenylpropanoid pathway is activated, leading to lignification, anthocyanin build-up and synthesis of other protective, secondary metabolites. Anthocyanins can fulfil many different functions. For long they have been discussed to act as anti-oxidants. While their efficient anti-oxidative function has been demonstrated *in-vitro*, their *in-vivo* function as antioxidants still is under debate (Agati and Tattini, 2010; Juadjur et al., 2015; Landi et al., 2015). Their *in-vivo* function as antioxidant is questioned, because anthocyanins are stored within the vacuole and are thus not in close proximity to possible sources of ROS generation. However, considering that the vacuole occupies 70 % or more of the cellular space, proximity to ROS generating organelles is virtually always given. Admittedly, regarding reactivity and thus possible diffusion distances of most ROS, an even closer proximity would be required for efficient anti-oxidative function. Nonetheless, the vacuolar membrane harbours aquaporins and thus provides a possibility for the influx of ROS, in particular H_2O_2, which due to its longer lifetime, actually can diffuse away from its production site over significant distances. Still, scavenging of ROS with higher reactivity by anthocyanins probably can be excluded, as these will not even reach the vacuole.

Another function ascribed to anthocyanin-synthesis is the delay of leaf senescence, especially in the case of macro-nutrient deficiencies. A typical reaction to nutrient deficiencies is reduced growth. Upon reduced growth, the sink strength of developing organs declines. This in turn leads to the accumulation of sugars in mature source leaves (Wingler et al., 2005). As described above, high sugar contents would then accelerate senescence progression. However, sugar accumulation also induces the phenylpropanoid pathway, and thus also anthocyanin synthesis. In that way, anthocyanins may simply provide another sink for excess carbon skeletons and thus decelerate the progression of sugar induced senescence (for detailed review, see Landi et al., 2015).

In conclusion, N starvation seems to induce a premature senescence program combined with a stress response. The decreased availability of nitrogen elicits an N shortage stress response. Growth in general slows down, because of that sink strength of previously developing organs drops drastically. As a consequence, nutrient export from source leaves also decreases and a local over-supply of carbon-skeletons in these leaves arises. This and the general lack of nitrogen increase sugar contents and thus C/N ratio significantly, thereby eliciting C/N ratio dependent senescence induction. Lastly, the stress response as well as the increased carbon availability in source leaves induces anthocyanin synthesis, which then might mask the senescence associated, temporary increase of H_2O_2 contents, elicited by the senescence induction associated reduction of anti-oxidative capacities.

Varying N-Supply Plants from the above introduced experiment treated with *normal CO_2* supply and either low nitrogen (N_L) or optimal nitrogen (N_O) were sampled also for MA aided gene expression analyses. This was carried out by the group of Prof. Dr. R. Kunze (FU Berlin) and results have been recently published in Safavi-Rizi et al. (2018). In addition to this analysis, we screened the data for genes with expression profiles (anti-)matching the pattern of H_2O_2 in- and decrease (Bieker et al., 2012, 2019). Surprisingly, transcripts of SSPs, usually expressed exclusively in seeds, were found to be expressed in *B. napus* leaf material. Besides others, members of the *NAPIN* and *CRUCIFERIN* SSP family were found to be present in the clusters following as well as the clusters contradicting the course of intracellular H_2O_2 contents.

For further analyses, an Arabidopsis Genome Initiative (AGI) code listing including seed storage protein and related loci was assembled and implemented in a repeated screen of the expression data. In more detail, under N_O conditions *CRUCIFERIN* transcripts were induced, whereas under N_L conditions expression of *NAPIN* transcripts was enhanced. Moreover, each time the expression of *NAPIN* or *CRUCIFERIN* was induced, transcript levels of the respective other SSP class were reduced.

We were able to reproduce this results in another experiment that included only the same fertilization treatments, but not climate simulation and adjustment of CO_2 concentrations. In this experiment, more leaf positions were sampled, including the terminal leaf (the last leaf residing beneath the first developing pods) as well as stem tissue below that leaf. Additionally, we analysed a third experiment which did neither entail CO_2 or climate adjustments nor the application of the different N regimes. Also here, more leaf positions as well as stem tissue were sampled.

In all three experiments, a progressive accumulation pattern of SSPs in leaf material could be observed on transcriptional as well as on translational level. Starting at a low/old leaf position, SSP accumulation coincided with the rise of intracellular H_2O_2 contents and seemingly progressed up the plant to the next oldest leaf, shortly before the former was shed. This suggested a supportive function during senescence associated nutrient remobilisation by providing an interim storage of amino acids liberated during protein degradation. According to ^{15}N data (measured and already partially published in Franzaring et al., 2011), early applied nitrogen was remobilised with much less efficiency than later assimilated N (see Figure 4, Bieker et al., 2019).

To be efficient, an interim N reservoir requires means for economical storage as well as for effective remobilisation. SSPs are extensively processed during their maturation. The final polypeptides are then able to multimerize to compact structures which are usually deposited in (seed) protein storage vacuoles (Shewry et al.,

1995). As the transcripts possess the according sorting signals, translation into the endoplasmatic reticulum (ER) is highly probable. However, for proper maturation of SSP polypeptides, the activity of vacuolar processing enzymes (VPEs) is necessary. Indeed, γ-VPE (AT4G32940) was found to be differentially regulated during both nitrogen treatments. However, in both cases absolute expression values were very low and thus negligible.

Nevertheless, experiments with *A. thaliana vpe* null mutant plants have shown that also other proteases can process primary SSP translation products. SSPs will not be cleaved properly and for this reason will not be stored in their usual, multimeric conformation. For this reason, storage efficiency most probably is reduced. Despite that, *A. thaliana vpe* null mutant plants do not display significant changes in seed protein content or in protein *remobilisation rates* during germination (Gruis et al., 2004). Thus, the efficiency of neither the synthesis nor the later remobilisation can be estimated based just on the presence or absence of the respective processing enzymes during translation.

Evidence on the possible impact of *non seed-located* SSPs on N remobilisation may be drawn from their temporary build-up also in stem tissue. Shoot tissue already has been proposed to fulfil interim storage functions during seed filling (Girondé et al., 2015). Also, Staswick (1994) has shown the build-up of the closely related VSPs in soybean leafs to up to 50 % of total leaf protein content prior senescence induction, as well as their remobilisation during leaf senescence. As SSPs are for the bigger part composed of N rich amino acids, as for example glutamine and asparagine, their build-up might serve an essential function during N remobilisation. During remobilisation processes, proteins are degraded and the liberated amino acids are converted into the primary transport form glutamine, asparagine, glutamate and aspartate (see Section 4.4). Although these amino acids may be stored inside the vacuole, the constant accumulation of a few types of products from always the same transamination reactions poses a central problem. The accumulation of reaction products inhibits further reactions into this direction by products binding to the corresponding enzyme and thus prohibiting binding of further substrate (*product inhibition*). This jam might not only be detrimental to further transamination reactions, but also it might backlog as far as to the actual degradation reactions. Thus, a temporary build-up of SSPs in leaf and stem tissue during leaf senescence might very well support nutrient remobilisation to reproductive tissue.

In addition to the observed progressive accumulation pattern from the oldest to the youngest parts of the plant, the N status dependent expression of either *CRU* or *NAP* suggests a connection to plant N management strategies. A CRUCIFERIN monomer contains 698 N atoms, whereas the much smaller NAPIN monomer con-

tains only 228. Thus, the synthesis of SSPs apparantly adapts to levels of available nitrogen. Similar plasticity was observed by Brunel-Muguet et al. (2015). Here, upon sulphur limitation, *B. napus* seeds showed a change in their composition, shifting to a higher content of NAPIN, which contains less sulphur than CRUCIFERIN. Thus, a mechanism to adapt seed filling processes also to N availability seems natural.

But most importantly, several binding motifs of TFs involved in senescence regulation as well as in plant nitrogen management were identified in SSP upstream regions, again supporting the theory of an N status dependent remobilisation strategy during leaf senescence (for details see Bieker et al., 2019). Interestingly, in the experiment without any adjustment of N fertilization also the N dependent transcriptional control of *NAPIN* and *CRUCIFERIN* seems to be lost. Both SSP classes were expressed coinciding with rising H_2O_2 contents. However, expression induction of *NAPIN* was 3-4 times higher than that of *CRUCIFERIN* (see Bieker et al., 2019, Figure 2).

But the expression of SSPs might not only serve an improved N remobilisation during seed filling. The overall expression pattern suggests an association to ROS accumulation. While this indeed indicates a link to the developmental senescence program, this might also serve anti-oxidative functions. Already in 2001 Desikan et al. identified SSPs to be responsive to oxidative stress in *A. thaliana*. Moreover, Nguyen et al. (2015) have shown anti-oxidative functions for CRUCIFERINs in *Arabidopsis* seeds. Earlier publications have reported SSPs to be massively oxidized, especially to be carbonylated (Barba-Espín et al., 2011; Job et al., 2005). Besides an easier access to SSP monomers after multimer-destabilization via carbonylation, a ROS scavenging mechanism has been proposed. Especially in seeds, SSPs are very abundant and thus might act as ROS scavenging system (El-Maarouf-Bouteau et al., 2013). Further support for this hypothesis results from the already mentioned study conducted by Nguyen et al. (2015). Here seeds generated from *Arabidopsis* triple *cruciferin* ko-lines (*crua/crub/cruc*) displayed a much more pronounced sensitivity to artificial ageing as well as considerably higher protein carbonylation.

In conclusion, adaptive systems for nutrient remobilisation during senescence and seed filling considering nutrient availability have been shown already earlier (e.g. Brunel-Muguet et al., 2015). Thus, such a system to be in place also for N appears natural. However, it is surprising that the expression of transcripts formerly annotated as seed specific outside the seeds remained unnoticed so far. Especially in a species, which is under constant scrutiny trying to achieve higher nutrient use efficiencies and better seed nutrient compositions.

7 Concluding Remarks and Outlook

The Use of *HyPer* In our use case, *HyPer* has proven to be inappropriate, at least for the *measurement* of senescence associated dynamics H_2O_2 contents. However, it has to be considered here, that the initiation of senescence is a highly complex process, which allows, but also requires, the contribution of many different cellular events and processes. These will finally culminate in the induction of leaf senescence, presumably by transgressing a certain threshold of H_2O_2 contents. The thus gradual increase of intracellular H_2O_2 contents often can be observed over a time-frame of 2–3 weeks before it reaches its maximum (see Figure 1, left).
In essence, the velocity of senescence inducing H_2O_2 accumulation is very low compared to other cellular responses involving the generation of ROS. This most probably allows for the observed H_2O_2 scavenging properties of *HyPer*. Still, this theory lacks tangible proof. A possible experiment to test for this would be for example to treat (non) *HyPer* expressing bacteria or yeast with increasing amounts of H_2O_2 and then analyse expression of H_2O_2 inducible genes (e.g. genes of the OxyR regulon in *E. coli* or CTT1 in yeast). The resulting dynamics would indicate if and to which extent *HyPer* scavenges H_2O_2 in a cellular environment. Similar experiments with *A. thaliana* protoplasts may be considered. On whole leaves the cuticula might represent a too large barrier to apply H_2O_2 in low enough concentrations needed for a quantifiable effect.

H_2O_2 as Signalling Molecule During Senescence Induction The general signalling function of H_2O_2 during senescence by now is beyond any dispute. Moreover, the presented research clearly indicates, that ROS signals derived from different origins have different downstream effects. However, a central question arising from these results is, how ROS can fulfil distinctive functions based only on their origin, considering that ROS can not carry any additional information, as for example regarding the upstream elicitor of ROS production.
One possibility of achieving specificity in ROS signalling is to put ROS production and the signal perceiving target in close proximity to each other. In plants, plastids can undergo multiple specialized differentiations. Plastid differentiation into chloroplasts takes place in photosynthetically active tissue, in non photosynthetic tissue to amyloplasts, chromoplasts occur in reproductive and senescent organs. Beltrán et al. (2018) revealed the existence of specialized *sensory plastids* localized to the epidermis and the vasculature parenchyma. They are different to chloroplasts in size, structure and function. They exhibit a distinctive proteome, seemingly spe-

cialized for the perception and integration of signalling events. While in mesophyll chloroplasts the predominant class of proteins is photosynthesis associated, the most abundant proteins in sensory plastids are related to oxidation-reduction processes, responses to cold, salt and oxidative stress and others. In more detail, transcriptome and translatome analysis of cells containing sensory plastids revealed differential transcription of multiple signalling specific elements. Besides others, this included for example Ca^{2+} signalling cascade elements as well as the ROS response related *MAPK phosphatase 2* (AT3G06110) and *WRKY25* (AT2G30250), indicating the participation of sensory plastids in ROS and Ca^{2+} mediated signalling (Beltrán et al., 2018). Furthermore, the differential translation of proteins associated with the DNA methylation machinery, chromatin silencing, splicing and spliceosome, and others was observed.
This strongly supports the hypothesis introduced above of the chloroplast (sensory plastid) being a central integrator of stress and developmental signalling. Further analysis of the in Beltrán et al. (2018) provided data as well as senescence phenotyping of plants disturbed in sensory plastid function (e.g. *muts homlog1 (msh1)* plants) with respect to their senescence behaviour may give more insights. MSH1 is a marker protein specifically found in sensory plastids and respective knockout plants show a range of different phenotypes related to stress and developmental signalling (Abdelnoor et al., 2003; Xu et al., 2012; Beltrán et al., 2018). A comparison of the *HyPer* line transcriptome data with the translatome of *A. thaliana* MSH1 expressing cells acquired by Beltrán et al. (2018) might give further insights into senescence specific (ROS mediated) signalling originating from (sensory) plastids.

In general, the data gained from the aforementioned RNAseq experiment will provide multiple leverage points for further research. For example, thorough evaluation of this data might enable us to identify common promoter elements of genes targeted by H_2O_2 associated signalling events. Even more excitingly, one might be able to distinguish genetic elements responsive to H_2O_2 originating from specific subcellular compartments. Based on these insights, identification and further studies of for example TFs binding to these elements will greatly assist the elucidation of the signalling cascade(s) involved in the induction of leaf senescence.
Crossings of the different *HyPer* lines already have been made. Analysis of the resulting lines will provide further valuable hints on the interplay and inter-dependence of H_2O_2 signals originating from different subcellular locations, especially the proposed role of the Ox_{Cyt}/Ox_{Chloro} ratio during stromule development. Depending on the resulting phenotype (delayed senescence *induction* versus *progression*), the hierarchic order of the ROS generating locations, their specific function in senescence induction and even the mechanisms of long distance signalling might be further confirmed.

Connecting Age- and Stress-Mediated Senescence Induction Also for further investigations of the integration of stress and age-dependent senescence induction the *HyPer* lines might prove valuable. Stress elicited cascades almost always include the production of *metabolic* as well as *signalling* ROS. Here, an analysis of the origin and the dynamics of the involved ROS might be feasible via ratio-metric *HyPer* measurements, especially as these cascades seem to be less prone to modulation via *HyPer* conferred scavenging.
The application of senescence inducing stresses to *HyPer* expressing plants also might yield more knowledge about the role of H_2O_2 as a stress and senescence connecting signalling element. As presented in section 6.1, the RNAseq data also indicated disturbances in stress related signalling processes that can lead to senescence induction (for example plant-pathogen interaction). Thus, analysis of the data in combination with experiments entailing for example pathogen infection of *HyPer* expressing plants will also yield further understanding of the role of ROS signals originating from different subcellular locations. Also, the above mentioned identification of promoter elements responsive to H_2O_2 mediated signalling and the respective genes also will reveal a closer look into the (ROS dependent) inter-connection of senescence and stress signalling.

The *Arabidopsis* histidine kinase 5 (AHK5) has been described to be employed in responses to biotic and abiotic stress as well as in developmental processes (Iwama et al., 2007; Pham et al., 2012; Pham and Desikan, 2012). It is the only member of the *Arabidopsis Histidine Kinase* multi-gene family which comprises no transmembrane domain and has been shown to be predominantly localized to the cytoplasm but also to be associated with the plasma membrane in *N. benthamiana* (Grefen et al., 2008; Desikan et al., 2008). Via FRET-FLIM analysis Heunemann (2016) could show the interaction of AHK5 with itself to a homo-dimer, but also with AtRBOHC, D and F. Moreover, its activity is dependent on the oxidation of the protein, which also allows for the formation of homo-dimers. In summary, the localisation to the plasma-membrane, the dimerisation with members of the RBOH family and its activation upon oxidation as well as its involvement in plant hormone and H_2O_2 dependent signalling during developmental and stress elicited processes (see Iwama et al., 2007; Desikan et al., 2008; Pham and Desikan, 2012; Pham et al., 2012; Mira-Rodado et al., 2012; Heunemann, 2016), render it a highly probable candidate to be involved in senescence signalling and the integration with developmental processes.
Indeed, Heunemann (2016) could show a delayed leaf senescence phenotype in *A. thaliana ahk5* plants. The here conducted senescence analysis was combined with measurements of multiple ROS associated elements of senescence signalling. However, while the delay in senescence was clearly shown, a perturbation of H_2O_2

dependent signalling was not obvious. Peroxidation of membrane lipids appeared to be delayed, but no significant differences in senescence associated H_2O_2 accumulation were detected between *A. thaliana* wildtype and *ahk5* plants (Heunemann, 2016). Moreover, also stress associated H_2O_2 accumulation did not seem to be disturbed in *Arabidopsis ahk5* lines (Heunemann, 2016). This indicates, that AHK5 is not involved in the initial production or amplification of senescence inducing H_2O_2, but rather it may be required for downstream signalling events. This is also supported by the required oxidation for dimerisation and activation of the kinase. Unfortunately, the by Heunemann (2016) acquired data regarding leaf colouration as well as the chlorophyll fluorescence measurements do not allow to distinguish between a delay of senescence induction or senescence progression. Obvious follow-up investigations would include another detailed analysis of senescence progression including the implementation of ACA and documentation of developmental hallmarks in the experimental procedures, which would then allow the discrimination between a senescence induction and a progression phenotype. Also here, application of senescence inducing stresses to *ahk5* plants and following analysis of senescence induction and progression might provide further hints on the general role of AHK5 during the integration of stress elicited pathways into the pathway of senescence induction.
Furthermore, because AHK5 also directly interacts with ethylene response 1 (ETR1) (Heunemann, 2016), its involvement in ethylene mediated senescence induction should also be subjected to further investigations. ETR1 has been demonstrated to be involved in ethylene mediated senescence induction (Grbić and Bleecker, 1995). An initial analysis of ethylene induced senescence in *A. thaliana* wildtype, *ahk5* and *etr1* lines should be able to provide further conclusions on the involvement of AHK5 in ethylene/ETR1 mediated senescence induction.

Seed Storage Protein Expression in Vegetative Tissue The analysis of *B. napus* (cv. *Mozart*) plants revealed SSPs to be expressed in vegetative tissue during senescence (i.e. stem and leaf). Although a supportive function during senescence associated N remobilisation seems natural, this hypothesis still lacks proof.
A complete knockout of SSPs would also impact nitrogen storage capabilities in seeds, and thus also limit sink strength. For this reason, only conditional knockout lines would be suitable to provide further confirmation or opposition of the suggested supportive function of leaf and stem localized SSP expression. Transgenic lines expressing artificial microRNA constructs under a for example leaf specific promoter would be a reasonable approach. An analysis of these plants grown under multiple different N regimes would facilitate to draw inferences about SSP mediated

overall support of N remobilisation and also could confirm the possible adaptation mechanism to different N conditions by switching between expression of 2S- and 12S-SSP genes.

With respect to agronomic use cases, knowledge of the origin of the nitrogen incorporated into leaf localized SSPs is of central importance as it could be implemented in optimized fertilization regimes. ^{15}N pulse-chase experiments comparable to Chardon and Masclaux-Daubresse (2011) would clarify whether senescence associated SSPs synthesis primarily relies on protein degradation and remobilisation or on post-vegetative N assimilation. Moreover, this also would provide a more general insight in the mechanisms of seed filling and nutrient remobilisation during senescence in *B. napus*. Another question to be addressed are the salvage and remobilisation of synthesized SSPs from leaves. In the case of N the prevalent remobilisation forms are small peptides, amino-acids urea, ammonium and nitrate (see Section 4.4). Clarification of leaf-localised SSP degradation mechanisms might offer starting points for further genetic enhancement of N use efficiencies. Lastly, all these experiments might be extended to other species, as for example soybean. Even though here VSP expression would have to be addressed, similar functions as proposed for SSP expression in *B. napus* might be present and exploitable to increase nutrient use efficiencies.

https://de.overleaf.com/project/5d1bcd1f12adb55f1b3af022

References

Abdelnoor, R. V., Yule, R., Elo, A., Christensen, A. C., Meyer-Gauen, G., and Mackenzie, S. A. (2003). Substoichiometric shifting in the plant mitochondrial genome is influenced by a gene homologous to muts. *Proceedings of the National Academy of Sciences*, 100(10):5968–5973.

Agati, G. and Tattini, M. (2010). Multiple functional roles of flavonoids in photoprotection. *New Phytologist*, 186(4):786–793.

Agüera, E. and De la Haba, P. (2018). Leaf senescence in response to elevated atmospheric co 2 concentration and low nitrogen supply. *Biologia plantarum*, pages 1–8.

Agüera, E., Cabello, P., and De La Haba, P. (2010). Induction of leaf senescence by low nitrogen nutrition in sunflower (helianthus annuus) plants. *Physiologia Plantarum*, 138(3):256–267.

Alscher, R. G., Erturk, N., and Heath, L. S. (2002). Role of superoxide dismutases (sods) in controlling oxidative stress in plants. *Journal of Experimental Botany*, 53(372):1331–1341.

Apel, K. and Hirt, H. (2004). Reactive oxygen species: Metabolism, oxidative stress, and signal transduction. *Annual Review of Plant Biology*, 55(1):373–399. PMID: 15377225.

Arking, R. (2019). *Biology of Longevity and Aging*. Oxford University Press.

Asada, K., Urano, M., and Takahashi, M.-a. (1973). Subcellular location of superoxide dismutase in spinach leaves and preparation and properties of crystalline spinach superoxide dismutase. *European Journal of Biochemistry*, 36(1):257–266.

Balazadeh, S., Kwasniewski, M., Caldana, C., Mehrnia, M., Zanor, M. I., Xue, G.-P., and Mueller-Roeber, B. (2011). Ors1, an h2o2-responsive nac transcription factor, controls senescence in arabidopsis thaliana. *Molecular plant*, 4(2):346–360.

Balazadeh, S., Siddiqui, H., Allu, A. D., Matallana-Ramirez, L. P., Caldana, C., Mehrnia, M., Zanor, M.-I., Köhler, B., and Mueller-Roeber, B. (2010a). A gene regulatory network controlled by the nac transcription factor anac092/atnac2/ore1 during salt-promoted senescence. *The Plant Journal*, 62(2):250–264.

Balazadeh, S., Wu, A., and Mueller-Roeber, B. (2010b). Salt-triggered expression of the anac092-dependent senescence regulon in arabidopsis thaliana. *Plant signaling & behavior*, 5(6):733–735.

Banerjee, A. and Roychoudhury, A. (2015). Wrky proteins: signaling and regulation of expression during abiotic stress responses. *The Scientific World Journal*, 2015.

Barba-Espín, G., Diaz-Vivancos, P., Job, D., Belghazi, M., Job, C., and Hernández, J. A. (2011). Understanding the role of h2o2 during pea seed germination: a combined proteomic and hormone profiling approach. *Plant, cell & environment*, 34(11):1907–1919.

Belousov, V. V., Fradkov, A. F., Lukyanov, K. A., Staroverov, D. B., Shakhbazov, K. S., Terskikh, A. V., and Lukyanov, S. (2006). Genetically encoded fluorescent indicator for intracellular hydrogen peroxide. *Nature methods*, 3(4):281.

Beltrán, J., Wamboldt, Y., Sanchez, R., LaBrant, E. W., Kundariya, H., Virdi, K. S., Elowsky, C., and Mackenzie, S. A. (2018). Specialized plastids trigger tissue-specific signaling for systemic stress response in plants. *Plant Physiology*, 178(2):672–683.

Berger, S., Bell, E., Sadka, A., and Mullet, J. E. (1995). Arabidopsis thaliana atvsp is homologous to soybean vspa and vspb, genes encoding vegetative storage protein acid phosphatases, and is regulated similarly by methyl jasmonate, wounding, sugars, light and phosphate. *Plant molecular biology*, 27(5):933–942.

Besseau, S., Li, J., and Palva, E. T. (2012). Wrky54 and wrky70 co-operate as negative regulators of leaf senescence in arabidopsis thaliana. *Journal of experimental botany*, 63(7):2667–2679.

Bieker, S., Riester, L., Doll, J., Franzaring, J., Fangmeier, A., and Zentgraf, U. (2019). Nitrogen supply drives senescence-related seed storage protein expression in rapeseed leaves. *Genes*, 10(2).

Bieker, S., Riester, L., Stahl, M., Franzaring, J., and Zentgraf, U. (2012). Senescence-

specific alteration of hydrogen peroxide levels in arabidopsis thaliana and oilseed rape spring variety brassica napus l. cv. mozartf. *Journal of Integrative Plant Biology*, 54(8):540–554.

Bienert, G. P. and Chaumont, F. (2014). Aquaporin-facilitated transmembrane diffusion of hydrogen peroxide. *Biochimica et Biophysica Acta (BBA)-General Subjects*, 1840(5):1596–1604.

Bilan, D. S. and Belousov, V. V. (2018). In vivo imaging of hydrogen peroxide with hyper probes. *Antioxidants & redox signaling*.

Bloom, A. J., Burger, M., Asensio, J. S. R., and Cousins, A. B. (2010). Carbon dioxide enrichment inhibits nitrate assimilation in wheat and arabidopsis. *Science*, 328(5980):899–903.

Bonaventure, G., Bao, X., Ohlrogge, J., and Pollard, M. (2004). Metabolic responses to the reduction in palmitate caused by disruption of the fatb gene in arabidopsis. *Plant Physiology*, 135(3):1269–1279.

Breeze, E., Harrison, E., McHattie, S., Hughes, L., Hickman, R., Hill, C., Kiddle, S., Kim, Y.-s., Penfold, C. A., Jenkins, D., et al. (2011). High-resolution temporal profiling of transcripts during arabidopsis leaf senescence reveals a distinct chronology of processes and regulation. *The Plant Cell*, pages tpc–111.

Bresson, J., Bieker, S., Riester, L., Doll, J., and Zentgraf, U. (2017). A guideline for leaf senescence analyses: from quantification to physiological and molecular investigations. *Journal of experimental botany*, 69(4):769–786.

Brown, A. V. and Hudson, K. A. (2015). Developmental profiling of gene expression in soybean trifoliate leaves and cotyledons. *BMC plant biology*, 15(1):169.

Brunel-Muguet, S., D'Hooghe, P., Bataillé, M.-P., Larré, C., Kim, T.-H., Trouverie, J., Avice, J.-C., Etienne, P., and Dürr, C. (2015). Heat stress during seed filling interferes with sulfur restriction on grain composition and seed germination in oilseed rape (brassica napus l.). *Frontiers in plant science*, 6:213.

Buchner, P., Tausz, M., Ford, R., Leo, A., Fitzgerald, G. J., Hawkesford, M. J., and Tausz-Posch, S. (2015). Expression patterns of c-and n-metabolism related genes in wheat are changed during senescence under elevated co2 in dry-land agriculture. *Plant Science*, 236:239–249.

Cameron, K., Di, H. J., and Moir, J. (2013). Nitrogen losses from the soil/plant system: a review. *Annals of Applied Biology*, 162(2):145–173.

Caplan, J. L., Kumar, A. S., Park, E., Padmanabhan, M. S., Hoban, K., Modla, S., Czymmek, K., and Dinesh-Kumar, S. P. (2015). Chloroplast stromules function during innate immunity. *Developmental Cell*, 34(1):45–57.

Cathcart, R., Schwiers, E., and Ames, B. N. (1983). Detection of picomole levels of hydroperoxides using a fluorescent dichlorofluorescein assay. *Analytical biochemistry*, 134(1):111–116.

Chardon, F. and Masclaux-Daubresse, C. (2011). Exploring nitrogen remobilization for seed filling using natural variation in Arabidopsis thaliana. *Journal of Experimental Botany*, 62(6):2131–2142.

Chen, D., Wang, S., Xiong, B., Cao, B., and Deng, X. (2015). Carbon/nitrogen imbalance associated with drought-induced leaf senescence in sorghum bicolor. *PloS one*, 10(8):e0137026.

Chen, H., Lai, Z., Shi, J., Xiao, Y., Chen, Z., and Xu, X. (2010). Roles of arabidopsis wrky18, wrky40 and wrky60 transcription factors in plant responses to abscisic acid and abiotic stress. *BMC plant biology*, 10(1):281.

Chen, Q., Soulay, F., Saudemont, B., Elmayan, T., Marmagne, A., and Masclaux-Daubresse, C. (2018). Overexpression of atg8 in arabidopsis stimulates autophagic activity and increases nitrogen remobilization efficiency and grain filling. *Plant and Cell Physiology*.

Chiba, A., Ishida, H., Nishizawa, N. K., Makino, A., and Mae, T. (2003). Exclusion of ribulose-1, 5-bisphosphate carboxylase/oxygenase from chloroplasts by specific bodies in naturally senescing leaves of wheat. *Plant and Cell Physiology*, 44(9):914–921.

Choudhury, F. K., Rivero, R. M., Blumwald, E., and Mittler, R. (2017). Reactive oxygen species, abiotic stress and stress combination. *The Plant Journal*, 90(5):856–867.

Corpas, F. J., Barroso, J. B., and del Rio, L. A. (2001). Peroxisomes as a source of reactive oxygen species and nitric oxide signal molecules in plant cells. *Trends in plant science*, 6(4):145–150.

Corpas, F. J., Barroso, J. B., Palma, J. M., and Rodriguez-Ruiz, M. (2017). Plant peroxisomes: a nitro-oxidative cocktail. *Redox biology*, 11:535–542.

Cosio, C. and Dunand, C. (2009). Specific functions of individual class iii peroxidase genes. *Journal of Experimental Botany*, 60(2):391–408.

De la Mata, L., De la Haba, P., Alamillo, J., Pineda, M., and Agüera, E. (2013). Elevated co2 concentrations alter nitrogen metabolism and accelerate senescence in sunflower (helianthus annuus l.) plants. *Plant, Soil and Environment*, 59(7):303–308.

del Rio, L. A., Sandalio, L. M., Palma, J. M., Bueno, P., and Corpas, F. J. (1992). Metabolism of oxygen radicals in peroxisomes and cellular implications. *Free Radical Biology and Medicine*, 13(5):557 – 580.

Desikan, R., Horák, J., Chaban, C., Mira-Rodado, V., Witthöft, J., Elgass, K., Grefen, C., Cheung, M.-K., Meixner, A. J., Hooley, R., et al. (2008). The histidine kinase ahk5 integrates endogenous and environmental signals in arabidopsis guard cells. *PLoS One*, 3(6):e2491.

Desikan, R., Soheila, A.-H., Hancock, J. T., Neill, S. J., et al. (2001). Regulation of the arabidopsis transcriptome by oxidative stress. *Plant physiology*, 127(1):159–172.

Desimone, M., Henke, A., and Wagner, E. (1996). Oxidative stress induces partial degradation of the large subunit of ribulose-1,5-bisphosphate carboxylase/oxygenase in isolated chloroplasts of barley. *Plant Physiology*, 111(3):789–796.

Dietz, K. J. and Hell, R. (2015). Thiol switches in redox regulation of chloroplasts: balancing redox state, metabolism and oxidative stress. *Biol. Chem.*, 396(5):483–494.

Dynowski, M., Schaaf, G., Loque, D., Moran, O., and Ludewig, U. (2008). Plant plasma membrane water channels conduct the signalling molecule h2o2. *Biochemical Journal*, 414(1):53–61.

El-Maarouf-Bouteau, H., Meimoun, P., Job, C., Job, D., and Bailly, C. (2013). Role of protein and mrna oxidation in seed dormancy and germination. *Frontiers in Plant Science*, 4:77.

Eubel, H., Meyer, E. H., Taylor, N. L., Bussell, J. D., O'Toole, N., Heazlewood, J. L.,

Castleden, I., Small, I. D., Smith, S. M., and Millar, A. H. (2008). Novel proteins, putative membrane transporters, and an integrated metabolic network are revealed by quantitative proteomic analysis of arabidopsis cell culture peroxisomes. *Plant physiology*, 148(4):1809–1829.

Even-Chen, Z. and Itai, C. (1975). The role of abscisic acid in senescence of detached tobacco leaves. *Physiologia Plantarum*, 34(2):97–100.

Exposito-Rodriguez, M., Laissue, P. P., Yvon-Durocher, G., Smirnoff, N., and Mullineaux, P. M. (2017). Photosynthesis-dependent h2o2 transfer from chloroplasts to nuclei provides a high-light signalling mechanism. *Nature Communications*, 8(1):49.

Farrington, J., Ebert, M., Land, E., and Fletcher, K. (1973). Bipyridylium quaternary salts and related compounds. v. pulse radiolysis studies of the reaction of paraquat radical with oxygen. implications for the mode of action of bipyridyl herbicides. *Biochimica et Biophysica Acta (BBA) - Bioenergetics*, 314(3):372 – 381.

Foyer, C. H., Lelandais, M., and Kunert, K. J. (1994). Photooxidative stress in plants. *Physiologia Plantarum*, 92(4):696–717.

Foyer, C. H. and Noctor, G. (2016). Stress-triggered redox signalling: what's in prospect? *Plant, cell & environment*, 39(5):951–964.

Franzaring, J., Weller, S., Schmid, I., and Fangmeier, A. (2011). Growth, senescence and water use efficiency of spring oilseed rape (*Brassica napus* l. cv. mozart) grown in a factorial combination of nitrogen supply and elevated co2. *Environmental and Experimental Botany*, 72(2):284–296.

Gepstein, S. and Thimann, K. V. (1980). Changes in the abscisic acid content of oat leaves during senescence. *Proceedings of the National Academy of Sciences*, 77(4):2050–2053.

Gilroy, S., Suzuki, N., Miller, G., Choi, W.-G., Toyota, M., Devireddy, A. R., and Mittler, R. (2014). A tidal wave of signals: calcium and ros at the forefront of rapid systemic signaling. *Trends in Plant Science*, 19(10):623 – 630.

Giri, M., Singh, N., Banday, Z., Singh, V., Ram, H., Singh, D., Chattopadhyay, S., and Kumar Nandi, A. (2017). Gbf1 differentially regulates cat2 and pad4

transcription to promote pathogen defense in arabidopsis thaliana. *The Plant journal : for cell and molecular biology*, 91.

Girondé, A., Etienne, P., Trouverie, J., Bouchereau, A., Le Cahérec, F., Leport, L., Orsel, M., Niogret, M.-F., Nesi, N., Carole, D., et al. (2015). The contrasting n management of two oilseed rape genotypes reveals the mechanisms of proteolysis associated with leaf n remobilization and the respective contributions of leaves and stems to n storage and remobilization during seed filling. *BMC plant biology*, 15(1):59.

Grbić, V. and Bleecker, A. B. (1995). Ethylene regulates the timing of leaf senescence in arabidopsis. *The Plant Journal*, 8(4):595–602.

Grefen, C., Stadele, K., Ruzicka, K., Obrdlik, P., Harter, K., and Horák, J. (2008). Subcellular localization and in vivo interactions of the arabidopsis thaliana ethylene receptor family members. *Molecular Plant*, 1(2):308–320.

Gruis, D., Schulze, J., and Jung, R. (2004). Storage protein accumulation in the absence of the vacuolar processing enzyme family of cysteine proteases. *The Plant Cell*, 16(1):270–290.

Guo, Y. and Gan, S. (2006). Atnap, a nac family transcription factor, has an important role in leaf senescence. *The Plant Journal*, 46(4):601–612.

Guo, Y. and Gan, S.-S. (2012). Convergence and divergence in gene expression profiles induced by leaf senescence and 27 senescence-promoting hormonal, pathological and environmental stress treatments. *Plant, Cell & Environment*, 35(3):644–655.

Hanson, G. T., Aggeler, R., Oglesbee, D., Cannon, M., Capaldi, R. A., Tsien, R. Y., and Remington, S. J. (2004). Investigating mitochondrial redox potential with redox-sensitive green fluorescent protein indicators. *Journal of Biological Chemistry*, 279(13):13044–13053.

He, P., Osaki, M., Takebe, M., Shinano, T., and Wasaki, J. (2005). Endogenous hormones and expression of senescence-related genes in different senescent types of maize. *Journal of Experimental Botany*, 56(414):1117–1128.

Heunemann, M. (2016). H2o2-perzeption und signaltransduktion: Funktionelle und strukturelle charakterisierung der arabidopsis histidinkinase 5 (ahk5).

Himelblau, E. and Amasino, R. M. (2001). Nutrients mobilized from leaves of arabidopsis thaliana during leaf senescence. *Journal of Plant Physiology*, 158(10):1317–1323.

Högy, P. and Fangmeier, A. (2008). Effects of elevated atmospheric co2 on grain quality of wheat. *Journal of Cereal Science*, 48(3):580 – 591.

Ishida, H., Nishimori, Y., Sugisawa, M., Makino, A., and Mae, T. (1997). The large subunit of ribulose-1, 5-bisphosphate carboxylase/oxygenase is fragmented into 37-kda and 16-kda polypeptides by active oxygen in the lysates of chloroplasts from primary leaves of wheat. *Plant and cell physiology*, 38(4):471–479.

Iwama, A., Yamashino, T., Tanaka, Y., Sakakibara, H., Kakimoto, T., Sato, S., Kato, T., Tabata, S., Nagatani, A., and Mizuno, T. (2007). Ahk5 histidine kinase regulates root elongation through an etr1-dependent abscisic acid and ethylene signaling pathway in arabidopsis thaliana. *Plant and cell physiology*, 48(2):375–380.

Jiang, J., Ma, S., Ye, N., Jiang, M., Cao, J., and Zhang, J. (2017). Wrky transcription factors in plant responses to stresses. *Journal of Integrative Plant Biology*, 59(2):86–101.

Jing, S., Zhou, X., Song, Y., and Yu, D. (2009). Heterologous expression of oswrky23 gene enhances pathogen defense and dark-induced leaf senescence in arabidopsis. *Plant Growth Regulation*, 58(2):181–190.

Job, C., Rajjou, L., Lovigny, Y., Belghazi, M., and Job, D. (2005). Patterns of protein oxidation in arabidopsis seeds and during germination. *Plant Physiology*, 138(2):790–802.

Jordan, W. R., Brown, K. W., and Thomas, J. C. (1975). Leaf age as a determinant in stomatal control of water loss from cotton during water stress. *Plant Physiology*, 56(5):595–599.

Juadjur, A., Mohn, C., Schantz, M., Baum, M., Winterhalter, P., and Richling, E. (2015). Fractionation of an anthocyanin-rich bilberry extract and in vitro antioxidative activity testing. *Food chemistry*, 167:418–424.

Kim, J., Kim, J. H., Lyu, J. I., Woo, H. R., and Lim, P. O. (2018). New insights into the regulation of leaf senescence in arabidopsis. *Journal of Experimental Botany*, 69(4):787–799.

Kim, J. H., Woo, H. R., Kim, J., Lim, P. O., Lee, I. C., Choi, S. H., Hwang, D., and Nam, H. G. (2009). Trifurcate feed-forward regulation of age-dependent cell death involving mir164 in arabidopsis. *Science*, 323(5917):1053–1057.

Kliebenstein, D. J., Monde, R.-A., and Last, R. L. (1998). Superoxide dismutase in arabidopsis: An eclectic enzyme family with disparate regulation and protein localization. *Plant Physiology*, 118(2):637–650.

Koo, J. C., Lee, I. C., Dai, C., Lee, Y., Cho, H. K., Kim, Y., Phee, B.-K., Kim, H., Lee, I. H., Choi, S. H., et al. (2017). The protein trio rpk1–cam4–rbohf mediates transient superoxide production to trigger age-dependent cell death in arabidopsis. *Cell reports*, 21(12):3373–3380.

Krueger, S., Niehl, A., Lopez Martin, M. C., Steinhauser, D., Donath, A., Hildebrandt, T., Romero, L. C., Hoefgen, R., Gotor, C., and Hesse, H. (2009). Analysis of cytosolic and plastidic serine acetyltransferase mutants and subcellular metabolite distributions suggests interplay of the cellular compartments for cysteine biosynthesis in Arabidopsis. *Plant Cell Environ.*, 32(4):349–367.

Landi, M., Tattini, M., and Gould, K. S. (2015). Multiple functional roles of anthocyanins in plant-environment interactions. *Environmental and Experimental Botany*, 119:4–17.

Lee, I. C., Hong, S. W., Whang, S. S., Lim, P. O., Nam, H. G., and Koo, J. C. (2011). Age-dependent action of an aba-inducible receptor kinase, rpk1, as a positive regulator of senescence in arabidopsis leaves. *Plant and Cell physiology*, 52(4):651–662.

Lee, S., Seo, P. J., Lee, H.-J., and Park, C.-M. (2012). A nac transcription factor ntl4 promotes reactive oxygen species production during drought-induced leaf senescence in arabidopsis. *The Plant Journal*, 70(5):831–844.

Li, J. et al. (2014). Role of wrky transcription factors in arabidopsis development and stress responses.

Li, Z., Wang, F., Zhao, Q., Liu, J., and Cheng, F. (2018). Involvement of nadph oxidase isoforms in the production of o2- manipulated by aba in the senescing leaves of early-senescence-leaf (esl) mutant rice (oryza sativa). *PLOS ONE*, 13(1):1–17.

Lim, P. O., Kim, H. J., and Gil Nam, H. (2007). Leaf senescence. *Annual Review of*

Plant Biology, 58(1):115–136.

Liu, Y., Ahn, J.-E., Datta, S., Salzman, R. A., Moon, J., Huyghues-Despointes, B., Pittendrigh, B., Murdock, L. L., Koiwa, H., and Zhu-Salzman, K. (2005). Arabidopsis vegetative storage protein is an anti-insect acid phosphatase. *Plant Physiology*, 139(3):1545–1556.

Liu, Z.-Q., Yan, L., Wu, Z., Mei, C., Lu, K., Yu, Y.-T., Liang, S., Zhang, X.-F., Wang, X.-F., and Zhang, D.-P. (2012). Cooperation of three wrky-domain transcription factors wrky18, wrky40, and wrky60 in repressing two aba-responsive genes abi4 and abi5 in arabidopsis. *Journal of experimental botany*, 63(18):6371–6392.

Love, N. R., Chen, Y., Ishibashi, S., Kritsiligkou, P., Lea, R., Koh, Y., Gallop, J. L., Dorey, K., and Amaya, E. (2013). Amputation-induced reactive oxygen species are required for successful xenopus tadpole tail regeneration. *Nature Cell Biology*, 15:222 EP –.

Manners, J. M., Penninckx, I. A., Vermaere, K., Kazan, K., Brown, R. L., Morgan, A., Maclean, D. J., Curtis, M. D., Cammue, B. P., and Broekaert, W. F. (1998). The promoter of the plant defensin gene pdf1.2 from arabidopsis is systemically activated by fungal pathogens and responds to methyl jasmonate but not to salicylic acid. *Plant molecular biology*, 38(6):1071–1080.

Masclaux-Daubresse, C., Daniel-Vedele, F., Dechorgnat, J., Chardon, F., Gaufichon, L., and Suzuki, A. (2010). Nitrogen uptake, assimilation and remobilization in plants: challenges for sustainable and productive agriculture. *Annals of botany*, 105(7):1141–1157.

Maxwell, D. P., Wang, Y., and McIntosh, L. (1999). The alternative oxidase lowers mitochondrial reactive oxygen production in plant cells. *Proceedings of the National Academy of Sciences*, 96(14):8271–8276.

Mhamdi, A., Queval, G., Chaouch, S., Vanderauwera, S., Van Breusegem, F., and Noctor, G. (2010). Catalase function in plants: a focus on arabidopsis mutants as stress-mimic models. *Journal of Experimental Botany*, 61(15):4197–4220.

Miao, Y., Laun, T., Zimmermann, P., and Zentgraf, U. (2004). Targets of the wrky53 transcription factor and its role during leaf senescence in arabidopsis. *Plant molecular biology*, 55(6):853–867.

Miller, A. J. and Smith, S. J. (1996). Nitrate transport and compartmentation in cereal root cells. *Journal of Experimental Botany*, 47(7):843–854.

Miller, E. W., Tulyathan, O., Isacoff, E. Y., and Chang, C. J. (2007). Molecular imaging of hydrogen peroxide produced for cell signaling. *Nature chemical biology*, 3(5):263–267.

Miller, G., Schlauch, K., Tam, R., Cortes, D., Torres, M. A., Shulaev, V., Dangl, J. L., and Mittler, R. (2009). The plant nadph oxidase rbohd mediates rapid systemic signaling in response to diverse stimuli. *Sci. Signal.*, 2(84):ra45–ra45.

Mira-Rodado, V., Veerabagu, M., Witthöft, J., Teply, J., Harter, K., and Desikan, R. (2012). Identification of two-component system elements downstream of ahk5 in the stomatal closure response of arabidopsis thaliana. *Plant signaling & behavior*, 7(11):1467–1476.

Miret, J. A., Munné-Bosch, S., and Dijkwel, P. P. (2018). Aba signalling manipulation suppresses senescence of a leafy vegetable stored at room temperature. *Plant Biotechnology Journal*, 16(2):530–544.

Mittler, R., Vanderauwera, S., Suzuki, N., Miller, G., Tognetti, V. B., Vandepoele, K., Gollery, M., Shulaev, V., and Van Breusegem, F. (2011). Ros signaling: the new wave? *Trends in plant science*, 16(6):300–309.

Mohanty, J., Jaffe, J. S., Schulman, E. S., and Raible, D. G. (1997). A highly sensitive fluorescent micro-assay of h2o2 release from activated human leukocytes using a dihydroxyphenoxazine derivative. *Journal of immunological methods*, 202(2):133–141.

Murray, S. L., Ingle, R. A., Petersen, L. N., and Denby, K. J. (2007). Basal resistance against pseudomonas syringae in arabidopsis involves wrky53 and a protein with homology to a nematode resistance protein. *Molecular Plant-Microbe Interactions*, 20(11):1431–1438.

Nguyen, T.-P., Cueff, G., Hegedus, D. D., Rajjou, L., and Bentsink, L. (2015). A role for seed storage proteins in arabidopsis seed longevity. *Journal of experimental botany*, 66(20):6399–6413.

Noctor, G. and Foyer, C. H. (1998). Ascorbate and glutathione: Keeping active

oxygen under control. *Annual Review of Plant Physiology and Plant Molecular Biology*, 49(1):249–279. PMID: 15012235.

Noctor, G. and Foyer, C. H. (2016). Intracellular redox compartmentation and ros-related communication in regulation and signaling. *Plant physiology*, 171(3):1581–1592.

Noctor, G., Mhamdi, A., and Foyer, C. H. (2016). Oxidative stress and antioxidative systems: recipes for successful data collection and interpretation. *Plant, cell & environment*, 39(5):1140–1160.

Ogawa, K., Kanematsu, S., and Asada, K. (1996). Intra- and extra-cellular localization of "cytosolic" cuzn-superoxide dismutase in spinach leaf and hypocotyl. *Plant and Cell Physiology*, 37(6):790–799.

Pal, L. and Kar, R. K. (2018). Role of reactive oxygen species in cotyledon senescence during early seedling stage of mung bean [vigna radiata (l.) wilczek]. *Journal of Plant Growth Regulation*, pages 1–10.

Peterhansel, C. and Maurino, V. G. (2011). Photorespiration redesigned. *Plant Physiology*, 155(1):49–55.

Peuke, A. D. (2009). Correlations in concentrations, xylem and phloem flows, and partitioning of elements and ions in intact plants. a summary and statistical re-evaluation of modelling experiments in ricinus communis. *Journal of Experimental Botany*, 61(3):635–655.

Pham, J. and Desikan, R. (2012). Modulation of ros production and hormone levels by ahk5 during abiotic and biotic stress signaling. *Plant signaling & behavior*, 7(8):893–897.

Pham, J., Liu, J., Bennett, M. H., Mansfield, J. W., and Desikan, R. (2012). Arabidopsis histidine kinase 5 regulates salt sensitivity and resistance against bacterial and fungal infection. *New Phytologist*, 194(1):168–180.

Philosoph-Hadas, S., Hadas, E., and Aharoni, N. (1993). Characterization and use in elisa of a new monoclonal antibody for quantitation of abscisic acid in senescing rice leaves. *Plant growth regulation*, 12(1-2):71–78.

Poburko, D., Santo-Domingo, J., and Demaurex, N. (2011). Dynamic regulation of

the mitochondrial proton gradient during cytosolic calcium elevations. *Journal of Biological Chemistry*, pages jbc–M110.

Podzimska-Sroka, D., O'Shea, C., Gregersen, P. L., and Skriver, K. (2015). Nac transcription factors in senescence: from molecular structure to function in crops. *Plants*, 4(3):412–448.

Potschin, M., Schlienger, S., Bieker, S., and Zentgraf, U. (2014). Senescence networking: Wrky18 is an upstream regulator, a downstream target gene, and a protein interaction partner of wrky53. *Journal of plant growth regulation*, 33(1):106–118.

Pourtau, N., Jennings, R., Pelzer, E., Pallas, J., and Wingler, A. (2006). Effect of sugar-induced senescence on gene expression and implications for the regulation of senescence in arabidopsis. *Planta*, 224(3):556–568.

Purvis, A. C. (1997). Role of the alternative oxidase in limiting superoxide production by plant mitochondria. *Physiologia Plantarum*, 100(1):165–170.

Qiu, K., Li, Z., Yang, Z., Chen, J., Wu, S., Zhu, X., Gao, S., Gao, J., Ren, G., Kuai, B., et al. (2015). Ein3 and ore1 accelerate degreening during ethylene-mediated leaf senescence by directly activating chlorophyll catabolic genes in arabidopsis. *PLoS genetics*, 11(7):e1005399.

Rennie, E. A. and Turgeon, R. (2009). A comprehensive picture of phloem loading strategies. *Proceedings of the National Academy of Sciences*, 106(33):14162–14167.

Reumann, S., Babujee, L., Ma, C., Wienkoop, S., Siemsen, T., Antonicelli, G. E., Rasche, N., Lüder, F., Weckwerth, W., and Jahn, O. (2007). Proteome analysis of arabidopsis leaf peroxisomes reveals novel targeting peptides, metabolic pathways, and defense mechanisms. *The Plant Cell*, 19(10):3170–3193.

Rodriguez-Serrano, M., Romero-Puertas, M. C., Sanz-Fernandez, M., Hu, J., and Sandalio, L. M. (2016). Peroxisomes extend peroxules in a fast response to stress via a reactive oxygen species-mediated induction of peroxin pex11a. *Plant physiology*, pages pp–00648.

Rogers, H. and Munné-Bosch, S. (2016). Production and scavenging of reactive oxygen species and redox signaling during leaf and flower senescence: similar but different. *Plant physiology*, 171(3):1560–1568.

Safavi-Rizi, V., Franzaring, J., Fangmeier, A., and Kunze, R. (2018). Divergent n deficiency-dependent senescence and transcriptome response in developmentally old and young brassica napus leaves. *Frontiers in plant science*, 9:48.

Sandalio, L. M. and Rio, L. A. D. (1987). Localization of superoxide dismutase in glyoxysomes from citrullus vulgaris. functional implications in cellular metabolism. *Journal of Plant Physiology*, 127(5):395 – 409.

Santiago, J. P. and Tegeder, M. (2016). Connecting source with sink: the role of arabidopsis aap8 in phloem loading of amino acids. *Plant physiology*, pages pp–00244.

Schrader, M. and Fahimi, H. D. (2006). Peroxisomes and oxidative stress. *Biochimica et Biophysica Acta (BBA)-Molecular Cell Research*, 1763(12):1755–1766.

Shahnejat-Bushehri, S., Nobmann, B., Devi Allu, A., and Balazadeh, S. (2016a). Jub1 suppresses pseudomonas syringae-induced defense responses through accumulation of della proteins. *Plant signaling & behavior*, 11(6):e1181245.

Shahnejat-Bushehri, S., Tarkowska, D., Sakuraba, Y., and Balazadeh, S. (2016b). Arabidopsis nac transcription factor jub1 regulates ga/br metabolism and signalling. *Nature plants*, 2(3):16013.

Shewry, P. R., Napier, J. A., and Tatham, A. S. (1995). Seed storage proteins: structures and biosynthesis. *The plant cell*, 7(7):945.

Sinclair, A. M., Trobacher, C. P., Mathur, N., Greenwood, J. S., and Mathur, J. (2009). Peroxule extension over er-defined paths constitutes a rapid subcellular response to hydroxyl stress. *The Plant Journal*, 59(2):231–242.

Smykowski, A. (2010). *The G-box Binding Factor 1 (GBF1) Regulates the Onset of Leaf Senescence in Arabidopsis Thaliana*. PhD thesis, University of Tuebingen.

Staswick, P. (1994). Storage proteins of vegetative plant tissues. *Annual review of plant biology*, 45(1):303–322.

Staswick, P. (1997). The occurrence and gene expression of vegetative storage proteins and a rubisco complex protein in several perennial soybean species. *Journal of experimental botany*, 48(12):2031–2036.

Suzuki, N., Miller, G., Salazar, C., Mondal, H. A., Shulaev, E., Cortes, D. F., Shuman, J. L., Luo, X., Shah, J., Schlauch, K., et al. (2013). Temporal-spatial interaction between reactive oxygen species and abscisic acid regulates rapid systemic acclimation in plants. *The Plant Cell*, pages tpc–113.

Tegeder, M. and Masclaux-Daubresse, C. (2018). Source and sink mechanisms of nitrogen transport and use. *New Phytologist*, 217(1):35–53.

Tegeder, M. and Rentsch, D. (2010). Uptake and partitioning of amino acids and peptides. *Molecular Plant*, 3(6):997–1011.

Tegeder, M. and Ward, J. (2012). Molecular evolution of plant aap and lht amino acid transporters. *Frontiers in Plant Science*, 3:21.

Teixeira, F. K., Menezes-Benavente, L., Margis, R., and Margis-Pinheiro, M. (2004). Analysis of the molecular evolutionary history of the ascorbate peroxidase gene family: Inferences from the rice genome. *Journal of Molecular Evolution*, 59(6):761–770.

Thimann, K. V. and Satler, S. O. (1979). Relation between leaf senescence and stomatal closure: senescence in light. *Proceedings of the National Academy of Sciences*, 76(5):2295–2298.

Thomas, H. and Stoddart, J. L. (1980). Leaf senescence. *Annual review of plant physiology*, 31(1):83–111.

Tian, S., Wang, X., Li, P., Wang, H., Ji, H., Xie, J., Qiu, Q., Shen, D., and Dong, H. (2016). Plant aquaporin atpip1;4 links apoplastic h2o2 induction to disease immunity pathways. *Plant Physiology*, 171(3):1635–1650.

Tyree, M. T. (2003). Plant hydraulics: the ascent of water. *Nature*, 423(6943):923.

Wang, D., Amornsiripanitch, N., and Dong, X. (2006). A genomic approach to identify regulatory nodes in the transcriptional network of systemic acquired resistance in plants. *PLoS pathogens*, 2(11):e123.

Wang, X., Li, S., Liu, Y., and Ma, C. (2015). Redox regulated peroxisome homeostasis. *Redox biology*, 4:104–108.

Waszczak, C., Carmody, M., and Kangasjärvi, J. (2018). Reactive oxygen species in plant signaling. *Annual review of plant biology*, 69:209–236.

Wiederschain, G. Y. (2011). The molecular probes handbook. a guide to fluorescent probes and labeling technologies. *Biochemistry (Moscow)*, 76(11):1276–1276.

Wierer, S., Elgass, K., Bieker, S., Zentgraf, U., Meixner, A., and Schleifenbaum, F. (2011). Determination of the in vivo redox potential using rogfp and fluorescence spectra obtained from one-wavelength excitation. In *Imaging, Manipulation, and Analysis of Biomolecules, Cells, and Tissues IX*, volume 7902, page 790211. International Society for Optics and Photonics.

Wingler, A., Purdy, S., MacLean, J. A., and Pourtau, N. (2005). The role of sugars in integrating environmental signals during the regulation of leaf senescence. *Journal of experimental botany*, 57(2):391–399.

Wingler, A. and Roitsch, T. (2008). Metabolic regulation of leaf senescence: interactions of sugar signalling with biotic and abiotic stress responses. *Plant Biology*, 10:50–62.

Woo, H. R., Koo, H. J., Kim, J., Jeong, H., Yang, J. O., Lee, I. H., Jun, J. H., Choi, S. H., Park, S. J., Kang, B., et al. (2016). Programming of plant leaf senescence with temporal and inter-organellar coordination of transcriptome in arabidopsis. *Plant physiology*, pages pp–01929.

Wu, A., Allu, A. D., Garapati, P., Siddiqui, H., Dortay, H., Zanor, M.-I., Asensi-Fabado, M. A., Munné-Bosch, S., Antonio, C., Tohge, T., et al. (2012). Jungbrunnen1, a reactive oxygen species–responsive nac transcription factor, regulates longevity in arabidopsis. *The Plant Cell*, pages tpc–111.

Wu, J., Sun, Y., Zhao, Y., Zhang, J., Luo, L., Li, M., Wang, J., Yu, H., Liu, G., Yang, L., Xiong, G., Zhou, J.-M., Zuo, J., Wang, Y., and Li, J. (2015). Deficient plastidic fatty acid synthesis triggers cell death by modulating mitochondrial reactive oxygen species. *Cell Res*, 25(5):621–633.

Wudick, M. M., Luu, D.-T., and Maurel, C. (2009). A look inside: localization patterns and functions of intracellular plant aquaporins. *New Phytologist*, 184(2):289–302.

Xu, X., Chen, C., Fan, B., and Chen, Z. (2006). Physical and functional interactions

between pathogen-induced arabidopsis wrky18, wrky40, and wrky60 transcription factors. *The Plant Cell*, 18(5):1310–1326.

Xu, Y.-Z., Santamaria, R. d. l. R., Virdi, K. S., Arrieta-Montiel, M. P., Razvi, F., Li, S., Ren, G., Yu, B., Alexander, D., Guo, L., Feng, X., Dweikat, I. M., Clemente, T. E., and Mackenzie, S. A. (2012). The chloroplast triggers developmental reprogramming when muts homolog1 is suppressed in plants. *Plant Physiology*, 159(2):710–720.

Yang, J., Worley, E., and Udvardi, M. (2014). A nap-aao3 regulatory module promotes chlorophyll degradation via aba biosynthesis in arabidopsis leaves. *The Plant Cell*, pages tpc–114.

Yang, L., Ye, C., Zhao, Y., Cheng, X., Wang, Y., Jiang, Y.-Q., and Yang, B. (2018). An oilseed rape wrky-type transcription factor regulates ros accumulation and leaf senescence in nicotiana benthamiana and arabidopsis through modulating transcription of rbohd and rbohf. *Planta*, 247(6):1323–1338.

Yang, Z. and Ohlrogge, J. B. (2009). Turnover of fatty acids during natural senescence of arabidopsis, brachypodium, and switchgrass and in arabidopsis β-oxidation mutants. *Plant Physiology*, 150(4):1981–1989.

Zeevaart, J. A. D. and Creelman, R. A. (1988). Metabolism and physiology of abscisic acid. *Annual Review of Plant Physiology and Plant Molecular Biology*, 39(1):439–473.

Zhang, J., Jia, W., Yang, J., and Ismail, A. M. (2006). Role of aba in integrating plant responses to drought and salt stresses. *Field Crops Research*, 97(1):111 – 119. Preparing Rice for a Water-Limited Future: from Molecular to Regional Scale.International Rice Research Congress.

Zhang, K. and Gan, S.-S. (2012). An abscisic acid-atnap transcription factor-sag113 protein phosphatase 2c regulatory chain for controlling dehydration in senescing arabidopsis leaves. *Plant Physiology*, 158(2):961–969.

Zhang, K., Xia, X., Zhang, Y., and Gan, S.-S. (2012). An aba-regulated and golgi-localized protein phosphatase controls water loss during leaf senescence in arabidopsis. *The Plant Journal*, 69(4):667–678.

Zhao, H.-F., Qiu, K., Ren, G.-D., Zhu, Y., and Kuai, B.-K. (2010). A pleiotropic

phenotype is associated with altered endogenous hormone balance in the developmentally stunted mutant (dsm1). *Journal of Plant Biology*, 53(1):79–87.

Zimmermann, P., Heinlein, C., Orendi, G., and Zentgraf, U. (2006). Senescence-specific regulation of catalases in arabidopsis thaliana (l.) heynh. *Plant, cell & environment*, 29(6):1049–1060.

Appendix

Determination of the *in vivo* redox potential using roGFP and fluorescence spectra obtained from one-wavelength excitation

S. Wierer[1*], K. Elgass[2], S. Bieker[3], U. Zentgraf[3], A. J. Meixner[1], F. Schleifenbaum[2]

[1]Institute of Physical and Theoretical Chemistry, University of Tuebingen, Auf der Morgenstelle 18, 72076 Tuebingen, Germany.
[2]Center for Plant Molecular Biology, Department of Plant Physiology, University of Tuebingen, Auf der Morgenstelle 1, 72076 Tuebingen, Germany.
[3]Center for Plant Molecular Biology, Department of Genetics, University of Tuebingen, Auf der Morgenstelle 28, 72076 Tuebingen, Germany.

* Post Box 706, University of Konstanz, 78457 Konstanz, Germany.

sebastian.wierer@uni-konstanz.de
kirstin.elgass@uni-tuebingen.de
stefan.bieker@student.uni-tuebingen.de
ulrike.zentgraf@uni-tuebingen.de
alfred.meixner@uni-tuebingen.de
frank.schleifenbaum@uni-tuebingen.de

ABSTRACT

The analysis of molecular processes in living (plant) cells such as signal transduction, DNA replication, carbon metabolism and senescence has been revolutionized by the use of green fluorescent protein (GFP) and its variants as specific cellular markers. Many cell biological processes are accompanied by changes in the intracellular redox potential. To monitor the redox potential, a redox-sensitive mutant of GFP (roGFP) was created, which shows changes in its optical properties in response to changes in the redox state of its surrounding medium.

For a quantitative analysis in living systems, it is essential to know the optical properties of roGFP *in vitro*. Therefore, we applied spectrally resolved fluorescence spectroscopy on purified roGFP exposed to different redox potentials to determine shifts in both the absorption and the emission spectra of roGFP. Based on these *in vitro* findings, we introduce a new approach using one-wavelength excitation to use roGFP for the *in vivo* analysis of cell biological processes. We demonstrate the ability this technique by investigating chloroplast-located Grx1-roGFP2 expressing *Arabidopsis thaliana* cells as example for dynamically moving intracellular compartments. This is not possible with the two-wavelength excitation technique established so far, which hampers a quantitative analysis of highly mobile samples due to the time delay between the two measurements and the consequential displacement of the investigated area

Keywords: roGFP, one-wavelength excitation, redox potential, sensor, *in vivo*, spectroscopy

1. INTRODUCTION

For many years, fluorescent labeling of proteins in living cells was mostly used as a marker light, neglecting the fact that the spectral and temporal properties of emitted fluorescence also reflect the physico-chemical properties of the chromophore´s direct environment. This has changed recently with the creation of *Aequorea victoria* green fluorescent protein (GFP) mutants, which change their optical properties with e.g. the local redox potential [1-6] and can therefore be used as an intracellular sensor for the respective physico-chemical parameter. By recording the optical properties of these sensor proteins, it is therefore possible to gain novel molecular, cell biological and functional information about the investigated fusion protein *in vivo*.

In the year 2004 Hanson et al. substituted surface-exposed residues on the *Aequorea victoria* green fluorescent protein (GFP) [2] with cysteines in appropriate positions to enable the reversible formation of disulfide bonds in dependence of the local redox potential. Thus, he created different redox-sensitive GFP variants (roGFPs) with distinct point mutations (roGFP1 to roGFP6). The roGFP2 construct, which was used in all experiments presented here, was shown to be the most suitable version to measure the redox potential in reducing compartments [6].

RoGFP, exhibits two excitation maxima (at about 400 and 475–490 nm), which can be attributed to an internal equilibrium between the neutral and anionic form of the chromophore, respectively. The same excitation maxima can be observed in wild-type GFP, but in roGFP, the relative amplitudes of these bands strongly depend on the redox-potential of the surrounding medium due to the newly introduced disulfide bond near the roGFP chromophore. Therefore, roGFP can be used as highly-sensitive, non-invasive local probe for the redox-potential *in vitro* and *in vivo*. Independent of the excitation maxima, both chromophoric forms emit in the same spectral range around 510 nm.

Using roGFP as an *in vivo* redox-potential sensor taking advantage of the different excitation maxima of the two chromophore forms .and recording the fluorescence intensity after excitation with two different wavelengths [5] suffers from serious limitations. Besides photobleaching and excitation power effects, potential mobility of the sample is an issue. Using the established two-wavelength excitation, the subsequently recorded images have to be merged to calculate the fluorescence intensity ratio. As soon, as sample movement cannot be excluded, displacement hampers the comparison of the two images and it is difficult if not impossible to obtain reliable results. Therefore a highly desirable aim is the development of a method, which provides identical information about the local redox state using only one-wavelength excitation measurements.

Here we demonstrate that the fluorescence spectra of the neutral form of the roGFP2 chromophore is slightly shifted compared to the anionic form of the roGFP2 chromophore. Therefore, high resolution fluorescence spectroscopy of roGFP2 can be used for the determination of the redox potential *in vitro* and *in vivo* with one-wavelength excitation, negotiating the mentioned limitations of two-wavelength excitation.

2. RESULTS AND DISCUSSION

2.1 Fluorescence Emission Maxima of Oxidized and Reduced roGFP2

It is known from literature, that the oxidized and reduced forms of the roGFP2 chromophore emit fluorescence light in the same spectral region. However, high resolution spectra are still missing. Therefore, we applied spectrally resolved fluorescence microscopy to fully oxidized and reduced roGFP2 solutions. Complete oxidation and reduction was ensured by adding hydrogen peroxide or dithiothreitol (DTT), respectively, in excess to the roGFP2 solutions and subsequent incubation for 30 min.

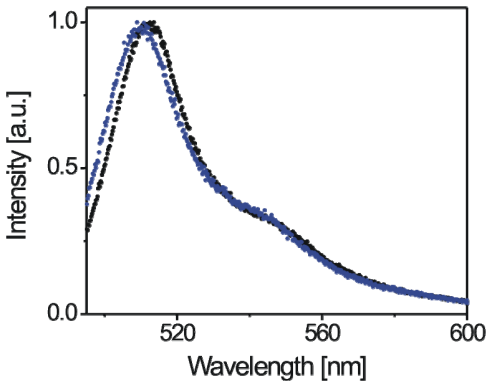

Figure 1: Fluorescence spectra of fully oxidized (blue line) and fully reduced (black line) roGFP2. Both chromophores emit in the same spectral range but the emission maximum of the reduced form is shifted to longer wavelengths by about 7 nm.

Figure 1 shows fluorescence emission spectra recorded for the oxidized (blue line) and the reduced (black line) form of the chromophore. Both chromophores emit in the same spectral range but the emission maximum of the reduced form is shifted to longer wavelengths by about 7 nm from 509 nm (oxidized form) to 516 nm (reduced form).

2.2. Fluorescence spectra of hybrid roGFP2 solutions

Based on this observation, we assumed that it should be possible to determine the relative ratio of oxidized and reduced chromophores of a hybrid roGFP2 solution by calculating the ratio of the emission maxima (EMR) at 509 nm and at 516 nm. To verify this hypothesis, we prepared a roGFP2 redox series by addition of different hydrogen peroxide and DTT concentrations. Afterwards, each of the solutions was characterized by recording a fluorescence spectrum and the fluorescence intensity ratio 509/516 was calculated.

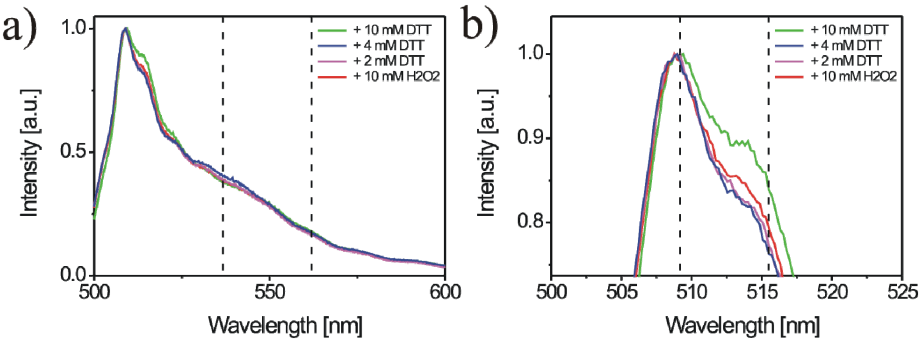

Figure 2: Fluorescence spectra of hybrid roGFP2 solutions, with different ratios of oxidized and reduced chromophores. The higher the amount of reduced chromophores, the higher the fluorescence intensity at 516 nm (right dashed line).

Table 1 lists the calculated ratios *r* for all recorded spectra. The error values have been calculated according to the Gaussian law of error propagation (Equation 1). After addition of hydrogen peroxide, the ratio values do not change, indicating that the roGFP2 is fully oxidized when extracted from E. coli.

roGFP2	509/516 ratio	error
+ 10 mM DTT	1.25	0.0100
+ 8 mM DTT	1.24	0.0099
+ 6 mM DTT	1.22	0.0096
+ 4 mM DTT	1.21	0.0095
+ 2 mM DTT	1.21	0.0095
+ 0 mM DTT	1.15	0.0088
+ 2 mM H_2O_2	1.14	0.0086
+ 4 mM H_2O_2	1.16	0.0089
+ 6 mM H_2O_2	1.13	0.0085
+ 8 mM H_2O_2	1.15	0.0088
+ 10 mM H_2O_2	1.17	0.0090

Table 1: List of calculated 509/516 nm fluorescence intensity ratios for all prepared hybrid roGFP2 solutions. Addition of hydrogen peroxide does not change the ratio indicating roGFP2 is fully oxidized when extracted from E. coli.

2.3 Calibration curve for roGFP2-EMR

For the determination of the absolute redox potential *in vitro* or *in vivo*, a calibration curve of roGFP2-EMR is essential. To obtain a calibration curve from the roGFP2-EMR calculated above, the actual redox potential of each roGFP2 hybrid solution was determined according to Meyer et al. and Schwarzlander et al. by roGFP-FIR using the Nernst equation [2,6] (Figure 3). Plotting the roGFP2-EMR values against the calculated environmental redox potentials reveals a linear behaviour of roGFP2 for changed redox potentials in the relevant redox potential range.

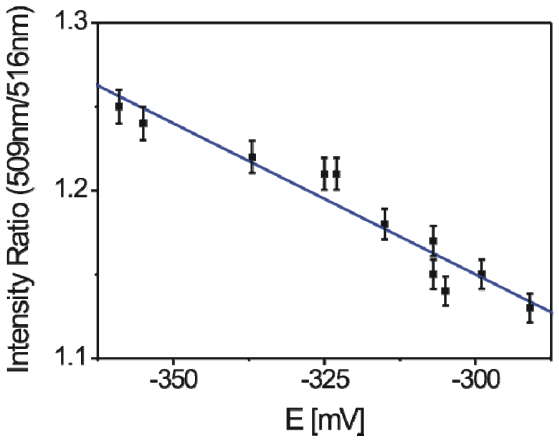

Figure 3: Correlation between the environmental redox potential E and the EMR of roGFP2. A linear relationship between E and the EMR of roGFP2 in the relevant redox potential range is revealed.

2.4 *In vivo* application of roGFP2-EMR

To verify, if the emission maxima ratio of roGFP2 (roGFP2-EMR) can be used for the investigation of moving compartments in living cells, we applied this method to plant chloroplasts. Chloroplasts mainly consist of two photosystems, PSI and PSII, with fluorescence intensity maxima at 730nm (PSI) or 680 nm (PSII), respectively (Figure 4a).

Chloroplasts of higher land plants have a heterogenic morphology of appressed and non-appressed thylakoid membrane domains, which are called the grana and the stroma lamellae. The PSII is enriched in the grana whereas the PSI is enriched in the stroma lamellae [7]. Therefore, the fluorescence intensity ratio PSI/PSII changes in dependence of the position in the chloroplast. PSI/PSII ratios were calculated from the corresponding spectra by dividing the fluorescence intensity maximum of PSI (λ_{emPSI} = 730 nm) by the fluorescence intensity maximum of PSII (λ_{emPSII} = 680 nm) after background correction (Figure 4a). Comparison of the fluorescence intensity ratio of roGFP2 and the photosystems reveals a relationship between both (Figure 4b), indicating that the redox potential in the grana lamellae differs from the redox potential in the stroma lamellae.

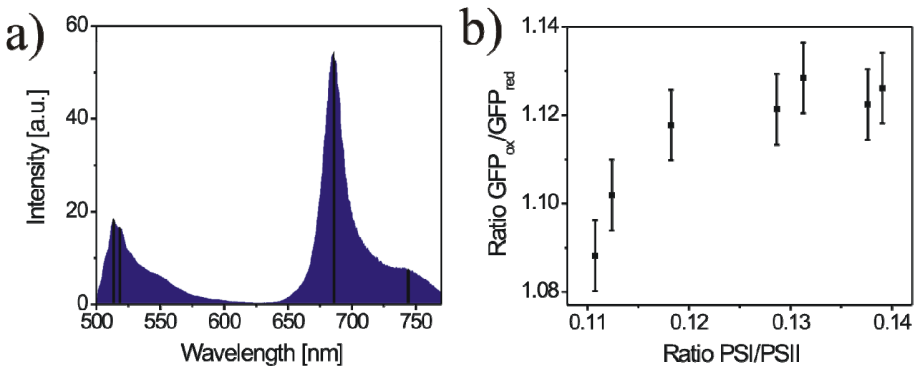

Figure 4: Relationship between the fluorescence intensity ratio of roGFP2 and the fluorescence intensity ratio of the photosystems. The data indicate different redox potential in the grana lamellae and in the stroma lamellae.

3. CONCLUSION

Up to now, the determination of the redox potential using roGFPs has been performed taking advantage of the different excitation maxima of the neutral and the anionic form of the roGFP chromophore and calculating the fluorescence intensity ratio (FIR) after excitation with two different wavelengths [1-5]. However, roGFP-FIR suffers from temporal restrictions and serious limitations inherent in intensity measurements such as photobleaching and excitation power effects.

Here we demonstrate the applicability of high resolution fluorescence spectroscopy for the *in vitro* determination of the environmental redox potential. The emission maximum of oxidized and reduced roGFP2 is shifted by 7 nm from 509 nm to 516 nm. Therefore, fluorescence intensity ratios (509nm/516nm) of high resolution roGFP2 spectra can be used to determine the environmental redox potential.

In contrast to roGFP-FIR, roGFP2-EMR can be performed using one-wavelength excitation, avoiding the limitations of two-wavelength excitation such as temporal restrictions, photobleaching and excitation power effects. This enables the *in vivo* investigation of movable compartments such as chloroplasts in living plant cells.

MATERIALS AND METHODS

Preparation of purified roGFP2 solution for in vitro measurements

The roGFP2 sequence was cloned into the expression vector pET30a (Novagen). A starter culture was grown overnight by inoculation of a single colony of transformed E.coli BL21(DE3). The culture was diluted to a total volume of 1l and grown on an orbital shaker to an OD of approx. 0.5 (37°C, 180 rpm). The culture was subsequently cooled to 18°C and protein expression was induced by addition of 1 mM IPTG. After overnight expression, cells were harvested and the His-tagged protein was purified by laboratory procedures.

Preparation of the roGFP2 redox series

For tuning the oxidation state of roGFP2, identical volumes of hydrogen peroxide or dithiolthreitol (DTT) were added in different concentrations to the same concentration and volumina of roGFP2 solution (4 µM roGFP2 and 0, 2, 4, 6, 8, 10, 20, 30, 40, 50 mM DTT or 4 µM roGFP2 and 2, 4, 6, 8 10 mMH_2O_2). This procedure resulted in a roGFP2 redox series which was used to determine the …calibration curves.

Optical and spectroscopic measurements

All optical measurements were performed using a custom built confocal laser-scanning microscope based on a Zeiss Axiovert 135 TV [8], equipped with a feedback-controlled precision x-, y-, z-scanning stage (P-517.3, Physik Instrumente) allowing for repositioning a certain spot precisely back into the focal area with a nominal accuracy of 2 nm. A spectral integrating avalanche photodiode (PDM series, MicroPhotonDevices (MPD), Italy) was used as a detector for image acquisition. Spectra were obtained using a spectrograph (Princeton Instruments Acton Spectra Pro 300i, 300 lines grating) coupled to a thermo-electric cooled CCD-camera (PIXIS 100, Roper Scientific).

A pulsed laser diode operating at 473 nm (Picoquant LDH-P-C470) and a repetition rate of 20 MHz was used as excitation source. A microscope objective with high numerical aperture (Plan-Neofluar, 100x/1.30 oil, Zeiss) was used to focus the excitation light as well as to collect the fluorescence emission. The setup was equipped with a 500 nm dichroic mirror (FF500-Di01-25x36, Semrock) to block back-scattered excitation light and with a 500 nm bandpass filter (Semrock BrightLine BL500/24) to detect GFP-fluorescence.

REFERENCES

[1] M. Gutscher, A. L. Pauleau, L. Marty, T. Brach, G. H. Wabnitz, Y. Samstag, A. J. Meyer, and T. P. Dick, "Real-Time Imaging of the Intracellular Glutathione Redox Potential", Nature Methods 5**,** 553 (2008).

[2] G. T. Hanson, R. Aggeler, D. Oglesbee, M. Cannon, R. A. Capaldi, R. Y. Tsien, and S. J. Remington, "Investigating Mitochondrial Redox Potential with Redox-Sensitive Green Fluorescent Protein Indicators", Journal of Biological Chemistry 279**,** 13044 (2004).

[3] K. Jiang, C. Schwarzer, E. Lally, S. B. Zhang, S. Ruzin, T. Machen, S. J. Remington, and L. Feldman, "Expression and Characterization of a Redox-Sensing Green Fluorescent Protein (Reduction-Oxidation-Sensitive Green Fluorescent Protein) in Arabidopsis", Plant Physiology 141**,** 397 (2006).

[4] A. J. Meyer and T. Brach, "Dynamic Redox Measurements with Redox-Sensitive Gfp in Plants by Confocal Laser Scanning Microscopy", Methods in Molecular Biology**,** 93 (2009).

[5] A. J. Meyer, T. Brach, L. Marty, S. Kreye, N. Rouhier, J. P. Jacquot, and R. Hell, "Redox-Sensitive Gfp in Arabidopsis Thaliana Is a Quantitative Biosensor for the Redox Potential of the Cellular Glutathione Redox Buffer", Plant Journal 52**,** 973 (2007).

[6] M. Schwarzlander, M. D. Fricker, C. Muller, L. Marty, T. Brach, J. Novak, L. J. Sweetlove, R. Hell, and A. J. Meyer, "Confocal Imaging of Glutathione Redox Potential in Living Plant Cells", Journal of Microscopy-Oxford 231**,** 299 (2008).
[7] J. M. Anderson, W. S. Chow, and D. J. Goodchild, "Thylakoid Membrane Organization in Sun Shade Acclimation", Australian Journal of Plant Physiology 15**,** 11 (1988).
[8] K. Elgass, K. Caesar, F. Schleifenbaum, Y.-D. Stierhof, A. J. Meixner, and K. Harter, "Novel Application of Fluorescence Lifetime and Fluorescence Microscopy Enables Quantitative Access to Subcellular Dynamics in Plant Cells", PLoS ONE 4**,** Article No.: e5716 (2009).

JIPB Journal of Integrative Plant Biology

Journal of Integrative Plant Biology 2012, **54** (8): 540–554

Research Article

Senescence-specific Alteration of Hydrogen Peroxide Levels in *Arabidopsis thaliana* and Oilseed Rape Spring Variety *Brassica napus* L. cv. Mozart

Stefan Bieker[1], Lena Riester[1], Mark Stahl[1], Jürgen Franzaring[2] and Ulrike Zentgraf[1*]

[1]ZMBP (Center for Plant Molecular Biology), University of Tübingen, Auf der Morgenstelle 28, 72076 Tübingen, Germany

[2]Institute for Landscape and Plant Ecology, Ökologiezentrum 2, August-von-Hartmann-Str. 3, 70599 Stuttgart, Germany

*Corresponding author

Tel: +49 7071 2978833; Fax: +49 7071 295042; E-mail: ulrike.zentgraf@uni-tuebingen.de

Articles can be viewed online without a subscription.

Available online on 16 July 2012 at www.jipb.net and www.wileyonlinelibrary.com/journal/jipb

doi: 10.1111/j.1744-7909.2012.01147.x

Abstract

In order to analyze the signaling function of hydrogen peroxide (H_2O_2) production in senescence in more detail, we manipulated intracellular H_2O_2 levels in *Arabidopsis thaliala* (L.) Heynh by using the hydrogen-peroxide-sensitive part of the *Escherichia coli* transcription regulator OxyR, which was directed to the cytoplasm as well as into the peroxisomes. H_2O_2 levels were lowered and senescence was delayed in both transgenic lines, but OxyR was found to be more effective in the cytoplasm. To transfer this knowledge to crop plants, we analyzed oilseed rape plants *Brassica napus* L. cv. Mozart for H_2O_2 and its scavenging enzymes catalase (CAT) and ascorbate peroxidase (APX) during leaf and plant development. H_2O_2 levels were found to increase during bolting and flowering time, but no increase could be observed in the very late stages of senescence. With increasing H_2O_2 levels, CAT and APX activities declined, so it is likely that similar mechanisms are used in oilseed rape and *Arabidopsis* to control H_2O_2 levels. Under elevated CO_2 conditions, oilseed rape senescence was accelerated and coincided with an earlier increase in H_2O_2 levels, indicating that H_2O_2 may be one of the signals to inducing senescence in a broader range of *Brassicaceae*.

Keywords: *Arabidopsis thaliana*; *Brassica napus*; *E. coli* Oxy-RD; intracellular hydrogen peroxide; senescence phenotype; catalase; ascorbate Peroxidase; elevated CO_2.

Bieker S, Riester L, Stahl M, Franzaring J, Zentgraf U (2012) Senescence-specific alteration of hydrogen peroxide levels in *Arabidopsis thaliana* and oilseed rape spring variety *Brassica napus* L. cv. Mozart. *J. Integr. Plant Biol.* **54**(8), 540–554.

Introduction

As the worldwide demand for food- and fuel crops steadily rises, the improvement of productivity has been of increasing focus, not only in regards to quantity of yield, but also to the quality of the harvested products. Leaf senescence is the last stage of the the foliar lifecycle, and predominantly serves as a mechanism for annual plants to recycle nutrients out of non-reproductive tissues into developing fruits and seeds. It is a highly complex and dynamic process modulated by nutrition status and various endogenous signals, as well as by biotic and abiotic stress conditions. All these triggers have to be interconnected to a certain degree in a complicated signaling network, and integration of these signals determines onset, progression, or even reversion of senescence. When the restructuring and remobilization of nutrients are terminated, senescing leaves eventually die and are shed by the plant.

In the crop plant oilseed rape, the reutilization of nutrients, especially nitrogen compounds, is inefficient in comparison to other crops. Most of the oilseed rape leaves are shed before or during early flowering, and thus do not contribute to remobilization but instead amount to a loss of up to 15% of the plant's total N reserves (Rossato et al. 2001). Phloem loading of amino acids is not limiting for nitrogen remobilization from senescing leaves in oilseed rape; therefore, other factors have to be considered that may limit nitrogen remobilization

and N efficiency. One strategy to improve the nitrogen use efficiency in oilseed rape would be to delay senescence until seed filling is completed (Tilsner et al. 2005). However, delayed senescence in wheat has been shown to correlate with low protein content (Uauy et al. 2006), whereas drought stress appears to enhance senescence and increase carbon remobilization and protection of stem tissue against oxidative stress (Bazargani et al. 2011). Even though high N availability and high CO_2 prolonged flowering time of oilseed rape plants, they did not lead to the production of more ripe pods, but instead more likely prevented apical switch off, thus leading to a strong branching out (Franzaring et al. 2011). Furthermore, high CO_2 caused a decline in seed oil content, indicating that nutrient remobilization appears to be very complex during senescence.

Despite the importance of senescence, our knowledge of the regulatory mechanisms of this process is still limited. Senescence is triggered by exogenous and endogenous parameters. The most important endogenous factors are the age of the leaves and the age or developmental stage of the plant. However, how these two parameters are sensed and translated into molecular signals is still unclear. The photosynthetic activity of leaves of annual plants decreases continuously after full expansion (Batt and Woolhause 1975; Hensel et al. 1993). A decline in photosynthetic activity under a certain threshold may act as a senescence-inducing signal (Matile et al. 1992; Smart 1994), but chlorophyll a/b ratio also appears to be important (Sakuraba et al. 2012). However, autumn senescence in free-growing aspen (*Populus tremula*) is exclusively initiated by the photoperiod (Keskitalo et al. 2005). Sugar accumulation as well as sugar starvation are believed to be signals to induce senescence; however, changes in the sugar to nitrogen content during the sink/source transition of leaves also appear to play a role in the induction of leaf senescence (Masclaux et al. 2000; van Doorn 2004; Pourtau et al. 2004; Wingler et al. 2004, 2009). Again, it remains unclear how these parameters are sensed and translated into molecular signals. Aside from photoperiod, sugars, and nitrogen, senescence is triggered by the interplay of many plant hormones acting at specific concentrations in synergistic or antagonistic ways and in concert with other signals like calcium and especially oxygen free radicals (ROS). Therefore, the complex signaling network that triggers senescence is far from being understood.

ROS play an important role during leaf senescence in two different aspects: signaling and molecule degradation. In contrast to calcium signaling, which is executed by storage and release of Ca^{2+}, ROS signaling is controlled by production and scavenging (Mittler et al. 2004). Thus, plants have developed a fine-tuned network of enzymatic and low-molecular-weight antioxidative components which act in different cellular compartments. Additionally, different plant species have developed diverse strategies to balance their redox potential and regulate their ROS status. In *Arabidopsis*, a network of at least 152 genes is involved in managing the ROS levels. This network is highly dynamic and redundant, and includes ROS-scavenging and ROS-producing proteins (Mittler et al. 2004).

We have already shown that *Arabidopsis* catalases (CAT) exhibit senescence-specific regulation. CAT2 activity decreased at a very early stage during the time of bolting. The increase in H_2O_2 levels is enforced by a decrease in ascorbate peroxidase 1 (APX1) activity at the same time point (Ye et al. 2000; Zimmermann et al. 2006). However, APX1 is not down-regulated at the transcriptional level during the time of bolting (Panchuk et al. 2005), but rather H_2O_2 itself most likely leads to the inactivation of APX1 (Miyake and Asada 1996; Zimmermann et al. 2006). Furthermore, we have shown that this inactivation is dependent on the developmental stage of the plants with the highest sensitivity during bolting time, suggesting a feedback amplification loop. This coordinated regulation of the hydrogen peroxide scavenging enzymes on the transcriptional and posttranscriptional level creates a distinct increase in H_2O_2 at the time point when the plants start to bolt and flower, and a coordinated senescence process of all rosette leaves should be induced (Zimmermann et al. 2006). This distinct increase in H_2O_2 most likely induces the expression of transcription factors and senescence-associated genes (SAGs). NAC and WRKY transcription factors constitute the two largest groups of transcription factors of the senescence transcriptome (Guo et al. 2004), and certain members of these two transcription factor families have been shown to play central roles in regulating senescence in wheat and *Arabidopsis* (Miao et al. 2004; Guo and Gan 2006; Uauy et al. 2006; Balazadeh et al. 2010, 2011; Breeze et al. 2011; Yang et al. 2011). Besides other triggers, the expression of these senescence-associated WRKY and NAC factors is controlled by H_2O_2 (Miao et al. 2007, 2008; Miao and Zentgraf 2010; Balazadeh et al. 2010, 2011).

A rapid turnover of the catalase protein necessitates continuous transcription and translation of mRNA (Feierabend et al. 1992). Using the yeast-one-hybrid system, G-box binding factor 1 (GBF1) has been identified as a negative regulator of *CAT2* expression (Smykowski et al. 2010). In *GBF1* knock-out (GBF1-KO) plants, *CAT2* down-regulation is abolished, the H_2O_2 peak disappears, and plants show delayed onset of leaf senescence, clearly indicating that H_2O_2 is used as a signal to induce the onset of senescence. Since GBF1 also controls other important senescence-down-regulated genes like *RUBISCO* (Smykowski et al. 2010), we wanted to isolate the effect of H_2O_2 regulation from effects related to other GBF1 target genes. Therefore, we manipulated H_2O_2 levels by overexpression of the hydrogen-peroxide-sensitive part of the *E. coli* transcription regulator OxyR to confirm that the loss of the H_2O_2 signal is leading to the delay of senescence. Furthermore, we investigated senescence processes in *Brassica napus* L. cv. Mozart, focusing on the role of H_2O_2 and its scavenging enzymes during leaf and plant development.

Results

To determine that the delayed senescence phenotype of the *gbf1* mutants is mainly due to *CAT2* down-regulation and to the lack of the hydrogen peroxide signal instead of due to the regulatory effects of GBF1 on other important target genes like *RUBISCO*, we aimed to alter the H_2O_2 content using a transgene which confers no alternative function in plants. To this end, we used a construct which combines the regulatory domain of the *E. coli* OxyR transcription factor for sensing H_2O_2 in bacteria with a cpYFP (Belousov et al. 2006). The *E. coli* OxyR transcription factor contains two domains: an H_2O_2-sensitive regulatory domain (amino acids 80–310, OxyR-RD), and a DNA-binding domain (amino acids 1–79). In the presence of H_2O_2, the reduced form of OxyR-RD is oxidized. The key residues for oxidation of OxyR-RD are Cys199 and Cys208. H_2O_2 converts Cys199 to a sulfenic acid derivative and forms a disulfide bond with Cys208, leading to a dramatic conformational change which allows DNA binding (Zheng et al. 1998). *In vitro* experiments conducted by Aslund et al. (1999) revealed that the hydrogen peroxide that they added to the reaction appears to be consumed because OxyR returns to its reduced form in the time course experiment. Thus, they proposed that OxyR is acting as a peroxidase in these *in vitro* reactions. This proposition is supported by the finding that significant NADPH consumption was observed (Aslund et al. 1999). Here, we used plants overexpressing OxyR-RD-cpYFP in the cytoplasm and in the peroxisomes where the CAT2 protein is predominately located. These lines were constructed by Costa and coworkers, and the YFP localization in the two different compartments was confirmed by confocal microscopy (Costa et al. 2010). Two cytoplasmic and two peroxisomal overexpressing lines with different levels of transgene expression were used for phenotypic analyses. Senescence was delayed in all lines expressing OxyR-RD-YFP. Interestingly, the delay was dependent on the compartment to which the OxyR-RD was directed, since the cytoplasmic lines (1 and 8) showed a more severe phenotype than the peroxisomal lines (2 and 9) even though OxyR-RD-YFP expression was higher in the peroxisomal lines (**Figure 1**). In order to determine if the senescence delay was due to altered H_2O_2 concentrations, we analyzed H_2O_2 concentrations using the fluorescent dye DCFDA for the peroxisomal line 2 (2/per) and the cytoplasmic line 8 (8/cyt), with both lines expressing OxyR-RD-YFP to approximately the same extent (**Figure 1**). The H_2O_2 peak which is observed in wildtype plants during bolting and the onset of flowering is diminished in both lines in young as well as in middle-aged leaves (**Figure 2**). However, the decrease was more pronounced in the 8/cyt line. This is in accordance with a more pronounced delay of chlorophyll loss and the overall senescence phenotype which is observed in 8/cyt. This clearly indicates that cytoplasmic H_2O_2 appears to be more effective in senescence signaling than peroxisomal H_2O_2.

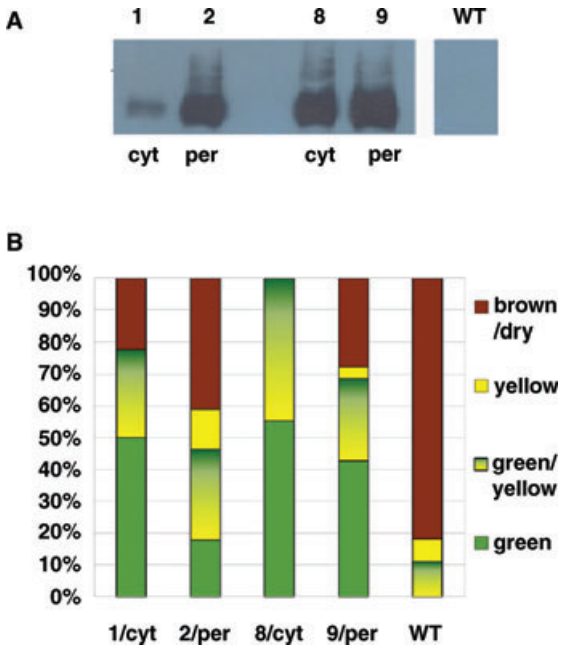

Figure 1. Analyses of transgenic *Arabidopsis* lines overexpressing cytoplasmic (cyt) or peroxisomal (per) OxyR-RD-cpYFP.

(A) Western blot analyses of protein extracts of two cytoplasmic (1/cyt, 8/cyt) and two peroxisomal (2/per, 9/per) expression lines immuno-detected with an anti-GFP antibody.
(B) Phenotypic analyses of the 4 lines by sorting the leaves into 4 categories (green/green-yellow/yellow/brown-dry).
Data represent mean ±*STDV* of nine replicates.

In order to characterize the role of H_2O_2 as a signaling molecule during early senescence in crop plants, we investigated the H_2O_2 levels in oilseed rape plants for individual leaves of one plant and for the same leaf position during plant development in the spring variety cv. Mozart grown under greenhouse conditions. H_2O_2 levels of young oilseed rape leaves were higher than H_2O_2 levels in old leaves independent of the age of the plant (**Figure 3A**). Overall levels increased with plant age when plants started to bolt and flower as has already been shown in *Arabidopsis* (Miao et al. 2004; Zimmermann et al. 2006), clearly indicating that the increase in H_2O_2 appears to be a systemic signal which is dependent only on plant age and not on leaf age (**Figure 3B**). However, in very old *Arabidopsis* plants, H_2O_2 increased to very high levels (Miao et al. 2004; Zimmermann et al. 2006), a phenomenon which was not observed in oilseed rape (**Figure 3C**), indicating that during bolting and flowering time H_2O_2 appears to be used as a signaling molecule in oilseed rape. H_2O_2 was not observed to

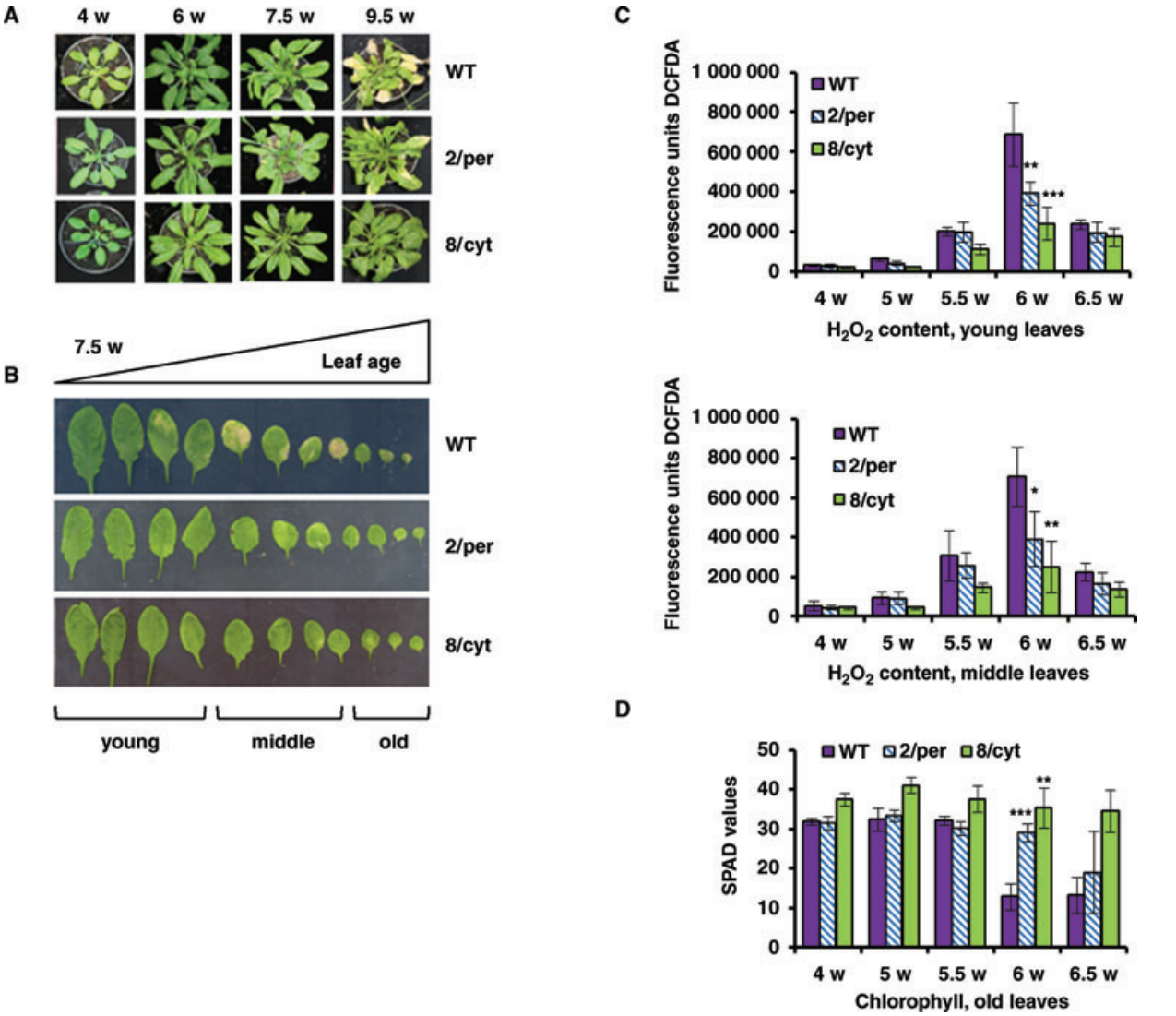

Figure 2. Phenotype, chlorophyll content and hydrogen peroxide levels of the 2/per and 8/cyt OxyR-RD-cpYFP overexpressing lines.

(A) Representative examples of the phenotypes of the whole rosettes of plants of different ages indicated in weeks (w).
(B) Rosette leaves of 7.5 week-old plants sorted according to their ages.
(C) Hydrogen peroxide levels were analyzed using DCFDA fluorescence of grouped rosettes leaves (young/middle).
(D) SPAD values representing chlorophyll contents of grouped rosette leaves (old).
Data represent mean ± *STDV* of at least three replicates. *T*-test analyses were performed, the level of significance is indicated by the asterisks * $P < 0.05$; ** $P < 0.01$ and *** $P < 0.005$ compared to WT values. cyt, cytoplasmic; per, peroxisomal; WT, wild type.

play a role in molecule degradation in late stages of senescence in oilseed rape plants.

The increase in H_2O_2 during bolting time in *Arabidopsis* is predominantly regulated by interplay of CAT2 and APX1 activity regulation (Zimmermann et al. 2006). Although CAT2 is down-regulated on the transcriptional level by the transcription factor GBF1 (Smykowski et al. 2010), APX1 down-regulation appears to be a secondary effect and is achieved on the post transcriptional level (Ye et al. 2000; Panchuk et al. 2005; Zimmermann et al. 2006). A matrix of CAT and APX activities of oilseed rape leaves revealed that CAT activity also declined during bolting and the onset of flowering (**Figure 4A**). The CAT activity pattern observed in oilseed rape leaves was very similar to that observed in *Arabidopsis* leaves, and by employing 3-aminotriazole (3-AT) treatment, the different protein bands in the gels stained for CAT activity could be clearly assigned

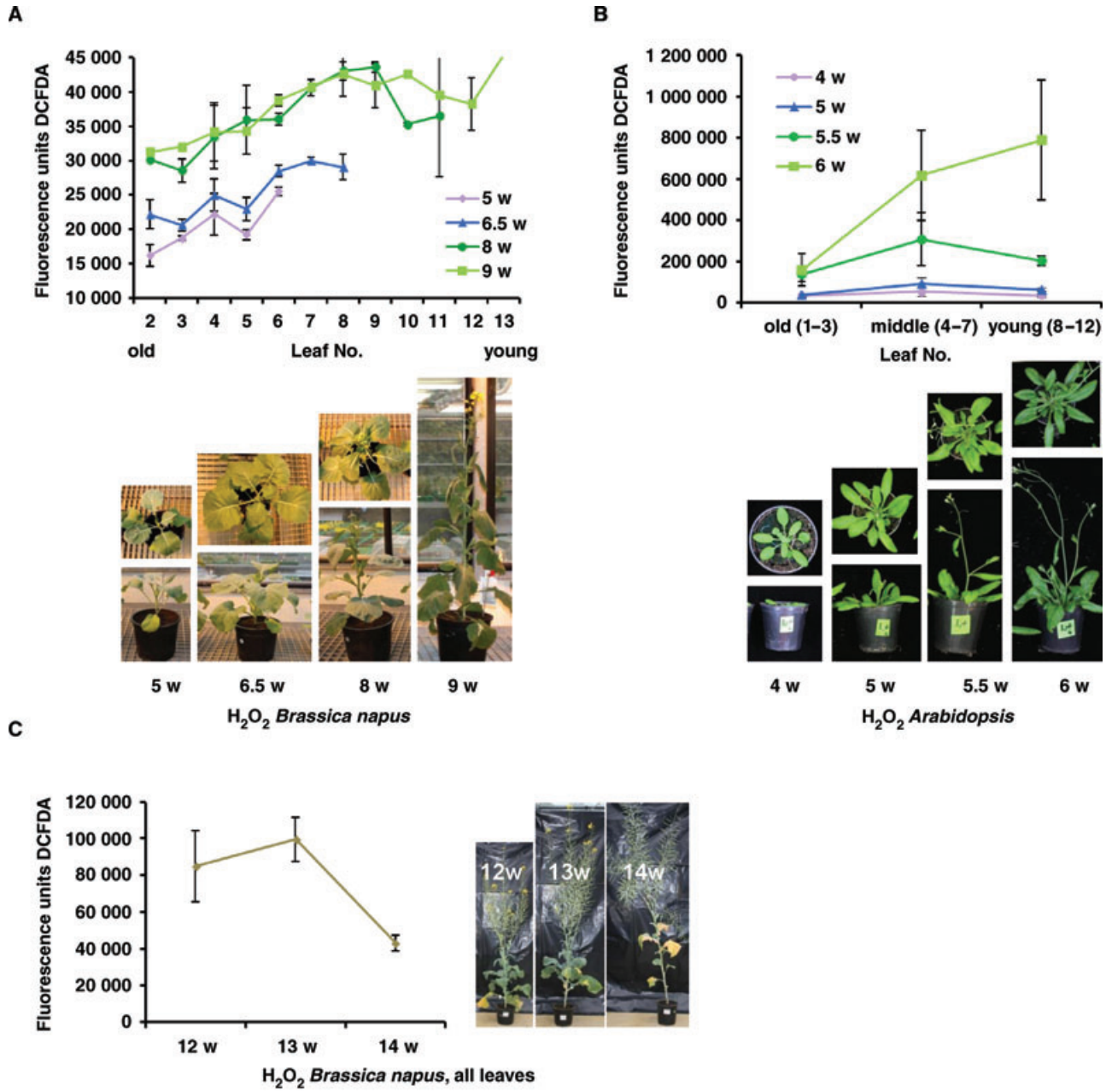

Figure 3. Hydrogen peroxide profiles of oilseed rape *Brassica napus* and *Arabdiopsis* plants.

Hydrogen peroxide levels were analyzed using DCFDA fluorescence of **(A)** individual leaves of one oilseed rape plant.
(B) Grouped *Arabidopsis* rosettes leaves (young/middle/old).
(C) All leaves of very old oilseed rape plants.
Age of the plants is indicated in weeks (w). Data represent mean ± *STDV* of at least three replicates. cyt, cytoplasmic; per, peroxisomal.

to CAT2 and CAT3 isoforms (**Figure 4B**; Orendi et al. 2001). However, the inhibition of APX during bolting time is less pronounced than in *Arabidopsis* plants (Ye et al. 2000; Zimmermann et al. 2006) and is only seen in younger leaves (Nos. 10 and 12). Furthermore, no clear relation to different APX isoforms could be drawn. Therefore, only the overall activity of APX was measured in the following experiments.

Developmental H_2O_2 profiles were recorded in more detail at three different leaf positions (leaf Nos. 5, 8, 12) and were accompanied by analyses of chlorophyll content, ascorbate and

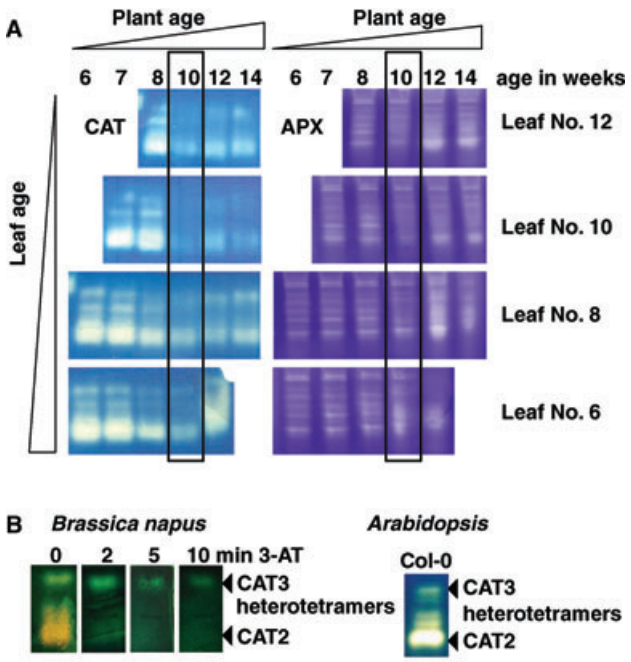

Figure 4. Characterization of catalase and ascorbate peroxdase activities.

(A) CAT and APX activity profiles of different oilseed rape leaves of one plant and leaves of the same position of plants with different ages.

Black boxes highlight 10-week old plants were CAT activity is reduced in all leaves whereas APX acitivity is only slightly diminished in leaf Nos. 10 and 12.

(B) Identification of the different catalase isoforms using 3-aminotriazole (3-AT), a very potent inhibitor for CAT2 being less efficient for CAT3.

Incubation time in 3-AT solution prior to activity staining is indicated above the lanes.

glutathione pools, CAT and APX activities, and total carbon (C) and nitrogen (N) contents (**Figure 5**). In this experiment, H_2O_2 increased and CAT and APX activities decreased again during bolting and the onset of flowering (**Figure 5D, E**). This was very similar for all three leaf positions; therefore, we exemplified the data gathered from leaf No. 8. With increasing plant age, the total glutathione pool decreased, with GSSG levels decreasing more dramatically at the beginning of development (**Figure 5B**). The total ascorbate pool also decreased with plant age, but no obvious difference between DHAsc and Asc was observed. Remarkably, glutathione as well as ascorbate pools slightly increased again after H_2O_2 had reached its maximum level in 9-week-old plants (**Figure 5C**), which might be a counter-regulation for the increasing H_2O_2 levels.

Furthermore, total C and N contents and the C/N ratio were determined as additional senescence parameters. C and N contents continually dropped during progression of development and senescence. During senescence, N content decreased more dramatically leading to an increase in the C/N ratio (**Figure 5F**), which has been reported to be a senescence signal (Wingler et al. 2009). However, these changes can be observed only in later stages of senescence in 13-week-old plants when 40% of the chlorophyll has already been lost (**Figure 5G**). Interestingly, the C/N ratio dropped again in 14-week-old plants.

Gene expression analyses of SAGs and SDGs using material derived from leaf No. 8 revealed that with the maximum of H_2O_2 expression of early SDGs like *CAB, RUBISCO* and *CAT2* (**Figure 6B**) started to decline while early SAGs like *SAG13* and *CAT3* were up-regulated (**Figure 6A**). In contrast, expression of the late senescence marker *SAG12* and of *glutamate synthase (GLS)* was still low when chlorophyll content had not yet started to decrease (**Figures 5G**, **6A**). The expression profile of the transcription factor *WRKY53,* which plays a central role in early senescence regulation in *Arabidopsis*, followed the H_2O_2 profile (**Figure 6C**). Taken together, hydrogen peroxide levels in oilseed rape appear to be regulated in a very similar way as observed in *Arabidopsis*, and might also be used as a signal in senescence regulation.

Since oilseed rape is an important crop plant, developmental senescence of oilseed rape was also analyzed in field-near conditions and under three different N (N min, N opt, N plus) and two different CO_2 (380 ppm and 550 ppm) regimens in fully-programmed growth chambers (Franzaring et al. 2011, 2012). Plants were grown under conditions simulating the seasonal increments of the day length and temperature of South-Western Germany. Here, we focused on H_2O_2 levels and chlorophyll content as determined by SPAD readings. In contrast to our greenhouse conditions, plants developed fewer leaves before flowering; therefore, leaf No. 5 was used for H_2O_2 measurements in this case (**Figure 7**). In leaf No. 5, H_2O_2 started to increase with bolting and flowering and reached its maximum level when full flowering was observed. The increase was more prominent in N plus and N min conditions compared to an optimal N supply. As a phenotypic indicator for senescence, chlorophyll content started to decrease when H_2O_2 reached its maximum under all three N conditions. In a high CO_2 atmosphere, chlorophyll started to decline one week earlier under low and optimal N conditions, and H_2O_2 also reached its peak one week earlier, indicating that under field-near conditions H_2O_2 is most likely used as a signal for the onset of senescence (**Figure 7**).

Discussion

Many different agriculturally-important traits are affected by plant senescence, so understanding and modulating

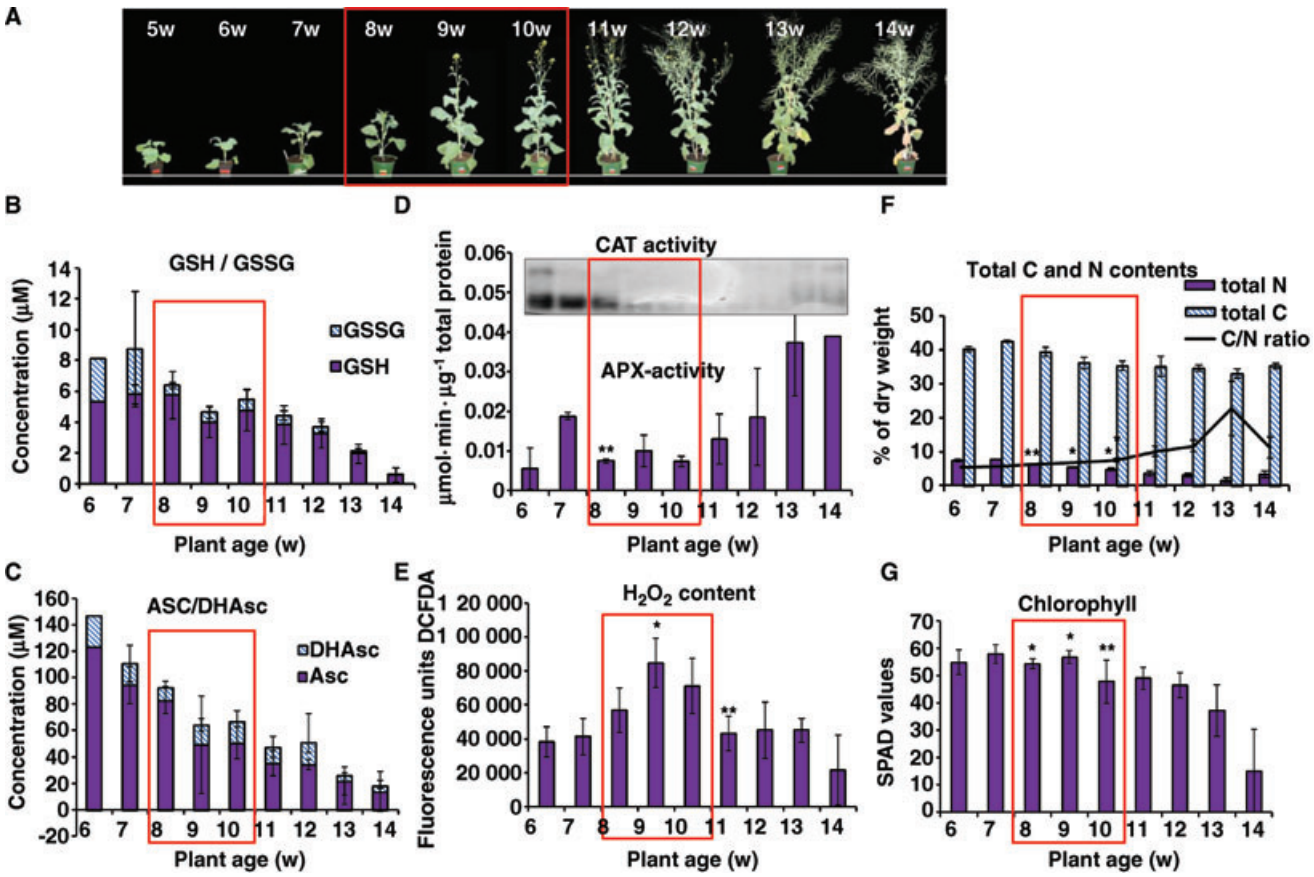

Figure 5. Phenotype, H_2O_2 content, CAT activity profiles, total APX activity, chlorophyll content, ascorbate and glutathione pools and total C and N contents of oilseed rape plants over development.

(A) Phenotypic appearance of oilseed rape plants of different ages.
(B) Reduced (GSH) and oxidized form (GSSG) of glutathione of leaf No. 8.
(C) Dehydroascorbate (DHAsc) and ascorbate (ASC) contents of leaf No. 8.
(D) CAT and APX activities of leaf No. 8.
(E) Hydrogen peroxide levels were analyzed using DCFDA fluorescence of leaf No. 8.
(F) Total C, total N and C/N ratio of leaf No. 8.
(G) SPAD values representing chlorophyll contents of leaf No. 8.
Age of the plants is indicated in weeks (w). Data represent mean $\pm STDV$ of at least three replicates. Comparison of means and the determination of statistically significant differences rest on T-tests with * $P < 0.05$; ** $P < 0.01$ and *** $P < 0.005$. Tests were made pair wise (7 w–8 w, 8 w–9 w, 9 w–10 w, 10 w–11 w).

senescence processes might help solve mounting problems such as drought stress that are due to global climatic changes. ROS appear to play an important role during senescence, since many senescence mutants are also linked to antioxidative capacity. The delayed leaf senescence mutants *ore1*, *ore3*, and *ore9*, exhibit increased tolerance to various types of oxidative stress (Woo et al. 2004). The *Arabidopsis crp5*/*old1* mutants exhibit early senescence through deregulation of the cellular redox balance, since transcriptome data suggest that presymptomatic *cpr5*/*old1* plants are in a state of high cellular oxidative stress (Jing et al. 2008). It is speculated that CPR5 behaves as a shuttling inner nuclear membrane-bound transcription cofactor that possibly interacts with multiple partners to induce pleiotropic effects (Perazza et al. 2011). Furthermore, *old5* mutants displaying a higher respiration rate also show an increased expression of oxidative stress markers (Schippers et al. 2008). Moreover, the *vtc1* mutant, being deficient in ascorbic acid, exhibits early senescence (Barth et al. 2004). Kurepa et al. (1998) also showed a strong correlation between longevity and resistance to oxidative stress.

Obviously, plants have developed a very fine-tuned network of enzymatic and low molecular weight antioxidative

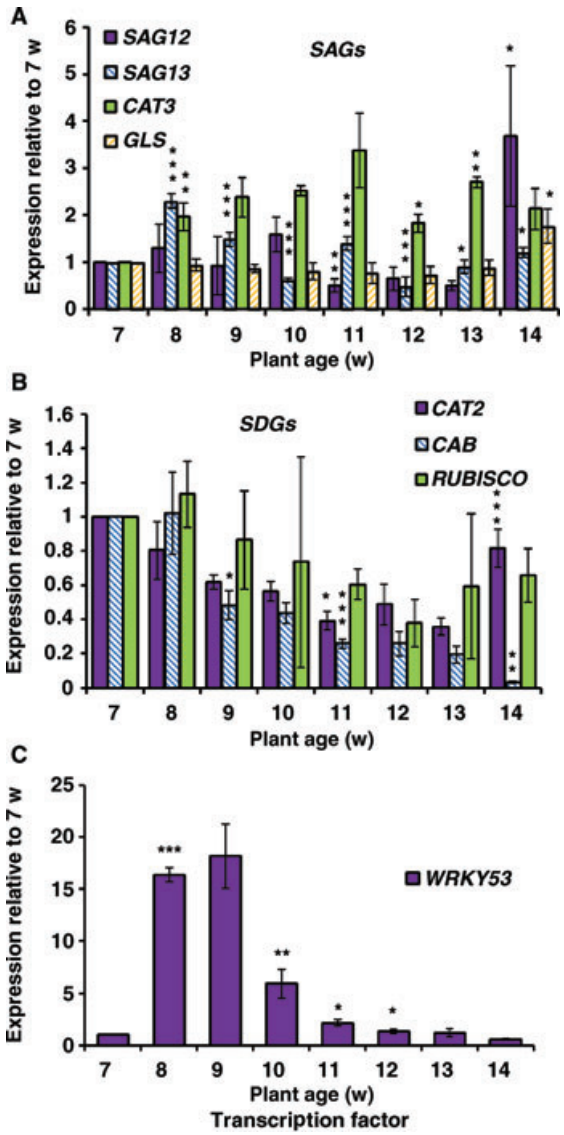

Figure 6. SDG and SAG expression.

qRT-PCR analyses of different genes for different developmental stages of oilseed rape plants.

(A) Senescence-associated genes (SAGs) *catalase3* (*CAT3*), *SAG12, SAG13*, *glutamine synthase* (*GLS*).

(B) Senescence down-regulated genes (SDGs) *catalase2* (*CAT2*), small subunit of ribulose-1,5-bisphophate decarboxylase (*RUBISCO*), *chlorophyll a,b-binding protein (CAB)*.

(C) Senescence associated transcription factor *WRKY53.*

The *ACTIN2* gene expression was used for normalization. Expression values are indicated relative to the values in 7-week-old plants, respectively. Data represent mean ± *STDV* of three replicates. Comparison of means and the determination of statistically significant differences rest on *T*-tests with * $P < 0.05$; ** $P < 0.01$ and *** $P < 0.005$. Tests were made pair wise (7 w–8 w, 8 w–9 w, 9 w–10 w, 10 w–11 w, 11 w–12 w, 12 w–13 w, 13 w–14 w)

components in different cell compartments, and different plant taxa have developed different strategies to balance their redox potential and regulate their ROS status. The network managing the ROS balance is highly dynamic and redundant, and includes ROS-scavenging and ROS-producing proteins.

More or less all cellular compartments produce ROS, but they also have their own scavenging systems. However, the types of ROS and the amounts produced can vary between those compartments in which H_2O_2 is able to pass through membranes and can be released from different compartments. Mitochondria, chloroplasts and peroxisomes carry out important functions associated with the senescence process; however, it is believed that chloroplasts play a principal role in the regulation of the leaf senescence process (Zapata et al. 2005; Martínez et al. 2008) and are the main target of age-associated oxidative stress in plants (Munné-Bosch and Alegre 2002). However, peroxisomes and ROS generated in these organelles were shown to play a central role in natural and dark-induced senescence in pea plants (del Río et al. 1998), and it has been discussed that peroxisomes could act as subcellular sensors of plant stress and senescence by releasing NO, superoxide, and H_2O_2 as signaling molecules into the cytosol, thereby triggering the expression of specific genes (Corpas et al. 2001, 2004; del Rio et al. 2006). The down-regulation of *CAT2* expression by the transcription factor *GBF1* induces the onset of leaf senescence (Smykowski et al. 2010), and assigns a regulatory role to peroxisomal H_2O_2.

By using *Arabidopsis* plants overexpressing the fusion protein *E. coli* OxyR-RD-YFP in peroxisomes and the cytoplasm, we intended to alter H_2O_2 levels in these two compartments independent of other cellular functions to evaluate the specific impact of these H_2O_2 molecules on leaf senescence. Our results show that altered cytoplasmic H_2O_2 levels appear to have a higher impact on senescence than altered H_2O_2 levels in peroxisomes (**Figure 1**), because the delay of senescence was more pronounced in the cytoplasmic lines even though expression of the transgene was higher in peroxisomes. H_2O_2 levels measured with a canonical technique were lower in transgenic lines and correlated with the decrease in chlorophyll and the severity of the phenotype (**Figure 2**). Since senescence is predominantly regulated on transcriptional level, the cytoplasmic compartment might have a direct influence on redox regulation of transcription factors like *WRKY53*. Moreover, cytoplasmic H_2O_2 can also directly activate a specific *Arabidopsis* MAP triple kinase, ANP1, which initiates a phosphorylation cascade involving two stress MAPKs, AtMPK3 and AtMPK6 (Kovtun et al. 2000). Expression of the MAP triple kinase1 (*MEKK1*) of *Arabidopsis* can also be induced by H_2O_2 and shows its expression maximum during onset of leaf senescence (Miao et al. 2007). Whether H_2O_2 induced expression of SAGs is transduced by MAPK signaling or directly by redox-sensitive transcription factors has yet to be elucidated. However, it is

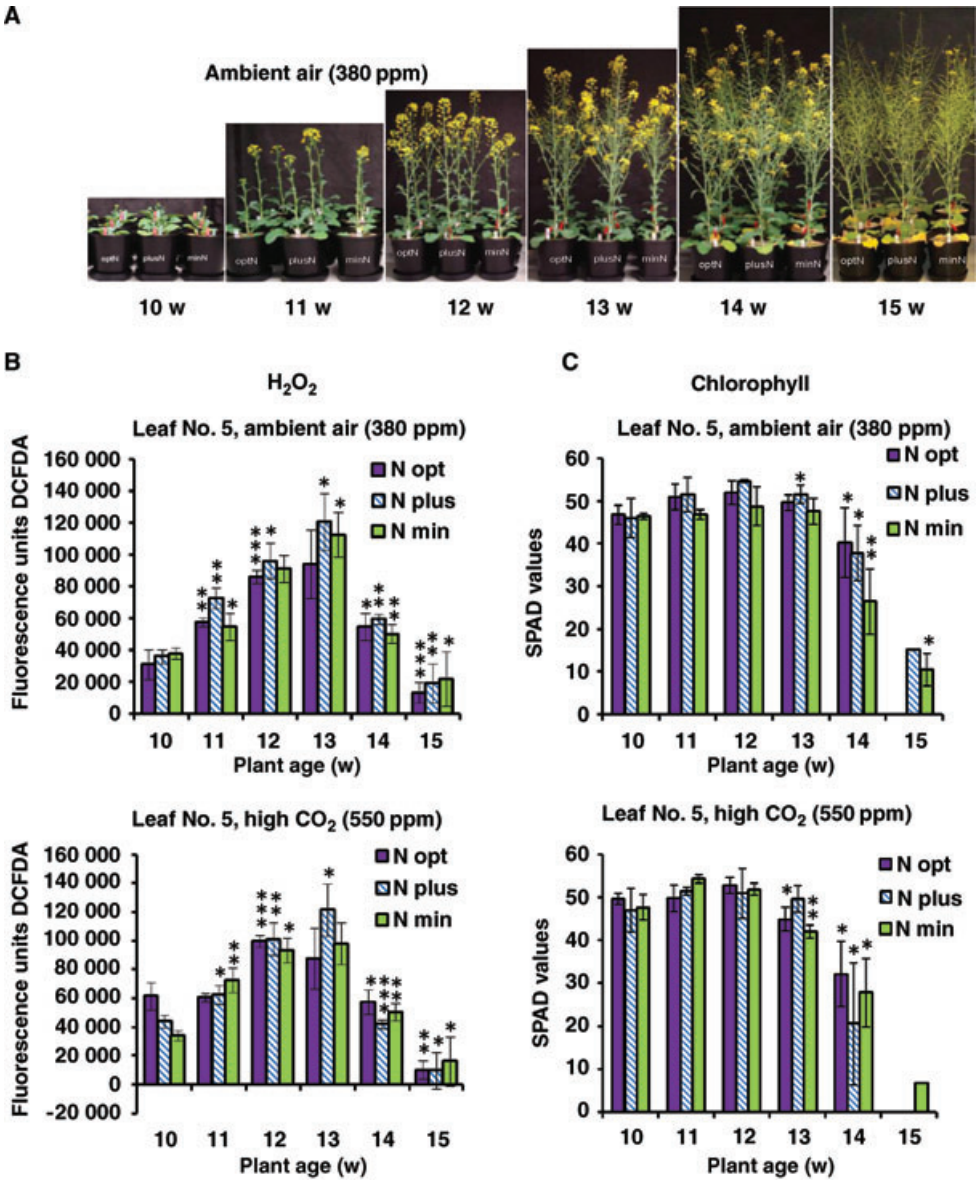

Figure 7. Different nitrogen and CO_2 regimes under field-near conditions.

Plants were grown in two different atmospheres (380 ppm and 550 ppm CO_2) and three levels of N fertilization representing 75 (min), 150 (opt) and 225 (plus) kg ha^{-1} were applied (Franzaring et al. 2011).

(A) Phenotypic appearance of oilseed rape plants of different ages grown under field-near in ambient air (week 10 to 15 after sowing).

(B) Hydrogen peroxide levels were analyzed using DCFDA fluorescence of leaf No. 5 in ambient air (top) and high CO_2 (bottom).

(C) SPAD values representing chlorophyll contents of leaf No. 5 in ambient air (top) and high CO_2 (bottom).

Age of the plants is indicated in weeks (w). Data represent mean $\pm$ *STDV* of three replicates. Comparison of means and the determination of statistically significant differences rest on *T*-tests with * $P < 0.05$; ** $P < 0.01$ and *** $P < 0.005$. Tests were made pair wise (10 w–11 w, 11 w–12 w, 12 w–13 w, 13 w–14 w, 14 w–15 w). Missing error bars at 15 w indicate that only one leaf was left over for the measurements.

reasonable to speculate that eukaryotic cells also evolved nuclear antioxidant systems distinct from the cytosolic ones, since nuclear redox-states influence the activity of a large number of nuclear proteins including transcription factors, and oxidative injury or DNA replication errors caused by ROS are serious problems for aerobic organisms. At least one family member of the peroxiredoxins has been reported to be localized in the nucleoplasm of rice and *Arabidopsis* (Dietz 2011).

In order to see whether H_2O_2 also serves as a senescence signal in the crop plant oilseed rape, we established a matrix of H_2O_2 levels and CAT and APX activities in oilseed rape plants. As for *Arabidopsis,* the hydrogen peroxide levels increased during bolting and flowering; however, in very late stages of senescence when H_2O_2 levels again increased substantially in *Arabidopsis* rosettes (coinciding with increased lipid peroxidation and fatty acid degradation), no such increase could be observed in oilseed rape, indicating that mobilization of the carbon skeletons of lipids during membrane deterioration might be less efficient. With increasing H_2O_2 levels, CAT and APX activity decreased, with CAT2 down-regulation being relatively severe and APX down-regulation being less pronounced and only observable in young oilseed rape leaves. Although *CAT2* down-regulation in *Arabidopsis* is achieved through transcriptional down-regulation by GBF1 (Smykowski et al. 2010), APX1 down-regulation appears to be posttranscriptional, most likely involves H_2O_2, and is dependent on the developmental stage; however, the precise mechanism is still unknown (Ye et al. 2000; Zimmermann et al. 2006). Down-regulation of CAT and APX activity and the increase of H_2O_2 are not restricted to *Brassicaceae*, and have also been observed in sunflower senescence (Agüera et al. 2010).

Total glutathione and ascorbate pools decreased during development, and interestingly, the reduction rate of both pools increased with the progression of senescence in oilseed rape leaves. In 6 and 7-week-old plants, the oxidized forms reached their maximum values, maintained comparable levels from weeks 8 to 12, and then decreased again to nearly undetectable levels of GSSG in 12 and 13-week-old plants, which coincides with low H_2O_2 levels in these final stages. This is in agreement with the characteristic high reduction state of the glutathione pool. In the absence of stress, tissues such as leaves typically maintain measurable GSH:GSSG ratios of approximately 20:1 with considerable variation in specific subcellular compartments (Meyer et al. 2007; Queval et al. 2011). In *cat2* mutants, the conversion of GSH to GSSG within h after the onset of H_2O_2 production was followed by a subsequent increase of the total glutathione pool over 3–4 d (Queval et al. 2009). The GSH:GSSG ratio of leaves dropped from approximately 20:1 to almost 1:1 after induction of endogenous H_2O_2 production at moderate rates (Mhamdi et al. 2010). Such effects were not observed during the developmental increase of H_2O_2 in oilseed rape. Only a slight increase in the glutathione pool was observed in 10-week-old plants after H_2O_2 had reached its maximum level (**Figure 5A**).

Since glutathione status is often used as a marker for oxidative stress, it can be speculated that the long-term increased H_2O_2 levels during development are not recognized as “oxidative stress” but as a developmental signal. However, the glutathione redox potential is not only governed by the GSH:GSSG ratio, but also depends on the absolute concentration of the total glutathione pool (Mullineaux and Rausch 2005; Meyer 2008). A decrease in a total glutathione pool with a constant GSH:GSSG ratio leads to an increase in redox potential, meaning that no clear conclusion can be drawn in regards to the actual redox potential (Queval et al. 2011). Decreasing glutathione pools in senescent leaves might also indicate sulfur remobilization, since glutathione is one of the major forms of organic sulfur translocated to the phloem, and high concentrations of glutathione have also been observed in the phloem sap of *Brassica napus* plants (Mendoza-Cózatl et al. 2008). Furthermore, sulfur availability and senescence are interconnected in oilseed rape; a transient S limitation in oilseed rape plants is compensated for by means of a fine management of leaf N-S remobilization, and causes delayed leaf senescence (Abdallah et al. 2011). The transport protein OPT6 might play a role in long-distance transport. The corresponding *Arabidopsis* gene is highly expressed in the vasculature, and has been discussed to transport GS-conjugates and GS-cadmium complexes as well as GSH and GSSG (Cagnac et al. 2004), although GSSG transport is still under debate (Pike et al. 2009). Moreover, glutathione is involved in various signaling processes, but the study of glutathione-dependent signaling is still at early stages (Noctor et al. 2012). Even though ascorbate and glutathione pools are often considered as interchangeable antioxidants and both pools decreased with oilseed rape plant age, glutathione or ascorbate deficiency mutants of *Arabidopsis* revealed that these two compounds have specific functions. Furthermore, ascorbate and glutathione are differentially influenced by environmental factors, and *cat2* mutants have been shown to produce oxidized glutathione after the onset of H_2O_2 production while ascorbate remains highly reduced (Queval et al. 2007; Mhamdi et al. 2010; Foyer and Nocter 2011). Although considerable amounts of oxidized glutathione can be measured in young oilseed rape plants which are reduced again with development, the ascorbate reduction state did not change significantly with age until week 13. Remarkably, the ascorbate pool increased slightly, though not significantly, after H_2O_2 levels had reached their maximum point in 9-week-old plants (**Figure 5C**). A change in SDG and SAG expression coincided with the H_2O_2 maximum, and preceded chlorophyll breakdown. Early SAGs like SAG13 increased, whereas early SDGs like *CAB* or *RUBISCO* decreased. Of particular note, the expression of the transcription factor *WRKY53* paralleled the H_2O_2 profile. For *Arabidopsis*, expression of *WRKY53* also parallels H_2O_2 profiles and can be induced within h by H_2O_2 treatment in presenescent plants. In addition, expression of the upstream and downstream regulating factors of *WRKY53* is also controlled by H_2O_2, indicating that the transcriptional reprogramming is at least in part regulated by H_2O_2 (Miao et al. 2007, 2008; Miao and Zentgraf 2010). There is some evidence that *WRKY53* itself is involved in the H_2O_2 response

of the *WRKY53* promoter, in which case the Zn-finger in the DNA binding region of the WRKY proteins could serve as the structural domain for direct redox-regulation (Arrigo 1999). Under close to field conditions, H_2O_2 levels also increased during flowering. Under low and excess nitrogen supplies, H_2O_2 production appeared to be slightly increased, but these slight differences had no impact on leaf senescence. In a high CO_2 atmosphere, low and optimal nitrogen supply led to an earlier decline of chlorophyll and N contents (Franzaring et al. 2011, 2012), and H_2O_2 also peaked earlier, indicating that H_2O_2 maxima correlated with the onset of senescence and senescence is accelerated under high CO_2 conditions. Accelerated senescence could also be observed in flag leaves of barley in a high CO_2 atmosphere (Fangmeier et al. 2000). However, under high N conditions, the H_2O_2 increase was exactly the same as under ambient air, but the decline was steeper for H_2O_2 as well as for chlorophyll. Even though high N availability and high CO_2 prolonged flowering time, they did not lead to the production of more ripe pods, but more likely prevented apical switch off leading to a strong branching out. In addition, a slight reddening of the youngest stem leaves and pod stalks was observed after flowering under high N availability and high CO_2, probably indicating nutrient deficiencies or imbalances. Furthermore, high CO_2 caused a decline in seed oil contents contents. Nevertheless, remobilization appears to remain effective since macronutrients in the seeds increased slightly, and a lower N content was measured in senescent leaves (Franzaring et al. 2011, 2012). Leaf senescence in sunflower plants was also accelerated by nitrogen deficiency, and also correlated with an early decrease in the antioxidant enzymes activities of CAT and APX (Agüera et al. 2010). In conclusion, H_2O_2 appears to be used as a signal to promote senescence in different plant species, and to be part of a complex regulatory network. Remarkably, transcriptome responses to both CO_2 and H_2O_2 are highly dependent on the photoperiod (Queval et al. 2012).

Materials and Methods

Plant material and cultivation

Arabidopsis thaliana (L.) Heynh ecotype Columbia was grown in a climate chamber at 22 °C, illuminated for 16 h at moderate light intensity (60 μmol s^{-1} m^{-2}). Under these conditions, the plants developed flowers within 5–6 weeks and the mature seeds were harvested after 12 weeks. During growth and development of the leaves, the respective positions within the rosette were color-coded with different colored threads, so that even in very late stages of development, individual leaves could be analyzed according to their age. *Brassica napus* L. cv. Mozart was grown in greenhouses at 19–22 °C during a 16 h photoperiod of approximately 150 μmol s^{-1} m^{-2} light intensity. Near-field conditions for *Brassica napus* L. cv. Mozart were simulated in large growth chambers at the University of Hohenheim, using the seasonal increments of day length and the temperature of South-Western Germany as described in Franzaring et al. (2011). Plants were harvested on a weekly basis, and samples were always taken at the same time in the morning to avoid circadian effects.

H_2O_2 measurements

Leaf discs (approximately 1 cm in diameter) were taken from approximately the same position of the respective leaf and incubated for exactly 45 min in DCFDA working-solution (Dichlorofluorescein-Diacetate, 200 μg in 40 mL MS-Medium pH 5.7–5.8). Discs were then rinsed with water and frozen in liquid nitrogen. After homogenization on ice, 500 μL 40 mM Tris pH 7.0 was added, and the samples were centrifuged at 4 °C for 30 min. Fluorescence (480 nm excitation, 525 nm emission) of the supernatant was measured in a Berthold TriStar LB941 plate reader. All samples were taken and processed at one time point and incubated in one DCFDA working-solution to avoid staining solution- and diurnal-variability.

SPAD measurements and phenotypic analysis

For assessment of the leaf senescence state, color-coded leaves were grouped into three categories: (leaf Nos. 1–3), middle aged (leaf Nos. 4–7) and young (leaf Nos. 8–12) leaves. Chlorophyll content was estimated with a Atleaf + SPAD-Meter or a Konica-Minolta SPAD 502. Each leaf was measured in triplicate at different positions, and values were averaged. For evaluation of leaf senescence phenotypes, all leaves were categorized into four groups according to their leaf color: 1) “green”, 2) leaves starting to display yellowing as “yellowgreen”, 3) completely yellow leafs as “yellow”, and 4) dry and/or brown leafs as “brown/dry”.

C and N content analysis

Whole leaves were homogenized in liquid nitrogen and 200 mg of the homogenized powder was lyophilized. Total carbon and nitrogen contents of the lyophilized material were determined with a CN-element analyzer (Elementar Vario EL III) via heat combustion at 1 150 °C and thermal conductivity detection.

Catalase and APX zymograms

Leaf discs (approximately 1 cm in diameter) were taken from approximately the same position of the respective leaf and frozen in liquid nitrogen. After homogenization on ice, a protein extraction buffer was added (100 mM Tris, 20% Glycerol (v/v), 30 mM DTT, pH 8) and the samples were centrifuged for 15 min at 14 000 rpm and 4 °C. Total protein concentration of

the supernatant was determined via Bradford assay (Bio-Rad Protein Assay), and 15 μg total protein was separated on native PAA gels (7.5% PAA, 1.5 M Tris, pH 8.8; running buffer: 25 mM Tris, 250 mM Glycin, pH 8.3). Subsequently, the gels were rinsed twice with water, incubated for exactly 2 min in a 0.01% H_2O_2 solution, again rinsed twice with water and stained in a solution containing 1% $FeCl_3$ and 1% $K_3(Fe(CN)_6)$; (w/v) until activity bands became visible (approximately 4 min). The staining reaction was stopped by decanting staining solution and rinsing gels with water. For isoform identification, slices of gels containing the same samples and sample amounts were incubated for 2–10 min in 10 mM 3-amino triazol (3-AT) solution prior to activity staining.

For APX activity, two leaf discs (approximately 1 cm in diameter) were taken from approximately the same position of the respective leaf and frozen in liquid nitrogen. After homogenization on ice, a protein extraction buffer was added (50 mM potassium phosphate pH 7.8, 2% Triton-X 100 (v/v), 5 mM ascorbic acid, 35 mM β-mercapto ethanol, 2% polyvinylpyrrolidon (w/v)) and the samples were centrifuged for 15 min at 14 000 rpm and 4 °C. Protein concentration of the supernatant was determined via Bradford assay (Biorad Protein Assay). The native PAA gels (10% PAA, 1.5 M Tris pH 8.8, 13% Glycerol (v/v); running buffer: 25 mM Tris, 250 mM Glycin, 2 mM ascorbic acid, pH 8.3) were run for 30 min at 120 V before samples were loaded, and then 30 μg of protein was loaded and the electrophoresis was conducted for approximately 3 h (120 V, 4 °C). After electrophoresis, the gels were incubated three times in 50 mM potassium phosphate buffer pH 7 containing 2 mM ascorbic acid for 10 min, and once in 50 mM potassium phosphate buffer pH 7 containing 4 mM ascorbic acid and 0.5 μM H_2O_2 for 10 min. Gels were rinsed twice with water after each incubation step. Gels were equilibrated for 1–2 min in 50 mM potassium phosphate buffer pH 7.8 before the staining reaction was started by adding 50 mM potassium phosphate buffer pH 7.8 containing 14 mM TEMED and 2.45 mM NBT. The staining reaction was stopped when the first bands became visible (after approximately 5–10 min) by decanting the staining solution and rinsing the gels with water.

APX activity measurement

Total protein extracts were obtained from homogenized leaf discs and stored in a 50 mM potassium phosphate buffer (pH 7.8) with 0.25 mM EDTA, 2% PVP (w/v), 10% Glycerol (v/v) and 5 mM ascorbic acid. 100 μL of these extracts were used for activity measurements in a 25 mM phosphate buffer (pH 7) with 0.1 mM EDTA, 1 mM H_2O_2 and 0.25 mM ascorbic acid in a total volume of 1 mL. The reaction was started by the addition of H_2O_2, and a decrease in ascorbic acid was recorded at 290 nm. For the final calculation, an ascorbic acid extinction coefficient of 2.8 mM $*$ cm^{-1} was used.

GSSG/GSH and DHAsc/Asc analytics

Four leaf discs were homogenized in 300 μL 5 N HCl in 15% methanol, sonicated for 3 min, and incubated for 15 min on ice. Subsequently, the samples were centrifuged at 4 °C for 15 min at 14 000 rpm. The supernatant was removed and directly used for LC/MS analysis (Acquity UPLC, SynaptG2 HDMS; Waters, Manchester) of ascorbic acid and glutathione pools. For the analysis, 5 μL of the supernatant was injected onto a 2.1 mm × 100 mm, 1.8 μm Acquity UPLC HSS T3 column operating at a flow rate of 0.3 mL/min. For chromatographic separation, an 8 min gradient from 99% water to 99% methanol (both solvents with 0.1% formic acid) was used. The mass spectrometer was equipped with an ESI source and operated in resolution scanning mode with a scan time of 0.2 s. For quantification, bracketing calibration was performed.

Protein extraction, western blot and immunodetection

150–300 mg leaf material was homogenized on ice with 300 μL protein extraction buffer (100 mM potassium phosphate, 1 mM EDTA, 1% Triton-X 100 (v/v) and 10% Glycerol (v/v)). After 15 min centrifugation at 14 000 rpm and 4 °C, protein concentration of the supernatant was determined. For western blotting, 30 μg of protein was loaded on a SDS-PAGE gel and transferred onto a nitrocellulose membrane by semi-dry blotting. The membrane was washed twice with Tris-buffered saline (TBS), and then blocked with 3% milk powder in TBS. The detection was performed with polyclonal Anti-GFP antibodies in 1.5% milk powder. After washing twice with TBS-Tween 20 (TBS-T), peroxidase-conjugated anti-mouse antibodies were used for the chemiluminescence detection.

Quantitative RT-PCR

Primer design for qRT-PCR was done via QuantPrime (Arvidsson et al. 2008). RNA extraction and cDNA synthesis were conducted with the InviTrap Spin Universal RNA Mini Kit (Invitek) and qScript cDNA SuperMix (Quanta Biosciences), respectively. qPCR was performed with Perfect CTa SybrGreen Fast Mix (Quanta Biosciences) in an iCycler iQ System (Biorad). Relative quantification to *ACTIN2* was calculated with the $\Delta\Delta C_T$ – Method (Pfaffl et al. 2001). *ACTIN2* was chosen as a reference gene for Senescence, since the variation of *ACTIN2* expression over different leaf and plant stages in *Arabidopsis* was very low in contrast to that of other housekeeping genes (Panchuk et al. 2005).

Acknowledgements

We thank Alex Costa from the University of Padua, Italy, for providing the plants overexpressing OxyR-RD-cpYFP in

the cytoplasm and peroxisomes. We thank Gabriele Eggers-Schumacher and Bettina Stadelhofer (ZMBP, University of Tuebingen, Germany) for their excellent technical assistance. This work was financially supported by the DFG (FOR948).

Received 4 Apr. 2012 Accepted 8 Jul. 2012

References

Abdallah M, Etienne P, Ourry A, Meuriot F (2011) Do initial S reserves and mineral S availability alter leaf S-N mobilization and leaf senescence in oilseed rape? *Plant Sci.* **180,** 511–520.

Agüera E, Cabello P, de la Haba P (2010) Induction of leaf senescence by low nitrogen nutrition in sunflower (*Helianthus annuus*) plants. *Physiol. Plant* **138,** 256–267.

Arrigo AP (1999) Gene expression and the thiol redox state. *Free Radical Biol. Med.* **27,** 936–944.

Arvidsson S, Kwasniewski M, Riaño-Pachón DM, Mueller-Roeber B (2008) QuantPrime – a flexible tool for reliable high-throughput primer design for quantitative PCR. *BMC Bioinformatics* **9,** 465.

Aslund F, Zheng M, Beckwith J, Storz G (1999) Regulation of the OxyR transcription factor by H_2O_2 and the cellular thiol-disulfide status. *Proc. Natl. Acad. Sci. USA* **96,** 6161–6165.

Balazadeh S, Siddiqui H, Allu AD, Matallana-Ramirez LP, Caldana C, Mehrnia M, Zanor MI, Köhler B, Mueller-Roeber B (2010) A gene regulatory network controlled by the NAC transcription factor ANAC092/AtNAC2/ORE1 during salt-promoted senescence. *Plant J.* **62,** 250–264.

Balazadeh S, Kwasniewski M, Caldana C, Mehrnia M, Zanor MI, Xue GP, Mueller-Roeber B (2011) ORS1, an H_2O_2-responsive NAC transcription factor, controls senescence in *Arabidopsis thaliana*. *Mol. Plant* **4,** 346–360.

Barth C, Moeder W, Klessig DF, Conklin PL (2004) The timing of senescence and response to pathogens is altered in the ascorbate-deficient *Arabidopsis* mutant *vitamin c-1*. *Plant Physiol.* **34,** 1784–1792.

Batt T, Woolhouse HW (1975) Changing activities during senescence and sites of synthesis of photosynthetic enzymes in leaves of labiate, *Perilla frutenscens* (L.) Britt. *British J. Exp. Bot.* **26,** 569–579.

Bazargani MM, Sarhadi E, Bushehri AA, Matros A, Mock HP, Naghavi MR, Hajihoseini V, Mardi M, Hajirezaei MR, Moradi F, Ehdaie B, Salekdeh GH (2011) A proteomics view on the role of drought-induced senescence and oxidative stress defense in enhanced stem reserves remobilization in wheat. *J. Proteomics* **74,** 1959–1973.

Belousov VV, Fradkov AF, Lukyanov KA, Staroverov DB, Shakhbazov KS, Terskikh AV, Lukyanov S (2006) Genetically encoded fluorescent indicator for intracellular hydrogen peroxide. *Nat. Methods* **3,** 281–286.

Breeze E, Harrison E, McHattie S, Hughes L, Hickman R, Hill C, Kiddle S, Kim YS, Penfold CA, Jenkins D, Zhang C, Morris K, Jenner C, Jackson S, Thomas B, Tabrett A, Legaie R, Moore JD, Wild DL, Ott S, Rand D, Beynon J, Denby K, Mead A, Buchanan-Wollaston V (2011) High-resolution temporal profiling of transcripts during *Arabidopsis* leaf senescence reveals a distinct chronology of processes and regulation. *Plant Cell* **23,** 873–894.

Cagnac O, Bourbouloux A, Chakrabarty D, Zhang MY, Delrot S (2004) AtOPT6 transports glutathione derivatives and is induced by primisulfuron. *Plant Physiol.* **135,** 1378–1387.

Corpas FJ, Barroso JB, Carreras A, Quirós M, León AM, Romero-Puertas MC, Esteban FJ, Valderrama R, Palma JM, Sandalio LM, Gómez M, del Río LA (2004) Cellular and subcellular localization of endogenous nitric oxide in young and senescent pea plants. *Plant Physiol.* **136,** 2722–2733.

Corpas FJ, Barroso JB, del Río LA (2001) Peroxisomes as a source of reactive oxygen species and nitric oxide signal molecules in plant cells. *Trends Plant Sci*. **6,** 145–150.

Costa A, Drago I, Behera S, Zottini M, Pizzo P, Schroeder JI, Pozzan T, Lo Schiavo F (2010) H_2O_2 in plant peroxisomes: An in vivo analysis uncovers a Ca^{2+}-dependent scavenging system. *Plant J.* **62,** 760–772.

del Río LA, Pastori, GM, Palma JM, Sandalio LM, Sevilla F, Corpas FJ, Jiménez A, López-Huertas E, Hernández JA (1998) The activated oxygen role of peroxisomes in senescence. *Plant Physiol.* **116,** 1195–1200.

del Rio LA, Sandalio LM, Corpas FJ, Palma JM, Barroso JB (2006) Reactive oxygen species and reactive nitrogen species in peroxisomes. Production, scavenging, and role in cell signaling. *Plant Physiol.* **141,** 330–335.

Dietz KJ (2011) Peroxiredoxins in plants and cyanobacteria. *Antioxid. Redox Signal.* **15,** 1129–1159.

Feierabend J, Schaan C, Hertwig B (1992) Photoinactivation of catalase occurs under both high and low temperature stress conditions and accompanies photoinhibition of photosystem II. *Plant Physiol.* **100,** 1554–1561.

Fangmeier A, Chrost B, Högy P, Krupinska K (2000) CO_2 enrichment enhances flag leaf senescence in barley due to greater grain nitrogen sink capacity. *Environ. Exp. Bot.* **44,** 151–164.

Franzaring J, Welle, S, Schmid I, Fangmeier A (2011) Growth, senescence and water use efficiency of spring oilseed rape (*Brassica napus* L. cv. Mozart) grown in a factorial combination of nitrogen supply and elevated CO_2. *Environ. Exp. Bot.* **72,** 284–296.

Franzaring J, Gensheimer G, Weller S, Schmid I, Fangmeier A (2012) Allocation and remobilisation of nitrogen in spring oilseed rape (*Brassica napus* L. cv. Mozart) as affected by N supply and elevated CO_2. *Environ. Exp. Bot.* **83,** 12–22.

Foyer CH, Nocter G (2011) Ascorbate and glutathione: The heart of the redox Hub. *Plant Physiol.* **155,** 2–18.

Guo Y, Cai Z, Gan S (2004) Transcriptome of *Arabidopsis* leaf senescence. *Plant Cell Environ.* **27,** 521–549.

Guo Y, Gan S (2006) AtNAP, a NAC family transcription factor, has an important role in leaf senescence. *Plant J.* **46,** 601–612.

Hensel LL, Grbić V, Baumgarten D, Bleecker AB (1993) Developmental and age-related processes that influence the longevity and senescence of photosynthetic tissues in *Arabidopsis*. *Plant Cell* **5,** 553–564.

Jing HC, Hebeler R, Oeljeklaus S, Sitek B, Stühler K, Meyer HE, Sturre MJ, Hille J, Warscheid B, Dijkwel PP (2008) Early leaf senescence is associated with an altered cellular redox balance in *Arabidopsis* cpr5/old1 mutants. *Plant Biol.* **10** (Suppl. s1), 85–98.

Keskitalo J, Bergquist G, Gardestrom P, Jansson S (2005) A cellular timetable of autumn senescence. *Plant Physiol.* **139,** 1635–1648.

Kovtun Y, Chiu WL, Tena G, Sheen J (2000) Functional analysis of oxidative stress-activated mitogen-activated protein kinase cascade in plants. *Proc. Natl. Acad. Sci. USA* **97,** 2940–2945.

Kurepa J, Smalle J, Van Montagu M, Inzé D (1998) Oxidative stress tolerance and longevity in *Arabidopsis*: The late flowering mutant gigantea is tolerant to paraquat. *Plant J.* **14,** 759–764.

Martínez DE, Costa ML, Guiamet JJ (2008) Senescence-associated degradation of chloroplast proteins inside and outside the organelle. *Plant Biol.* **10** (Suppl. s1), 15–22.

Masclaux C, Valadie, **MH, Brugière N, Morot-Gaudry JF, Hirel B** (2000) Characterization of the sink/source transition in tobacco (*Nicotiana tabacum* L.) shoots in relation to nitrogen management and leaf senescence. *Planta* **211,** 510–518.

Matile P, Schellenberg M, Peisker C (1992) Production and release of a chlorophyll catabolite in isolated senescent chloroplasts. *Planta* **18,** 230–235.

Mendoza-Cózatl DG, Butko E, Springer F, Torpey JW, Komives EA, Kehr J, Schroeder JI (2008) Identification of high levels of phytochelatins, glutathione and cadmium in the phloem sap of *Brassica napus*. A role for thiol-peptides in the long-distance transport of cadmium and the effect of cadmium on iron translocation. *Plant J.* **54,** 249–259.

Meyer AJ, Brach T, Marty L, Kreye S, Rouhier N, Jacquot JP, Hell R (2007) Redox-sensitive GFP in *Arabidopsis thaliana* is a quantitative biosensor for the redox potential of the cellular glutathione redox buffer. *Plant J.* **52,** 973–986.

Meyer AJ (2008) The integration of glutathione homeostasis and redox signaling. *J. Plant Physiol.* **165,** 1390–1403.

Mhamdi A, Hager J, Chaouch S, Queval G, Han Y, Taconnat L, Saindrenan P, Gouia H, Issakidis-Bourguet E, Renou JP, Nocter G (2010) *Arabidopsis* GLUTATHIONE REDUCTASE1 plays a crucial role in leaf responses to intracellular hydrogen peroxide and in ensuring appropriate gene expression through both salicylic acid and jasmonic acid signaling pathways. *Plant Physiol.* **153,** 1144–1160.

Miao Y, Laun T, Zimmermann P, Zentgraf U (2004) Targets of the WRKY53 transcription factor and its role during leaf senescence in *Arabidopsis*. *Plant Mol. Biol.* **55,** 853–867.

Miao Y, Laun T, Smykowski A, Zentgraf U (2007) *Arabidopsis* MEKK1 can take a short cut: It can directly interact with senescence-related WRKY53 transcription factor on the protein level and can bind to its promoter. *Plant Mol. Biol.* **65,** 63–76.

Miao Y, Smykowski A, Zentgraf U (2008) A novel upstream regulator of WRKY53 transcription during leaf senescence in *Arabidopsis* thaliana. *Plant Biol.* **10** (Suppl. s1), 110–120.

Miao Y, Zentgraf U (2010) A HECT E3 ubiquitin ligase negatively regulates *Arabidopsis* leaf senescence through degradation of the transcription factor WRKY53. *Plant J.* **63,** 179–188.

Mittler R, Vanderauwera S, Gollery M, Van Breusegem F (2004) Reactive oxygen gene network of plants. *Trends Plant Sci.* **9,** 490–498.

Miyake C, Asada K (1996) Inactivation mechanism of ascorbate peroxidase at low concentrations of ascorbate: Hydrogen peroxide decomposes compound I of ascorbate peroxidase. *Plant Cell Physiol.* **37,** 423–430.

Mullineaux PM, Rausch T (2005) Glutathione, photosynthesis and the redox regulation of stress-responsive gene expression. *Photosyn. Res.* **86,** 459–474.

Munné-Bosch S, Alegre L (2002) Plant aging increases oxidative stress in chloroplasts. *Planta* **214,** 608–615.

Noctor G, Mhamdi A, Chaouch S, Han Y, Neukermans J, Marquez-Garcia B, Queval G, Foyer CH (2012) Glutathione in plants: An integrated overview. *Plant Cell Environ.* **35,** 454–484.

Orendi G, Zimmermann P, Baar C, Zentgraf U (2001) Loss of stress-induced expression of cata-lase3 during leaf senescence in *Arabidopsis thaliana* is restricted to oxidative stress. *Plant Sci.* **161,** 301–314.

Panchuk II, Zentgraf U, Volkov RA (2005) Expression of the *Apx* gene family during leaf senescence of *Arabidopsis thaliana*. *Planta* **222,** 926–932.

Perazza D, Laporte F, Balagué C, Chevalier F, Remo S, Bourge M, Larkin J, Herzog M, Vachon G (2011) GeBP/GPL transcription factors regulate a subset of CPR5-dependent processes. *Plant Physiol.* **157,** 1232–1242.

Pfaffl MW (2001) A new mathematical model for relative quantification in real-time RT-PCR. *Nucl. Acids Res.* **29,** 2002–2007.

Pike S, Patel A, Stacey G, Gassmann W (2009) *Arabidopsis* OPT6 is an oligopeptide transporter with exceptionally broad substrate specificity. *Plant Cell Physiol.* **50,** 1923–1932.

Pourtau N, Marès M, Purdy S, Quentin N, Ruël A, Wingler A (2004) Interactions of abscisic acid and sugar signalling in the regulation of leaf senescence. *Planta* **219,** 765–772.

Queval G, Issakidis-Bourguet E, Hoeberichts FA, Vandorpe M, Gakière B, Vanacker H, Miginiac-Maslow M, Van Breusegem F, Noctor G (2007) Conditional oxidative stress responses in the *Arabidopsis* photorespiratory mutant *cat2* demonstrate that redox state is a key modulator of daylength-dependent gene expression, and define photoperiod as a crucial factor in the regulation of H_2O_2-induced cell death. *Plant J.* **52,** 640–657.

Queval G, Thominet D, Vanacker H, Miginiac-Maslow M, Gakière B, Noctor G (2009) H_2O_2-activated up-regulation of glutathione in *Arabidopsis* involves induction of genes encoding enzymes

involved in cysteine synthesis in the chloroplast. *Mol. Plant* **2,** 344–356.

Queval G, Jaillard D, Zechmann B, Noctor G (2011) Increased intracellular H_2O_2 availability preferentially drives glutathione accumulation in vacuoles and chloroplasts. *Plant Cell Environ.* **34,** 21–32.

Queval G, Neukermans J, Vanderauwera S, Van Breusegem F, Noctor G (2012) Day length is a key regulator of transcriptomic responses to both CO_2 and H_2O_2 in *Arabidopsis*. *Plant Cell Environ.* **35,** 374–387.

Rossato L, Laine P, Ourry A (2001) Nitrogen storage and remobilization in *Brassica napus* L. during the growth cycle: Nitrogen fluxes within the plant and changes in soluble protein patterns. *J. Exp. Bot.* **52,** 1655–1663.

Sakuraba Y, Balazadeh S, Tanaka R, Mueller-Roeber B, Tanaka A (2012) Overproduction of chlorophyll b retards senescence through transcriptional re-programming in *Arabidopsis*. *Plant Cell Physiol.* **53,** 505–517.

Schippers JH, Nunes-Nesi A, Apetrei R, Hille J, Fernie AR, Dijkwel PP (2008) The *Arabidopsis* onset of leaf death5 mutation of quinolinate synthase affects nicotinamide adenine dinucleotide biosynthesis and causes early ageing. *Plant Cell* **20,** 2909–2925.

Smart CM (1994) Gene expression during leaf senescence. *New Phytol.* **126,** 419–448.

Smykowski A, Zimmermann P, Zentgraf U (2010) G-Box Binding Factor1 reduces *CATALASE2* expression and regulates the onset of leaf senescence in *Arabidopsis*. *Plant Physiol.* **153,** 1321–1331.

Tilsner J, Kassner N, Struck C, Lohaus G (2005) Amino acid contents and transport in oilseed rape (*Brassica napus* L.) under different nitrogen conditions. *Planta* **221,** 328–338.

Uauy C, Distelfeld A, Fahima T, Blechl A, Dubcovsky J (2006) A *NAC* Gene regulating senescence improves grain protein, zinc, and iron content in wheat. *Science* **314,** 1298–1301.

van Doorn WG (2004) Is petal senescence due to sugar starvation? *Plant Physiol.* **134,** 35–42.

Wingler A, Marès M, Pourtau N (2004) Spatial patterns and metabolic regulation of photosynthetic parameters during leaf senescence. *New Phytol.* **161,** 781–789.

Wingler A, Masclaux-Daubresse C, Fischer AM (2009) Sugars, senescence, and ageing in plants and heterotrophic organisms. *J. Exp. Bot.* **60,** 1063–1066.

Woo HR, Kim JH, Nam HG, Lim PO (2004) The delayed leaf senescence mutants of *Arabidopsis*, ore1, ore3, and ore9 are tolerant to oxidative stress. *Plant Cell Physiol.* **45,** 923–932.

Yang SD, Seo PJ, Yoon HK, Park CM (2011) The *Arabidopsis* NAC transcription factor VNI2 integrates abscisic acid signals into leaf senescence via the *COR*/*RD* genes. *Plant Cell* **23,** 2155–2168.

Ye ZZ, Rodriguez R, Tran A, Hoang H, de los Santos D, Brown S, Vellanoweth RL (2000) The developmental transition to flowering represses ascorbate peroxidase activity and induces enzymatic lipid peroxidation in leaf tissue in *Arabidopsis thaliana*. *Plant Sci.* **158,** 115–127.

Zapata JM, Guera A, Esteban-Carrasco A, Martin M, Sabater B (2005) Chloroplasts regulate leaf senescence: Delayed senescence in transgenic ndhF-defective tobacco. *Cell Death Diff.* **12,** 1277–1284.

Zheng M, Aslund F, Storz G (1998) Activation of the OxyR transcription factor by reversible disulfide bond formation. *Science* **279,** 1718–1721.

Zimmermann P, Heinlein C, Orendi G, Zentgraf U (2006) Senescence specific regulation of catalases in *Arabidopsis thaliana* (L.) Heynh. *Plant Cell Environ.* **29,** 1049–1060.

(Co-Editor: Hai-Chun Jing)

Chapter 3

Plant Senescence and Nitrogen Mobilization and Signaling

Stefan Bieker and Ulrike Zentgraf

Additional information is available at the end of the chapter

http://dx.doi.org/10.5772/54392

1. Introduction

1.1. Senescence

Very early during their reproductive phase, annual plants initiate the process of senescence. Monocarpic senescence describes the last steps in these plants' development; senescence on organ level starts shortly after entering reproductive phase while after anthesis the whole plant undergoes senescence and dies.

In the following we will focus on leaf senescence. Two different processes can be distinguished in annual plants relying on different genetic programs. Before anthesis, sequential leaf senescence recycles nutrients from old to developing leaves which is mainly under the control of the growing apex and is arrested when no more new leaves develop and when the plant starts to flower and sets fruit. Monocarpic leaf senescence recovers valuable nutrients from the leaves during flower induction and anthesis to provide these to the developing reproductive organs [1, 2]. The latter is crucial for fruit and seed development and has a major impact on yield quantity and quality. In wheat salvaged nitrogen (N) from the leaves accounts for up to 90% of the total grain N content [3]. A complex regulation of many different metabolic pathways and expression of numerous genes underlies this process. How coordination and interplay of many controlling factors, like hormones, genetic reprogramming, biotic and abiotic stresses are achieved is far from being understood, but it is already clear that this regulatory network is highly complex and dynamic.

Thousands of genes are differentially regulated during senescence induction and progression. To date forward and reverse genetic approaches as well as large-scale transcript profiling have identified almost 6.500 genes being differentially expressed during the course of leaf senescence including up-regulated as well as down-regulated genes [4]. The high num-

ber of differentially regulated senescence-associated transcription factors (TF) demonstrates the dimensions of genetic reprogramming taking place. These TFs include 20 distinct families of which NAC-, WRKY-, C2H2-type zinc finger, EREBP- and MYB-families are most abundant [5]. Recently, Breeze et al. (2011) [4] published extremely important results of a high-resolution temporal transcript profiling of senescing Arabidopsis leaves giving insight into the temporal order of genetic events. One of the first steps at the onset of senescence is a shift from anabolic to catabolic processes. Amino acid metabolism and protein synthesis are down-regulated while expression of autophagy- and reactive oxygen species-related, and water-response genes is enhanced. In contrast to the following elevation of abscisic acid (ABA) and jasmonic acid (JA) signaling-related gene expression, cytokinin-mediated signaling is lowered just as chlorophyll and carotenoid biosynthesis. The next phases include down-regulation of carbon utilization and enhanced expression of cystein-aspartat proteases, carotene metabolism-associated genes and pectinesterases which is then followed by the reduction of photosynthetic activity and degradation of the photosynthetic apparatus coinciding with the increased activity of lipid catabolism, ethylene signaling and higher abundance of cytoskeletal elements [4].

Hormonal control of senescence is conveyed especially by ethylene, jasmonic and salicylic acid, cytokinin and auxin. Many mutants with a delayed senescence phenotype could be traced back to impaired or up-regulated ethylene or cytokinin signaling, respectively [6, 7]. In adition, ABA acts as a positive regulator of leaf senescence. Recently a membrane-bound, leucine rich repeat containing receptor kinase (RPK1) has been identified to play an important role in ABA-mediated senescence induction in an age-dependent manner. Strikingly, *rpk1* mutant lines did not show significant alterations in developmental processes, which have been reported for numerous other ABA signaling defective mutant lines [5], except slightly shorter growth [8]. This kinase has been indentified to integrate ABA signals during seed germination, plant growth, stomatal closure and stress responses. Overexpression lines showed enhanced expression of several stress and H_2O_2-responsive genes [9, 10]. Mutant lines showed a delayed senescence phenotype with slower progression of chlorophyll degradation and cell death.

Induction and progression of leaf senescence demands a tight regulation of numerous processes. Integration of nutritional cues, biotic and abiotic influences, plant development and age has to take place for the correct timing of onset and temporal advance of this complex developmental process. Despite the enormous efforts and achievements in this field, many of the regulatory mechanisms remain elusive.

1.2. Nitrogen and agriculture

The nowadays growth of population and thus increasing demand for food and oil crops forces agricultural industry to increase quantitative as well as qualitative yields. Until 2050 world's population is predicted to be as high as 9-10 billion people [11] and grain requirement is projected to be doubled, mostly resulting from a higher demand for wheat fed meat [12]. As most of the cropping systems are naturally deficient in nitrogen, there is a fundamental dependency on inorganic nitrogen fertilizers. 85-90 million tons of these fertilizers

http://dx.doi.org/10.5772/54392

are applied annually worldwide [13-15]. However, 50-70% of these nitrogenous fertilizer are lost to the environment [16], mostly due to volatilization of N_2O, NO, N_2 and NH_3 and leaching of soluble NO_3^- into the water. Thus nitrogen is not only one of the most expensive nutrients to provide, but it also has a strong detrimental impact on the environment. Since surrounding ecosystems and potable water supply are endangered by oversaturation with nitrogenous compounds, it is necessary to improve application techniques and plant's nitrogen use efficiencies.

Several different definitions of nitrogen and nutrient use efficiencies are on hand. The most common is the *nitrogen use efficiency* (NUE), which is defined as shoot dry weight divided by total nitrogen content of the shoots. The *usage index* (UI) takes absolute biomass into account as it is denoted by the shoot fresh weight times the NUE. Likewise, the *N uptake efficiency* (NUpE) takes into account the whole N content of the plant and the N supplied by fertilization per plant. The fraction of the N taken up, which is then distributed to the grain, can be obtained by calculating the *N utilization efficiency* (NUtE) (Grain weight per total N content). Other efficiencies, which seem to be more suitable for the use in applied sciences, are the *agronomic efficiency* (AE), *apparent nitrogen recovery* (AR) and the *physiological efficiency* (PE). AE, AR and PE do require an unfertilized control to be calculated. While AE measures the efficiency to redirect applied nitrogen to the grains, AR defines the efficiency to capture N from the soil. PE puts the N uptake into relationship with the outcome of grain (reviewed in [15]). *Nitrogen remobilization efficiency* (NRE) describes the plant's capacity to translocate already assimilated nitrogen to developing organs. Finally, the *harvest index* (HI) and the *nitrogen harvest index* (NHI) are often used terms. HI is the total yield weight per plant mass, while NHI states the grain N content per whole plant N content.

Emission of nitrogen to the environment could be strongly reduced by application of 'best management techniques' in agricultural practice like e.g. rectifying the rate of appliance by accounting for all other possible sources of nitrogen influx (carryover from previous crops, atmospheric deposits etc.), ameliorating the timing and also changing the method of appliance to reduce atmospheric losses [13]. Food production has doubled in the last 40 years. Most of this increase could be achieved by selection of new strains, breeding and application of greater amounts of fertilizer and pesticides and other techniques [12]. Amending of nutrient use efficiencies of the crop plants was mostly accomplished via breeding programs by now. QTL selection for higher yields, increased oil or protein content has been pursued for decades. In wheat for example, increasing yield and grain protein content has been extensively studied, but improving both is restrained by the negative genetic relationship between these traits [17, 18].

2. Nitrogen uptake, assimilation and distribution

Nitrogen sources vary extremely encompassing organic and inorganic forms, small peptides and single amino acids, thus uptake systems need to be adjusted and well regulated in spatial and temporal activity. Although the predominant form in which N is taken up mainly

depends on the plants adaption to the given environment and influences like fertilization, soil pH, temperature, precipitation and others [14, 19], most plants cover their N demand primarily through soil nitrate being provided by fertilization, bacterial nitrification and other processes [15]. However, a wide range of different uptake system has evolved in plants. For example, oligopeptides can be taken up via OPT-proteins (oligopeptide transporters), ammonium via ammonium transporters (AMTs) and amino acids via amino acid transporters and amino acid permeases. Besides the *AtCLC* (ChLoride Channel) gene family, comprising 7 members of which two (*AtCLCa* and *AtCLCb*) have been shown to encode tonoplast located NO_3^-/H^+ antiporters [20, 21], two families of nitrate transporters have been identified in higher plants (NRT1 and NRT2), representing low- and high affinity transporter systems, respectively. Moreover the *NRT1*-family has been shown to comprise also di-/tripeptide transporters (PTR) [22].

2.1. Nitrogen transporter systems

Four constituents of nitrate uptake are known, constitutive (c) and inducible (i) high- (HAT) and low-affinity (LAT) transporters, respectively. The high-affinity system's K_M ranges from ~ 5-100 μM, varying with plant species, and a maximal influx via this system of 1 μMol * g^{-1} * h^{-1} has been determined [23, 24]. At nitrate concentrations of 10 mM the influx rate via the LATs can reach up to ~24 μMol * g^{-1} * h^{-1} [24].

The *NRT1*-family comprises 53 genes in Arabidopsis which are classified as LATs. *AtNRT1-1* (*CHL1*) was the first member to be identified in 1993 and has been shown to encode a proton-coupled nitrate transporter [25]. Studies with *Xenopus* oocytes have shown that this transporter protein possesses two different states, one serving low-affinity and the other one high-affinity nitrate uptake [26, 27], thus the distinction between high and low-affinity nitrate transporters is overridden in this case. Switching between these two modes of action is conferred by phosphorylation of threonin at position 101 [28]. *AtNRT1-1* is expressed in the cortex and endodermis of mature roots and in the epidermis of root tips. Additionally, a nitrate sensing function regulating the plants primary nitrate response has been strongly indicated for the AtNRT1-1 protein by several lines of evidence. The *chl1-5 (atnrt1-1-5)* mutant, a deletion mutant with no detectable *CHL1* transcript, is deficient in nitrate uptake and initiation of the primary nitrate response. The *chl1-9* mutant is defective in nitrate uptake but not in the primary nitrate response. The *chl1*-9 mutant has a point mutation between two transmembrane domains. When threonine 101 was mutated to mimic or repress phosphorylation and transformed into the *chl1-5* background, primary nitrate response could be repressed or enhanced [29]. Constitutive expression identifies AtNRT1-2 as part of the Arabidopsis cLATs. Its transcript is only found in root epidermal cells [22]. Expression of *AtNRT1-5* is nitrate inducible; however, the response to nitrate is much slower than for *AtNRT1-1*. AtNRT1-5 has been shown to be a pH-dependent, bidirectional nitrate transporter, with subcellular localization in the plasma membrane of root pericycle cells near the xylem implicating an involvement in long-distance nitrate transport [30]. Experimental evidence suggests nitrate storage in leaf petioles to be associated with the function of AtNRT1-4. Here, nitrate content is relatively high, while nitrate reductase (NR) activity is

http://dx.doi.org/10.5772/54392

low. Additionally, *AtNRT1-4* is predominantly expressed in the leaf petiole and the *atnrt1.4* mutant shows a nitrate content decreased by half in the petiole [22, 31]. *AtNRT1-6* is expressed in the silique's and funiculus' vascular tissue and thought to play a nitrate providing role in early embryonic development [32]. AtNRT1-8 functions in nitrate unloading from the xylem sap and is mainly located in xylem parenchyma cells within the vasculature [33], whereas AtNRT1-9 facilitates nitrate loading into the root phloem from root phloem companion cells [34].

High affinity nitrate uptake is conducted by members of the *NRT2*-family, comprising 7 genes in Arabidopsis. AtNRT2-1 has been shown to be one of the main components of the HATs. Mutant *atnrt2-1* plants displayed a loss of nitrate uptake capacity up to 75% at HAT-specific NO_3^- concentrations [35]. Furthermore, lateral root growth is repressed under low nitrate combined with high sucrose supply, where NRT2-1 acts either as sensor or transducer [36]. Experiments with *Xenopus* oocytes revealed the requirement of a AtNAR2 protein for AtNRT2-1 function [37]. Mutants of either of these two components showed impaired nitrate uptake at HAT-specific concentrations and hampered growth with display of N-starvation symptoms, in which, remarkably, the *atnar2* mutant phenotype appeared to be more pronounced [38]. The phenotype of the *atnrt2-7* mutant is similar to the phenotype of the *atclca* mutant. The *AtCLCa* gene has been shown to encode a NO_3^-/H^+ antiporter enabling accumulation of nitrate in the vacuole. Mutation of either of these resulted in lower nitrate content. Ectopic overexpression of *AtNRT2-7* led to higher nitrate contents in dried seeds, where the gene is highly expressed under wild type conditions, and an increase in the nitrate HATs uptake capacity by 2-fold. However, normal development was not impaired in the mutants as well as overexpressor plants [14, 20, 39]. Despite its high homology to *AtNRT2-1, AtNRT2-4* is not dependent on the function of *AtNAR2*. *AtNRT2-4* expression is highly induced upon nitrogen starvation in the outermost layer of young lateral roots [40].

Members of the *AMT1*- and *AMT2*-subfamilies are thought to be the main high affinity ammonium transporters in plants. Due to ammonium's toxic nature and convertibility from NH_4^+ to NH_3 and the thus varying membrane permeability, its uptake and transport needs to be tightly regulated [41, 42]. AMTs are regulated transcriptionally by N-supply, sugar and daytime and provide an additive contribution to ammonium transport [41]. AtAMT1-1 contributes 30-35 % as does AtAMT1-3, while AtAMT1-2 provides only 18-25% [43, 44]. AtAMT1-1 transports ammonium as well as its analog methyl-ammonium. Additionally, its activity is regulated posttranscriptionally via the availability of nitrate [42].

2.2. Nitrogen assimilation

Assimilation of NO_3^- and NH_4^+ almost always includes incorporation into amino acids (AA). The most abundant transport forms are glutamine, glutamate, asparagine and aspartate [45] although direct transport of NO_3^- and NH_4^+ also takes place but to a much lesser extend [46]. Nitrate assimilation thus requires reduction to ammonium. Nitrate reductase (NR) realizes the first step by reducing NO_3^- to NO_2^-. This reaction takes place in the cytoplasm, while the reduction of nitrite to ammonium is carried out in the plastids. Here, nitrite reductase (NiR) converts NO_2^- to NH_4^+ making it readily available for the in-

corporation into AAs in a NADH-dependent manner. Assimilation of ammonium into AAs involves chloroplastic glutamine synthetase 2 (GS2) and glutamate synthase (Fd-GOGAT), which generates glutamine and glutamate (for detailed review see [14]). Glutamine as well as glutamate serve as ammonium donor for the synthesis of all other amino acids including aspartate and asparagine, which in turn function as active NH_4^+ donor or as long-range nitrogen transport and storage form, respectively [47]. Alternatively carbamoylphosphate synthase can be involved in ammonium assimilation by producing carbamoylphosphate and successively citrulline and arginine. Assimilation in non-green tissues is achieved in plastids in a similar manner, although here GOGAT depends on NADH instead of ferredoxin. Carbon skeletons are essential for the acquisition of inorganic nitrogen in AAs. Especially the demand for keto-acids has to be met (see [14] and references within). These are predominantly obtained from the TCA-Cycle in the form of 2-oxoglutarate (2OG) [47, 48]. 2OG is used for incorporation of photorespiratory ammonium, resulting in the production of glutamate, which in turn can be utilized by GS1 and GS2 to produce glutamine. This displays the intricate interconnection between carbon and nitrogen metabolism, in which N uptake and assimilation is also influenced via photosynthetic rates [47]. Besides direct assimilation into AAs, nitrate can also be stored in the vacuole and in the chloroplast. Vacuolar nitrate concentrations can vary enormously, as vacuolar nitrate also contributes to turgor maintenance and might have a nitrate storage function to maintain the cytosolic nitrate concentrations which are more constant [49].

3. Senescence induction and nitrogen mobilization

As mentioned above, induction of senescence is a highly complex regulated and dynamic process. Besides developmental cues, there are numerous other possible impacts. Nutritional starvation, photosynthetic activity, pathogen infections, carbon accumulation, carbon to nitrogen ratio, photoperiod and various other cues can lead to senescence induction on either organ or whole plant level. Both natural and stress induced senescence are accompanied with the remobilization of valuable nutrients from various organs of the plant. In the following we will again focus on the situation in leaves.

3.1. Senescence induction

Correct timing of leaf senescence is crucial for proper plant development. Too early senescence induction would decrease the ability to assimilate CO_2, while too late induction would reduce the plant's capacity to remobilize nutrients from old leaves to developing organs [50]. Nevertheless, timing of senescence can also be regarded as an active adaption to the given nutritional and environmental conditions. For example under limited nutrition, continued growth of vegetative tissues would result in a reduced ability to develop reproductive organs.

Nutritional limitation, especially in concerns of nitrogen, has been shown to be able to enhance leaf senescence. Sunflower (*Helianthus annuus*) plants grown under low nitrogen sup-

ply showed a stronger decline of photosynthetic activity and more pronounced senescence symptoms than plants sufficiently supplied with nitrogen [51]. Furthermore these plants showed a more pronounced and earlier drop in (Glu+Asp)/(Gln+Asn) ratio during the progression of senescence indicating an additional adaption to low nitrogen conditions through enhanced nitrogen remobilization. In this experiment, also a significant increase in the ratio of hexose to sucrose was observed at the beginning of senescence which was higher in N-starved plants. This indicates that sugar-related senescence induction is dependent on the availability of nitrogen [51]. However, high sugar contents repress photosynthesis and can induce early SAG expression while late SAG expression is repressed. Diaz et al. (2005) [52] showed sugar accumulation to be lower in some recombinant inbred lines which display early leaf yellowing, thus pointing out a mayor function for sugar accumulation alone but the regulating function of the C/N balance during induction of monocarpic senescence is widely discussed. Recently, trehalose-6-phosphate (T6P) was identified as a main signaling component in this pathway. T6P inhibits the activity of Snf1-related protein kinase (SnRK1). Zhang et al. (2009) [53] showed the T6P/SnRK1 interaction in Arabidopsis seedling extracts and other young tissues treated with T6P. Additionally, Delatte et al. (2011) [54] confirmed the inhibition of SnRK1 by T6P with plants overexpressing the SnRK1 catalytic subunit gene *KIN10.* These plants were insensitive to trehalose treatments. Further verification of T6P as signaling molecule was provided by several studies. In wheat the interaction of T6P and SnRK1 has been suggested to play a role during grain filling [55]. Wingler et al. (2012) [56] conducted a study with *otsA* and *otsB* expressing Arabidopsis plants *otsA* encodes the bacterial T6P synthase gene, *otsB* the T6P phosphatase gene; therefore, overexpression leads to increasing or decreasing T6P contents, respectively. A significantly higher accumulation of glucose, fructose and sucrose was observed in *otsB* expressing plants and these plants displayed a delayed senescence phenotype. But most interestingly, these plants were rendered less susceptible to the induction of senescence-associated genes by sugar feeding in combination with low nitrogen supply, whereas *otsA* plants induced senescence and anthocyanin synthesis upon external supply of 2% glucose.

Another signaling component involved in senescence induction is light quantity and quality. Senescence can be induced by the darkening of individual leaves. However, darkening of the whole plant resulted in delay rather than in induction of leaf senescence in Arabidopsis and sunflower plants [57, 58]. Brouwer et al. (2012) [59] recently revealed the involvement of photoreceptors in dark and shading induced leaf responses. They applied different shading conditions to single leaves of Arabidopsis plants. Depending on the amount of light perceived, different biological programs were induced, leading to either acclimation to the new light conditions or leaf senescence. Furthermore, *phytochrome A* mutant lines displayed accelerated chlorophyll degradation under all shading conditions except darkness, displaying its involvement in the perception of and adaption to changing light conditions [59].

A tight linkage between stress response and leaf senescence is demonstrated by the function of several members of the NAC- and WRKY-family [60]. For example, *At NTL9 (NAC TRANSCRIPTION FACTOR LIKE 9)* mediates osmotic stress signaling during leaf senes-

cence [61] and *At VNI2 (ANAC083)* has been shown to integrate abscisic acid (ABA)-mediated abiotic stress signals into leaf senescence [62].

Besides various other cues like the stage of plant development, pathogens, extreme temperatures, source-sink transitions and drought, the action of reactive oxygen species (ROS) has been shown to have a severe impact on the induction of leaf senescence. Cellular H_2O_2 levels increase at the onset of senescence due to a complex regulation of hydrogen peroxide scavenging enzymes [63]. The increase in intracellular H_2O_2 levels is initiated via the down-regulation of the expression of the hydrogen peroxide scavenging enzyme CATALASE2 by the transcription factor GBF1 (G-Box binding factor 1). In *gbf1* knock-out plants, the senescence specific elevation in H_2O_2 levels is absent leading to a significant delay of leaf senescence [64]. We have demonstrated recently using a specific *in vivo* hydrogen peroxide monitoring and scavenging system that the pivotal role of H_2O_2 during the induction of developmental leaf senescence in Arabidopsis is depending on the subcellular localization and concentration. Furthermore, a similar senescence-specific up-regulation of H_2O_2 levels and down-regulation of the respective scavenging enzymes was also observed in *Brassica napus* [65]. Knock-out and overexpression plants of *AtOSR1* (*ANAC059* or *ATNAC3*) or *AtJUB1* (*ANAC042*), which are both highly inducible by H_2O_2, were delayed or accelerated, respectively, concerning the onset of leaf senescence in which JUB1 also modulates cellular H_2O_2 levels [66, 67]. Besides their important role in disease resistance [68], several WRKY transcription factors have been suggested to have a striking role in the regulation of leaf senescence. For example AtWRKY53, a H_2O_2-responsive transcription factor, has been indicated to have a function as important control element during the onset of leaf senescence [69].

Conclusively, leaf senescence is governed not only by developmental age but a wide range of various different external and internal factors, biotic and abiotic influences, molecules and cues, which have to be integrated. Despite its enormous agricultural importance, our knowledge of these integrative mechanisms is still limited and needs much more efforts to get complete insight into the regulatory network controlling the onset and progression of leaf senescence.

3.1.1. N-uptake during senescence

Nitrogen uptake and partitioning after beginning anthesis varies greatly between different species and even between ecotypes. An analysis of different Arabidopsis accessions revealed that the fate of nitrogen absorbed during flowering can be different, depending on general N availability and accession. At low nitrogen concentrations most of the N assimilated post-flowering was allocated to the seeds, while under high N regimes the main part of it was distributed to the rosette leaves and successively lost in the dry remains, except for four tested accessions. N13, Sakata, Bl-1 and Oy-0 allocated the nitrogen taken up post-flowering also to the seeds under high N supply [70]. In wheat, a minor portion of grain N is derived from N uptake post-flowering, whereas up to 90-95% is remobilized from other plant tissues [3, 71]. In oilseed rape (*Brassica napus*) the induction of the reproductive phase is accompanied with a drastic down-regulation of nitrogen uptake systems. HATs and HATs + LATs activities are decreased thus almost resulting in an arrest of nitrogen uptake during seed fill-

ing and flowering [14, 72-74]. Grown under non-limiting nitrogen conditions, Arabidopsis displays a lowered nitrate influx during the reproductive stage in comparison to the influx during the vegetative stage [14]. Although many plants seem to continue N uptake during seed filling, this nitrogen is not always allocated to the seeds, thus rendering nitrogen remobilization from senescing organs a central component for the proper development of reproductive organs.

3.2. Nitrogen mobilization

3.2.1. Senescence associated proteases

Protein degradation is most likely the most important degradation process that occurs during senescence [75]. With a combined ^{15}N tracing/proteomics approach, Desclos et al. (2009) [76] have shown that HSP70, chaperonin10 and disulfide isomerase are synthesized during the whole progression of senescence in *B. napus* illustrating the necessity to prevent the aggregation of denatured proteins. In addition, almost all protease families have been associated with some aspects of plant senescence [75].

The aminopeptidase LAP2 has been characterized as exopeptidase liberating N-terminal leucine, methionine and phenylalanine. Arabidopsis *lap2* mutants displayed a significant change in amino acid contents. In particular, nitrogen rich AAs like glutamate and glutamine were dramatically reduced while leucine levels were the same as in wild type plants. Furthermore, a premature leaf senescence phenotype was observed in these plants. Different recombinant inbred lines, which are also modified in Glu, Gln, Asp and Asn contents, also show a senescence phenotype tempting the authors to speculate that the senescence phenotype of *lab2* might be related to a decreased turnover of defective proteins and the marked decrease of nitrogen rich AAs [77].

Chloroplast targeted proteases comprise proteases of the Lon, PreP, Clp, FtsH and DegP type [78-80]. Their substrates include, besides others, chlorophyll apoproteins like LHCII, the D1 protein of the photosystem II reaction center and Rubisco. The Clp protease complex is the most abundant stromal protease, where PreP is also located [78, 79]. Several catalytic subunits of the Clp proteases display up-regulated expression during dark-induced senescence in Arabidopsis, like e.g. ClpD/ERD1 and ClpC1. They possess sequence similarity to the chaperon HSP100 indicating that they might function as recognition subunit in the Clp protease complex to recruit denatured proteins [80]. FtsH proteases are thylakoid bound facing the stroma while Deg proteases are also thylakoid bound but facing stroma as well as thylakoid lumen [81, 82]. DegP2 is responsible for an initial cleavage of the D1 protein, where after FtsH proteases complete the full degradation [80, 83]. These two proteases belong to the family of serine proteases. In wheat, serine proteases are the most important family of proteases participating in N remobilization [84]. Subtilases have been reported to be highly expressed in barley during natural and senescence induced via artificial carbohydrate accumulation. Additionally induced proteases were SAG12, CND41-like, papain-like, serine carboxypeptidase III precursor, aspartic endopeptidases and others [85]. Roberts et al. (2012) [75] suggest a classification of senescence-associated proteases according to their expression

profile and probable function during natural senescence. Class I includes all proteases being expressed in non-senescent and in senescent tissue. Although no senescence specific expression change can be observed, their continued expression in a catabolic environment displays their significance for a normal progression of senescence. Class II contains proteases being expressed at a low level in non-senescent tissue and induced upon senescence onset. Class III comprises proteases which are induced exclusively during senescence. This suggests a role in the late stages of senescence and a probable function in cell death execution. Class IV proteases constitute proteases transiently expressed during onset of senescence which could be involved in early breakdown processes like e.g. chloroplast dismantling. Finally, class V proteases are down-regulated during senescence. These enzymes are likely to fulfill housekeeping protein turnover and other proteolytic functions, which are no longer needed during the progression of leaf senescence [75].

3.2.2. Chloroplast dismantling

Chloroplasts are the first organelles to show visible symptoms of degradation processes during senescence. Containing up to 75% of total leaf nitrogen, chloroplasts are the main source for its remobilization [86]. Four different pathways have been proposed for chloroplast and chloroplastic protein degradation: I) endogenous proteases degrade proteins intra-plastidial, II) degradation of stroma fragments in an extraplastidic, non-autophagic pathway, as well as III) extraplastidic degradation by autophagy-associated pathways, and IV) autophagic degradation of entire plastids [87]. Chloroplast breakdown is not a chaotic decay, but rather an organized and selective process. As chloroplasts are one of the plants main ROS-producing organelles, and due to the potential phototoxicity of many chloroplastic components and their degradation intermediates, a coordinated dismantling process is necessary to prevent severe cell damage [88, 89].

Within these organelles Rubisco represents the most abundant protein. Its abundance exceeds the requirements for photosynthesis by far, thus a nitrogen storage function has been suggested for it [90]. In chloroplasts isolated from senescing leaves a 44 kDa fragment of Rubisco's large subunit accumulates, but seems not to be degraded further [91]. The chloroplastic aspartate protease CND41 has been shown to degrade denatured Rubisco, but not active Rubisco *in vitro* [92]. This protease might be involved directly in Rubisco degradation, as accumulation of CND41 correlates with loss of Rubisco [93]. However, tobacco CND41 antisense lines also show a dwarf phenotype, reduced gibberellin levels and reduced leaf expansion, thus this correlation could be an indirect effect through gibberellin homeostasis [94]. Rubisco containing bodies (RCB) have been found to be shuttling from the chloroplast to the central vacuole via an autophagy-dependent pathway [95]. The autophagy-dependency of these bodies was shown using *atg4a4b-1*mutants which are impaired in autophagy. Chloroplast fate was investigated in individually darkened leaves (IDLs) of wild type plants and *atg4a4b-1* mutants since individual darkening of leaves has been shown to rapidly induce senescence [57]. Wild type plants showed a decrease in chloroplast number and size as well as formation of RCBs. A*tg4a4b-1* mutant lines also displayed a decrease in chloroplast size but RCB formation was abolished and also the count of chloroplasts stayed constant.

However, Rubisco, nitrogen, soluble protein and chlorophyll contents decreased at almost the same rate in wild type plants as in *atg4a4b-1* mutant plants. This suggests alternative, autophagy-independent protein degradation pathways [96]. Lastly, despite the earlier mentioned 44 kDa Rubisco fragment observed in isolated chloroplasts, oxidative stress conditions might also initiate degradation of Rubisco's large subunit, as under these conditions the large subunit is split into a 37 and a 16 kDa fragment [97].

Besides the RCBs, senescence-associated vacuoles (SAVs) have been described. These vacuoles, enclosed by a single membrane layer, are enriched in Rubisco and display a high proteolytic activity at a pH more acidic than the central vacuole's. SAVs are structurally not related to RCBs which posses a double layer membrane [95, 98]. The double layer membrane enclosing the RCBs appears to be derived from the chloroplast envelope [95]. Furthermore, SAV development seems to be autophagy-independent, as Arabidopsis *atapg7-1* mutant lines show normal SAV formation [98]. SAVs are only formed in leaf mesophyll cells. They are approximately 700 nm in diameter and can be labeled with antibodies against the (H+)-pyrophosphatase, an Arabidopsis vacuolar marker indicating these organelles indeed to be vacuoles [98]. Accumulation of stromal proteins in the SAVs was proven via plastid localized GFP which localized in SAVs in senescing tobacco leaves. In addition, high levels of chloroplastic glutamine synthase could be detected within these vacuoles [89]. Although the chlorophyll degradation pathway has been elucidated to a large extend and the first steps are regarded to occur within the plastid [88, 99], chlorophyll *a* has been found in SAVs under certain conditions, thus an alternative degradation pathway can be proposed [89]. Despite SAG12 has been shown to localize in SAVs, *sag12* mutant lines did neither show impairment in SAV formation nor in the proteolytic activity within the SAVs [98].

Even though chlorophyll represents about 2% of the total cellular nitrogen content [86], N fixed in chlorophyll is not exported from the leaf but rather remains in the vacuole [100]. However, around 20% N are fixed in proteins associated with or directly binding chlorophyll [88] and removal of chlorophyll seems to be a prerequisite for degradation of the corresponding apoproteins [88]. Pheophorbide a oxygenase (PAO) is an iron-dependent monooxygenase localized to the inner envelope of maturing gerontoplasts and catalyzes the conversion of pheophorbide a to red chlorophyll catabolites, one of the first steps during chlorophyll degradation. It represents a key control point in regulation of chlorophyll degradation [88, 101, 102]. In *pao* mutants and other stay green mutants affected in PAO activity and thus impaired chlorophyll degradation, this retention is accompanied with the accumulation of chlorophyll apoproteins like LHCII (see [88] and references within).

3.2.3. Autophagy

Autophagy plays a crucial role for nitrogen remobilization. The most striking phenotype of all *atg* mutants is hypersensitivity to nitrogen starvation ([103] and references within). Furthermore, an age dependent early senescence phenotype can be observed. As autophagy is involved in molecule degradation one would expect delayed senescence if this pathway is blocked. One hypothesis explaining this contradiction is that the autophagy pathway is normally activated at an early stage of senescence starting to degrade plastid proteins while

leaving the photosynthetic apparatus intact. However, when autophagy is blocked, it is speculated that autophagy-independent pathways for chloroplast protein degradation might be activated untimely leading to premature chloroplast and chlorophyll degradation and thus to an early senescence phenotype [104]. Recently, Guiboileau et al. (2012) [103] conducted a study on the impact of *atg* mutants *(atg5, atg9* and RNAi18) on nitrogen remobilization. These plants were grown under ample and low nitrate conditions. In comparison to wild type plants the dry weight as well as the seed weight was lowered. However, when calculating the harvest index, *atg* mutants did not display a significant difference, except for the *atg5* mutant line at low N conditions. When the nitrogen use and remobilization efficiency was investigated via ^{15}N tracing experiments, all *atg* lines showed a decrease in this feature. It was demonstrated that remobilization was significantly impaired, as N contents in the plants dry remains were enriched and ^{15}N previously partitioned to the leaves was not mobilized to the seeds. To verify that this impairment rests on an autophagy defect and not on premature senescence and cell death symptoms, *atg5* mutants were combined with two SA signaling mutants, *sid2* and *nahG*, overriding the early senescence phenotype. These mutants reached nearly wild type biomass levels, but did not compensate the decrease in NRE. These results and the finding that autophagy regulates SA levels in a negative feedback loop [105] suggest, that the premature senescence phenotype in *atg* mutants is at least in part mediated by increased SA levels [104]. Conclusively, blocked autophagy pathways might result in an early senescence phenotype because of the accumulation of damaged and thus potentially toxic molecules in combination with a missing negative feedback on SA levels leading to cell death and activation of alternative pathways for bulk protein degradation.

3.2.4. Re-assimilation and translocation of salvaged nitrogen

As mentioned above, chloroplastic glutamine synthetase (GS2), GOGAT, NiR and Rubisco are targeted for rapid degradation already during early phases of senescence, disrupting primary nitrogen assimilation. Proteolysis in the vacuole feeds into the cellular pool of free AAs during the progression of senescence. The steady-state concentrations of free AAs depend on the rate of their release due to proteolysis and their efflux into growing structures [106]. Soudry et al. (2005) [106] have utilized a bioluminescence assay combined with auxotrophic bacteria for the detection of free tryptophan levels. They assumed that tryptophan reflects the overall pool of free AAs, as it is not modified before its export into sink organs. An accumulation of free AAs was observed in detached oat and Arabidopsis leaves. While attached oat leaves showed a gradual decrease in tryptophan levels during further progression of senescence, the attached Arabidopsis leaves did not or only due to membrane leakage resulting from the experimental procedure. The authors concluded that not only source strength but also sink strength is important for successful nutrient remobilization and suggested that the small reproductive organs of Arabidopsis exerted too weak sink strength. However, these findings might be related to the experimental design, as Arabidopsis does indeed remobilize N for seed filling [70] and Diaz et al. (2005) [52] reported decreasing levels for several AAs during the progression of leaf senescence in Arabidopsis. Protein breakdown increases free AAs in the cell. While some seem to be exported without prior modification, many are probably modified, hydrolyzed or interconverted. Expressional

profiling revealed that, besides others, the cytosolic GS1, glutamate dehydrogenase (GDH) and asparagine synthetase (AS) are specifically induced during senescence [14]. A series of transamination reactions would result in an accumulation of glutamate, which could serve as substrate for GDH. Deamination of glutamate via GDH provides then 2OG and ammonia. NH_3 could then in turn be used as substrate for cytosolic GS1, giving rise to glutamine, which is one of the major nitrogen transport forms during nutrient remobilization. In fact many studies strengthen a positive correlation between GS activity and yield as well as grain and stem N content. Martin et al. (2006) [107] identified two cytosolic glutamine synthetase isoforms in maize which have a major impact on kernel size and yield. In wheat, GS activity was also positively linked with grain and stem N content [71]. Recently, two rice varieties with different levels of GS2 activity were analyzed and plants with higher activity displayed less NH_3 emission due to photorespiration and a better ability to recycle and reassimilate ammonia within the plant [108]. In barley amino acid permeases (AAP) seem to play a significant role during N retranslocation and grain filling. Recent RNA-Seq data revealed an overrepresentation of this gene family in both source and sink tissues. Furthermore, the grain-specific HvAAP3, which was also identified in this study, has high sequence similarity to Arabidopsis AAP1 and AAP8, which have been already shown to be involved in seed N supply (see [109] and references within).

Asparagine amounts also increase significantly in whole rosettes darkened for several days as well as in senescent leaves (see e.g. [1, 80]). Besides the senescence specific up-regulation of AS, pyruvate orthophosphate dikinase (PPDK) expression is also significantly increased during dark-induced senescence [80]. PPDK might have a role in carbon salvage after lipid degradation, thus Lin and Wu (2004) [80] also investigated other pathways possibly involved in this process. Remarkably, they found only a few components of these pathways to be up-regulated and many others even down-regulated. Based on their expressional profiling data, they postulated a alternative pathway for asparagine synthesis, where PPDK delivers metabolic precursors [80]. Additionally, seed protein contents were elevated and viability of seedlings was increased on nitrogen-limiting media in Arabidopsis *ASN1* overexpressor lines (*35S*::*ASN1*). Furthermore, they observed more Asn to be allocated to flowers and developing siliques and also higher Asn contents in phloem exudates [80, 110].

Nitrogen is not only remobilized from older leaves via amino acids. Nitrate and ammonia are also translocated to developing sink tissues. Fan et al. (2009) [111] identified a nitrate transporter (NRT1-7) which is involved in remobilization processes. Arabidopsis *nrt1-7* mutants displayed retarded growth under nitrogen starvation conditions. Also the spatial expression of this transporter in phloem tissue of older leaves and the expressional induction upon nitrogen starvation points out its function in nitrogen remobilization. Finally, the inability of *nrt1-7* mutants to remobilize ^{15}N from old to young leaves and the high accumulation of nitrate in old leaves in this mutants further underlines this assumption [111]. Another nitrate transporter involved in remobilization is NRT2-4. This transporter acts in the high-affinity range and its expression is also induced upon nitrogen starvation. Additionally, *nrt2-4* mutant lines had lower phloem sap nitrate contents. However, *nrt2-4* mutants were not altered in growth or development, indicating that the decreased NO_3-levels

are not limiting for the adaption to N starvation and most likely functionally redundant transporter systems exist [40].

4. Reactive oxygen and nitrogen species in signaling

Reactive oxygen and nitrogen species (ROS, RNS) play a central role in many aspects of plant development and response to environmental influences. These include among others responses to wounding, pathogen infection, drought and water stress, high salinity, cold and heat. In the case of ROS, research has focused especially on H_2O_2. As this reactive oxygen molecule is relatively long lived (~1 ms half life), small and uncharged, and thus is able to pass membranes, a central position in various signaling pathways has been attributed to it. Nitric oxide (NO) has been shown to be involved in many of the H_2O_2-mediated pathways in either a synergistic or antagonistic mode of action. In the following we will briefly introduce the production and scavenging mechanisms for this two reactive oxygen and nitrogen compounds and their interplay in regulation of developmental processes, stress responses and senescence will be outlined.

4.1. ROS and RNS: Molecule types, production and scavenging

Many of the reactive oxygen species in the cell are formed as toxic byproducts of metabolic processes. Photorespiration and β-oxidation of fatty acids produce H_2O_2 in peroxisomes and glyoxisomes, which is normally scavenged by an extensive protection system mainly consisting of catalases (CAT) and ascorbate peroxidases (APX). Xanthine oxidase generates superoxide anions in the peroxisomes, which is converted by superoxide dismutases (SOD) into O_2 and H_2O_2. Chloroplasts are the main site for ROS production in plants. Due to the photooxidative nature of many of their components they can give rise to superoxide radicals, hydrogen peroxide, hydroxyl radicals and singlet oxygen. ROS produced in the chloroplasts are mainly scavenged by the ascorbate-glutathione cycle [112]. SODs scavenge superoxide anions and dismutate them to O_2 and H_2O_2, which is then in turn reduced to water by the action of ascorbate peroxidase and ascorbate. The resulting monodehydro-ascorbate (MDHA) is regenerated either via the MDHA reductase (MDHAR) under the use of NADPH or it spontaneously converts into dehydroascorbate (DHA) which is then reduced to ascorbate again via the DHA reductase (DHAR). DHAR uses glutathione (GSH) as second substrate. The reduced state of GSH is reconstituted by glutathione reductase (GR). Excess oxidized GSSG seems to be exported from the cytosol to the central vacuole and the chloroplasts to maintain a reduced environment and redox homeostasis in the cytosol and possibly the nucleus [113]. Finally, superoxide radicals can be produced as a byproduct during respiration in mitochondria. Here, also SOD and the ascorbate-glutathione cycle removes the ROS. Further ROS scavenging in this organelle is mediated by peroxiredoxins and thioredoxins, as it is also observed in chloroplasts. Additionally, non-enzymatic components like tocopherols, flavonoids, ascorbic acid and others are employed in the extensive and elaborate ROS detoxification system (reviewed in [114-119]). Under optimal growth conditions,

http://dx.doi.org/10.5772/54392

ROS production is relatively low; however, during stress, the production of ROS is rapidly enhanced [120].

Active production of ROS or the so called "oxidative burst" is initiated upon several stresses and developmental stimuli. The main enzymes generating these ROS are the respiratory burst oxidase homologs (RBOH) [121]. In a NADPH-dependent reaction they form O_2^- in the apoplast. This is then converted by SODs to H_2O_2. The function of the 10 different RBOH proteins identified in Arabidopsis [122] is important in various developmental and regulatory processes. Root elongation is reduced in *atrbohD/F* mutants [122]. ROS produced upon pathogen attack are generated by RBOHs (see for example [123]). Also the response to heavy metals seems to be at least in part mediated by RBOH proteins. Cadmium treated sunflower leaf discs showed an altered expression and activity of the NADPH oxidase [124]. The function of these proteins is often associated with the action of Ca^{2+}. Arabidopsis *rbohC/rhd2* mutants displayed lowered ROS contents in growing root hairs and a distortion in Ca^{2+} uptake due to a missing activation of Ca^{2+} channels [125], although for the rice RBOHB homolog calcium was needed to activate the oxidase itself [126].

Reactive nitrogen species (RNS) comprise NO and NO-derived molecules as di-nitrogen trioxide, nitrogen dioxide, peroxynitrite, S-nitrosothiols and others [127]. NO production in plant cells is under continuous debate. Especially the existence of a plant nitric oxide synthase (NOS) is a controversial topic. Until today, there is no clear proof for the existence of NOS in plants although there is indirect evidence through the application of NOS inhibitors, which have been established for mammalian cells (e.g. L-NAME a L-arginine analogue) in combination with NR inhibitors, or the measurement of NOS-like activity, like the conversion of L-arginine to citrulline, where NO is assumed to be produced at the same time [128-130]. AtNOS1 was identified in 2003 by Guo et al. (2003) [131], but is under controversial discussion ever since. Indeed, *atnos1* mutant plants do exhibit significantly lower NO contents, a chlorotic phenotype in seedlings which can be rescued by NO application and an early-senescence phenotype, but expression of the corresponding genes from Arabidopsis, maize and rice revealed no NOS activity *in-vitro*, and even the mammalian orthologous displayed no NOS function [132]. Thus *AtNOS1* was renamed to *AtNOA1* (NO associated 1). Nevertheless, there are other enzymatic ways known to produce NO. NR was found to be able to generate NO. It was shown to be involved in NO generation during the transition to flowering Arabidopsis *nr1* and *nr2* mutants display a low endogenous NO content [133, 134]. Additionally, a NR- and NiR-independent pathway of NO production has been proposed via electron carriers of the mitochondrial respiratory chain [135] and an oxidation-associated pathway for NO synthesis has been suggested as hydroxylamines can be oxidized by superoxide and H_2O_2 generating NO [136].

Despite all the controversy on the topic of NO generation, it seems clear, that there are many ways to generate NO in plant cells and the pivotal role in many regulatory pathways cannot be denied. Involvement in fruit ripening, leaf senescence, flowering and stomatal closure and many other processes has been shown ([129] and references within).

4.2. ROS and RNS: Signaling

The role of H_2O_2 and NO during the onset of leaf senescence has been investigated in many studies. Recently, an upstream regulator of the ROS network during ABA-mediated drought-induced leaf senescence has been identified. The drought-responsive NAC transcription factor AtNTL4 (ANAC053) has been shown to promote ROS production by directly binding to promoters of genes encoding ROS biosynthetic enzymes [137]. In guard cells, an ABA-H_2O_2-NO signaling cascade has been proposed for stomatal closure. H_2O_2-induced generation of NO in guard cells has been reported for mung bean [138], Arabidopsis [139] and other plant species (see for example [140]). Removal of H_2O_2 as well as the blocking of calcium channels was able to suppress NO generation [138, 141]. A further interaction of NO and H_2O_2 was studied in tomato (*Lycopersicon esculentum* Mill. cv. "Perkoz") where the effect of application of exogenous NO scavengers and generators was analyzed in combination with *Botrytis cinerea* inoculation. NO generators specifically reduced H_2O_2 generation and thus allowed the infection to spread significantly under control conditions and in comparison to NO scavenger pre-treated leaves [142]. Moreover, cytoplasmic H_2O_2 can also directly activate a specific Arabidopsis MAP triple kinase, AtANP1, which initiates a phosphorylation cascade involving two stress AtMAPKs, AtMPK3 and AtMPK6 [143]. A direct interaction between AtMPK6 and AtNR2 during lateral root development has been shown *in-vitro* and *in-vivo*. During this interaction MPK6 phosphorylates and thus activates NR2 resulting in enhanced NO production [144]. Finally, another point of crosstalk between the NO and H_2O_2 signaling pathways has been referred to by positional cloning of the rice *NOE1*. This gene codes for a rice catalase, a knock-out leads to increased H_2O_2 contents which in turn enhance the activity of NR, resulting in elevated NO concentrations. The removal of excess NO ameliorated the cell death symptoms of the *noe1* mutants pointing out a cooperative function of H_2O_2 and NO during induction of PCD. Here, specifically S-nitrosylated proteins were identified, and overexpression of a rice S-nitrosoglutathione reductase could also alleviate the cell death symptoms [145].

Senescence-inhibiting features of NO have long been recognized, while H_2O_2 has often been attributed with senescence-promoting features. Exogenous NO application extends postharvest life of fruits and vegetables and, during leaf maturation in pea, NO contents gradually decrease [146, 147]. Furthermore, NO-deficient mutants display an early-senescence phenotype and the heterologues expression of an NO-degrading enzyme in Arabidopsis also leads to early leaf senescence and SAG up-regulation, which could be inhibited by external supply of NO [148]. Remarkably, the senescence delaying features of NO might be achieved due its ability to scavenge various kinds of ROS. In barley aleuron cells, NO has been shown to act as an antioxidant and thus alleviating GA-mediated PCD induction [149].

4.3. Specificity in ROS and RNS signaling

Some amino acids are more susceptible for modification by ROS and RNS than others. For example cysteins are often found to be preferentially oxidized. These residues are sensitive for ROS-derived protein carbonylation and RNS-mediated nitrosylation (-SNO) and glutahionylation. Additionally, sulfenic acid and disulfide formation also can be mediat-

ed via ROS and RNS on these residues. Tryptophane residues have been shown to be specifically di-oxygenized in plant mitochondria, thus forming N-formylkynurenine. The proteins found to be specifically oxygenized did, with one exception, all posses redox-activity or were involved in redox-active proteins [150]. Another good example for this specificity is Rubisco. Preferential oxidation of certain cysteine residues mediates the binding of Rubisco to the chloroplast envelope, thus causing catalytic inactivation and marking it for degradation [151, 152]. Recently, it has been shown, that chloroplast peroxidases are present in an inactivated form and become activated in part by proteolytic cleavage upon a H_2O_2 signal; in combination with newly synthesized peroxidases, they regulate plastidial ROS content in neem (*Azadirachta indica* A. juss) chloroplasts [153]. This displays a specificity of ROS induced processes, rather than undirected, detrimental impacts. However, how the cell responds differentially to the variety of H_2O_2 signals in different signaling pathways is still unclear. With regard to leaf senescence induction, a dependency of H_2O_2-mediated effects on the subcellular location was discovered. By using an *in-vivo* H_2O_2-scavenging system, we manipulated H_2O_2 contents in the cytosol and peroxisomes in Arabidopsis. While both lines showed lowered H_2O_2 contents and a delayed leaf senescence phenotype, the delay of the cytoplasmic line was more pronounced, despite the higher expression of the peroxisomal transgene [65]. Furthermore, lowering mitochondrial H_2O_2 production by blocking cytochrome *c* dependent respiration with the fungal toxin antimycin A had no effect on induction of leaf senescence [154]. Since senescence is predominantly regulated on transcriptional level, the cytoplasmic compartment might have a direct influence on redox regulation of transcription factors. Expression of the MAP triple kinase1 (*MEKK1*) of Arabidopsis can also be induced by H_2O_2 and shows its expression maximum during onset of leaf senescence [155]. Whether H_2O_2 induced expression of SAGs is transduced by MAPK signaling or directly by redox-sensitive transcription factors has yet to be elucidated.

Moreover, the already mentioned evidence of numerous selective oxidation reactions on specific amino acid residues depending on the type of ROS/RNS might lead to the degradation of the damaged proteins, thus generating distinct peptide patterns. These peptides would contain information being ROS- and source-specific (see [150] and references within). Spatial control might also be a source of specificity, as for example RBOH proteins are membrane bound and, therefore, localization of the ROS signal could be highly specific. Additionally, through the extensive detoxification system, ROS signals also might be spatially confined. In contrast, ROS signal auto-propagation over long distances via RBOHD induced by various stimuli has been shown in Arabidopsis [156]. Interestingly, temporal oscillation of ROS bursts has been observed to modulate root tip growth of Arabidopsis root hairs [157]. Finally, integration of metabolic reactions also seems to be a convenient way of specific signaling. Local blockage or enhancement of certain pathways would lead to the accumulation of intermediates, which in turn could serve for signaling functions (reviewed in [158]).

5. Concluding remarks

The intriguing connection between efficient nutrient remobilization and progression of leaf senescence is obvious. The correct timing of onset and progression of senescence has great influence on seed and fruit development and viability. Therefore, manipulating leaf senescence seems to be a promising trait to increase yield in various crop species. Functional stay green traits can prolong carbon assimilation and thus increase yield. However, a too strong delay in leaf senescence might hamper nutrient and especially nitrogen remobilization from the leaves. For various wheat mutants, Derkx et al. (2012) [159] speculated that the stay green phenotype might be associated with a decrease in grain N sink strength. Gpc-B1, a QTL locus in wheat, which is among others associated with increased grain protein content, has been shown to encode a NAC transcription factor (*NAM-B1*). It accelerates senescence and enhances nutrient remobilization from leaves. RNA interference mediated silencing of multiple homologues resulted in a delay of leaf senescence by approximately 3 weeks and decreased grain protein, iron and zinc content by more than 30% [160]. This indicates that the relation between senescence and nitrogen mobilization is very complicated and cannot be modified as easy as expected.

Besides QTL selection, transgenic approaches to increase nitrogen use efficiency in crop plants have been extensively studied. For example expression of alanine aminotransferase and asparagine synthase often resulted in enhanced seed protein content and higher seed yield. Increased cytokinin biosynthesis almost always resulted in delayed senescence and was sometimes associated with higher seed yield, seed protein content and increased biomass. Expression of amino acid permease from V*icia faba* under the *LeB4* promoter increased the seed size by 20-30%, as well as the abundance of nitrogen rich AAs and the content of seed storage proteins in the seeds (reviewed in [161]).

Nevertheless, although transgenic approaches have proven to enhance nitrogen use efficiencies and yield quantity as well as quality, these techniques have to cope with general skepticism on the consumer's side. Although approval for the agricultural use of genetically modified organisms has been extensively performed like e.g. in the Swiss National Research program NRP 59 (Benefits and risks of the deliberated release of genetically modified plants) clearly indicating a low risk and a enormously high potential of transgenic crop plants, problems with the acceptance of this technology, especially in Europe, still have to be faced.

Author details

Stefan Bieker and Ulrike Zentgraf

General Genetics, University of Tuebingen, Tuebingen, Germany

http://dx.doi.org/10.5772/54392

References

[1] Diaz C, Lemaître T, Christ A, Azzopardi M, Kato Y, Sato F, et al. Nitrogen Recycling and Remobilization Are Differentially Controlled by Leaf Senescence and Development Stage in Arabidopsis under Low Nitrogen Nutrition. Plant Physiology. 2008 July 2008;147(3):1437-49.

[2] Luquez VMC, Sasal Y, Medrano M, Martín MI, Mujica M, Guiamét JJ. Quantitative trait loci analysis of leaf and plant longevity in Arabidopsis thaliana. Journal of Experimental Botany. 2006 March 2006;57(6):1363-72.

[3] Kichey T, Hirel B, Heumez E, Dubois F, Le Gouis J. In winter wheat (Triticum aestivum L.), post-anthesis nitrogen uptake and remobilisation to the grain correlates with agronomic traits and nitrogen physiological markers. Field Crop Res. 2007 Apr 30;102(1):22-32.

[4] Breeze E, Harrison E, McHattie S, Hughes L, Hickman R, Hill C, et al. High-resolution temporal profiling of transcripts during Arabidopsis leaf senescence reveals a distinct chronology of processes and regulation. Plant Cell. 2011 Mar;23(3):873-94.

[5] Lim PO, Kim HJ, Nam HG. Leaf senescence. Annual Review of Plant Biology. 2007;58:115-36.

[6] Grbic V, Bleecker AB. Ethylene Regulates the Timing of Leaf Senescence in Arabidopsis. Plant Journal. 1995 Oct;8(4):595-602.

[7] Kim HJ, Ryu H, Hong SH, Woo HR, Lim PO, Lee IC, et al. Cytokinin-mediated control of leaf longevity by AHK3 through phosphorylation of ARR2 in Arabidopsis. P Natl Acad Sci USA. 2006 Jan 17;103(3):814-9.

[8] Lee IC, Hong SW, Whang SS, Lim PO, Nam HG, Koo JC. Age-Dependent Action of an ABA-Inducible Receptor Kinase, RPK1, as a Positive Regulator of Senescence in Arabidopsis Leaves. Plant and Cell Physiology. 2011 Apr;52(4):651-62.

[9] Osakabe Y, Maruyama K, Seki M, Satou M, Shinozaki K, Yamaguchi-Shinozaki K. Leucine-rich repeat receptor-like kinase1 is a key membrane-bound regulator of abscisic acid early signaling in Arabidopsis. Plant Cell. 2005 Apr;17(4):1105-19.

[10] Osakabe Y, Mizuno S, Tanaka H, Maruyama K, Osakabe K, Todaka D, et al. Overproduction of the Membrane-bound Receptor-like Protein Kinase 1, RPK1, Enhances Abiotic Stress Tolerance in Arabidopsis. J Biol Chem. 2010 Mar 19;285(12):9190-201.

[11] Division DoEaSAP. World Population Prospects: The 2008 Revision, Highlights. Popul Dev Rev. 2010 Dec;36(4):854-5.

[12] Tilman D, Cassman KG, Matson PA, Naylor R, Polasky S. Agricultural sustainability and intensive production practices. Nature. 2002 Aug 8;418(6898):671-7.

[13] Ribaudo M, Delgado J, Hansen LT, Livingston M, Mosheim R, Williamson JM. Nitrogen in Agricultural Systems: Implications for Conservation Policy. United States Department of Agriculture, Economic Research Service, 2011.

[14] Masclaux-Daubresse C, Daniel-Vedele F, Dechorgnat J, Chardon F, Gaufichon L, Suzuki A. Nitrogen uptake, assimilation and remobilization in plants: challenges for sustainable and productive agriculture. Ann Bot. 2010 Jun;105(7):1141-57.

[15] Good AG, Shrawat AK, Muench DG. Can less yield more? Is reducing nutrient input into the environment compatible with maintaining crop production? Trends in Plant Science. 2004 Dec;9(12):597-605.

[16] Peoples MB, Freney JR, Mosier AR. Minimizing gaseous losses of nitrogen. In: Bacon PE, editor. Nitrogen fertilization in the environment. New York et al.: Marcel Dekker, Inc.; 1995. p. 565-602.

[17] Bogard M, Jourdan M, Allard V, Martre P, Perretant MR, Ravel C, et al. Anthesis date mainly explained correlations between post-anthesis leaf senescence, grain yield, and grain protein concentration in a winter wheat population segregating for flowering time QTLs. Journal of Experimental Botany. 2011 Jun;62(10):3621-36.

[18] Oury FX, Godin C. Yield and grain protein concentration in bread wheat: how to use the negative relationship between the two characters to identify favourable genotypes? Euphytica. 2007 Sep;157(1-2):45-57.

[19] Maathuis FJM. Physiological functions of mineral macronutrients. Current Opinion in Plant Biology. 2009 Jun;12(3):250-8.

[20] De Angeli A, Monachello D, Ephritikhine G, Frachisse JM, Thomine S, Gambale F, et al. The nitrate/proton antiporter AtCLCa mediates nitrate accumulation in plant vacuoles. Nature. 2006 Aug 24;442(7105):939-42.

[21] von der Fecht-Bartenbach J, Bogner M, Dynowski M, Ludewig U. CLC-b-Mediated NO3-/H+ Exchange Across the Tonoplast of Arabidopsis Vacuoles. Plant and Cell Physiology. 2010 Jun;51(6):960-8.

[22] Tsay YF, Chiu CC, Tsai CB, Ho CH, Hsu PK. Nitrate transporters and peptide transporters. Febs Letters. 2007 May 25;581(12):2290-300.

[23] Huang NC, Liu KH, Lo HJ, Tsay YF. Cloning and functional characterization of an Arabidopsis nitrate transporter gene that encodes a constitutive component of low-affinity uptake. Plant Cell. 1999 Aug;11(8):1381-92.

[24] Touraine B, Glass ADM. NO3- and ClO3- fluxes in the chl1-5 mutant of Arabidopsis thaliana - Does the CHL1-5 gene encode a low-affinity NO3- transporter? Plant Physiology. 1997 May;114(1):137-44.

[25] Tsay YF, Schroeder JI, Feldmann KA, Crawford NM. The Herbicide Sensitivity Gene Chl1 of Arabidopsis Encodes a Nitrate-Inducible Nitrate Transporter. Cell. 1993 Mar 12;72(5):705-13.

[26] Liu KH, Huang CY, Tsay YF. CHL1 is a dual-affinity nitrate transporter of arabidopsis involved in multiple phases of nitrate uptake. Plant Cell. 1999 May;11(5):865-74.

[27] Wang RC, Liu D, Crawford NM. The Arabidopsis CHL1 protein plays a major role in high-affinity nitrate uptake. P Natl Acad Sci USA. 1998 Dec 8;95(25):15134-9.

[28] Liu KH, Tsay YF. Switching between the two action modes of the dual-affinity nitrate transporter CHL1 by phosphorylation. EMBO J. 2003 Mar 3;22(5):1005-13.

[29] Ho CH, Lin SH, Hu HC, Tsay YF. CHL1 functions as a nitrate sensor in plants. Cell. 2009 Sep 18;138(6):1184-94.

[30] Lin SH, Kuo HF, Canivenc G, Lin CS, Lepetit M, Hsu PK, et al. Mutation of the Arabidopsis NRT1.5 nitrate transporter causes defective root-to-shoot nitrate transport. Plant Cell. 2008 Sep;20(9):2514-28.

[31] Chiu CC, Lin CS, Hsia AP, Su RC, Lin HL, Tsay YF. Mutation of a nitrate transporter, AtNRT1:4, results in a reduced petiole nitrate content and altered leaf development. Plant & cell physiology. 2004 Sep;45(9):1139-48.

[32] Almagro A, Lin SH, Tsay YF. Characterization of the Arabidopsis nitrate transporter NRT1.6 reveals a role of nitrate in early embryo development. Plant Cell. 2008 Dec; 20(12):3289-99.

[33] Li JY, Fu YL, Pike SM, Bao J, Tian W, Zhang Y, et al. The Arabidopsis nitrate transporter NRT1.8 functions in nitrate removal from the xylem sap and mediates cadmium tolerance. Plant Cell. 2010 May;22(5):1633-46.

[34] Wang YY, Tsay YF. Arabidopsis Nitrate Transporter NRT1.9 Is Important in Phloem Nitrate Transport. Plant Cell. 2011 May;23(5):1945-57.

[35] Filleur S, Dorbe MF, Cerezo M, Orsel M, Granier F, Gojon A, et al. An Arabidopsis T-DNA mutant affected in Nrt2 genes is impaired in nitrate uptake. Febs Letters. 2001 Feb 2;489(2-3):220-4.

[36] Little DY, Rao HY, Oliva S, Daniel-Vedele F, Krapp A, Malamy JE. The putative high-affinity nitrate transporter NRT2.1 represses lateral root initiation in response to nutritional cues. P Natl Acad Sci USA. 2005 Sep 20;102(38):13693-8.

[37] Zhou JJ, Fernandez E, Galvan A, Miller AJ. A high affinity nitrate transport system from Chlamydomonas requires two gene products. Febs Letters. 2000 Jan 28;466(2-3): 225-7.

[38] Orsel M, Chopin F, Leleu O, Smith SJ, Krapp A, Daniel-Vedele F, et al. Characterization of a two-component high-affinity nitrate uptake system in Arabidopsis. Physiology and protein-protein interaction. Plant Physiology. 2006 Nov;142(3):1304-17.

[39] Chopin F, Orsel M, Dorbe MF, Chardon F, Truong HN, Miller AJ, et al. The Arabidopsis ATNRT2.7 nitrate transporter controls nitrate content in seeds. Plant Cell. 2007 May;19(5):1590-602.

[40] Kiba T, Feria-Bourrellier AB, Lafouge F, Lezhneva L, Boutet-Mercey S, Orsel M, et al. The Arabidopsis nitrate transporter NRT2.4 plays a double role in roots and shoots of nitrogen-starved plants. Plant Cell. 2012 Jan;24(1):245-58.

[41] Loque D, von Wiren N. Regulatory levels for the transport of ammonium in plant roots. J Exp Bot. 2004 Jun;55(401):1293-305.

[42] Yuan L, Loque D, Ye F, Frommer WB, von Wiren N. Nitrogen-dependent posttranscriptional regulation of the ammonium transporter AtAMT1;1. Plant Physiol. 2007 Feb;143(2):732-44.

[43] Loque D, Yuan L, Kojima S, Gojon A, Wirth J, Gazzarrini S, et al. Additive contribution of AMT1;1 and AMT1;3 to high-affinity ammonium uptake across the plasma membrane of nitrogen-deficient Arabidopsis roots. Plant J. 2006 Nov;48(4):522-34.

[44] Kaiser BN, Rawat SR, Siddiqi MY, Masle J, Glass AD. Functional analysis of an Arabidopsis T-DNA "knockout" of the high-affinity NH4(+) transporter AtAMT1;1. Plant Physiol. 2002 Nov;130(3):1263-75.

[45] Okumoto S, Pilot G. Amino Acid Export in Plants: A Missing Link in Nitrogen Cycling. Molecular Plant. 2011 February 15, 2011.

[46] Schjoerring JK, Husted S, Mack G, Mattsson M. The regulation of ammonium translocation in plants. J Exp Bot. 2002 Apr;53(370):883-90.

[47] Zheng Z-L. Carbon and nitrogen nutrient balance signaling in plants. Plant Signaling & Behavior. 2009;4(7):584-91.

[48] Lawlor DW. Carbon and nitrogen assimilation in relation to yield: mechanisms are the key to understanding production systems. Journal of Experimental Botany. 2002 April 15, 2002;53(370):773-87.

[49] Dechorgnat J, Nguyen CT, Armengaud P, Jossier M, Diatloff E, Filleur S, et al. From the soil to the seeds: the long journey of nitrate in plants. J Exp Bot. 2011 Feb;62(4): 1349-59.

[50] Wingler A, Purdy S, MacLean JA, Pourtau N. The role of sugars in integrating environmental signals during the regulation of leaf senescence. J Exp Bot. 2006;57(2): 391-9.

[51] Aguera E, Cabello P, de la Haba P. Induction of leaf senescence by low nitrogen nutrition in sunflower (Helianthus annuus) plants. Physiol Plant. 2010 Mar;138(3): 256-67.

[52] Diaz C, Purdy S, Christ A, Morot-Gaudry J-F, Wingler A, Masclaux-Daubresse C. Characterization of Markers to Determine the Extent and Variability of Leaf Senescence in Arabidopsis. A Metabolic Profiling Approach. Plant Physiology. 2005 June 2005;138(2):898-908.

[53] Zhang Y, Primavesi LF, Jhurreea D, Andralojc PJ, Mitchell RAC, Powers SJ, et al. Inhibition of SNF1-Related Protein Kinase1 Activity and Regulation of Metabolic Pathways by Trehalose-6-Phosphate. Plant Physiology. 2009 April 2009;149(4):1860-71.

[54] Delatte TL, Sedijani P, Kondou Y, Matsui M, de Jong GJ, Somsen GW, et al. Growth Arrest by Trehalose-6-Phosphate: An Astonishing Case of Primary Metabolite Control over Growth by Way of the SnRK1 Signaling Pathway. Plant Physiology. 2011 September 1, 2011;157(1):160-74.

[55] Martinez-Barajas E, Delatte T, Schluepmann H, de Jong GJ, Somsen GW, Nunes C, et al. Wheat Grain Development Is Characterized by Remarkable Trehalose 6-Phosphate Accumulation Pregrain Filling: Tissue Distribution and Relationship to SNF1-Related Protein Kinase1 Activity. Plant Physiology. 2011 May;156(1):373-81.

[56] Wingler A, Delatte TL, O'Hara LE, Primavesi LF, Jhurreea D, Paul MJ, et al. Trehalose 6-Phosphate Is Required for the Onset of Leaf Senescence Associated with High Carbon Availability. Plant Physiology. 2012 Mar;158(3):1241-51.

[57] Weaver LM, Amasino RM. Senescence is induced in individually darkened Arabidopsis leaves but inhibited in whole darkened plants. Plant Physiology. 2001 Nov; 127(3):876-86.

[58] Ono K, Nishi Y, Watanabe A, Terashima I. Possible Mechanisms of Adaptive Leaf Senescence. Plant Biology. 2001;3(3):234-43.

[59] Brouwer B, Ziolkowska A, Bagard M, Keech O, Gardestrom P. The impact of light intensity on shade-induced leaf senescence. Plant Cell and Environment. 2012 Jun; 35(6):1084-98.

[60] Olsen AN, Ernst HA, Leggio LL, Skriver K. NAC transcription factors: structurally distinct, functionally diverse. Trends Plant Sci. 2005 Feb;10(2):79-87.

[61] Yoon HK, Kim SG, Kim SY, Park CM. Regulation of leaf senescence by NTL9-mediated osmotic stress signaling in Arabidopsis. Molecules and cells. 2008 May 31;25(3): 438-45.

[62] Yang SD, Seo PJ, Yoon HK, Park CM. The Arabidopsis NAC transcription factor VNI2 integrates abscisic acid signals into leaf senescence via the COR/RD genes. Plant Cell. 2011 Jun;23(6):2155-68.

[63] Zimmermann P, Heinlein C, Orendi G, Zentgraf U. Senescence-specific regulation of catalases in Arabidopsis thaliana (L.) Heynh. Plant Cell Environ. 2006 Jun;29(6): 1049-60.

[64] Smykowski A, Zimmermann P, Zentgraf U. G-Box binding factor1 reduces CATALASE2 expression and regulates the onset of leaf senescence in Arabidopsis. Plant Physiol. 2010 Jul;153(3):1321-31.

[65] Bieker S, Riester L, Stahl M, Franzaring J, Zentgraf U. Senescence-specific Alteration of Hydrogen Peroxide Levels in Arabidopsis thaliana and Oilseed Rape Spring Variety Brassica napus L. cv. Mozart(F). J Integr Plant Biol. 2012 Aug;54(8):540-54.

[66] Balazadeh S, Kwasniewski M, Caldana C, Mehrnia M, Zanor MI, Xue GP, et al. ORS1, an H(2)O(2)-responsive NAC transcription factor, controls senescence in Arabidopsis thaliana. Molecular plant. 2011 Mar;4(2):346-60.

[67] Wu A, Allu AD, Garapati P, Siddiqui H, Dortay H, Zanor MI, et al. JUNGBRUNNEN1, a reactive oxygen species-responsive NAC transcription factor, regulates longevity in Arabidopsis. Plant Cell. 2012 Feb;24(2):482-506.

[68] Eulgem T, Somssich IE. Networks of WRKY transcription factors in defense signaling. Curr Opin Plant Biol. 2007 Aug;10(4):366-71.

[69] Miao Y, Laun T, Zimmermann P, Zentgraf U. Targets of the WRKY53 transcription factor and its role during leaf senescence in Arabidopsis. Plant Mol Biol. 2004 Aug; 55(6):853-67.

[70] Masclaux-Daubresse C, Chardon F. Exploring nitrogen remobilization for seed filling using natural variation in Arabidopsis thaliana. J Exp Bot. 2011 Mar;62(6):2131-42.

[71] Habash DZ, Bernard S, Schondelmaier J, Weyen J, Quarrie SA. The genetics of nitrogen use in hexaploid wheat: N utilisation, development and yield. Theor Appl Genet. 2007 Feb;114(3):403-19.

[72] Rossato L, Laine P, Ourry A. Nitrogen storage and remobilization in Brassica napus L. during the growth cycle: nitrogen fluxes within the plant and changes in soluble protein patterns. J Exp Bot. 2001 Aug;52(361):1655-63.

[73] Malagoli P, Laine P, Le Deunff E, Rossato L, Ney B, Ourry A. Modeling nitrogen uptake in oilseed rape cv Capitol during a growth cycle using influx kinetics of root nitrate transport systems and field experimental data. Plant Physiol. 2004 Jan;134(1): 388-400.

[74] Beuve N, Rispail N, Laine P, Cliquet JB, Ourry A, Le Deunff E. Putative role of γ - aminobutyric acid (GABA) as a long-distance signal in up-regulation of nitrate uptake in Brassica napus L. Plant, Cell & Environment. 2004;27(8):1035-46.

[75] Roberts IN, Caputo C, Criado MV, Funk C. Senescence-associated proteases in plants. Physiologia Plantarum. 2012 May;145(1):130-9.

[76] Desclos M, Etienne P, Coquet L, Jouenne T, Bonnefoy J, Segura R, et al. A combined N-15 tracing/proteomics study in Brassica napus reveals the chronology of proteomics events associated with N remobilisation during leaf senescence induced by nitrate limitation or starvation. Proteomics. 2009 Jul;9(13):3580-608.

[77] Waditee-Sirisattha R, Shibato J, Rakwal R, Sirisattha S, Hattori A, Nakano T, et al. The Arabidopsis aminopeptidase LAP2 regulates plant growth, leaf longevity and stress response. The New phytologist. 2011 Sep;191(4):958-69.

[78] Martinez M, Cambra I, Gonzalez-Melendi P, Santamaria ME, Diaz I. C1A cysteine-proteases and their inhibitors in plants. Physiologia Plantarum. 2012 May;145(1): 85-94.

[79] Kmiec B, Glaser E. A novel mitochondrial and chloroplast peptidasome, PreP. Physiologia Plantarum. 2012 May;145(1):180-6.

[80] Lin J-F, Wu S-H. Molecular events in senescing Arabidopsis leaves. The Plant Journal. 2004;39(4):612-28.

[81] Wagner R, Aigner H, Funk C. FtsH proteases located in the plant chloroplast. Physiol Plant. 2011 May;145(1):203-14.

[82] Clarke AK. The chloroplast ATP-dependent Clp protease in vascular plants – new dimensions and future challenges. Physiologia Plantarum. 2011;145(1):235-44.

[83] Haussuhl K, Andersson B, Adamska I. A chloroplast DegP2 protease performs the primary cleavage of the photodamaged D1 protein in plant photosystem II. EMBO J. 2001 Feb 15;20(4):713-22.

[84] Chauhan S, Srivalli S, Nautiyal AR, Khanna-Chopra R. Wheat cultivars differing in heat tolerance show a differential response to monocarpic senescence under high-temperature stress and the involvement of serine proteases. Photosynthetica. 2009 Dec;47(4):536-47.

[85] Parrott DL, McInnerney K, Feller U, Fischer AM. Steam-girdling of barley (Hordeum vulgare) leaves leads to carbohydrate accumulation and accelerated leaf senescence, facilitating transcriptomic analysis of senescence-associated genes. New Phytologist. 2007;176(1):56-69.

[86] Peoples MB, Dalling MJ. The interplay between proteolysis and amino acid metabolism during senescence and nitrogen reallocation. In: Senescence and Aging in Plants, LD Nooden and AC Leopold (eds), pp 181-217. 1988.

[87] Reumann S, Voitsekhovskaja O, Lillo C. From signal transduction to autophagy of plant cell organelles: lessons from yeast and mammals and plant-specific features. Protoplasma. 2010 Dec;247(3-4):233-56.

[88] Hörtensteiner S. Chlorophyll degradation during senescence. Annu Rev Plant Biol. 2006;57:55-77.

[89] Martínez DE, Costa ML, Gomez FM, Otegui MS, Guiamet JJ. 'Senescence-associated vacuoles' are involved in the degradation of chloroplast proteins in tobacco leaves. The Plant Journal. 2008;56(2):196-206.

[90] Feller U, Anders I, Mae T. Rubiscolytics: fate of Rubisco after its enzymatic function in a cell is terminated. Journal of Experimental Botany. 2008 May 1, 2008;59(7): 1615-24.

[91] Kokubun N, Ishida H, Makino A, Mae T. The Degradation of the Large Subunit of Ribulose-1,5-bisphosphate Carboxylase/oxygenase into the 44-kDa Fragment in the

Lysates of Chloroplasts Incubated in Darkness. Plant and Cell Physiology. 2002 November 15, 2002;43(11):1390-5.

[92] Kato Y, Murakami S, Yamamoto Y, Chatani H, Kondo Y, Nakano T, et al. The DNA-binding protease, CND41, and the degradation of ribulose-1,5-bisphosphate carboxylase/oxygenase in senescent leaves of tobacco. Planta. 2004 Nov;220(1):97-104.

[93] Kato Y, Yamamoto Y, Murakami S, Sato F. Post-translational regulation of CND41 protease activity in senescent tobacco leaves. Planta. 2005 Nov;222(4):643-51.

[94] Nakano T, Nagata N, Kimura T, Sekimoto M, Kawaide H, Murakami S, et al. CND41, a chloroplast nucleoid protein that regulates plastid development, causes reduced gibberellin content and dwarfism in tobacco. Physiologia Plantarum. 2003;117(1): 130-6.

[95] Ishida H, Yoshimoto K, Izumi M, Reisen D, Yano Y, Makino A, et al. Mobilization of rubisco and stroma-localized fluorescent proteins of chloroplasts to the vacuole by an ATG gene-dependent autophagic process. Plant Physiol. 2008 Sep;148(1):142-55.

[96] Wada S, Ishida H, Izumi M, Yoshimoto K, Ohsumi Y, Mae T, et al. Autophagy plays a role in chloroplast degradation during senescence in individually darkened leaves. Plant Physiol. 2009 Feb;149(2):885-93.

[97] Ishida H, Nishimori Y, Sugisawa M, Makino A, Mae T. The large subunit of ribulose-1,5-bisphosphate carboxylase/oxygenase is fragmented into 37-kDa and 16-kDa polypeptides by active oxygen in the lysates of chloroplasts from primary leaves of wheat. Plant & cell physiology. 1997 Apr;38(4):471-9.

[98] Otegui MS, Noh YS, Martinez DE, Vila Petroff MG, Staehelin LA, Amasino RM, et al. Senescence-associated vacuoles with intense proteolytic activity develop in leaves of Arabidopsis and soybean. Plant J. 2005 Mar;41(6):831-44.

[99] Büchert AM, Civello PM, Martinez GA. Chlorophyllase versus pheophytinase as candidates for chlorophyll dephytilation during senescence of broccoli. J Plant Physiol. 2011 Mar 1;168(4):337-43.

[100] Hörtensteiner S, Feller U. Nitrogen metabolism and remobilization during senescence. Journal of Experimental Botany. 2002 Apr;53(370):927-37.

[101] Chung DW, Pruzinská A, Hörtensteiner S, Ort DR. The Role of Pheophorbide a Oxygenase Expression and Activity in the Canola Green Seed Problem. Plant Physiology. 2006 September 2006;142(1):88-97.

[102] Matile P, Schellenberg M. The cleavage of phaeophorbide a is located in the envelope of barley gerontoplasts. Plant Physiology and Biochemistry. 1996 Jan-Feb;34(1):55-9.

[103] Guiboileau A, Yoshimoto K, Soulay F, Bataille MP, Avice JC, Masclaux-Daubresse C. Autophagy machinery controls nitrogen remobilization at the whole-plant level under both limiting and ample nitrate conditions in Arabidopsis. New Phytologist. 2012 May;194(3):732-40.

[104] Liu Y, Bassham DC. Autophagy: pathways for self-eating in plant cells. Annu Rev Plant Biol. 2012 Jun 2;63:215-37.

[105] Yoshimoto K. Plant autophagy puts the brakes on cell death by controlling salicylic acid signaling. Autophagy. 2010 Jan;6(1):192-3.

[106] Soudry E, Ulitzur S, Gepstein S. Accumulation and remobilization of amino acids during senescence of detached and attached leaves: in planta analysis of tryptophan levels by recombinant luminescent bacteria. J Exp Bot. 2005 Feb;56(412):695-702.

[107] Martin A, Lee J, Kichey T, Gerentes D, Zivy M, Tatout C, et al. Two Cytosolic Glutamine Synthetase Isoforms of Maize Are Specifically Involved in the Control of Grain Production. The Plant Cell Online. 2006 November 2006;18(11):3252-74.

[108] Kumagai E, Araki T, Hamaoka N, Ueno O. Ammonia emission from rice leaves in relation to photorespiration and genotypic differences in glutamine synthetase activity. Annals of Botany. 2011 September 20, 2011.

[109] Kohl S, Hollmann J, Blattner FR, Radchuk V, Andersch F, Steuernagel B, et al. A putative role for amino acid permeases in sink-source communication of barley tissues uncovered by RNA-seq. BMC plant biology. 2012 Aug 30;12(1):154.

[110] Lam H-M, Wong P, Chan H-K, Yam K-M, Chen L, Chow C-M, et al. Overexpression of the ASN1 Gene Enhances Nitrogen Status in Seeds of Arabidopsis. Plant Physiology. 2003 June 1, 2003;132(2):926-35.

[111] Fan S-C, Lin C-S, Hsu P-K, Lin S-H, Tsay Y-F. The Arabidopsis Nitrate Transporter NRT1.7, Expressed in Phloem, Is Responsible for Source-to-Sink Remobilization of Nitrate. The Plant Cell Online. 2009 September 2009;21(9):2750-61.

[112] Khanna-Chopra R. Leaf senescence and abiotic stresses share reactive oxygen species-mediated chloroplast degradation. Protoplasma. 2012 Jul;249(3):469-81.

[113] Queval G, Jaillard D, Zechmann B, Noctor G. Increased intracellular H(2)O(2) availability preferentially drives glutathione accumulation in vacuoles and chloroplasts. Plant Cell Environ. 2011 Jan;34(1):21-32.

[114] Apel K, Hirt H. Reactive oxygen species: metabolism, oxidative stress, and signal transduction. Annu Rev Plant Biol. 2004;55:373-99.

[115] Foyer CH, Noctor G. Redox Homeostasis and Antioxidant Signaling: A Metabolic Interface between Stress Perception and Physiological Responses. The Plant Cell Online. 2005 July 2005;17(7):1866-75.

[116] Noctor G, Foyer CH. ASCORBATE AND GLUTATHIONE: Keeping Active Oxygen Under Control. Annu Rev Plant Physiol Plant Mol Biol. 1998 Jun;49:249-79.

[117] Foyer CH, Noctor G. Ascorbate and Glutathione: The Heart of the Redox Hub. Plant Physiology. 2011 January 1, 2011;155(1):2-18.

[118] Asada K. Production and Scavenging of Reactive Oxygen Species in Chloroplasts and Their Functions. Plant Physiology. 2006 June 2006;141(2):391-6.

[119] Asada K. The Water-Water Cycle in Chloroplasts: Scavenging of Active Oxygens and Dissipation of Excess Photons. Annu Rev Plant Physiol Plant Mol Biol. 1999 Jun; 50:601-39.

[120] Miller GAD, Suzuki N, Ciftci-Yilmaz S, Mittler RON. Reactive oxygen species homeostasis and signalling during drought and salinity stresses. Plant, Cell & Environment. 2010;33(4):453-67.

[121] Torres MA, Dangl JL. Functions of the respiratory burst oxidase in biotic interactions, abiotic stress and development. Current Opinion in Plant Biology. 2005;8(4):397-403.

[122] Kwak JM, Mori IC, Pei ZM, Leonhardt N, Torres MA, Dangl JL, et al. NADPH oxidase AtrbohD and AtrbohF genes function in ROS-dependent ABA signaling in Arabidopsis. EMBO J. 2003 Jun 2;22(11):2623-33.

[123] Daudi A, Cheng Z, O'Brien JA, Mammarella N, Khan S, Ausubel FM, et al. The Apoplastic Oxidative Burst Peroxidase in Arabidopsis Is a Major Component of Pattern-Triggered Immunity. The Plant Cell Online. 2012 January 1, 2012;24(1):275-87.

[124] Groppa M, Ianuzzo M, Rosales E, Vázquez S, Benavides M. Cadmium modulates NADPH oxidase activity and expression in sunflower leaves. Biologia Plantarum. 2012;56(1):167-71.

[125] Foreman J, Demidchik V, Bothwell JH, Mylona P, Miedema H, Torres MA, et al. Reactive oxygen species produced by NADPH oxidase regulate plant cell growth. Nature. 2003 Mar 27;422(6930):442-6.

[126] Takahashi S, Kimura S, Kaya H, Iizuka A, Wong HL, Shimamoto K, et al. Reactive oxygen species production and activation mechanism of the rice NADPH oxidase OsRbohB. Journal of Biochemistry. 2012 July 1, 2012;152(1):37-43.

[127] Molassiotis A, Fotopoulos V. Oxidative and nitrosative signaling in plants: two branches in the same tree? Plant Signal Behav. 2011 Feb;6(2):210-4.

[128] Jin CW, Du ST, Shamsi IH, Luo BF, Lin XY. NO synthase-generated NO acts downstream of auxin in regulating Fe-deficiency-induced root branching that enhances Fe-deficiency tolerance in tomato plants. Journal of Experimental Botany. 2011 July 1, 2011;62(11):3875-84.

[129] Hancock JT. NO synthase? Generation of nitric oxide in plants. Period Biol. 2012 Mar; 114(1):19-24.

[130] Lozano-Juste J, León J. Enhanced Abscisic Acid-Mediated Responses in nia1nia2noa1-2 Triple Mutant Impaired in NIA/NR- and AtNOA1-Dependent Nitric Oxide Biosynthesis in Arabidopsis. Plant Physiology. 2010 February 2010;152(2): 891-903.

[131] Guo F-Q, Okamoto M, Crawford NM. Identification of a Plant Nitric Oxide Synthase Gene Involved in Hormonal Signaling. Science. 2003 October 3, 2003;302(5642):100-3.

[132] Zemojtel T, Fröhlich A, Palmieri MC, Kolanczyk M, Mikula I, Wyrwicz LS, et al. Plant nitric oxide synthase: a never-ending story? Trends in Plant Science. 2006;11(11):524-5.

[133] Seligman K, Saviani EE, Oliveira HC, Pinto-Maglio CAF, Salgado I. Floral Transition and Nitric Oxide Emission During Flower Development in Arabidopsis thaliana is Affected in Nitrate Reductase-Deficient Plants. Plant and Cell Physiology. 2008 July 1, 2008;49(7):1112-21.

[134] Modolo LV, Augusto O, Almeida IMG, Magalhaes JR, Salgado I. Nitrite as the major source of nitric oxide production by Arabidopsis thaliana in response to Pseudomonas syringae. FEBS Letters. 2005;579(17):3814-20.

[135] Planchet E, Jagadis Gupta K, Sonoda M, Kaiser WM. Nitric oxide emission from tobacco leaves and cell suspensions: rate limiting factors and evidence for the involvement of mitochondrial electron transport. The Plant Journal. 2005;41(5):732-43.

[136] Rümer S, Gupta KJ, Kaiser WM. Plant cells oxidize hydroxylamines to NO. Journal of Experimental Botany. 2009 May 1, 2009;60(7):2065-72.

[137] Lee S, Seo PJ, Lee HJ, Park CM. A NAC transcription factor NTL4 promotes reactive oxygen species production during drought-induced leaf senescence in Arabidopsis. Plant J. 2012 Jun;70(5):831-44.

[138] Lum HK, Butt YKC, Lo SCL. Hydrogen Peroxide Induces a Rapid Production of Nitric Oxide in Mung Bean (Phaseolus aureus). Nitric Oxide. 2002;6(2):205-13.

[139] Bright J, Desikan R, Hancock JT, Weir IS, Neill SJ. ABA-induced NO generation and stomatal closure in Arabidopsis are dependent on H2O2 synthesis. The Plant Journal. 2006;45(1):113-22.

[140] He J, Xu H, She X, Song X, Zhao W. The role and the interrelationship of hydrogen peroxide and nitric oxide in the UV-B-induced stomatal closure in broad bean. Functional Plant Biology. 2005;32(3):237-47.

[141] Neill S, Barros R, Bright J, Desikan R, Hancock J, Harrison J, et al. Nitric oxide, stomatal closure, and abiotic stress. Journal of Experimental Botany. 2008 February 1, 2008;59(2):165-76.

[142] Malolepsza U, Rózlska S. Nitric oxide and hydrogen peroxide in tomato resistance: Nitric oxide modulates hydrogen peroxide level in o-hydroxyethylorutin-induced resistance to Botrytis cinerea in tomato. Plant Physiology and Biochemistry. 2005;43(6): 623-35.

[143] Kovtun Y, Chiu W-L, Tena G, Sheen J. Functional analysis of oxidative stress-activated mitogen-activated protein kinase cascade in plants. Proceedings of the National Academy of Sciences. 2000 March 14, 2000;97(6):2940-5.

[144] Wang P, Du Y, Li Y, Ren D, Song CP. Hydrogen peroxide-mediated activation of MAP kinase 6 modulates nitric oxide biosynthesis and signal transduction in Arabidopsis. Plant Cell. 2010 Sep;22(9):2981-98.

[145] Aihong L, Wang Y, Tang J, Xue P, Li C, Liu L, et al. Nitric Oxide and Protein S-nitrosylation Are Integral to Hydrogen Peroxide Induced Leaf Cell Death in Rice. Plant Physiology. 2011 November 21, 2011.

[146] Leshem YaY, Wills RBH, Ku VV-V. Evidence for the function of the free radical gas - nitric oxide (NO) - as an endogenous maturation and senescence regulating factor in higher plants. Plant Physiology and Biochemistry. 1998;36(11):825-33.

[147] del Rio LA, Corpas FJ, Barroso JB. Nitric oxide and nitric oxide synthase activity in plants. Phytochemistry. 2004 Apr;65(7):783-92.

[148] Mishina TE, Lamb C, Zeier J. Expression of a nitric oxide degrading enzyme induces a senescence programme in Arabidopsis. Plant, Cell & Environment. 2007;30(1): 39-52.

[149] Beligni MV, Fath A, Bethke PC, Lamattina L, Jones RL. Nitric Oxide Acts as an Antioxidant and Delays Programmed Cell Death in Barley Aleurone Layers. Plant Physiology. 2002 August 1, 2002;129(4):1642-50.

[150] Møller IM, Sweetlove LJ. ROS signalling - specificity is required. Trends in Plant Science. 2010;15(7):370-4.

[151] Moreno J, Garcia-Murria MJ, Marin-Navarro J. Redox modulation of Rubisco conformation and activity through its cysteine residues. J Exp Bot. 2008;59(7):1605-14.

[152] Marin-Navarro J, Moreno J. Cysteines 449 and 459 modulate the reduction-oxidation conformational changes of ribulose 1.5-bisphosphate carboxylase/oxygenase and the translocation of the enzyme to membranes during stress. Plant Cell Environ. 2006 May;29(5):898-908.

[153] Goud PB, Kachole MS. Role of chloroplastidial proteases in leaf senescence. Plant Signal Behav. 2011 Sep;6(9):1371-6.

[154] Zentgraf U, Zimmermann P, Smykowski A. Role of Intracellular Hydrogen Peroxide as Signalling Molecule for Plant Senescence. In: Nagata T, editor. Senescence. Agricultural and Biological Sciences: InTech; 2012.

[155] Miao Y, Laun T, Smykowski A, Zentgraf U. Arabidopsis MEKK1 can take a short cut: it can directly interact with senescence-related WRKY53 transcription factor on the protein level and can bind to its promoter. Plant Molecular Biology. 2007;65(1):63-76.

[156] Miller G, Schlauch K, Tam R, Cortes D, Torres MA, Shulaev V, et al. The Plant NADPH Oxidase RBOHD Mediates Rapid Systemic Signaling in Response to Diverse Stimuli. Sci Signal. 2009 August 18, 2009;2(84):ra45-.

[157] Monshausen GB, Bibikova TN, Messerli MA, Shi C, Gilroy S. Oscillations in extracellular pH and reactive oxygen species modulate tip growth of Arabidopsis root hairs.

Proceedings of the National Academy of Sciences. 2007 December 26, 2007;104(52): 20996-1001.

[158] Mittler R, Vanderauwera S, Suzuki N, Miller G, Tognetti VB, Vandepoele K, et al. ROS signaling: the new wave? Trends in Plant Science. 2011;16(6):300-9.

[159] Derkx AP, Orford S, Griffiths S, Foulkes MJ, Hawkesford MJ. Identification of differentially senescing mutants of wheat and impacts on yield, biomass and nitrogen partitioning(f). J Integr Plant Biol. 2012 Aug;54(8):555-66.

[160] Uauy C, Distelfeld A, Fahima T, Blechl A, Dubcovsky J. A NAC Gene Regulating Senescence Improves Grain Protein, Zinc, and Iron Content in Wheat. Science. 2006 November 24, 2006;314(5803):1298-301.

[161] McAllister CH, Beatty PH, Good AG. Engineering nitrogen use efficient crop plants: the current status. Plant biotechnology journal. 2012 May 18.

J Plant Growth Regul (2014) 33:106–118
DOI 10.1007/s00344-013-9380-2

Senescence Networking: WRKY18 is an Upstream Regulator, a Downstream Target Gene, and a Protein Interaction Partner of WRKY53

Maren Potschin · Silke Schlienger · Stefan Bieker · Ulrike Zentgraf

Received: 19 August 2013 / Accepted: 3 September 2013 / Published online: 18 October 2013

Abstract Transcriptional reprogramming is a central feature of senescence regulation, implying an essential role for transcription factors. A regulatory function has already been attributed to different members of the plant-specific NAC and WRKY families in *Arabidopsis* but also in other plant species. WRKY53 is one important senescence regulator of the *Arabidopsis* WRKY family that is tightly regulated on different levels. In this study we show that WRKY18, which was formerly characterized as a downstream target of WRKY53 in the WRKY network, also regulates the expression of *WRKY53*. WRKY18 is able to bind directly to different W-boxes in the *WRKY53* promoter region and to repress expression of a *WRKY53* promoter-driven reporter gene in a transient transformation system using *Arabidopsis* protoplasts. Consistent with its repressing function on *WRKY53* as a positive senescence regulator, *WRKY18* overexpression led to delayed senescence, whereas *wrky18* mutant plants exhibited a clearly accelerated senescence. In addition, a direct interaction between WRKY53 and WRKY18 proteins could be detected in yeast using the split ubiquitin system and *in planta* in transiently transformed tobacco epidermal cells via FRET-FLIM. In contrast to WRKY18/18 homodimers, WRKY18/53 heterodimers positively influenced *WRKY53* promoter-driven reporter gene expression but appear to act only on a shorter 1.1 kbp promoter fragment but not on a 2.8 kbp longer fragment, indicating a more complex protein-protein-DNA interaction on the longer *WRKY53* promoter, most likely also triggered by the accessibility of the promoter on the chromatin level.

Keywords WRKY transcription factors · Senescence · DPI-ELISA · Feedback regulation · Yeast split ubiquitin · FRET-FLIM

Introduction

Senescence is associated with massive changes in the transcriptome, implying an important role for transcription factors (Buchanan-Wollaston and others 2005; Breeze and others 2011). The two plant-specific transcription factor families WRKY and NAC are both overrepresented in the senescence transcriptome of *Arabidopsis*, and several members of both families have already been characterized as playing important roles in senescence regulation, not only in *Arabidopsis* but also in other plant species (Guo and others 2004; Uauy and others 2006; Ulker and others 2007; Balazadeh and others 2010, 2011; Besseau and others 2012; Gregersen and others 2013). The *Arabidopsis* WRKY transcription factor family consists of at least 75 members playing diverse biological roles in plant growth, development, and responses to biotic and abiotic stress. The name is derived from the almost invariant WRKYGQK sequence at the N-terminus, which is followed by a more variable zinc-finger motif. The WRKY proteins have been grouped into three subgroups according to their structural features (Eulgem and others 2000; Rushton and others 2010); nevertheless, almost all analyzed WRKY proteins recognize the TTGACC/T W-box sequence. W-boxes are found in many promoters of senescence- and pathogen-associated genes (SAGs and PR

Electronic supplementary material The online version of this article (doi:10.1007/s00344-013-9380-2) contains supplementary material, which is available to authorized users.

M. Potschin · S. Schlienger · S. Bieker · U. Zentgraf (✉)
Center for Plant Molecular Biology, University of Tuebingen, Auf der Morgenstelle 32, 72076 Tuebingen, Germany
e-mail: ulrike.zentgraf@zmbp.uni-tuebingen.de

genes), but also in almost all *WRKY* promoters, indicating that a WRKY transcriptional network exists. Besides regulating transcription of each other, WRKY factors are also able to form heterodimers leading to a change in DNA-binding specificity (Xu and others 2006). In addition, many other proteins have been shown to physically interact with WRKY proteins, influencing their activity and stability (see Chi and others 2013 for review). A firm link between plant-specific NAC and WRKY proteins was deduced from low-resolution X-ray structures and small-angle X-ray scattering on complexes in the presence of DNA in which both use a β-strand motif for DNA binding (Welner and others 2012). Moreover, family members of both groups have been shown to react on elevated levels of reactive oxygen species, especially hydrogen peroxide, and are even involved in regulating the intracellular levels of these molecules (Miao and others 2004; Balazadeh and others 2011; Besseau and others 2012; Wu and others 2012).

Within the WRKY family, several factors have already been associated with senescence, namely, WRKY6 (Robatzek and Somssich 2002), WRKY70 (Ülker and others 2007; Besseau and others 2012), WRKY54 (Besseau and others 2012), WRKY22 (Zhou and others 2011), and WRKY53 (Hinderhofer and Zentgraf 2001; Miao and others 2004). Senescence-specific regulation of WRKY53 has already been analyzed in detail. The *WRKY53* gene shows a very interesting expression pattern, with a switch from leaf-age-dependent to a plant-age-dependent expression during bolting and flowering (Hinderhofer and Zentgraf 2001). Expression is most likely switched by increasing hydrogen peroxide levels at this time point (Miao and others 2004; Bieker and others 2012). Furthermore, epigenetic changes can also be observed at the promoter of *WRKY53* during leaf senescence induction in which histone modifications H3K4me2 and H3K4me3 are specifically enriched at the *WRKY53* promoter region (Ay and others 2009; Brusslan and others 2012), whereas DNA methylation remains low and unchanged (Zentgraf and others 2010). A transcriptional activator with homology to a HPT kinase (AD protein) was characterized to be one of the upstream regulatory proteins of WRKY53 (Miao and others 2008). Moreover, a mitogen-activated protein kinase kinase kinase (MEKK1) directly binds to the *WRKY53* promoter region, which is responsible for the switch from leaf-age- to plant-age-dependent expression (Miao and others 2007). However, MEKK1 does not directly activate transcription but acts most likely through phosphorylation of other promoter-associated proteins. One of these proteins could be WRKY53 itself sitting at its own promoter since, at least in vitro, MEKK1 is able to directly phosphorylate WRKY53 and thereby increase its DNA-binding activity (Miao and others 2004, 2007). In contrast, the AD protein could not be phosphorylated by MEKK1 (Miao and others 2008). The DNA-binding activity of WRKY53 is also triggered by the interaction with ESP/ESR, but in this case interaction leads to inhibition of DNA binding (Miao and Zentgraf 2007). In addition, WRKY53 protein levels are controlled by degradation through the HECT-domain ubiquitin ligase UPL5 (Miao and Zentgraf 2010).

In this study we analyzed which WRKY factors interact directly with the *WRKY53* promoter and what impact these factors have on the expression of *WRKY53*. One of the strongest interactions was detected between the *WRKY53* promoter and WRKY18, which was formerly characterized to be a downstream target of WRKY53 (Miao and others 2004). In a transient transformation assay of *Arabidopsis* protoplasts, WRKY18 could be characterized as a negative regulator of the *WRKY53* promoter-driven reporter gene expression. In consistence, a *WRKY18* T-DNA insertion line exhibited accelerated senescence, whereas a *WRKY18* overexpressing line showed a delay. Because both proteins can bind to *WRKY53* promoter elements, we analyzed whether the proteins can also form heterodimers. Protein-protein interaction between WRKY18 and WRKY53 was observed in yeast using the split ubiquitin system and in transiently transformed tobacco leaves using FRET-FLIM. Cotransformation of *WRKY18* and *WRKY53* overexpression constructs in *Arabidopsis* protoplasts together with a *WRKY53* promoter-driven reporter gene revealed that heterodimers resulted in a different outcome, as expected if the single effects of both factors were simply combined.

Material and Methods

Plant Material

Arabidopsis thaliana plants were grown in a climatic chamber at 20 °C under long-day conditions (16 h of light) with only moderate light intensity (60–100 μmol s^{-1} m^{-2}) to slow down development for better phenotyping. Under these conditions, the plants developed bolts and flowers within 5–6 weeks. During growth and development, the positions of individual leaves within the rosette were color-coded with different colored threads so that even at very late stages of development individual leaves could be analyzed according to their age (Hinderhofer and Zentgraf 2001). Plants were harvested in a weekly rhythm and samples were always taken at the same time in the morning to avoid circadian effects. T-DNA insertion lines of *WRKY18* (SALK_093916C) were obtained from the Nottingham *Arabidopsis* Stock Centre (NASC). Homozygous plants were characterized by PCR using gene-specific and T-DNA left border primers. Plants overexpressing *WRKY18* were transformed by a floral dip of Col-0 plants into *Agrobacterium tumefaciens* cultures carrying a

35S:*WRKY18* construct and subsequent selection of over-expressing plants by BASTA selection and qRT-PCR.

Senescence Phenotyping

Chlorophyll content was estimated using an atLeaf+ chlorophyll meter. Each leaf was measured in triplicate and values were averaged. For the evaluation of leaf senescence phenotypes, rosettes were scanned upside down for better visualization of the older leaves and leaves were sorted according to their age using a color code. In addition, leaves of at least five plants were categorized into four groups according to their leaf color: (1) "green"; (2) "yellow-green," leaves starting to get yellow from the tip; (3) "yellow," completely yellow leaves; and (4) "brown/dry," dry and/or brown leaves. Furthermore, expression of the senescence-associated marker genes *SAG12* (At5g45890), encoding a cysteine protease, and *SAG13* (At2g29350), encoding a short-chain alcohol dehydrogenase, was analyzed by qRT-PCR and normalized to the expression of the *ACTIN2* gene (At3g18780). In addition, expression of *WRKY53* (At4g23810) and *WRKY18* (At4g31800) were analyzed in the same way.

Protein Expression and Extraction for DPI-ELISA

The coding sequences of *WRKY18* and *WRKY53* and several other *WRKY*s were cloned into the pETG-10A vector for expression of the proteins with N-terminal-fused 6 × His-tag. The *E. coli* strain BL21-SI was used for protein expression. The cells were grown in 10 ml of selective medium overnight and subsequently diluted 1:20 in a final volume of 100 ml in medium without antibiotics. Protein expression was induced after 1.5 h by the addition of 1 mM IPTG and the cells were grown overnight at 18 °C. After centrifugation (2,500 g, 20 min, 4 °C) and washing [10 mM Tris-HCl (pH 7.5) and 100 mM NaCl], the bacterial pellet was resuspended in protein extraction buffer [4 mM Hepes (pH 7.5), 100 mM KCl, 8 % (v/v) glycerol, 1× complete proteinase inhibitor without EDTA (Roche)] and protein extraction was performed by sonication under native conditions. The protein concentration of the crude extract was measured by Bradford assay (Bio-Rad).

DPI ELISA

The DNA-protein interaction assay was performed basically as described by Brand and others (2010). 5′-Biotinylated complementary oligonucleotides were annealed (final concentration 2 µM) to get double-stranded DNA fragments. The sequences of the individual fragments containing different W-boxes are listed in Fig. 1a. These double-stranded oligonucleotides were added to a streptavidin-coated ELISA plate (Nunc Immobilizer) for binding for 1 h at 37 °C. After blocking using blocking reagent (Roche) for 30 min, the blocking reagent was removed and crude extracts were added in different protein concentrations (5, 10, and 25 µg) and incubated for 1 h at room temperature. Subsequently, biotinylated DNA-protein complexes were washed two times for 10 min at room temperature (blocking solution, Qiagen) and incubated with anti-His-HRP conjugate antibodies (Qiagen) 1:1,500 diluted in blocking solution for 1 h at room temperature. After washing, interaction was detected by a peroxidase reaction with ortho-phenylenediamine [OPD tablets, Agilent Technologies (Dako)] for 15 min in darkness. After stopping the reaction with 0.5 M H_2SO_4 solution, positive interactions that resulted in a yellow color could be measured with an ELISA reader (TriStar LB 941 plate reader, Berthold).

Real-time PCR

mRNA extraction from pooled leaves (leaf No. 5) of five different plants per plant line and time point was performed using the chemagic mRNA Direct Kit (chemagen). Subsequent cDNA synthesis was done with qScript™ cDNA SuperMix Kit (Quanta BioSciences). For the qRT-PCR, the iQ™ SYBR® Green Supermix (Bio-Rad) was used following the manufacturer's protocol. *ACTIN2* was chosen as the reference gene for senescence because the variation of *ACTIN2* expression over different leaf and plant stages in *Arabidopsis* was very low in contrast to other housekeeping genes (Panchuk and others 2005). Expression of analyzed genes was normalized to *ACTIN2* expression according to Pfaffl (2001). Each value represents three technical replicates of a pool of five biological replicates (Table 1).

Protoplast Transformation

The transient expression assays were performed by transforming protoplasts derived from a cell culture of *Arabidopsis thaliana* var. Columbia 0. Cells were transformed with 5 µg of effector and reporter plasmid DNA each, roughly following the protocol of Negrutiu and others (1987) (for details see the protocol at http://www.zmbp.uni-tuebingen.de/CentralFacilities/transf/index.html). Protoplasts were used for GUS assays or FRET-FLIM analyses.

Tobacco Leaf Infiltration

Agrobacteria tumefaciens cells (strain GV3101 RK) were transformed with 35S constructs carrying the coding sequences of *WRKY18* and *WRKY53* fused N-terminal to *CFP* or *YFP* coding sequences. *Agrobacteria* were grown overnight at 28 °C in 5 ml of LB medium containing the

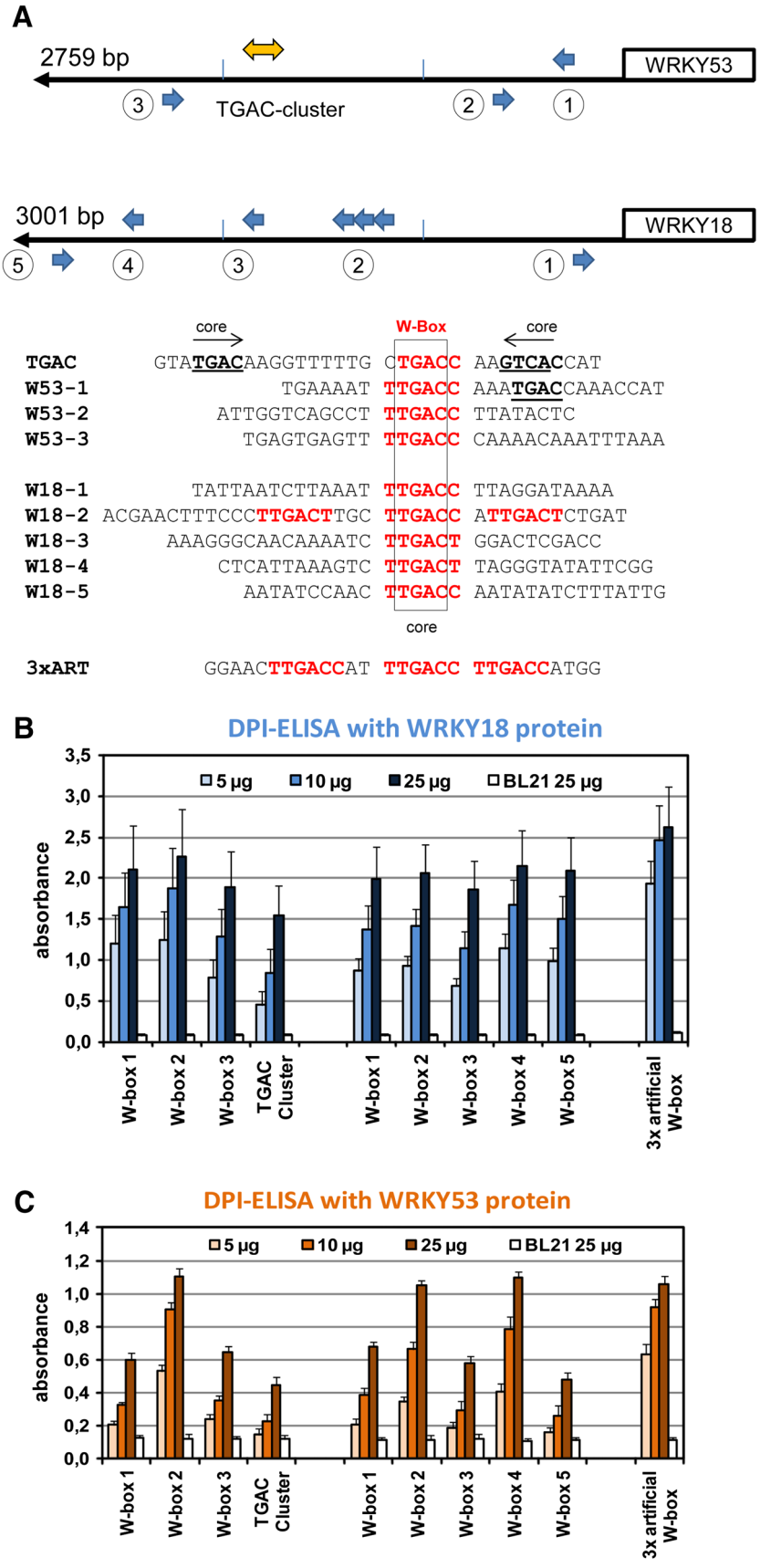

Fig. 1 **a** Schematic drawing of the W-boxes in the *WRKY53* and *WRKY18* promoter and sequence comparison of the DNA fragments used for DPI ELISAs. Perfect W-box motifs are highlighted in *red*; the core sequence TGAC is indicated in *bold* and *underlined*, and the direction of the motif is indicated by the *arrows*. An artificial sequence containing three perfect W-boxes was used as a positive control (3× ART). **b** Quantification of DPI-ELISAs performed with different amounts of crude extracts of *E. coli* BL21 cells expressing WRKY18 proteins combined with different biotinylated DNA fragments containing different W-boxes of the *WRKY53* and *WRKY18* promoter. **c** Quantification of DPI-ELISAs with different amounts of crude extracts of *E. coli* BL21 cells expressing WRKY53 proteins combined with different biotinylated DNA fragments containing different W-boxes of the *WRKY53* and *WRKY18* promoter. *Error bars* indicate standard deviation of three biological and two technical replicates

Table 1 Primers used for expression analyses by qRT-PCR

Gene	Forward primer	Reverse primer
WRKY53	5′-CAGACGGGGATGCTACGG-3′	5′-GGCGAGGCTAATGGTGGT-3′
SAG12	5′-GCTTTGCCGGTTTCTGTTG-3′	5′-GTTTCCCTTTCTTTATTTGTGTTG-3′
SAG13	5′- GTGCCAGAGACGAAACTC-3′	5′-GCTGTAAACTCTGTGGTC-3′
WRKY18	5′-TGGACGGTTCTTCGTTTCTCGAC-3′	5′-TCGTAACTCACTTGCGCTCTCG-3′
ACTIN2	5′-AAGCTCTCCTTTGTTGCTGTT-3′	5′-GACTTCTGGGCATCTGAATCT-3′

antibiotics of the strain and the plasmid. The preculture was transferred to 20 ml of LB medium supplemented with antibiotics for the plasmid only and grown further overnight at 28 °C. After centrifugation (4,000 rpm, 10 min) the pellet was resuspended in H_2O to an $OD_{600} = 0.8$. These cultures were combined to equal amounts with *Agrobacteria* cultures carrying p19 silencing inhibitor before infiltration. The *Agrobacteria* mixture was applied to the tobacco leaf using a syringe. After infiltration, plants were grown for 3–4 days before analyses of interaction using FRET-FLIM.

GUS Reporter Assay

Arabidopsis protoplasts were transformed as described above. A luciferase construct was cotransfected as an internal control. The protoplasts were incubated overnight in the dark and then used for GUS enzyme activity assays as described by Jefferson and others (1987). GUS fluorescence values were normalized to luciferase fluorescence to correct for transformation efficiency. A 1,099 bp fragment and a 2,759 bp fragment upstream of the *WRKY53* start codon were cloned into the binary vector pBGWFS7.0 and served as reporter construct. For *WRKY18*, a 1,500 bp sequence and a 3,001 bp sequence upstream of the start codon were used.

Protein-Protein Interaction via Yeast Split Ubiquitin

Protein-protein interaction was analyzed in yeast using the split-ubiquitin system of the DUALhunter kit following the manufacturer's protocol (Dualsystems Biotech, for details see http://www.dualsystems.com). The full-length cDNA of *WRKY53*, *WRKY18*, *WRKY6*, and *WRKY30* were cloned in-frame into bait vector (pDHB1) and prey vector (pPR3-N), respectively. All constructs were confirmed by sequencing. Empty vectors were used as negative controls. For the interaction analyses, the bait constructs were cotransformed with the prey constructs in the yeast strain NMY51 and grown at 30 °C for 4 days on SD media without Leu and Trp to select for transformation of both constructs. Subsequently, the yeast was transferred to quadruple dropout media without Leu, Trp, His, and Ade for analyses of protein-protein interaction. A Cub and a NubG construct were provided by the manufacturer as a negative control for the bait and prey, respectively.

Fluorescence Lifetime Imaging Microscopy

The full-length cDNAs of *WRKY18* and *WRKY53* were cloned into the pENSG-CFP:GW and pENSG-YFP:GW vectors for expression of the proteins with N-terminal-fused CFP or YFP (Wenkel and others 2006). Image and data acquisition was done with a Leica TCS SP8, combined with a PicoHarp 300 TCSPC Module and a Sepia Multichannel Picosecond Diode Laser (PDL 808-SC) (PicoQuant). Excitation was done with a 440-nm pulsed laser, with the intensity regulated via a Thorlabs Laser Combining Unit (PBH51502/SS/SPL-S6) and the emission recorded at 480 ± 25 nm. Analysis was performed using PicoQuant SymphoTime Software (ver. 5.3.2.2). The bi-exponential decay function was used for fluorescence decay analysis.

Results

To identify WRKY factors involved in the regulation of *WRKY53* expression, we cloned cDNAs of those WRKY factors that are expressed during onset of senescence according to genevestigator expression profiles (https://www.genevestigator.com/) into bacterial expression vectors fusing a 6xHis-tag to the WRKY proteins, namely, WRKY6, 13, 15, 18, 22, 25, 29, 30, 33, 38, 40 53, 60, 62, and 70. Crude extracts from *E. coli* cells expressing these proteins were used to perform DNA-protein interaction ELISAs (DPI-ELISAs) to screen for DNA binding to the *WRKY53* promoter. For WRKY18-6xHis, the strongest interaction with *cis* elements in the *WRKY53* promoter was observed; therefore, we concentrated our further analyses on the role of WRKY18 in *WRKY53* regulation.

Influence of *WRKY18* on *WRKY53* Expression

Several W-boxes or W-box-like *cis* elements can be detected in the upstream region of *WRKY53* as well as in

the upstream region of the *WRKY18* coding region (Fig. 1a). Five perfect W-box motifs of the *WRKY18* and three of the *WRKY53* promoter were used for DPI-ELISAs. In both promoters, motif clusters of at least three very closely linked motifs are present and were also used for DNA-binding studies in which the cluster in the *WRKY18* promoter consists of three perfect W-boxes and the cluster in the *WRKY53* promoter consists of only three core motifs (TGAC). Increasing amounts of crude extracts of *E. coli* BL21 cells (5, 10, and 25 µg) which were induced for expression of the 6× His-tagged versions of WRKY53 and WRKY18, respectively, were used for binding assays to the biotinylated double-stranded DNAs containing the different W-box motifs indicated in Fig. 1a. All W-box *cis* elements were bound in a concentration-dependent manner by both proteins. Both WRKY proteins showed the highest affinity to a 3× perfect but artificial W-box cluster (3× ART), which was used as positive control. Only very low background signals could be detected for extracts of empty BL21 cells, which were used as negative control. WRKY18 appears to have the same binding affinity to all perfect W-boxes in both promoters and a lower affinity to the imperfect TGAC cluster of the *WRKY53* promoter (Fig. 1b). In contrast, WRKY53 has a clear preference for W-box-2 of the *WRKY53* promoter and W-box-2 and -4 of the *WRKY18* promoter, whereas the affinity to the perfect W-box-5 of the *WRKY18* promoter is as low as it is to the imperfect TGAC cluster of the *WRKY53* promoter, indicating that WRKY53 appears to be more selective in DNA binding (Fig. 1c). However, no obvious further conservation in the surrounding DNA sequences of the preferred W-box motifs, which might be responsible for further selectivity, could be detected.

To investigate which effect *WRKY18* has on the expression of *WRKY53* and vice versa, transient cotransformation of *Arabidopsis* protoplasts with *WRKY53* and *WRKY18* promoter:*GUS* and 35S:*WRKY18* and 35S:*WRKY53* overexpression effector constructs was performed. *WRKY18* expression was activated by overexpression of *WRKY53* in protoplasts. This was already expected because in earlier experiments performed for *wrky53* and 35S:*WRKY53* plants (Miao and others 2004), expression of *WRKY18* was also activated by overexpression of *WRKY53* and reduced by the lack of a functional *WRKY53* protein in the *wrky53* mutant. In contrast, expression of *WRKY53* was inhibited by WRKY53 itself when only a short promoter fragment of 1 kb was used for the transient *GUS* expression experiments (Miao and others 2004). However, if a slightly longer fragment of 1.1 kb was used containing one additional W-box-like element, the negative effect was eliminated and was reversed into a slightly activating potential (Fig. 2). If the longer 2.8 kb fragment was used, an even more pronounced induction could be observed for the *WRKY53* promoter-

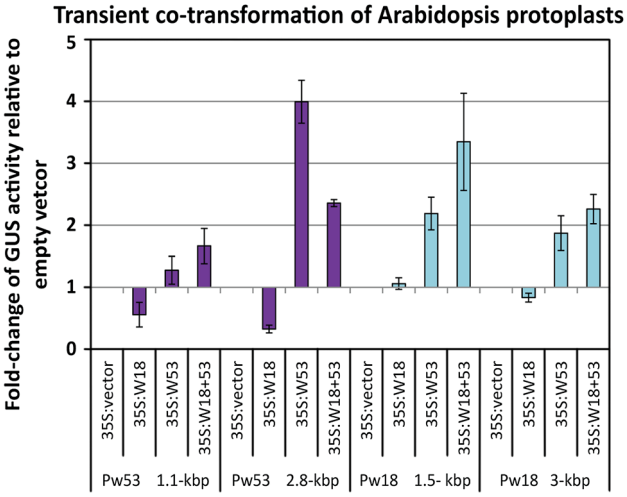

Fig. 2 *Arabidopsis* protoplasts were transiently transformed with 5 µg of effector and reporter plasmid DNA each, and a luciferase construct was cotransfected as an internal control. GUS fluorescence values were normalized to luciferase fluorescence to correct for transformation efficiency. A 1.1- and a 2.8-kb fragment of the *WRKY53* promoter and a 1.5 and a 3.0 kbp sequence of the *WRKY18* promoter fused to the *GUS* gene were used as reporter constructs. 35S:*WRKY18* and 35S:*WRKY53* constructs were used as effector plasmids. Values of empty vector construct were set to 1. *Error bars* indicate standard deviations of at least three biological and three technical replicates

driven reporter gene, suggesting that most likely complex protein–protein–DNA interactions are formed on the longer promoter, changing the impact of WRKY53 on its own promoter. This might also indicate that chromatin structure and accessibility of the promoter are key elements of *WRKY53* transcriptional regulation. Overexpression of *WRKY18* did not or only marginally influenced its own expression, even though WRKY18 could bind to all W-boxes of its own promoter, indicating that binding does not automatically result in effects on gene expression and that WRKY18 has no autoregulatory potential. *WRKY53* expression was clearly inhibited by overexpressed *WRKY18*, with a stronger effect on the longer 3.0 kb fragment, clearly suggesting that WRKY18 works as a repressor on the *WRKY53* expression (Fig. 2). In contrast to protoplasts transformed with a single WRKY expression construct, the effect of double transformation was not simply additive but different from a simple combination of the single effects. This is very obvious when single transformations and double transformation of the 1.1 kb promoter fragment of the *WRKY53* promoter are compared. *WRKY18* single transformation led to a reduction of reporter gene expression, whereas *WRKY53* single transformation led to a slight induction of reporter gene expression. Simultaneous expression of both constructs led to an induction of the reporter gene expression, which was higher than that by WRKY53 alone, even though WRKY18 would rather

contribute repression than activation. A very similar effect could be observed for the 1.5 and the 3.0 kb fragment of the *WRKY18* promoter in which WRKY18 alone had no or a slightly negative effect, but double transformation of both WRKY constructs induced reporter gene expression to a higher extent than *WRKY53* single transformation. This clearly indicates that WRKY18 and WRKY53 form heterodimers and that these heterodimers have a positive activation potential. However, on the 3.0 kb *WRKY53* promoter fragment, the effect of a double transformation appears to be only additive (Fig. 2), suggesting that heterodimers are not formed in all cases or that additional and higher-order complexes can be formed on the longer promoter fragment.

Phenotype of *WRKY18* T-DNA insertion and *WRKY18* overexpression lines

To verify the negative effect on *WRKY53* expression *in planta* and test for the relevance of these regulatory cues, we used a SALK T-DNA insertion line in the first exon of *WRKY18* (SALK_093916C) which was already characterized by Xu and others (2006). The homozygous insertion line was confirmed by PCR. In addition, *WRKY18*-overexpressing plants were produced by transformation of a 35S:*WRKY18* construct using *Agrobacteria tumefaciens* and floral dip. Overexpression and severe knockdown of the *WRKY18* gene was confirmed by qRT-PCR (Supplementary Fig. 1); the line showing the highest expression of *WRKY18* was grown side by side with the *wrky18* and wild-type (WT) plants under long-day conditions for detailed senescence phenotyping. Overall development of the plants was not impaired in both lines (Supplementary Fig. 2). However, the *wrky18* mutant showed slightly earlier flowering and the number of leaves was slightly but significantly lower (9.13; *t* test, $p = 0.0168$) than in WT (10.88) and overexpressing plants (10.79).

During early development of the plants, the leaves were color-coded with colored threads according to their age. Whole rosettes in different developmental stages (5- and 7-week-old plants) were scanned upside down to visualize the older leaves (Fig. 3a). In addition, the leaves were sorted with the help of the age-based color code (Fig. 3a). Furthermore, the leaves of at least five plants were categorized into four groups according to their leaf color (fully green, green/yellow, fully yellow, and brown/dry) to assure the senescence phenotype statistically (Fig. 3b). Chlorophyll contents of leaves 3 and 5 were measured by using an atLeaf+ chlorophyll meter (Fig. 4a), and expression of the senescence marker genes *SAG12* and *SAG13* as well as *WRKY53* itself as a marker gene was analyzed by qRT-PCR (Fig. 4b). Whereas in young plants no differences in expression of the senescence marker genes *SAG12* and *SAG13* could be observed between the lines, clear differences were detected in later stages. In comparison to the wild-type plants, *WRKY18*-overexpressing plants showed a delayed senescence phenotype accompanied by a delay in chlorophyll loss and delayed and lower expression of *SAG12*, *SAG13*, and *WRKY53*. In contrast, senescence, chlorophyll degradation, and *SAG* expression were accelerated in *wrky18* mutants, clearly indicating that WRKY18 is a negative regulator of *WRKY53* expression also *in planta* and has a clear impact on senescence regulation. qRT-PCR analyses of *WRKY53* expression in the *wrky18* and *WRKY18*-overexpressing plants also confirmed the negative effect of WRKY18 on *WRKY53* expression (Fig. 4B).

Protein-Protein Interaction between WRKY18 and WRKY53

Because both WRKY proteins bind equally well to the *WRKY53* promoter and to the *WRKY18* promoter and double transformation assays did not show simple additive effects, we analyzed whether these two proteins can physically interact using the yeast split ubiquitin system. The split ubiquitin system is advantageous for studying the interactions between transcription factors compared to the yeast-two-hybrid system based on the yeast GAL4 transcription factor because no deletion variants have to be used. In the yeast split ubiquitin system, homodimers of WRKY53 as well as of WRKY18 could be detected, but both WRKYs were also able to physically interact with each other forming heterodimers. Yeast cells were selected for transformation of both constructs by plating on double-selection medium SD-Leu-Trp. These yeast cells were then transferred on quadruple-dropout medium SD-Leu-Trp-His-Ade to test for the interaction. A clear interaction between WRKY53 and WRKY18 could be detected by the growth of the yeast on the quadruple-dropout medium and the white color, as weak interactions would lead to a pink color of the growing yeast cells (Fig. 5a). Protein complex formation between different WRKYs appears to be selective because WRKY6 did not interact with WRKY53. Besseau and others (2012) have already shown that WRKY53 also did not interact with WRKY70 and WRKY54. However, we clearly detected a homodimer formation of WRKY53 and of WRKY18 which was not observed previously (Besseau and others 2012). To verify these interactions *in planta*, we used a CFP/YFP Foerster resonance energy transfer (FRET) with subsequent fluorescence lifetime imaging microscopy (FLIM) analyses in transiently transformed tobacco leaves and *Arabidopsis* protoplasts. An interaction of two proteins is indicated by a reduction of the fluorescence lifetime of CFP after FRET from CFP to YFP. A strong interaction between WRKY53 and WRKY18 could be confirmed by FLIM in epidermal cells of tobacco leaves (Fig. 5b, c). Additional

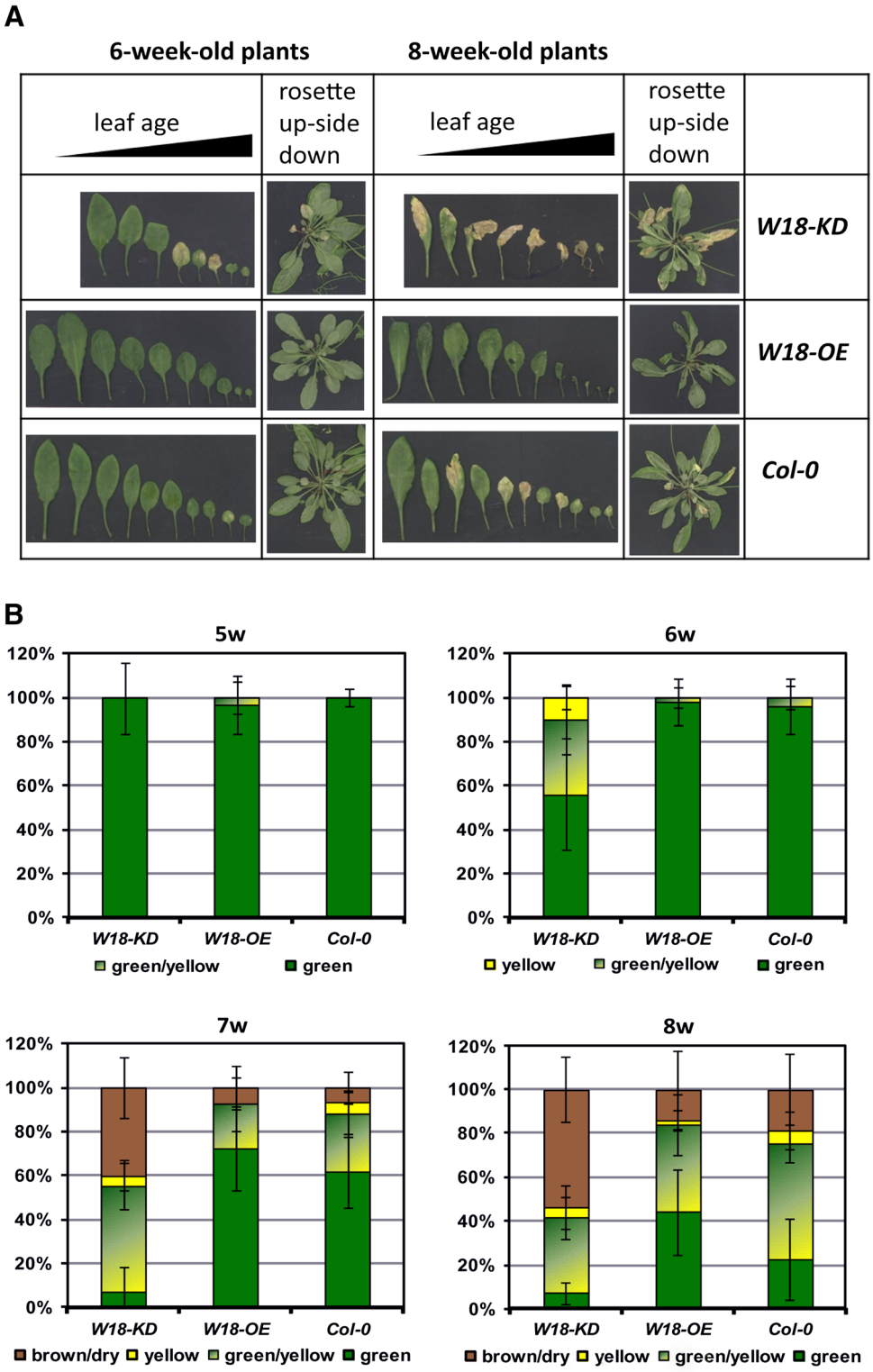

Fig. 3 Wild type (Col-0), *wrky18* mutant, and *WRKY18*-overexpressing plants were analyzed over development. **a** Rosette leaves of 6- and 8-week-old plants were sorted according to their age; whole rosettes were photographed from upside down to visualize also the older leaves. **b** For a quantitative evaluation of leaf senescence, plant leaves of at least five plants were categorized into four groups according to their leaf color: (1) "green"; (2) "yellow-green," that is, leaves starting to get yellow from the tip; (3) "yellow," completely yellow leaves; and (4) "brown/dry," dry and/or brown leaves. The percentages of each group with respect to total leaf numbers are presented. *Error bars* indicate standard deviation of at least five plants

confirmation of the homodimer formation of WRKY53 and WRKY18 could be achieved in tobacco (Fig. 5c) and in the *Arabidopsis* protoplast system (Supplementary Fig. 3). As already suggested by the results shown in Fig. 2, heterodimers are indeed formed *in planta* and they appear to have different effects on transcription than the homodimers. The complex cross-regulation between WRKY18 and WRKY53 is summarized in a model shown in Fig. 6.

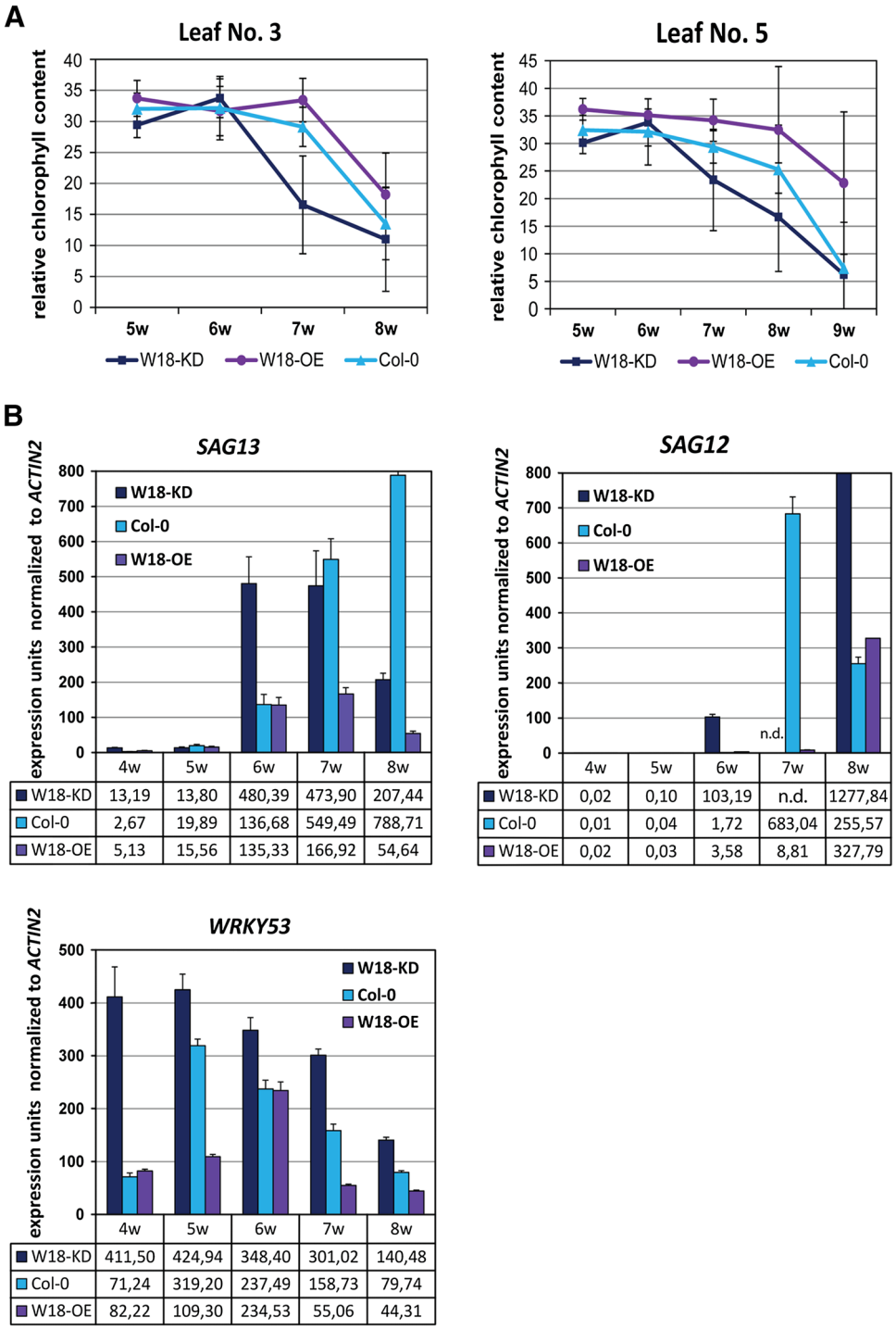

Fig. 4 **a** Chlorophyll values of leaves No. 3 and 5 were measured from 5- to 8-week-old plants of wild-type (Col-0), *wrky18* mutant, and *WRKY18*-overexpressers using an atLeaf+ chlorophyll meter. *Error bars* indicate standard deviation. **b** qRT-PCR expression analyses of the senescence marker genes *SAG12*, *SAG13*, and *WRKY53* normalized to *ACTIN2* according to Pfaffl (2001). Pools of leaf No. 5 of 4- to 8-week-old plants of five biological replicates were analyzed. *Error bars* indicate standard deviation of three technical replicates. *n.d.* not determined

Discussion

Senescence is characterized by a massive transcriptional reprogramming (Breeze and others 2011) to assure reorganization for reallocation of nutrients and minerals out of senescing tissue into developing parts of the plants such as fruits and seeds. This implies an important role for transcription factors, and NAC and WRKY transcription factors have a significant impact in *Arabidopsis* but also in other plant species. WRKY transcription factors can influence transcription of their target genes positively as well as negatively and are also able to regulate transcription of each other in a complex regulatory network. Besides senescence, WRKY transcription factors are involved mainly in plant responses to biotic and abiotic stress conditions and are often discussed as a node of

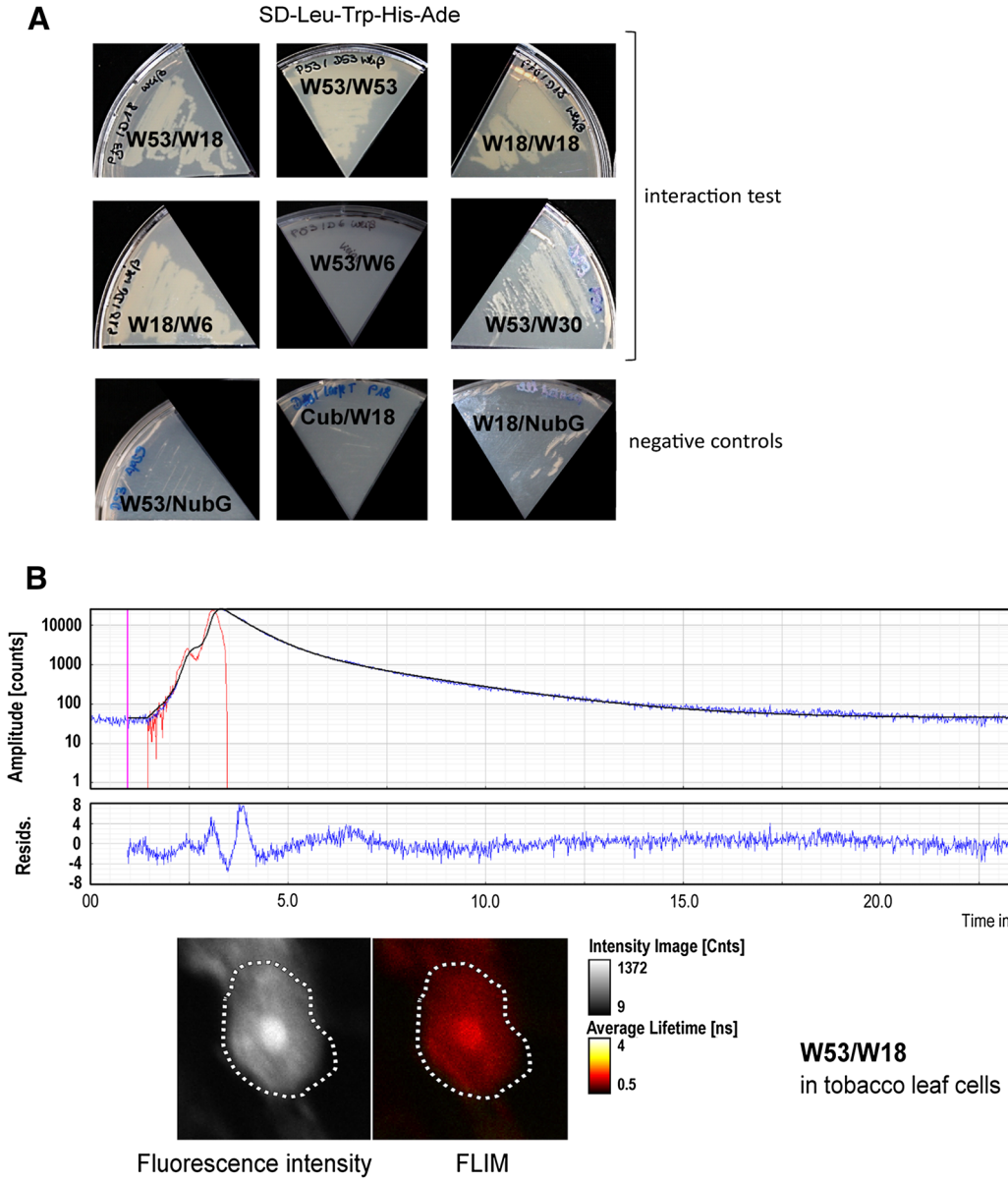
A
SD-Leu-Trp-His-Ade
W53/W18
W53/W53
W18/W18
interaction test
W18/W6
W53/W6
W53/W30
W53/NubG
Cub/W18
W18/NubG
negative controls
B
Amplitude [counts]
10000
1000
100
10
1
Resids.
8
4
0
-4
-8
00
5.0
10.0
15.0
20.0
25.0
Time in[ns]
Intensity Image [Cnts]
1372
9
Average Lifetime [ns]
4
0.5
W53/W18
in tobacco leaf cells
Fluorescence intensity
FLIM
C
FLIM measurements
tobacco
Arabidopsis
FLIM in ns
3,5
3
2,5
2
1,5
1
0,5
0
**
***
*
***
***
W53/18
W18/18
W53/53
control

◀ **Fig. 5** Protein–protein interaction between WRKY53 and WRKY18. **a** Yeast split ubiquitin system. Yeasts were cotransformed using prey-and-bait constructs of different WRKY factors indicated in the figure and were grown on selective medium SD-Leu-Trp to select for cotransformation. Subsequently, yeast cells were transferred to SD-Leu-Trp-His-Ade medium to analyze protein-protein interaction by growth of the yeasts. White colonies indicate strong interaction and pink colonies indicate weaker interaction. To show selectivity, WRKY6 was used interacting only with WRKY18 but not with WRKY53. Cub and NubG were provided by the manufacturer and were used as a negative control for the bait and prey, respectively. **b** Protein-protein interaction in transiently transformed tobacco epidermal leaf cells using FRET-FLIM analyses. In the upper graph, the *red line* describes the instrument response function, the *blue line* describes the actual decay, and the *black line* describes the bi-exponential fit. The *blue line* in the lower graph describes the residuals. Fluorescence lifetime is indicated by a color code reaching from *dark red* (very short decay times, ~0.5 ns) to yellow (long decay times, ~4.5 ns). The position of the nucleus is indicated by the dotted line. **c** Fluorescence lifetime was measured in *Arabidopsis* protoplasts and transiently transformed tobacco leaves for the WRKY53/53 homodimer, the WRKY18/18 homodimer, and the WRK53/18 heterodimer. Empty CFP and YFP vectors were used as control. *Error bars* indicate standard deviation of two to five replicates, $n = 2$–6; *n.d.* not determined. *t* tests have been performed and * indicated significance compared to control: $*p < 0.05$, $**p < 0.01$, $***p < 0.001$

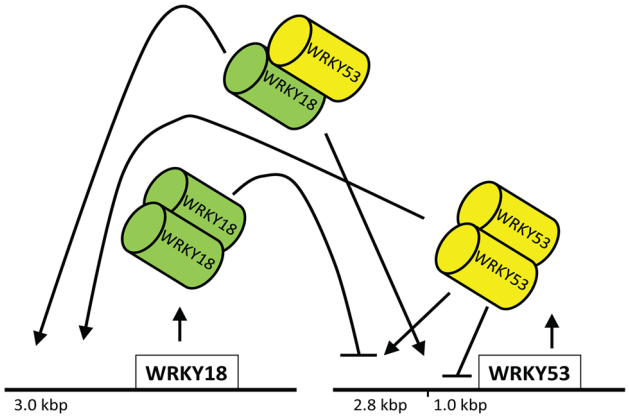

Fig. 6 Schematic drawing of the cross-regulation of WRKY18 and WRKY53

convergence between stress response and senescence. WRKY18 was initially characterized as being involved in the response of plants to pathogen attack because transgenic plants overexpressing *WRKY18* showed a marked increase in the expression of PR genes and resistance to the bacterial pathogen *Pseudomonas syringae* (Chen and Chen 2002). Potentiation of developmentally regulated defense responses by WRKY18 was not associated with enhanced biosynthesis of salicylic acid but required the disease resistance regulatory protein NPR1. In addition, WRKY18 together with WRKY40 negatively modulated the expression of positive regulators of defense such as CYP71A13, EDS1, and PAD4, but positively modulated the expression of some key JA-signaling genes by partly suppressing the expression of JAZ repressors (Pandey and others 2010). Besides the response to pathogen attack, WRKY18, 40, and 60 are involved in abiotic stress response to salt and osmotic stress and in ABA signaling. Both WRKY18 and WRKY40 are rapidly induced by ABA, and a delayed response of WRKY60 argues that *WRKY60* might be a direct target gene of WRKY18 and WRKY40 in ABA signaling. The requirement of both WRKY18 and WRKY40 for induction of WRKY60 suggests an involvement of the WRKY18/WRKY40 heterodimers that may recognize the W-boxes in the *WRKY60* promoter and activate the expression of the *WRKY70* gene (Chen and others 2010). Moreover, an indispensable role for WRKY18 in bacterial volatile responses was described (Wenke and others 2012). Wang and others (2006) took a genomics-directed approach and positioned the five group III WRKY factors 18, 53, 54, 58, and 60 in the complex transcriptional regulatory network of systemic acquired resistance (SAR). During SAR, salicylic acid (SA) accumulation triggers nuclear localization of the transcription factor NPR1, leading to the activation of WRKY transcription. *WRKY18*, *53*, *54*, *58*, and *60* are activated in this SA-mediated response pathway in which WRKY54 and 60 are also involved in a feedback loop in the regulation of SA production (Wang and others 2006). Remarkably, also in SAR, WRKY18 and WRKY53 act in the same regulatory cue.

WRKY53, a factor in group III of the WRKY family according to structural features, was characterized as a positive regulator of leaf senescence in *Arabidopsis* and appears to be very tightly regulated (Zentgraf and others 2010). Other group III factors like WRKY54 and WRKY70 cooperate as negative regulators of leaf senescence in *Arabidopsis* (Besseau and others 2012). Analyses of the SA-deficient *sid2* mutant revealed that expression of WRKY30, 53, 54, and 70 during senescence is partially SA-dependent. In addition to SA, WRKY30 and WRKY53 can be induced by H_2O_2 and both factors are tightly coexpressed during development. In contrast to *wrky53* mutant plants, miRNA-*WRKY30*-silenced plants displayed no significant senescence phenotype compared to wild-type plants (Miao and others 2004; Besseau and others 2012), indicating that WRKY30 does not directly regulate senescence. However, WRKY30 can form heterodimers with all other tested group III WRKYs, and one can speculate that WRKY30 acts as an integrator of WRKY function. In this study, we could show that not only group III factors are involved in cross-talk and feedback regulation of leaf senescence; the group IIa factor WRKY18 is also involved in the WRKY network regulation of senescence. *WRKY18* overexpression and knockdown clearly revealed an inhibitory function of WRKY18 on senescence. WRKY18 can

directly bind to different W-boxes in the *WRKY53* promoter so that senescence regulation is most likely mediated at least in part by *WRKY53* regulation. Comparison of the gene expression pattern according to the developmental map of the *Arabidopsis* eFP-Browser (http://bar.utoronto.ca/efp/cgi-bin/efpWeb.cgi) reveals that *WRKY18* is highly expressed in young leaves with a decrease toward old and senescence leaves, whereas *WRKY53* is expressed antagonistically, with its highest expression in senescence leaves and low expression in young leaves. Genevestigator profiles (https://www.genevestigator.com) and our own qRT-PCR analyses revealed (Supplementary Fig. 4) that *WRKY18* expression increased with progression of senescence, suggesting that increasing *WRKY18* expression might restrict *WRKY53* expression in later stages of senescence. Interestingly, WRKY53 itself induces the expression of WRKY18 so that WRKY18 can be positioned in an autoregulatory feedback loop of *WRKY53* expression. However, because there are many more proteins directly binding to the promoter of *WRKY53*, and, in addition, the length of the accessible promoter fragment also has to be taken into account, the regulation of WRKY53 appears to be much more complex.

Moreover, WRKY18 can form heterodimers with WRKY53, as demonstrated in yeast using the split ubiquitin system and *in planta* via transient expression in tobacco leaves with a subsequent FRET FLIM analysis. Homodimer and heterodimer formation between members of WRKY group IIa have already been described as mediated by leucine zipper motifs in the N-terminus of the proteins (Xu and others 2006). For these group IIa factors, heterodimer formation modulated the selectivity of DNA binding. Group III factors do not contain canonical leucine zipper motifs but nevertheless are able to interact with each other (Besseau and others 2012) and also across group borders, as shown in this study by the direct interaction of WRKY53 and WRKY18. Transient coexpression of both factors resulted in a different outcome as expected, if the effects of both factors were simply combined, indicating that heterodimers are most likely formed and responsible for these differences. Heterodimer formation in vivo was confirmed in yeast using the split ubiquitin system, and FRET FLIM analyses supported that heterodimers also occur *in planta*. The WRKY18/53 heterodimers appear to act only on a short version of the *WRKY53* promoter, suggesting that accessibility of the *cis* elements in the *WRKY53* promoter might determine whether heterodimers form. Changes in chromatin structure and histone modification have already been observed in the promoter of *WRKY53* (Ay and others 2009; Brusslan and others 2012) during plant development, disclosing a further level of regulation in the WRKY network. Moreover, WRKY factors not only interact with each other but also with many other regulatory proteins, integrating even more signals into the network. A very nice overview on protein interactions of WRKY factors has recently been published by Chi and others (2013). WRKY53 appears to be an important integration point between senescence, pathogen response, and SA and JA signaling. MEKK1 and ESP/ESR have already been characterized as mediating the cross-talk between senescence regulation and pathogen response via interaction with WRKY53 (Miao and others 2007; Miao and Zentgraf 2007). Cross-talk between WRKY18 and WRKY53 is another node of convergence between pathogen response and senescence.

In conclusion, the WRKY network regulation appears to be extremely complex, because in addition to transcriptional cross-regulation between different WRKYs and autoregulatory feedback loops, heterodimer formation modulates WRKY action (Fig. 6). Imaging of the dynamics of protein-protein interactions and competition between different interaction partners will be a future challenge to understand the complex regulatory WRKY network.

Acknowledgments We are grateful for the excellent technical assistance of Gabriele Eggers-Schumacher. We thank the NASC for supplying seeds of the *WRKY18* T-DNA insertion lines. This work was financially supported by the DFG (ZE 313, 9-1).

References

Ay N, Irmler K, Fischer A, Uhlemann R, Reuter G, Humbeck K (2009) Epigenetic programming via histone methylation at WRKY53 controls leaf senescence in *Arabidopsis thaliana*. Plant J 58(2):333–346

Balazadeh S, Siddiqui H, Allu AD, Matallana-Ramirez LP, Caldana C, Mehrnia M, Zanor MI, Köhler B, Mueller-Roeber B (2010) A gene regulatory network controlled by the NAC transcription factor ANAC092/AtNAC2/ORE1 during salt-promoted senescence. Plant J 62(2):250–264

Balazadeh S, Kwasniewski M, Caldana C, Mehrnia M, Zanor MI, Xue GP, Mueller-Roeber B (2011) ORS1, an H2O2-responsive NAC transcription factor, controls senescence in Arabidopsis thaliana. Mol Plant 4(2):346–360

Besseau S, Li J, Palva ET (2012) WRKY54 and WRKY70 co-operate as negative regulators of leaf senescence in Arabidopsis thaliana. J Exp Bot 63:2667–2679

Bieker S, Riester L, Stahl M, Franzaring J, Zentgraf U (2012) Senescence-specific alteration of hydrogen peroxide levels in Arabidopsis thaliana and oilseed rape spring variety Brassica napus L. cv. Mozart. J Integr Plant Biol 54(8):540–554

Brand LH, Kirchler T, Hummel S, Chaban C, Wanke D (2010) DPI-ELISA: a fast and versatile method to specify the binding of plant transcription factors to DNA in vitro. Plant Methods 25:6–25

Breeze E, Harrison E, McHattie S, Hughes L, Hickman R, Hill C, Kiddle S, Kim YS, Penfold CA, Jenkins D, Zhang C, Morris K, Jenner C, Jackson S, Thomas B, Tabrett A, Legaie R, Moore JD, Wild DL, Ott S, Rand D, Beynon J, Denby K, Mead A, Buchanan-Wollaston V (2011) High-resolution temporal profiling of transcripts during Arabidopsis leaf senescence reveals a

distinct chronology of processes and regulation. Plant Cell 23(3):873–894

Brusslan JA, Rus Alvarez-Canterbury AM, Nair NU, Rice JC, Hitchler MJ, Pellegrini M (2012) Genome-wide evaluation of histone methylation changes associated with leaf senescence in Arabidopsis. PLoS ONE 7(3):e33151

Buchanan-Wollaston V, Page T, Harrison E, Breeze E, Lim PO, Nam HG, Lin JF, Wu SH, Swidzinski J, Ishizaki K, Leaver CJ (2005) Comparative transcriptome analysis reveals significant differences in gene expression and signalling pathways between developmental and dark/starvation-induced senescence in Arabidopsis. Plant J 42(4):567–585

Chen C, Chen Z (2002) Potentiation of developmentally regulated plant defense response by AtWRKY18, a pathogen-induced Arabidopsis transcription factor. Plant Physiol 129(2):706–716

Chen H, Lai Z, Shi J, Xiao Y, Chen Z, Xu X (2010) Roles of Arabidopsis WRKY18, WRKY40 and WRKY60 transcription factors in plant responses to abscisic acid and abiotic stress. BMC Plant Biol 10:281

Chi Y, Yang Y, Zhou Y, Zhou J, Fan B, Yu JQ, Chen Z (2013) Protein-protein interactions in the regulation of WRKY transcription factors. Mol Plant 6(2):287–300

Eulgem T, Rushton PJ, Robatzek S, Somssich IE (2000) The WRKY superfamily of plant transcription factors. Trends Plant Sci 5:199–206

Gregersen PL, Culetic A, Boschian L, Krupinska K (2013) Plant senescence and crop productivity. Plant Mol Biol 82(6):603–622

Guo Y, Cai Z, Gan S (2004) Transcriptome of Arabidopsis leaf senescence. Plant Cell Environ 27(5):521–549

Hinderhofer K, Zentgraf U (2001) Identification of a transcription factor specifically expressed at the onset of leaf senescence. Planta 213(3):469–473

Jefferson RA, Kavanagh TA, Bevan MW (1987) GUS fusions: β-glucuronidase as a sensitive and versatile gene fusion marker in higher plants. EMBO J 6:3901–3907

Miao Y, Zentgraf U (2007) The antagonist function of Arabidopsis WRKY53 and ESR/ESP in leaf senescence is modulated by the jasmonic and salicylic acid equilibrium. Plant Cell 19(3):819–830

Miao Y, Zentgraf U (2010) A HECT E3 ubiquitin ligase negatively regulates Arabidopsis leaf senescence through degradation of the transcription factor WRKY53. Plant J 63(2):179–188

Miao Y, Laun T, Zimmermann P, Zentgraf U (2004) Targets of the WRKY53 transcription factor and its role during leaf senescence in Arabidopsis. Plant Mol Biol 55(6):853–867

Miao Y, Laun TM, Smykowski A, Zentgraf U (2007) Arabidopsis MEKK1 can take a short cut: it can directly interact with senescence-related WRKY53 transcription factor on the protein level and can bind to its promoter. Plant Mol Biol 65(1–2):63–76

Miao Y, Smykowski A, Zentgraf U (2008) A novel upstream regulator of WRKY53 transcription during leaf senescence in Arabidopsis thaliana. Plant Biol 10(Suppl 1):110–120

Negrutiu I, Shillito RD, Potrykus I, Biasini G, Sala F (1987) Hybrid genes in the analysis of transformation conditions I. Setting up a simple method for direct gene transfer in plant protoplasts. Plant Mol Biol 8:363–373

Panchuk II, Zentgraf U, Volkov RA (2005) Expression of the APX gene family during leaf senescence of Arabidopsis thaliana. Planta 222:926–932

Pandey SP, Roccaro M, Schön M, Logemann E, Somssich IE (2010) Transcriptional reprogramming regulated by WRKY18 and WRKY40 facilitates powdery mildew infection of Arabidopsis. Plant J 64(6):912–923

Pfaffl MW (2001) A new mathematical model for relative quantification in real-time RT-PCR. Nucleic Acids Res 29(9):e45

Robatzek S, Somssich IE (2002) Targets of AtWRKY6 regulation during plant senescence and pathogen defense. Genes Dev 16:1139–1149

Rushton PJ, Somssich IE, Ringler P, Shen QJ (2010) WRKY transcription factors. Trends Plant Sci 15:247–258

Uauy C, Distelfeld A, Fahima T, Blechl A, Dubcovsky J (2006) A NAC gene regulating senescence improves grain protein, zinc, and iron content in wheat. Science 314(5803):1298–1301

Ulker B, Shahid Mukhtar M, Somssich IE (2007) The WRKY70 transcription factor of Arabidopsis influences both the plant senescence and defense signaling pathways. Planta 226:125–137

Wang D, Amornsiripanitch N, Dong X (2006) A genomic approach to identify regulatory nodes in the transcriptional network of systemic acquired resistance in plants. PLoS Pathog 2(11):e123

Welner DH, Lindemose S, Grossmann JG, Møllegaard NE, Olsen AN, Helgstrand C, Skriver K, Lo Leggio L (2012) DNA binding by the plant-specific NAC transcription factors in crystal and solution: a firm link to WRKY and GCM transcription factors. Biochem J 444(3):395–404

Wenke K, Wanke D, Kilian J, Berendzen K, Harter K, Piechulla B (2012) Volatiles of two growth-inhibiting rhizobacteria commonly engage AtWRKY18 function. Plant J 70(3):445–459

Wenkel S, Turck F, Singer K, Gissot L, Le Gourrierec J, Samach A, Coupland G (2006) CONSTANS and the CCAAT box binding complex share a functionally important domain and interact to regulate flowering of Arabidopsis. Plant Cell 18(11):2971–2984

Wu A, Allu AD, Garapati P, Siddiqui H, Dortay H, Zanor MI, Asensi-Fabado MA, Munné-Bosch S, Antonio C, Tohge T, Fernie AR, Kaufmann K, Xue GP, Mueller-Roeber B, Balazadeh S (2012) JUNGBRUNNEN1, a reactive oxygen species-responsive NAC transcription factor, regulates longevity in Arabidopsis. Plant Cell 24(2):482–506

Xu X, Chen C, Fan B, Chen Z (2006) Physical and functional interactions between pathogen-induced Arabidopsis WRKY18, WRKY40, and WRKY60 transcription factors. Plant Cell 18:1310–1326

Zentgraf U, Laun T, Miao Y (2010) The complex regulation of WRKY53 during leaf senescence of Arabidopsis thaliana. Eur J Cell Biol 89(2–3):133–137

Zhou X, Jiang Y, Yu D (2011) WRKY22 transcription factor mediates dark-induced leaf senescence in *Arabidopsis*. Mol Cells 31(4):303–313

Journal of Experimental Botany, Vol. 69, No. 4 pp. 769–786, 2018
doi:10.1093/jxb/erx246 Advance Access publication 1 August 2017

REVIEW

A guideline for leaf senescence analyses: from quantification to physiological and molecular investigations

Justine Bresson[1,†,*], Stefan Bieker[1,†], Lena Riester[1,†], Jasmin Doll[1,†] and Ulrike Zentgraf[1]

[1] ZMBP, General Genetics, University of Tübingen, Auf der Morgenstelle 32, 72076 Tübingen, Germany

* Correspondence: j.bresson34@gmail.com
† These authors contributed equally to this work.

Received 31 March 2017; Editorial decision 22 June 2017; Accepted 23 June 2017

Editor: Christine Foyer, Leeds University, UK

Abstract

Leaf senescence is not a chaotic breakdown but a dynamic process following a precise timetable. It enables plants to economize with their resources and control their own viability and integrity. The onset as well as the progression of leaf senescence are co-ordinated by a complex genetic network that continuously integrates developmental and environmental signals such as biotic and abiotic stresses. Therefore, studying senescence requires an integrative and multi-scale analysis of the dynamic changes occurring in plant physiology and metabolism. In addition to providing an automated and standardized method to quantify leaf senescence at the macroscopic scale, we also propose an analytic framework to investigate senescence at physiological, biochemical, and molecular levels throughout the plant life cycle. We have developed protocols and suggested methods for studying different key processes involved in senescence, including photosynthetic capacities, membrane degradation, redox status, and genetic regulation. All methods presented in this review were conducted on *Arabidopsis thaliana* Columbia-0 and results are compared with senescence-related mutants. This guideline includes experimental design, protocols, recommendations, and the automated tools for leaf senescence analyses that could also be applied to other species.

Keywords: *Arabidopsis thaliana*, automated colourimetric assay, genetic regulation, ion leakage, leaf senescence, lipid peroxidation, photosynthetic capacities, redox regulation.

Introduction

Senescence in annual plants is described as the essential last developmental stage aimed at recycling and reallocation of valuable resources to actively growing organs. When plants are confronted with drastic stresses, senescence can also be an exit strategy to ensure the most optimal survival chances for its offspring. However, senescence is not a chaotic breakdown but a highly complex and dynamic process, following a precise timetable driven by genetic, developmental, and environmental factors (Jansson and Thomas, 2008). Senescence can thus be affected in different ways: in the onset and/or in the intensity and the rate of progression. As senescence is a relatively long process, it can be conceptually divided into three phases: initiation, reorganization, and termination.

Abbreviations: ACA, Automated colourimetric assay; carboxy-H_2DCFDA 5(6), carboxy-dichloro-fluorescein diacetate; Chl, chlorophyll; ChlF, chlorophyll fluorescence; DAB, 3,3′-diaminobenzidine; DCF, dichlorofluorescein; EL, electrolyte leakage; F_0, minimal fluorescence emission of a dark-adapted plant; F_m, maximum fluorescence emission after a short pulse of a saturating light; F_v, variable fluorescence, the difference between F_0 and F_m; F_v/F_m, maximum quantum efficiency of PSII photochemistry (photosynthetic efficiency); H_2O_2, hydrogen peroxide; HSV, hue saturation value; MDA, malondialdehyde; PAM, pulse amplitude modulation; PS, photosystem; ROS, reactive oxygen species; SAG, senescence-associated gene; SDG, senescence down-regulated gene; TBARS, thiobarbituric acid-reactive-substances; TF, transcription factor.

The onset of senescence is the consequence of a constant integration between intrinsic and environmental signals at cellular, tissue, and organ levels. Generally, plants grow continuously until they reach a maximum size, after which senescence can occur (Thomas, 2013). Without exogenous stress input, leaf senescence mainly depends on two endogenous parameters: leaf age and developmental stage at the whole-plant level (Zentgraf *et al.*, 2004). In *Arabidopsis thaliana*, the initiation of senescence usually coincides with the transition to flowering and is concomitant with cessation of vegetative meristem activity (Thomas, 2013). However, senescence can be triggered and modulated by a wide variety of abiotic and biotic stresses such as drought, shade, and pathogen infection (Lim *et al.*, 2007). The timing of leaf senescence initiation is crucial: if it is too late, it would allow only partial and incomplete remobilization of nutrients, whereas if initiated too early, it would reduce carbon assimilation and nitrogen uptake (Malagoli *et al.*, 2004; Masclaux-Daubresse *et al.*, 2010). The initiation of senescence is driven by multiple and co-ordinated signals through hormones, sugars, reactive oxygen species (ROS), and calcium (Lim *et al.*, 2007). At the molecular level, many different transcription factors (TF) are successively activated, forming a clear schedule of events taking place in the course of senescence. Almost 6500 differentially regulated genes have been identified via reverse-genetic approaches and large-scale transcriptome profiling in *A. thaliana* senescence, grouped into 48 clusters according to their differential expression patterns, thus indicating the complexity of the regulatory network (Breeze *et al.*, 2011).

Senescence progresses until fruit development and maturation is finished and ends with the complete disintegration of leaf tissues (Hensel *et al.*, 1993). During the reorganization phase, the cells are subjected to an intensive restructuring, notable by the breakdown of macromolecules, e.g. chlorophyll (Chl), and the remobilization of salvaged nutrients. Breakdown of proteins involves many plastidial and nuclear proteases and regulators of their activities, but also dynamic protein trafficking to bring about the conversion of larger macromolecular structures into transportable and useful breakdown products (Diaz-Mendoza *et al.*, 2016). Moreover, chaperones can also play important roles during the reorganization phase, as for example in protein carbonylation leading to irreversible oxidation, and thereby to a loss of function of the modified proteins (Johansson *et al.*, 2004). However, the extensive degradation of macromolecules can lead to the accumulation of toxic intermediates and by-products, which have to be dealt with by the senescing cells. In particular, antioxidative enzymes, such as peroxidases and catalases, play a crucial role in detoxifying highly reactive compounds generated during degradation processes (Buchanan-Wollaston *et al.*, 2003; Zimmermann *et al.*, 2006). Anthocyanin, a natural antioxidant, which has also been reported to protect against oxidative stress-induced damage, increases during senescence (He and Giusti, 2010). Detoxification is essential as the nucleus as well as the mitochondria have to remain functional in order to maintain transcriptional control and to provide sufficient energy throughout the whole process. During the termination phase, the vacuoles are disrupted and collapse, thus releasing nucleases and proteases into the cytoplasm, which is then contracted and acidified. This leads to the gradual degradation of the cytoplasm, fragmentation of the nuclear DNA and the organelles, and the deterioration of the membranes (Kuriyama and Fukuda, 2002; Ondzighi *et al.*, 2008). Cell death is thus initiated, progressively leading to an irreversible loss of cell integrity (Zimmermann and Zentgraf, 2005).

As senescence occurs in a progressive manner, its quantification throughout the plant life cycle needs reproducible and standardized methods in order to allow comparisons between genotypes and experiments. In addition, studying senescence requires an integrative multi-scale analysis of the dynamic changes occurring in different key processes. However, senescence phenotyping is still diverse, leading to low comparability of plant lines and experiments. Single time-point comparisons often clearly reveal that senescence is somehow disturbed, but they do not precisely indicate in which sense: the time-point of onset, the velocity of progression, or specific processes could be altered. Due to the lack of a general agreement on how senescence phenotyping should be conducted, we suggest a guideline that attempts to standardize leaf senescence analyses. In this review, we first propose an experimental design concerning environmental conditions, growth, and plant sampling for measuring key senescence-related markers. We describe a complete set of methods to assess senescence at physiological, biochemical, and molecular levels. In addition, we provide a novel automated quantification of leaf senescence based on macroscopic colourimetric assays. These complementary analyses will allow an overview of the whole process to be gained, and thus provide an ability to decide whether the initiation, reorganization, and termination phases are differently affected. We conducted the senescence analyses using the widely used *A. thaliana* Columbia-0 (Col-0) genotype as an example, and as a proof of concept we compared the results of our current and previous experiments in senescence-related mutants. All methods and computing tools are described in detail and all protocols, including ImageJ and R scripts, are provided to serve as recommendations for measurements and data analyses.

General considerations for experimental design

Environmental growth conditions such as photoperiod, light intensity, ambient temperature, and nutrient availability are key factors when analysing plant growth. Therefore, choosing the growth conditions is of utmost importance in the experimental design of senescence phenotyping. Amongst these conditions, light plays a crucial role in plant development and leaf morphogenesis, but also in senescence initiation and progression (Biswal and Biswal, 1984; Vasseur *et al.*, 2011). In Arabidopsis, light can promote or retard senescence in a photoperiodic and dose-dependent manner (Nooden *et al.*, 1996). Here, we grew our plants in standard soil (9:1 soil and sand; see Supplementary Table S1 at *JXB* online) in long days (16 h day; 8 h night), low light (~70–80 µE m^{-2} s^{-1}

at plant height), and an ambient temperature of 21 °C. Long days accelerate development (i.e. flowering time), while low light can lead to an extended period of senescence (Nooden *et al.*, 1996). This allows detailed analyses of all three different phases of senescence. A further advantage of plants grown under long days is a lower leaf number and thus less overlapping of the leaf blades within the rosette, compared with plants grown at photoperiods of 12 h or 8 h. This greatly facilitates the analysis of plant growth and quantification of senescence, especially at the whole-rosette level. In addition, to improve later image acquisition, the soil was covered with black sand to enhance the contrast between plant and soil and to reduce background noise.

The timing of sampling and measurements is also a crucial point. We have established a precise design for sampling and measurements that allows analyses of both growth and senescence (Fig. 1). Growth and development were non-invasively examined in all plants (80 in total) through measurements of rosette area and leaf number until the bolting stage (determined by macroscopic examination of flower buds). Stem and total silique dry mass were assessed every week from flowering time (first flower open) until first yellowish siliques stage (Fig. 1). In parallel, leaf senescence was analysed weekly for five consecutive weeks, including the specific developmental hallmarks. Depending on the experiment, sampling can be done according to days/weeks after sowing or germination. However, plant development should be considered when comparing different plant lines with significant differences in their growth (e.g. different bolting times). In this case, sampling could be done at different defined developmental stages

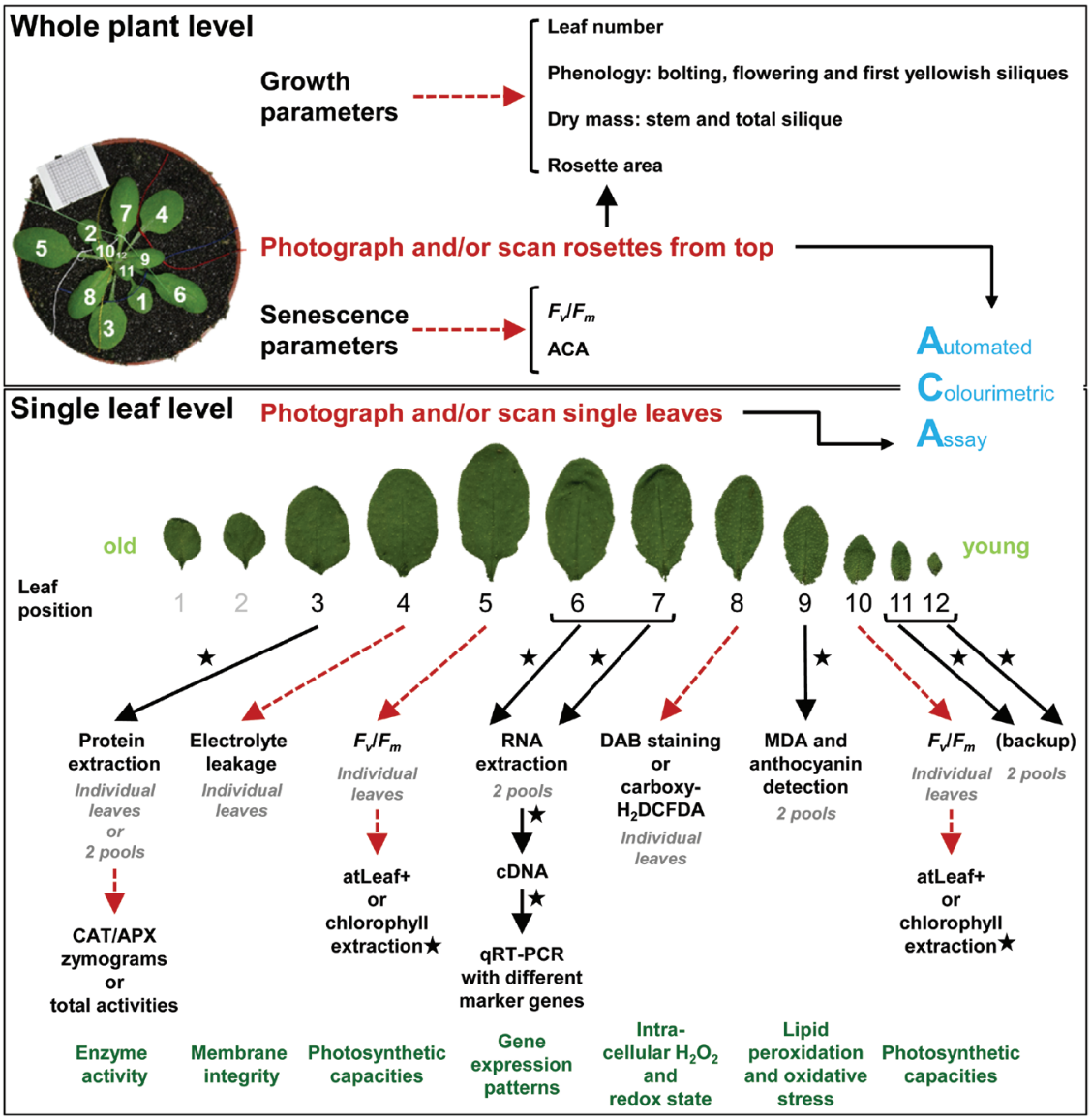

Fig. 1. Flow chart of the senescence phenotyping guideline. The upper part presents the analysis of growth and senescence at the whole-plant level with non-invasive and invasive measurements. The lower part represents the senescence phenotyping at the leaf level taking into account leaf position (age) within the rosette. Black lines and asterisks indicate that the processing can be done later and the plant material can be frozen and stored at –80 °C. Red dashed lines indicate immediate processing is required. ACA can be done at both the whole-rosette and leaf levels non-invasively from photographs or invasively from scans.

such as bolting, flowering, or first silique shattered. In our conditions, Col-0 plants started to bolt and flower at approximately 19 and 28 d, respectively (Fig. 2A–C). Sampling was started when the plants reached their maximal rosette area at bolting time (week 3) and was continued until rosette, stem, and silique walls were almost completely senescent at approximately 50 d after sowing (week 7; Fig. 2A–C). Sampling and measurements were done at the same time of the day to avoid circadian effects.

Senescence was evaluated at both the whole-rosette and leaf levels using different early and late markers involved in key senescence-related processes. Four plants were dissected each week to analyse senescence at the whole-rosette level by using Chl fluorescence (ChlF; i.e. photosynthetic efficiency, F_v/F_m) and an automated colourimetric assay (ACA; Fig. 1). The other markers were assessed in individual leaves of 12 plants taking into account the leaf position (age) within the rosette (Fig. 1). Since old and young leaves also show extensive differences in gene expression (Hinderhofer and Zentgraf, 2001; Zentgraf *et al.*, 2004), using the same leaf position for distinct measurements is crucial for reliable, reproducible, and comparable data. The leaves emerging after the cotyledons were numbered continuously from old to young, starting at the two first leaves and ending before the emergence of the cauline leaves, which are recognizable by their small and pointed leaf blade and lack of petioles (Steynen *et al.*, 2001). Leaf positions were labelled when the first leaves were fully expanded by marking each leaf with a coloured thread following a colour-code (Fig. 1; Hinderhofer and Zentgraf, 2001). After growth cessation, Col-0 rosettes displayed 10 leaves on average (Fig. 2B), meaning that all senescence-markers could routinely be analysed in the same plant but in different detached leaves (Fig. 1). The decline of photosynthetic capacity, mainly occurring during the reorganization phase, was analysed by direct and indirect measurements of Chl levels via measurements relying on light transmittance through the leaves (atLeaf+ Chl meter), ChlF, and Chl extractions. These measurements were done consecutively in the same leaves but at two different leaf positions: position 5 and 10 (except for Chl extraction, only at leaf position 5). These young and middle-aged leaves allow the analysis of early and late effects of senescence on the photosynthetic capacity. Membrane deterioration was estimated by measuring electrolyte leakage (EL) and lipid peroxidation. For measuring EL, leaves at position 4 were used. These relatively old leaves were selected because membrane integrity is mainly affected during the termination phase of senescence. Membrane damage through lipid peroxidation is mostly driven by increased ROS production, which has been shown to be higher in young leaves than in old leaves (Bieker *et al.*, 2012). Hence, lipid peroxidation and total anthocyanin content were measured in two pools, each composed of six leaves at position 9. For the same reason, hydrogen peroxide (H_2O_2) was quantified in leaves at position 8 to determine changes in the redox status during senescence. Finally, developmental gene regulation was analysed in leaves at positions 6 and 7, through expression of key senescence-related genes by quantitative real-time polymerase chain reaction (qRT-PCR) in two distinct pools by leaf position (composed of six leaves each). Leaf positions were chosen here in order to have enough material and to be able to compare expression levels to the reference transcriptome provided for leaf seven by Breeze *et al.* (2011). Leaves at position 3 can be used to profile the activity of anti-oxidative enzymes such as catalases or ascorbate peroxidases. Leaves 11 and 12 were used as backups for other analyses. Methods and results are presented and explained in detail in the sections below. All protocols used are provided in the supplementary information.

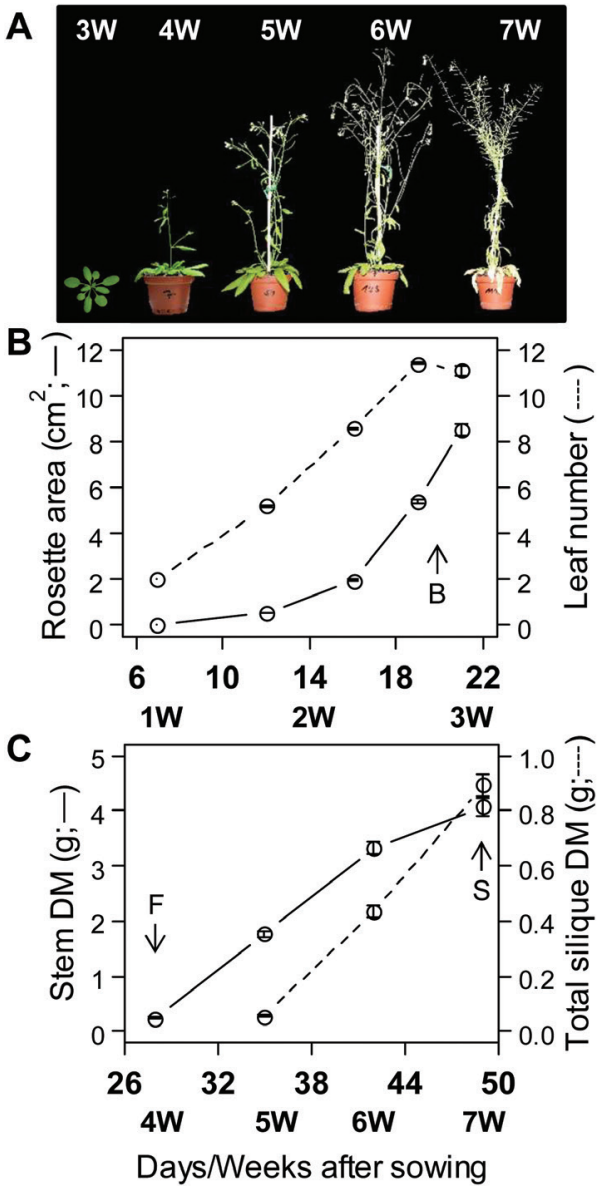

Fig. 2. Plant growth and development analyses. (A) A representative picture of Col-0 growth and senescence over 3–7 weeks after sowing. (B) Rosette area (solid line) and leaf number (dashed line), and (C) total stem (solid line) and silique dry mass (DM; dashed line) per d/week after sowing. Data are means (±SE) of 16–80 leaves. Arrows indicate bolting (B), flowering (F), and first yellowish siliques (S) stages.

Quantifying leaf senescence based on the breakdown of photosynthetic capacity

The different methods to analyse the breakdown of photosynthetic activity specified below are complementary and describe different aspects related to Chl degradation during senescence. Applying all of them gives the most holistic view of this process; however, if specific instruments are not at hand, e.g. atLeaf+ Chl meter or ChlF imaging, these measurements can be skipped in favour of Chl extraction and ACA.

Chlorophyll content through extraction and relative measurements

Photosynthesis is gradually inactivated during senescence and accompanied by degradation of Chl. Total leaf Chl content is the most popular trait for characterizing senescence progression related to the photosynthetic capacity. In higher plants, two forms of pigments prevail, Chl *a* and Chl *b*, which are differently involved in light harvesting. Chl *a* is linked to energy-processing centres of the photosystems (PS) whereas Chl *b* is considered an accessory pigment that transfers light energy to Chl *a* (Tanaka and Tanaka, 2006). During senescence, the Chl *a*/*b* ratio gives a valuable indication of the underlying process of chloroplast degradation (Pruzinská *et al.*, 2005; Sakuraba *et al.*, 2012). There are different methods to assess Chl levels in leaves. Traditionally, leaf Chl concentration is determined by spectrophotometric measurements of an 80% acetone extract. Absorbance is then converted to Chl concentration using standard equations derived from Arnon (1949; see Supplementary Protocol S1). In addition to the quantification of total Chl amount, this method allows Chl *a* and *b* levels to be distinguished based on their distinct absorption peaks, at 662.6 nm and 645.6 nm, respectively. Chl concentrations can be normalized by fresh weight (FW) or by leaf area (i.e. mg Chl g^{-1} FW or mg Chl cm^{-2}). Depending on plant growth conditions, Chl concentrations start to decrease at different time points during development. For example, decreased Chl levels have been shown at approx. 10 d after *A. thaliana* flowering under long days, 250 µmol m^{-2} s^{-1} light, 22 °C and 70% relative humidity (Breeze *et al.*, 2011). In our conditions, the total Chl concentration per unit FW was reduced by 27% one week after flowering (week 5 after sowing), parallel to an increased Chl *a*/*b* ratio (Fig. 3A). While Chl *a* level stayed almost constant, a decline in Chl *b* content was observed. This phenomenon mainly results from the conversion of Chl *b* to Chl *a* during degradation (Ito *et al.*, 1996). During silique maturation (week 7), the Chl *a*/*b* ratio was reduced and returned to values close to 1, due to equally low levels of Chl *a* and *b* in fully senescent leaves (Fig. 3A). In Arabidopsis, an increased Chl *a*/*b* ratio has also been shown during dark-induced senescence (Pruzinská *et al.*, 2005; Sakuraba *et al.*, 2012). However, senescence can affect the Chl *a*/*b* ratio differently depending on the species. An increase at late senescence stages was shown in barley (Krupinska *et al.*, 2012), whereas a decrease occurred in *Phaseolus vulgaris* and *Acer pseudoplatanus* (Jenkins *et al.*, 1981; Maunders and Brown, 1983).

A handheld Chl meter, relying on light transmittance through the leaf surface, provides a convenient and non-invasive method to measure relative Chl content. Optical values obtained from Chl meters are highly correlated to extractable leaf Chl levels (Novichonok *et al.*, 2016). In principle, optical values can be directly converted into Chl content. Here, we used the atLeaf+ Chl meter, which measures leaf absorbance of both 660 nm (red) and 940 nm (near-infrared) wavelengths. Red light is strongly absorbed by Chl, whilst near-infrared light is used as a reference wavelength to compensate for differences in leaf structure, notably leaf thicknesses (Markwell *et al.*, 1995). A single measurement takes only a few seconds and the measuring device is small enough to use on the small leaves of Arabidopsis (bigger than 0.2 cm^2). As environmental and measurement conditions can substantially influence atLeaf+ readings, measurements should be standardized as far as possible. Moreover, the non-uniform Chl distribution that occurs in leaves during senescence also has to be considered. For reproducible measurements, the readings should be done with the same leaf orientation (i.e. abaxial side up) and repeated several times over the flattened surface of the whole leaf (e.g. from the tip to the base). The proportion of leaf veins in larger leaves has an influence on the light transmittance, and therefore primary and secondary veins should generally be excluded from the measurements (Uddling *et al.*, 2007). The timing of readings is also important as the diurnal chloroplast movements in response to light affect the degree of heterogeneity in the Chl distribution (Hoel and Solhaug, 1998). Over the course of our study, 12 samples of detached leaves of both young and middle-age (positions 10 and 5, respectively) were analysed, and the atLeaf+ values could be converted into total chlorophyll content in mg cm^{-2} (http://www.atleaf.com/SPAD.aspx). As expected based on their position inside the rosette, leaf 5 globally presented lower atLeaf+ values compared to leaf 10 over the time course of the experiment (Fig. 3B). Leaf 5 displayed a significant decrease in atLeaf+ values one week after flowering, with reductions of 34% and 51% at weeks 5 and 6, respectively. Leaf 10 presented a lower decrease relatively to leaf 5, shown by a constant reduction (around 13%) until week 6 followed by a strong decline (Fig. 3B). atLeaf+ values for leaf 5 were linearly and positively correlated to the extracted total Chl concentration (R^2=0.82; P≤0.001). However, the relationship between atLeaf+ and the Chl *a*/*b* ratio was more complex and showed a curvilinear regression (data not shown). These two methods allow the time point of Chl breakdown to be defined as being during weeks 5 and 6 after sowing, and to schedule senescence initiation at flowering (week 4).

Chlorophyll fluorescence imaging

ChlF imaging, such as the pulse amplitude modulation (PAM) method, is also a widely used tool to assess photosynthetic status (Maxwell and Johnson, 2000). This method provides a non-invasive evaluation of the efficiency of PSII to supply electrons to the photosynthetic machinery. It also has the advantage of being applicable at the whole-rosette or leaf levels in various different plant species (Murchie and Lawson, 2013).

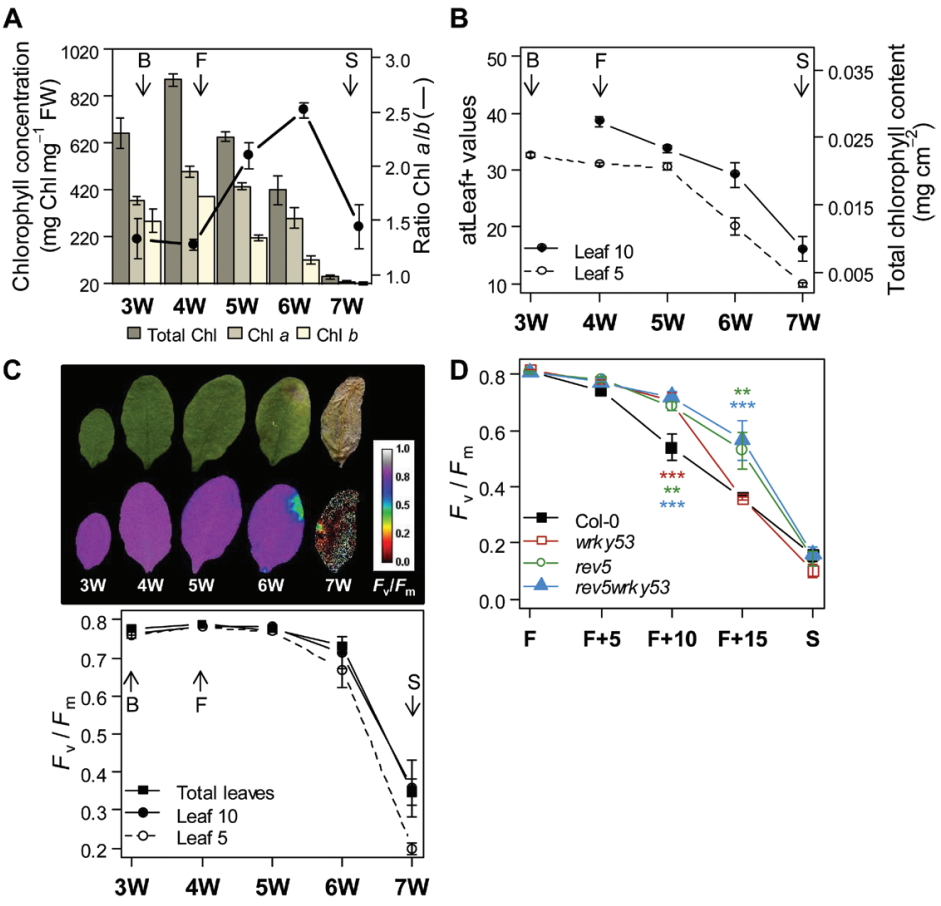

Fig. 3. Breakdown of photosynthetic capacity during leaf senescence. These measurements were taken consecutively on the same leaves at positions 5 and 10 (except for chlorophyll, Chl, content, only for leaf 5). (A) Total Chl, Chl *a*, and Chl *b* concentrations expressed by leaf fresh weight (FW) are indicated by the bars and the Chl *a*/*b* ratio by the black line. (B) Chl contents were measured using an atLeaf+ chlorophyll meter in Col-0 leaves over 3–7 weeks after sowing. Optical atLeaf+ values can be directly converted to total Chl content (right axis; http://www.atleaf.com/SPAD.aspx). (C) Top: representative leaves at position 5 in a false colour scale of photosynthetic efficiency (F_v/F_m), ranging from black (value 0) through red, yellow, green, blue to purple (ending at 1). Bottom: F_v/F_m values at the whole-rosette and leaf levels over time. Data are means (±SE) of 4–12 leaves. (D) Example of F_v/F_m measurements in knockout mutants delayed in senescence (*wrky53*, *rev5*, and *rev5wrky53*) from flowering (F) until the first siliques started yellowing (S). F+5, F+10, and F+15 indicate days after flowering. Data are means (±SE) of 5–8 plants per genotype. Significant differences were analysed using the Kruskal–Wallis test: **P*≤0.05, ***P*≤0.001, and ****P*≤0.0001. Arrows in (A–C) indicate bolting (B), flowering (F), and first yellowish siliques (S) stages.

ChlF is based on the quantification of the light re-emitted in red wavebands by dark-adapted leaves, after having been subjected to a saturating flash. Amongst the ChlF parameters, the F_v/F_m ratio, reflecting the maximal quantum yield of PSII photochemistry, is used as a sensitive and rapid indicator of physiological status (Genty *et al.*, 1989). Senescence- or stress-induced damage to the photosynthetic apparatus leads to a reduction of F_v/F_m values (Maxwell and Johnson, 2000; Bresson *et al.*, 2015). F_v/F_m has been shown to be closely related to the leaf relative water content and the Chl *a* content (Woo *et al.*, 2008; Filipovic *et al.*, 2013). Measurement of F_v/F_m is initiated by exposing dark-adapted leaves to a low modulated light beam to elicit a minimum value of ChlF, F_0. Dark-adaptation of leaves is a crucial step and should last 15–20 min for Arabidopsis. F_0 represents the basal fluorescence when excitation energy is not being transferred to the PSII reaction centres. After dark adaptation, the application of a brief saturating flash induces a maximum value of ChlF, F_m, which reflects the electron accumulation through PSII. The difference between F_0 and F_m is the variable fluorescence, F_v, and F_v/F_m is given by $(F_m–F_0)/F_m$ (Genty *et al.*, 1989). The settings for the light pulses are dependent on both growth conditions and the device used, and should be adjusted in order to reach F_v/F_m values of approximately 0.83 for healthy (fully green) plants. Values significantly under this threshold are indicative of an impaired physiological status, and under 0.3 the leaf tissues are considered as dead (Woo *et al.*, 2008). Our ChlF measurements were performed using the Imaging-PAM chlorophyll fluorometer and ImagingWin software application (Maxi version; ver. 2-46i, Heinz Walz GmbH; see Supplementary Protocol S2). The plants were dissected and leaves were fixed on the abaxial side with increasing age from left to right on black paper using double-sided tape. Data extraction from the ChlF images was done with an ImageJ (1.47v, Rasband, Bethesda, Maryland, USA) macro modified from Bresson *et al.* (2015). False-colour images of F_v/F_m permit the visualization of the spatio-temporal progression of senescence in leaves (Fig. 3C).

Senescence is often described as progressing from the leaf tip to the base with a bleaching gradient, but this is not a fixed

rule. From our experience, senescence progression can be spatially heterogeneous within the leaf, starting for example from the margins or in some cases even from the base. When examining the mean F_v/F_m value of all detached leaves over time, it displayed a similar pattern as if only leaves at positions 5 and 10 were considered (Fig. 3C). F_v/F_m dropped rather suddenly 6 weeks after sowing when senescence was clearly visible and Chl levels and atLeaf+ values were drastically reduced (Fig. 3A–C). In an independent experiment, ChlF was analysed in different lines delayed in their senescence progression, such as *wrky53*, *rev5*, and the double-knockout mutant *wrky53rev5* (Fig. 3D). WRKY53 is a well-known positive key regulator of age-induced leaf senescence (Zentgraf *et al.*, 2010) while REVOLUTA (REV) has been recently identified as a direct and positive regulator of *WRKY53* expression (Xie *et al.*, 2014). The plants were harvested according to their developmental stages from flowering until the first siliques started yellowing. Fig. 3D shows that the different mutants exhibited a significantly slower decline of F_v/F_m 10 d after flowering and reached equal F_v/F_m levels compared to Col-0 only during maturation of siliques. *rev5* and *wrky53rev5* presented an even more pronounced delay of senescence than *wrky53*, as previously shown by Xie *et al.* (2014). Although ChlF is a powerful tool to discriminate senescence mutant lines, F_v/F_m appears to be a later marker during the reorganization phase compared to extracted Chl and atLeaf+ values. However, ChlF imaging allows the easy analysis of the F_v/F_m patterns of the rosette in a dynamic manner and the estimation of the switch points of leaf senescence, as shown for example in *rev5* compared to Col-0 (see Supplementary Fig. S1).

Automated colourimetric assay (ACA)

Chl degradation is the earliest and most significant change that is visible to the naked eye. This is generally manifested by progressive leaf colour modifications from deep green to pale green, to yellow, and to brown (dry) as the final step. One of our former methods used to monitor senescence was to assign each leaf of the rosette to different categories according to its colour by visual inspection (e.g. green, green-yellow, yellow, and brown) and to calculate the proportion of each compared to the total leaf number (Miao and Zentgraf, 2010). Although this method can provide a reliable measure, it can be somewhat subjective due to the difficulties to assigning a general colour to leaves presenting colour heterogeneity. To avoid bias in leaf colour assignment, we have developed an automated colourimetric assay, which allows clustering each pixel within a leaf depending on its colour (see Supplementary Protocol S3 and http://www.zmbp.uni-tuebingen.de/gen-genetics/research-groups/zentgraf.html). ACA allows the single colour categorization by leaf to be ignored by instead giving an accurate quantification of each colour percentage within the leaf. ACA can be used in a non-invasive manner at the whole-rosette level, or in detached leaves. Non-invasive application on whole-rosettes also allows pre-screening of many plant lines before starting with detailed phenotyping of selected lines, or even the use of automated phenotyping platforms. Here, the *A. thaliana* rosettes were dissected; leaf blades were separated from their petiole, sorted by age, stuck to black paper, and scanned. Zenithal photographs can be used but the image acquisition settings (especially the lighting) must be homogeneous within an image and constant over experiments. Scans of leaves usually offer the best homogeneity. Leaves were then individually separated in single images using a semi-automatic ImageJ macro (see Supplementary Protocol S3). After manual selection of a leaf, the analysis permitted the automatic separation of the region of interest from the background and also the labelling of pictures by plant identification and leaf position number. Using R scripts (R Development Core Team, 2009), ACA was designed to automatically extract information such as genotype and plant age as well as leaf and plant number on the basis of the file name. ACA is based on grouping of each pixel of a picture depending on its position in the hue saturation value (HSV) colour-space. The three-dimensional representation of the HSV colour-space offers the opportunity to define ranges of colours taking into account three different channels (see Supplementary Protocol S3). We have defined six colour groups using Col-0 leaf pictures from four independent experiments with different growth conditions, notably with regard to light intensity (see Supplementary Fig. S2). The black background was first identified by filtering pixels based on both V and S channels, defined by V≤15% and S≤10%. The remaining pixels were grouped into bins describing green, green-yellow, yellow, brown, purple, or unknown (Fig. 4A). To achieve that, H, S, and V distributions of pictures of green, yellow, and brown leaves (classified visually) were examined, thus allowing definition of thresholds for each colour (see Fig. 3 in Supplementary Protocol S3). The purple category comprises all pinkish-purplish colours that are related to anthocyanin production (Fig. 4A). Although in some cases anthocyanin accumulates during senescence, the purple colour did not only appear in the last stage of senescence progression (from green to brown) but was also found independent of leaf age (e.g. in fully green leaves). All pixels that did not belong to the five defined classes were categorized as unknown. The percentage of each class was then calculated by subtracting background from the total pixel count. Unknown pixels represented only 0.002% across the different experiments. Fig. 4A shows a comparison of colour assignments between ACA and visual inspection. For example, a leaf considered by eye as being globally yellow displayed colour heterogeneity, with 22.6, 75.8, and 1.6% of green-yellow, yellow, and brown colours, respectively.

Here, in long-day and low-light conditions, green-yellow colours reflecting the onset of Chl breakdown during the reorganization phase of senescence appeared 6 weeks after sowing at the whole-rosette level and in leaf 5, and 7 weeks after sowing in leaf 10 (Fig. 4B). This is one week after the first decrease in Chl content and in atLeaf+ values, but in accordance with modifications observed in F_v/F_m values (Fig 3). Indeed, green percentage was linearly and positively correlated to F_v/F_m values (R^2=0.76; P≤0.001), whereas green-yellow, yellow, and brown were negatively correlated (R^2=0.18, 0.17, and 0.68, respectively; P≤0.001). The purple class was represented only marginally over the experiment, reaching a

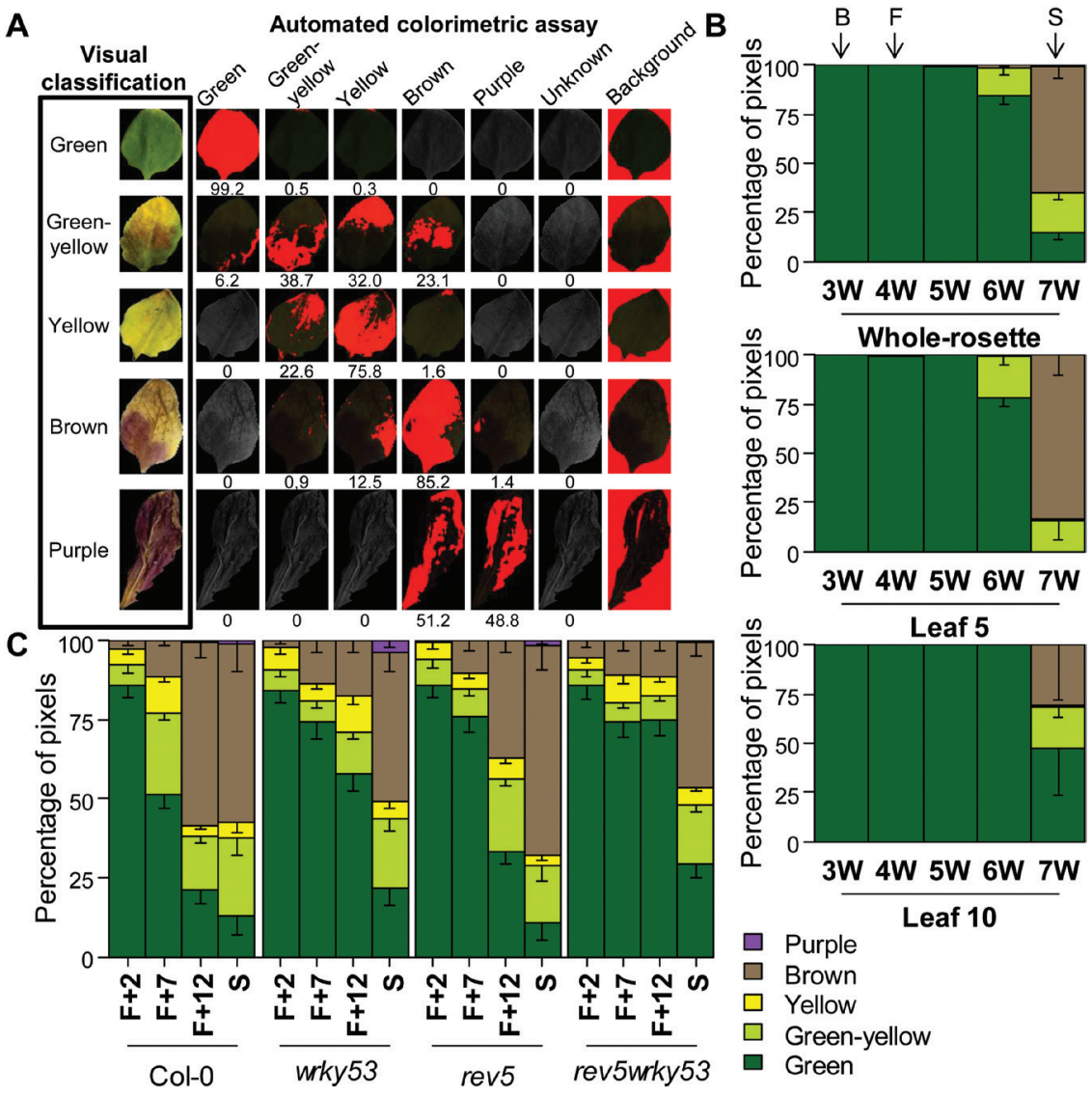

Fig. 4. Automated colourimetric assay (ACA). (A) Comparison of leaf colour assignment between visual inspection and ACA. Numbers indicate percentage of pixels of the respective colours. (B) ACA in Col-0 plants grown in long-day and low-light conditions, presented for the whole-rosette and in leaves 5 and 10 over 3–7 weeks after sowing. Data are means (±SE) of four plants. (C) Example of ACA in knockout mutants delayed in senescence (*wrky53*, *rev5*, and *rev5wrky53*) from flowering (F) until the first siliques started yellowing (S). F+2, F+7, and F+12 indicate days after flowering. Data are means (±SE) of 3–4 plants. Colour classes are organized from top to bottom: purple, brown, yellow, green-yellow, and green. Purple colours are related to anthocyanin production and do not reflect the last stage of senescence progression (from green to brown). Arrows indicate bolting (B), flowering (F), and first yellowish siliques (S) stages.

maximum of 0.9% in the termination phase (week 7). ACA was also performed on the *wrky53*, *rev5*, and *wrky53rev5* senescence-delayed lines over the period of development after flowering (Fig. 4C). While the different plants displayed a nearly similar whole-rosette pattern 2 d after flowering, Col-0 had a higher green-yellow percentage 7 d after flowering, resulting in a higher brown percentage 12 d after flowering. ACA thus validated the fact that senescence was delayed in these mutants. As for F_v/F_m values, the different mutants presented similar patterns compared to Col-0 during the maturation of the siliques (Fig. 4C). ACA thus permits quantification of senescence that is closely correlated to other Chl content-related measurements and can be robust across a variety of image samples.

Molecular and physiological investigations for analysing leaf senescence

Redox regulation: the case of hydrogen peroxide

Living cells constantly balance generation and scavenging of ROS in all cellular compartments to keep the redox status under tight control. In Arabidopsis, a network of at least 152 genes including ROS-scavenging and ROS-producing proteins is involved in managing ROS levels (Mittler *et al.*, 2004). Throughout senescence ROS, especially H_2O_2, play a pivotal role in signalling and molecule degradation (Zentgraf *et al.*, 2012). Many senescence-associated TFs are highly responsive to H_2O_2 including, for example, *WRKY53* (Miao *et al.*, 2004), *ORS1* (Balazadeh *et al.*, 2011), *JUB1* (Wu *et al.*, 2012), and

ATAF1 (Garapati *et al.*, 2015). Additionally, plants affected in H_2O_2 production or with changes in scavenging capacities show altered senescence phenotypes (Barth *et al.*, 2004; Bieker *et al.*, 2012). In Arabidopsis, the initiation of senescence coincides with an increase in intracellular H_2O_2 concentrations (Fig. 5A, B). This temporal loss of anti-oxidative capacity appears to be mainly achieved by a decrease in CATALASE2 (CAT2) and ASCORBATE PEROXIDASE1 (APX1) activities, two key H_2O_2-scavenging enzymes (Ye *et al.*, 2000; Zimmermann *et al.*, 2006). Initially, transcriptional down-regulation of *CAT2* leads to increasing H_2O_2 levels, which in turn induce post-translational inactivation of APX1 (Panchuk *et al.*, 2005). The inhibition of APX1 activity creates a positive feedback loop driving the first H_2O_2 peak, which appears to be restricted to the bolting period. As a consequence of high H_2O_2 levels, *CAT3* expression and activity are induced, which then lower the H_2O_2 levels and contribute to the recovery of APX1 activity. An even more substantial second H_2O_2 peak occurs during the termination phase of senescence, which most likely originates from degradation processes such as lipid degradation, membrane deterioration, and disruption of the electron transport chains.

Due to the inherent reactivity and instability of ROS, the specific and sensitive detection of intracellular ROS in a biological system is difficult and laborious. Here, we measured H_2O_2 contents in detached Col-0 leaves (Fig. 5B) using a semi-quantitative method according to Cathcart *et al.* (1983). This fluorescent assay uses 5(6)-carboxy-dichloro-fluorescein diacetate (carboxy-H_2DCFDA), which can react with several ROS including H_2O_2, hydroxyl radicals, and peroxynitrite.

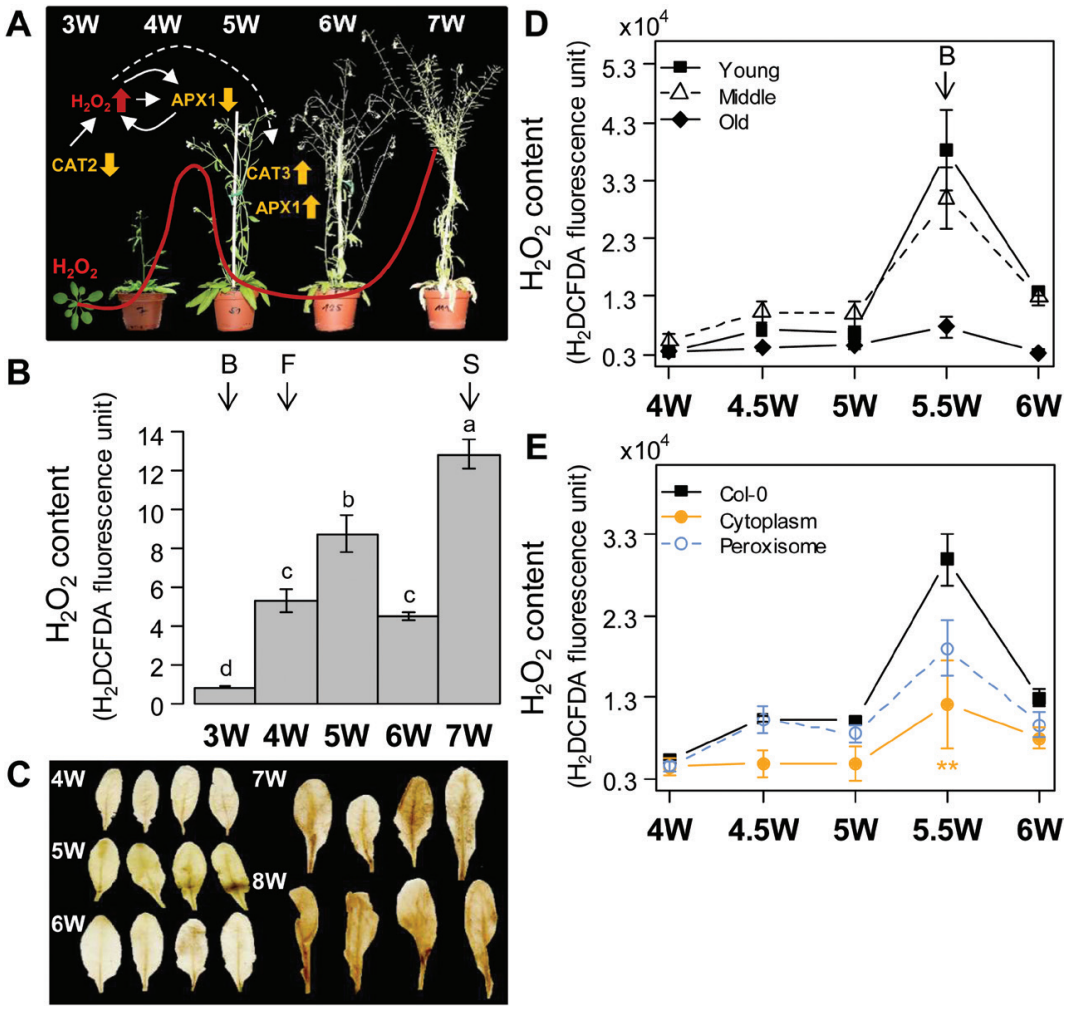

Fig. 5. Hydrogen peroxide plays a pivotal role during age-induced senescence initiation and progression. (A) Model of hydrogen peroxide (H_2O_2) regulation throughout senescence via H_2O_2-scavenging enzyme activities, notably CATALASES (CATs) and ASCORBATE PEROXIDASE 1 (APX1; according to Zimmermann *et al.*, 2006). (B) H_2O_2 content in Col-0 leaves over 3–7 weeks after sowing. H_2O_2 content was measured using a carboxy-H_2DCFDA fluorescence assay in independent leaves at position 9. Data are means (±SE) of 12 leaves. Different letters indicate significant differences according to the Kruskal–Wallis test at $P \leq 0.05$. (C) Illustration of DAB staining in four independent Col-0 leaves from 4–8 weeks after sowing. (D) H_2O_2 content over 4–6 weeks after sowing depending on Col-0 leaf position: young (leaves 8–12), middle-aged (leaves 4–7), and old (leaves 1–3), according to Bieker *et al.* (2012). Data are means (±SE) of at least three replicates. (E) Example of changes in H_2O_2 pattern in middle-aged leaves using two different lines having altered H_2O_2 levels in either the peroxisome or cytoplasm, according to Bieker *et al.* (2012). Values are means (±SE) of 10–15 biological replicates. Significant differences were analysed according to the Kruskal–Wallis test (*$P \leq 0.05$). Arrows indicate bolting (B), flowering (F), and first yellowish siliques (S) stages.

Although more H_2O_2-specific dyes such as di-amino-benzidine exist, they are often highly toxic and thus not easy to handle. Furthermore, techniques such as cerium-chloride staining or spin trapping require special equipment such as an electron microscope or an electron paramagnetic resonance spectroscope, respectively. Additionally, cerium chloride has a low cell-penetration efficiency, and thus requires relatively long incubation times. Carboxy-H_2DCFDA is a non-polar dye able to passively diffuse across cellular membranes. It is trapped inside the cells after deacetylation by an intracellular esterase, rendering the molecule polar. Deacetylated carboxy-H_2DCFDA can then be oxidized by ROS and is converted to highly fluorescent dichlorofluorescein (DCF). Only intracellular DCF is measured, as extracellular oxidized dye is not able to enter the cells and leaves are rinsed after incubation. In order to get comparable results with different dye stock solutions, calibration of the dye is required. Two options are given here, both include chemical deacetylation followed by oxidation of the dye via H_2O_2 (see Supplementary Protocol S4). H_2O_2 content can be expressed on a per leaf basis, or it can be normalized by leaf FW or area in cases of significant size differences between genotypes. For other plant species having larger leaves, a combination of FW and area (e.g. weighed leaf discs with the same diameter) usually gives the best results.

Another possibility to visualize *in situ* modifications in leaf H_2O_2 content during senescence is the 3,3′-diaminobenzidine (DAB) staining method, which has to be used with caution because of its toxicity (see Supplementary Protocol S4). Although this method can also be conducted quantitatively, we used it here to analyse the spatio-temporal H_2O_2 accumulation in leaves (Fig. 5C). DAB is oxidized by H_2O_2 in the presence of haem-containing proteins, such as peroxidases, leading to an easily visible dark brown precipitate. This is exploited as a stain to detect the presence and localization of H_2O_2 in plant cells (Daudi and O'Brien, 2012). Fig. 5C illustrates DAB staining of individual Col-0 leaves from 4 to 8 weeks after sowing, from an independent experiment. The variations of stain intensity were comparable with the measured fluctuations in leaf H_2O_2 content during plant development (Fig. 5B, C). It is also important to note that the leaf position for H_2O_2 measurement is crucial, because levels increase differently depending on age and position of the respective leaves. The youngest and middle-aged leaves (leaves 8–12 and 4–7, respectively) show a higher increase in H_2O_2 whereas the oldest leaves (1–3) present a poor and negligible H_2O_2 peak (Fig. 5D; Bieker *et al.*, 2012).

To illustrate the contribution of H_2O_2 measurement for senescence analyses, we present some examples of Arabidopsis lines affected in leaf senescence. Two prevalent changes in H_2O_2 pattern can be observed, mainly related to modifications in H_2O_2 peaks. Fig. 5E shows results of two different lines having an altered H_2O_2 level in either peroxisomes or cytoplasm by the overexpression of the fusion *Escherichia coli* protein OxyR-RD-cpYFP (Belousov *et al.*, 2006; Costa *et al.*, 2010) that consumes H_2O_2. Both transgenic lines have clearly shown a slower senescence progression (Bieker *et al.*, 2012). The H_2O_2 peak observed in wild-type plants at bolting (here at 5.5 weeks after sowing) occurred at the same time point in both transgenic lines but with significantly reduced amplitudes (Fig. 5E). On the other hand, a delay in senescence can also translate into a delay of the H_2O_2 peak with equal amplitude compared to Col-0 plants, as it was shown for *wrky53* knockout lines, which are delayed in senescence initiation (see Supplementary Fig. S3).

As well as the intracellular H_2O_2 content, CAT and APX activities can also be used as early physiological markers of senescence. Their activities decrease in Arabidopsis at a very early stage during bolting time and before the beginning of Chl breakdown (Supplementary Fig. S4; Zimmermann *et al.*, 2006). This has also been observed in other plant species, for example oilseed rape and sun flowers (Agüera *et al.*, 2010; Bieker *et al.*, 2012). Here, we give two different protocols to monitor the activity of these enzymes (see Supplementary Protocol S5). Native PAGE followed by in-gel activity staining allows the visualization of changes at the isoform level, but quantification is not easily feasible in a reproducible manner. In contrast to in-gel activity profiling, photometric assays can easily quantify total enzyme activities, but isoform-specific alterations cannot be detected.

Genetic regulation of age-induced leaf senescence markers

Identifying the dynamic changes in transcript levels gives helpful clues about key switch points in the different leaf senescence phases. Transcriptome studies using expressed sequence tag libraries and *A. thaliana* genomic arrays have revealed that senescence involves the expression of thousands of genes and many signalling pathways (Zentgraf *et al.*, 2004; Buchanan-Wollaston *et al.*, 2005; Breeze *et al.*, 2011). Genes up- or down-regulated in expression are grouped into two categories: senescence-associated genes (SAGs; Lohman *et al.*, 1994) and senescence down-regulated genes (SDGs). Among these genes, many TFs have been identified as key regulators in the control of senescence and can be used for characterizing senescence progression, such as *NAC*, *WKRY*, *MYB*, *bZIP*, and *bHLH* family members (Liu *et al.*, 2010; Li *et al.*, 2012). In this large network, we have chosen some *A. thaliana* key SAG and SDG markers at both early and late senescence stages, which we recommend as a basic set (Table 1, Fig. 6). However, other marker genes might also be suitable if specific functional aspects of senescence need to be analysed in detail. Gene expression levels were followed by qRT-PCR of Col-0 leaves over four consecutive weeks (Fig. 6; see Supplementary Protocol S6). Samples harvested in the last week (week 7) were removed from the analyses because leaves were almost completely senescent and dead, and hence only very low amounts of RNA could be isolated and no reliable transcript levels were detected. Transcriptional changes were calculated based on the comparative C_T method (Pfaffl, 2001) and normalized to *ACTIN2* levels (Panchuk *et al.*, 2005).

SAGs are up-regulated during senescence but their expression patterns in the course of plant development are quite variable due to the large spectrum of their functions (Lohman *et al.*, 1994; Weaver *et al.*, 1998). Many SAGs also respond

Table 1. *List of key genes involved in age-induced senescence*

Name	Locus	Description	Relevant papers
Senescence-associated genes (SAGs): up-regulated during senescence			
SAG12	At5g45890	Encodes a cysteine protease	Lohman *et al.*, 1994; Weaver *et al.*, 1998; Noh and Amasino, 1999
SAG13	At2g29350	Encodes a short-chain alcohol dehydrogenase	Gan, 1995; Weaver *et al.*, 1998
WRKY53	At4g23810	Member of WRKY transcription factor family (group III)	Hinderhofer and Zentgraf, 2001; Miao *et al.*, 2004; Zentgraf *et al.*, 2010
ANAC092	At5g39610	Encodes a NAC-domain transcription factor (also called *AtNAC2*, *ORE1*)	Balazadeh *et al.*, 2008, 2010; Kim *et al.*, 2009
ATG7	At5g45900	Encodes an E1 enzyme for the ubiquitin-like autophagy proteins (also called *APG7* and *AtAPG7*)	Doelling *et al.*, 2002; Thompson and Vierstra, 2005; Breeze *et al.*, 2011
ZAT12	At5g59820	Encodes a zinc finger protein	Rizhsky *et al.*, 2004*a*; Davletova *et al.*, 2005; Miller *et al.*, 2008
CAT3	At1g20620	Encodes a heme-containing enzyme with catalase activity to detoxify H_2O_2	Orendi *et al.*, 2001; Zimmermann *et al.*, 2006; Du *et al.*, 2008
Senescence down-regulated (SDGs): down-regulated during senescence			
CAT2	At1g58030	Encodes a heme-containing enzyme with catalase activity to detoxify H_2O_2	Orendi *et al.*, 2001; Zimmermann *et al.*, 2006; Du *et al.*, 2008
RBCS1A	At1g67090	Encodes a member of the Rubisco small subunit (RBCS) multigene family	Mae *et al.*, 1984; Izumi *et al.*, 2012
CAB1	At1g29930	Encodes a subunit of light-harvesting complex II (also called *LHCB1.3*)	Green *et al.*, 1991; Weaver *et al.*, 1998

to environmental stresses and can be considered as integrators of the different signalling pathways controlling stress responses and/or age-dependent senescence (Weaver *et al.*, 1998). Generally, *SAG12* and *SAG13* expression are the most extensively used SAG markers, reflecting late and early status of senescence, respectively. *SAG12* has been strictly associated with naturally induced senescence (Noh and Amasino, 1999). It encodes a putative cysteine protease, located predominantly in senescence-associated vacuoles involved in protein degradation (Carrión *et al.*, 2013). In oilseed rape, the *SAG12*/*Cab* expression pattern has been shown to reflect the transition from sink to source tissue for nitrogen (Gombert *et al.*, 2006). Although *SAG12* is involved in the massive proteolytic processes in later senescence stages, its specific targets and functions in Arabidopsis senescence are still unclear as mutants have shown no altered senescence phenotype and display normal growth and development (Otegui *et al.*, 2005; Masclaux-Daubresse *et al.*, 2010). Nevertheless, its expression is regulated in a developmentally controlled, senescence-specific manner (Noh and Amasino, 1999). *SAG12* is highly up-regulated at the mRNA level only in senescent tissues (week 6; Fig. 6A). *SAG13* encodes a protein related to a short-chain alcohol dehydrogenase and/or oxidoreductase (Gan, 1995) and is quite differently regulated from *SAG12*. Expression rose slightly before senescence initiation (week 4) and then progressively increased (Fig. 6B). Modifications in the dynamics of *SAG12* and *SAG13* expression have been shown in various mutants affected in senescence (e.g. He and Gan, 2002; Miao *et al.*, 2004).

In addition, the *NAC* and *WRKY* families constitute the two largest groups of TFs in the senescence transcriptome (Guo *et al.*, 2004). They represent valuable markers playing central roles in senescence (Guo and Gan, 2006; Zentgraf *et al.*, 2010). As key senescence-related TFs, *WRKY53* and *ANAC092* have been shown to affect the expression of many known senescence-regulated genes involved in, for example, reallocation of nutrients, cell wall modifications, and amino acid and hormone metabolism (Balazadeh *et al.*, 2010). Here, qRT-PCR analyses revealed that *WRKY53* expression can be used as a very early senescence marker, showing a strong increase at 4 weeks after sowing, when plants started to flower but no visible signs of senescence and no significant increase in *SAG12* and *SAG13* expression were observed (Figs 3, 4, 6A–C). *ANAC092* expression also increased with senescence initiation, but reached its maximum expression levels at later stages in senescent leaves (week 6; Fig. 6D), as previously determined by Balazadeh *et al.* (2008).

Some other SAGs involved in senescence-related processes were chosen to complete the overall picture. *ATG7* belongs to the autophagy-associated gene family, composed of 30 genes identified in yeast and *A. thaliana* (Bassham *et al.*, 2006). Extensive cell death and early yellowing have been shown in leaves of a number of *atg*-defective Arabidopsis mutants such as *apg7-1* (Doelling *et al.*, 2002), *atg5* (Sakuraba *et al.*, 2014), *apg9-1* (Hanaoka *et al.*, 2002), and *atg4a4b-1* (Yoshimoto *et al.*, 2004). *ATG7* encodes an E1 enzyme, which is a ubiquitin-like autophagy protein involved in intracellular protein degradation (Thompson and Vierstra, 2005). It has been shown to be required for proper nutrient recycling and senescence (Doelling *et al.*, 2002). The timing of *ATG7* expression might be a control point for autophagy activation in senescing leaf cells. Moreover, its expression is heavily enhanced in parallel with the breakdown of photosynthetic capacity during the reorganization phase (Breeze *et al.*, 2011). In our growth conditions, *ATG7* expression showed a slight initial up-regulation 5 weeks after sowing, indicating the first step of the degradative processes while photosynthetic capacity did not appear to be affected. The latter started to decline when *ATG7* expression was maximal (Figs 3C, 6E).

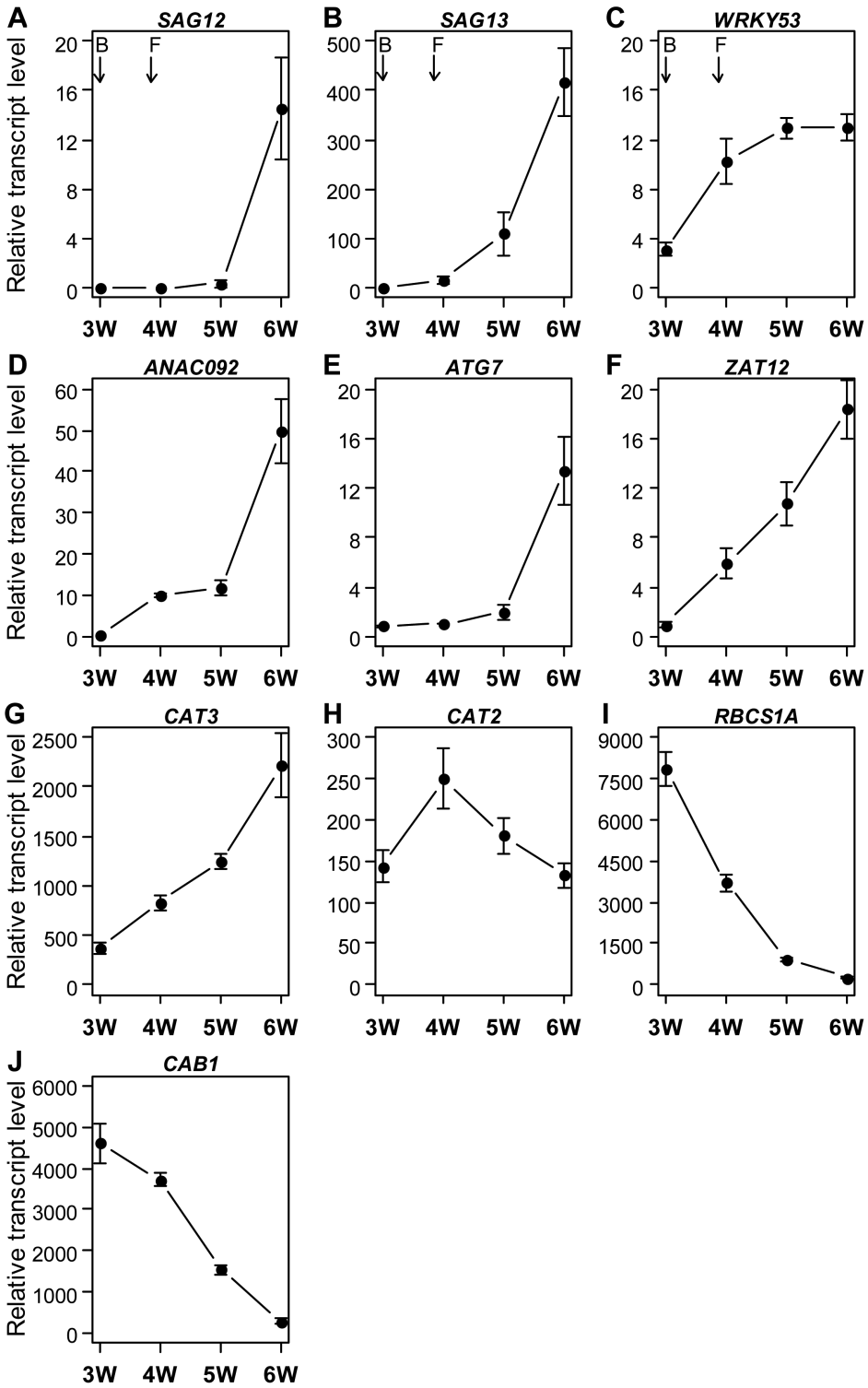

Fig. 6. Genetic regulation of senescence-related genes. qRT-PCR of different key markers in Col-0 leaves (positions 6 and 7) over 3–6 weeks after sowing: (A) *SAG12*, (B) *SAG13*, (C) *WRKY53*, (D) *ANAC092*, (E) *ATG7*, (F) *ZAT12*, (G) *CAT3*, (H) *CAT2*, (I) *RBCS1A*, and (J) *CAB1*. qRT-PCR was performed in two distinct pools by leaf position, each comprising six independent leaves. Transcriptional levels were calculated based on the comparative $\Delta\Delta C_T$ method and normalized to *ACTIN2* levels. Arrows indicate the bolting (B) and flowering (F) stages. Data are means (±SE) of four biological replicates with 1–2 technical replicates.

The TF *ZAT12* responds at transcript levels to a plethora of abiotic and biotic stresses and is notably involved in cold and oxidative stress signalling in Arabidopsis (Rizhsky *et al.*, 2004*b*; Vogel *et al.*, 2005). *ZAT12* might be related to leaf senescence by its strong implication in ROS signal transduction (Miller *et al.*, 2008). *ZAT12* expression is notably induced by H_2O_2 (Davletova *et al.*, 2005), which accumulates in *A. thaliana* cells during senescence initiation at bolting

(Fig. 5A–C). In addition, during oxidative stress, ZAT12 was shown to be required for *APX1* expression (Rizhsky *et al.*, 2004*a*). In our experiment, *ZAT12* transcript abundance showed a strong rise at very early stages (week 4), which is concomitant with an increase in H_2O_2 content at this time point. However, the *ZAT12* expression increased steadily during senescence progression, not following the H_2O_2 leaf content dynamics (Figs 5, 6F). Furthermore, *APX1* expression is also not induced during senescence progression (Panchuk *et al.*, 2005), indicating a more complex function of *ZAT12* in the senescence regulatory network.

CAT2 and *CAT3* also play a key role in H_2O_2 metabolism (Fig. 5A), as they catalyse the decomposition of H_2O_2 to water and oxygen without need of reducing equivalents (Du *et al.*, 2008). The Arabidopsis CAT family is a good example of a gene family containing SAGs as well as SDGs. While two members, *CAT3* and *CAT1*, are SAGs with different dynamics, *CAT2* belongs to the group of SDGs. Their role during leaf senescence is well documented (e.g. Orendi *et al.*, 2001; Zimmermann *et al.*, 2006). The development of senescence symptoms is correlated with modifications of CAT activities: CAT2 activity decreases at an early stage during bolting, whereas CAT3 activity increases with plant age (Zimmermann *et al.*, 2006). Consistent with this, *CAT3* expression started to increase with senescence initiation and reached maximal expression in senescent leaves. In contrast, *CAT2* is down-regulated during leaf senescence (Fig. 6G, H).

In contrast to SAGs, SDGs are not generally assumed to actively participate in the senescence regulatory network itself but instead they reflect a more general reduction of the leaf maintenance machinery. Interestingly, using multi-parallel qRT-PCR, Balazadeh *et al.* (2008) have found more TF genes being down-regulated than up-regulated during senescence. Here, we have chosen two key SDGs that are often used as senescence-markers and that reflect the breakdown of photosynthetic capacity (Table 1, Fig. 6I, J). The *RBCS1A* and *CAB1* genes both have important roles in photosynthetic CO_2 fixation (Izumi *et al.*, 2012). Senescence-correlated losses in photosynthetic capacity are usually associated with alterations in their protein activities. Rubisco is a critical enzyme of the Calvin cycle and the most abundant chloroplast protein, comprising approximately 50% of soluble proteins (Wittenbach, 1978). Rubisco content changes greatly during a leaf's life span and is one of the proteins broken down early during senescence. Fragmentation of the Rubisco large subunits is notably induced by ROS (Desimone *et al.*, 1996). Rubisco is transported from chloroplasts to the vacuole by autophagy for degradation (Ishida *et al.*, 2008). It has been shown in wheat that the amount of Rubisco decreases rapidly in the early leaf senescence stages, although more slowly in the later stages (Mae *et al.*, 1984). Moreover, Rubisco subunits were found to be controlled at the translational levels during rice leaf senescence (Suzuki and Makino, 2013). Here, *RBCS1A* in Col-0 leaves showed a reduction of 50% of its transcript levels at 4 weeks after sowing, which appears to be early compared to the breakdown of photosynthetic capacity. Its expression then gradually decreased during senescence progression (Figs 3C, 6I). *CAB1* belongs to the *LHC* gene family and encodes for a subunit of the light-harvesting complex II (Green *et al.*, 1991). It has been shown that *LHCB* gene expression is tightly regulated by developmental cues as well as by multiple environmental signals, particularly including light or oxidative stresses (see references in Liu *et al.*, 2013). Decreased *CAB1* expression is also associated with reduced photosynthetic activity as plants senesce (Li *et al.*, 2013). Fig. 6J shows that *CAB1* presented a similar pattern to *RBCS1A*, but with a weaker decrease at 4 weeks after sowing.

All these markers acting in various key senescence-related processes give a global picture that includes the initiation, reorganization, and termination phases of leaf senescence. Moreover, they do not act individually but in a complex network with many possible interconnections.

Membrane integrity

During senescence, the membrane undergoes biochemical and biophysical changes leading to the final collapse of the cell. The plasma membrane of senescing cells becomes fragile and permeable. Membrane proteins and lipids are oxidized and degraded. This leads to dramatic modifications in lipid composition and a decrease in solute retention (Dhindsa *et al.*, 1981). We suggest estimating cell membrane integrity during senescence through measurements of EL and lipid peroxidation. EL is a well-established method to analyse disruption of cell membranes manifested by the leaking of solutes out of leaves that occurs under various stresses (e.g. Debrunner and Feller, 1995; Campos *et al.*, 2003) or ageing (e.g. Rolny *et al.*, 2011). An increase of EL reflects an extensive disruption of plasma membranes during leaf senescence (Lim *et al.*, 2007). During the reorganization phase, although cell membranes exhibit no massive degradation, EL can also increase due to the accumulation of leaf ammonium resulting from protein degradation (Rolny *et al.*, 2011). Slower increases in EL indicate a delayed senescence phenotype, as shown for example in *ore1* mutants affected in ageing-induced cell death (Kim *et al.*, 2009). EL is often quantified in detached leaves by measuring conductivity of a bathing solution (e.g. Saltveit, 2002; Campos *et al.*, 2003; Rolny *et al.*, 2011). Here, we present senescence-induced effects on EL for single detached leaves of Col-0 measured by a conductivity meter (CM100-2, Reid & Associates, Durban, South Africa; Fig. 7A, B). Leaves were first washed in deionized water to remove solutes from the surface. The conductivity of the bathing solution (deionized water) was measured every hour for 20 h. The slope of a fitted linear curve was then used to quantify the EL velocity, which can be normalized by leaf FW or area (see Supplementary Protocol S7). EL expressed by FW showed an initial increase during senescence initiation at flowering (week 4), which also coincides with the first increase in H_2O_2 content (Figs 5B, 7A). EL then showed a slight but still constant increase during the reorganization phase (weeks 5–6) and a strong peak in fully senescent leaves in the termination phase (week 7), which reflects cell death (Fig. 7A).

Lipid peroxidation can also be used as an indicator of membrane deterioration during senescence (Dhindsa *et al.*, 1981; Ahmad and Tahir, 2016). Lipid peroxidation is the

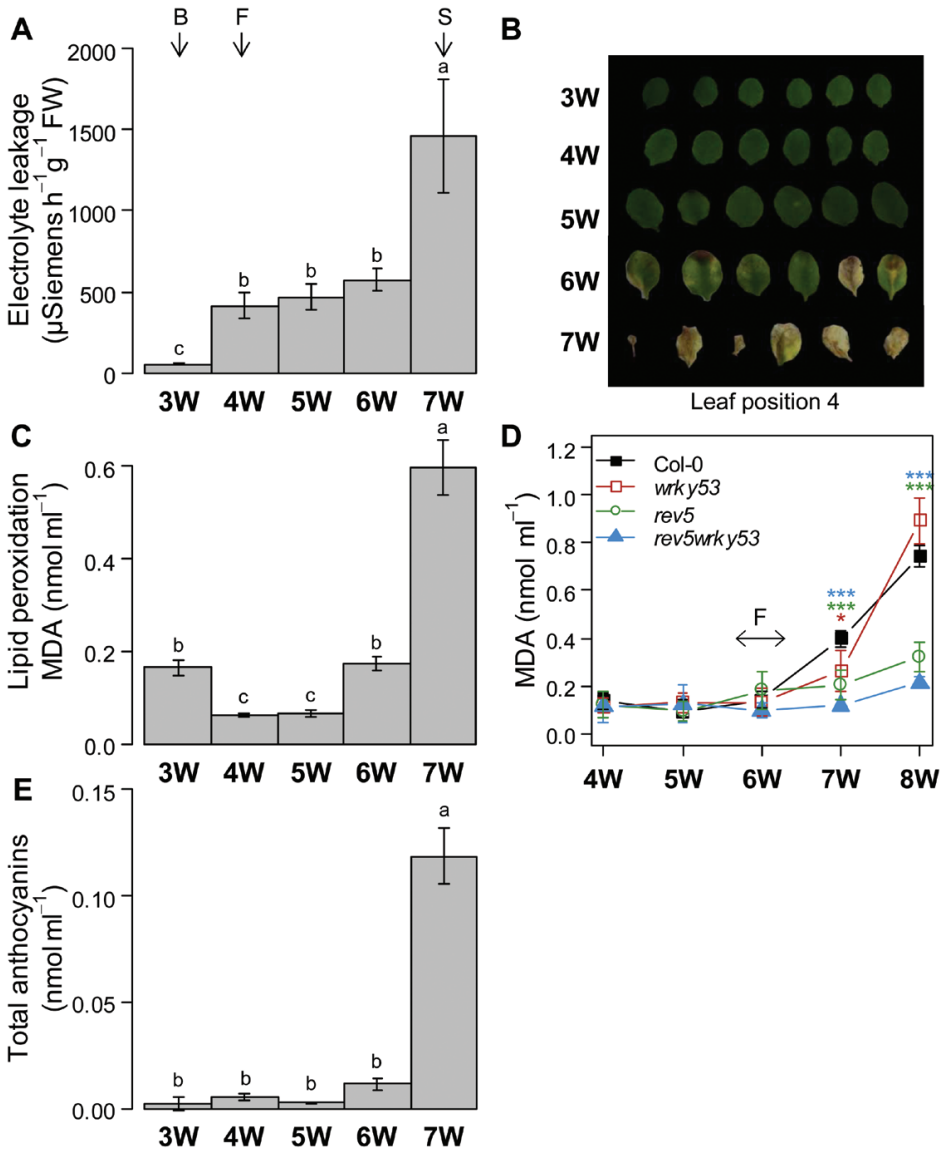

Fig. 7. Loss of membrane integrity during leaf senescence. (A) Electrolyte leakage (EL) in Col-0 leaves over 3–7 weeks after sowing. EL was measured in single detached leaves (position 4) using a conductivity meter (CM100-2, Reid & Associates, Durban, South Africa) and normalized to leaf fresh weight (FW). Data are means (±SE) of 12 leaves. (B) A representative picture of leaves used for EL. (C) Lipid peroxidation in Col-0 leaves over 3–7 weeks after sowing. Lipid peroxidation was measured using two distinct pools each of six independent leaves (position 9). Data are means (±SE) of two biological and two technical replicates. Different letters indicate significant differences according to the Kruskal–Wallis test at $P \leq 0.05$. (D) Example of lipid peroxidation measurements in knockout mutants delayed in senescence (*wrky53*, *rev5*, and *rev5wrky53*) according to Xie *et al.* (2014). Data are means (±SD) of at least three biological replicates. Comparison of means and determination of statistical differences was carried out using Student's *t*-test (*$P \leq 0.05$, **$P \leq 0.005$, and ***$P \leq 0.0005$). (E) Total anthocyanin content in Col-0 leaves over 3–7 weeks after sowing, measured during lipid peroxidation determination. Arrows in (A, C–E) indicate bolting (B), flowering (F), and first yellowish siliques (S) stages.

consequence of the oxidative degradation of polyunsaturated fatty acids, through auto-oxidation or ROS, occurring during ageing. This induces the production of a large variety of oxidation products such as malondialdehyde (MDA), propanal, hexanal, and 4-hydroxynonenal (Ayala *et al.*, 2014). MDA concentration is one of the most widespread and reliable markers of lipid peroxidation in plant tissues (Del Rio *et al.*, 2005). Here, we utilized an improved thiobarbituric acid-reactive-substances assay (TBARS) developed by Hodges *et al.* (1999). This method is based on spectrophotometric measurement of a pinkish-red adduct between MDA and two molecules of TBA with a maximum absorbance at 532 nm (Janero, 1990; Hodges *et al.*, 1999). Certain compounds, such as anthocyanin and carbohydrates, may interfere with the measurements at this wavelength and thus could lead to an over-estimation of MDA levels. To estimate and correct for the interference of non TBA-complexes, another reaction with the same plant extracts but without TBA is used and the values are subtracted from the corresponding reaction containing TBA. Total anthocyanin levels are determined as the difference between absorbance at 532 and 600 nm (Hodges and Nozzolillo, 1995), which is also used as a physiological parameter of senescence progression. Furthermore, in addition to lipid peroxides, sugars can also bind to TBA,

and therefore a further measurement at 440 nm is made. The MDA concentration is then corrected using these three measurements according to Hodges *et al.* (1999). For senescence analyses, corrections for interfering compounds are indispensable as plants can accumulate anthocyanin and sugars in their leaves during senescence. Normalization of MDA levels is not normally necessary as the same amount of sample is used for extraction (see Supplementary Protocol S8). If this is not the case, normalization to allow for differing amounts of sample is still possible. Here, MDA levels measured in Col-0 leaves showed a global increase over the time course, which was highly correlated with increased EL (Fig. 7A, C; R^2=0.81; P≤0.001). This illustrated the age-dependent degradation of cell membranes, which showed a progressive loss of integrity from flowering until irreversible and fatal damage occurred in fully senescent leaves during the termination phase. As an example, we have compared Col-0 plants to *wrky53*, *rev5*, and *wrky53rev5* mutants that are delayed in senescence. Lipid peroxidation showed an accelerated increase in Col-0 leaves at 7 weeks after sowing compared to the mutants. As shown for the results for F_v/F_m and ACA, *wrky53* recovered to Col-0 values in the termination phase of senescence (Figs 3D, 4C, 7D; Xie *et al.*, 2014). Interestingly, it could be shown that levels of lipid peroxidation were related to levels of senescence (via Chl content) in the different mutants (Xie *et al.*, 2014). As for lipid peroxidation, total anthocyanin levels started to increase in week 6 and reached very high levels during the terminal phase in week 7. This also correlated with the results obtained from the ACA (Figs 4, 7E).

Conclusion and perspectives

This paper proposes a guideline for analysing senescence in a dynamic manner using different early and late markers in key senescence-related processes involved during the initiation, reorganization, and termination phases. We provide a novel simple and automated quantification of leaf senescence, which also allows the quantification of anthocyanin in senescing leaves. We did not want to make an exhaustive list of all the methods that exist, but rather give a simple directive for starting analysis of different plants and/or abiotic and biotic stresses, which could affect leaf senescence. This can serve as a basis for identifying senescence-associated genes as well as natural diversity that can then be extended to a deeper analysis to answer specific questions depending on the study. For example, amongst the different key markers, hormone and sugar signalling can be investigated for senescence analyses.

We also wanted to emphasize that a clear distinction must be made between plant development and the onset or progression of leaf senescence. Bolting/flowering time (and by extension stem length) is often considered as a marker of the *onset* of senescence in annual plants; however, although senescence usually starts at bolting, it is not correlated to the *progression* of senescence across leaves. For instance, Koornneef *et al.* (1991) have shown that two *A. thaliana* mutants (*co-2* and *fca*) exhibit a delay in flowering but have a normal progression of leaf senescence. This clearly illustrates that leaf senescence and reproductive development should be considered as dissectible processes.

All the methods presented here were described for Arabidopsis but can easily be adapted to other plant species, for example as already shown for oilseed rape (Bieker *et al.*, 2012). As senescence is an important trait in agriculture, analysing senescence in crop plants is already a significant issue and will become more and more important. Therefore, a detailed analysis as described here but applied to crop plants showing altered senescence will lead to a better understanding as to which part of the senescence program is actually affected by specific genome changes. This would give early hints on whether the modifications in senescence might interfere with yield stability and stress resistance of high-performance crop plant lines.

Supplementary Data

Supplementary data are available at *JXB* online.

Table S1. Composition of the soil used in our experiments.

Fig. S1. F_v/F_m rosette patterns of Col-0 and of the delayed-senescence mutant *rev5* over the course of plant development.

Fig. S2. Automated colourimetric assays in different experiments with varying light conditions.

Fig. S3. Hydrogen peroxide content in the delayed-senescence mutant *wrky53* over the course of plant development.

Fig. S4. Activity zymograms for catalases and ascorbate peroxidase over the course of development.

Protocol S1. Chlorophyll extraction.

Protocol S2. Chlorophyll fluorescence imaging.

Protocol S3. Automated colourimetric assay.

Protocol S4. Hydrogen peroxide measurement.

Protocol S5. Anti-oxidative enzyme activities.

Protocol S6. Quantitative real-time polymerase chain reaction (qRT-PCR).

Protocol S7. Electrolyte leakage.

Protocol S8. Lipid peroxidation.

Acknowledgments

We thank Gesine Seibold and Manuela Freund for their technical support. We also thank François Vasseur for comments on previous versions of the present paper. The authors' research was supported by grants from the Deutsche Forschungsgemeinschaft (FOR948 ZE 313/8-2, ZE 313/9-1, and the CRC1101, B06). JB was funded by the Alexander von Humboldt Foundation.

References

Agüera E, Cabello P, de la Haba P. 2010. Induction of leaf senescence by low nitrogen nutrition in sunflower (*Helianthus annuus*) plants. Physiologia Plantarum **138,** 256–267.

Ahmad SS, Tahir I. 2016. Increased oxidative stress, lipid peroxidation and protein degradation trigger senescence in *Iris versicolor* L. flowers. Physiology and Molecular Biology of Plants **22,** 507–514.

Arnon DI. 1949. Copper enzymes in isolated chloroplasts. polyphenoloxidase in *Beta vulgaris*. Plant Physiology **24,** 1–15.

Ayala A, Muñoz MF, Argüelles S. 2014. Lipid peroxidation: production, metabolism, and signaling mechanisms of malondialdehyde and

4-hydroxy-2-nonenal. Oxidative Medicine and Cellular Longevity **2014,** 360438.

Balazadeh S, Kwasniewski M, Caldana C, Mehrnia M, Zanor MI, Xue GP, Mueller-Roeber B. 2011. ORS1, an H_2O_2-responsive NAC transcription factor, controls senescence in *Arabidopsis thaliana*. Molecular Plant **4,** 346–360.

Balazadeh S, Riaño-Pachón DM, Mueller-Roeber B. 2008. Transcription factors regulating leaf senescence in *Arabidopsis thaliana*. Plant Biology **10**(Suppl 1), 63–75.

Balazadeh S, Siddiqui H, Allu AD, Matallana-Ramirez LP, Caldana C, Mehrnia M, Zanor MI, Köhler B, Mueller-Roeber B. 2010. A gene regulatory network controlled by the NAC transcription factor ANAC092/AtNAC2/ORE1 during salt-promoted senescence. The Plant Journal **62,** 250–264.

Barth C, Moeder W, Klessig DF, Conklin PL. 2004. The timing of senescence and response to pathogens is altered in the ascorbate-deficient Arabidopsis mutant *vitamin c-1*. Plant Physiology **134,** 1784–1792.

Bassham DC, Laporte M, Marty F, Moriyasu Y, Ohsumi Y, Olsen LJ, Yoshimoto K. 2006. Autophagy in development and stress responses of plants. Autophagy **2,** 2–11.

Belousov VV, Fradkov AF, Lukyanov KA, Staroverov DB, Shakhbazov KS, Terskikh AV, Lukyanov S. 2006. Genetically encoded fluorescent indicator for intracellular hydrogen peroxide. Nature Methods **3,** 281–286.

Bieker S, Riester L, Stahl M, Franzaring J, Zentgraf U. 2012. Senescence-specific alteration of hydrogen peroxide levels in *Arabidopsis thaliana* and oilseed rape spring variety *Brassica napus* L. cv. Mozart. Journal of Integrative Plant Biology **54,** 540–554.

Biswal U, Biswal B. 1984. Photocontrol of leaf senescence. Photochemistry and Photobiology **39,** 875–879.

Breeze E, Harrison E, McHattie S, *et al*. 2011. High-resolution temporal profiling of transcripts during Arabidopsis leaf senescence reveals a distinct chronology of processes and regulation. The Plant Cell **23,** 873–894.

Bresson J, Vasseur F, Dauzat M, Koch G, Granier C, Vile D. 2015. Quantifying spatial heterogeneity of chlorophyll fluorescence during plant growth and in response to water stress. Plant Methods **11,** 23.

Buchanan-Wollaston V, Earl S, Harrison E, Mathas E, Navabpour S, Page T, Pink D. 2003. The molecular analysis of leaf senescence–a genomics approach. Plant Biotechnology Journal **1,** 3–22.

Buchanan-Wollaston V, Page T, Harrison E, *et al*. 2005. Comparative transcriptome analysis reveals significant differences in gene expression and signalling pathways between developmental and dark/starvation-induced senescence in Arabidopsis. The Plant Journal **42,** 567–585.

Campos PS, Quartin V, Ramalho JC, Nunes MA. 2003. Electrolyte leakage and lipid degradation account for cold sensitivity in leaves of *Coffea* sp. plants. Journal of Plant Physiology **160,** 283–292.

Carrión CA, Costa ML, Martínez DE, Mohr C, Humbeck K, Guiamet JJ. 2013. *In vivo* inhibition of cysteine proteases provides evidence for the involvement of 'senescence-associated vacuoles' in chloroplast protein degradation during dark-induced senescence of tobacco leaves. Journal of Experimental Botany **64,** 4967–4980.

Cathcart R, Schwiers E, Ames BN. 1983. Detection of picomole levels of hydroperoxides using a fluorescent dichlorofluorescein assay. Analytical Biochemistry **134,** 111–116.

Costa A, Drago I, Behera S, Zottini M, Pizzo P, Schroeder JI, Pozzan T, Lo Schiavo F. 2010. H_2O_2 in plant peroxisomes: an *in vivo* analysis uncovers a Ca^{2+}-dependent scavenging system. The Plant Journal **62,** 760–772.

Daudi A, O'Brien JA. 2012. Detection of hydrogen peroxide by DAB staining in Arabidopsis leaves. Bio-protocol **2,** e263.

Davletova S, Schlauch K, Coutu J, Mittler R. 2005. The zinc-finger protein Zat12 plays a central role in reactive oxygen and abiotic stress signaling in Arabidopsis. Plant Physiology **139,** 847–856.

Debrunner N, Feller U. 1995. Solute leakage from detached plant parts of winter wheat: influence of maturation stage and incubation temperature. Journal of Plant Physiology **145,** 257–260.

Del Rio D, Stewart AJ, Pellegrini N. 2005. A review of recent studies on malondialdehyde as toxic molecule and biological marker of oxidative stress. Nutrition, Metabolism, and Cardiovascular Diseases **15,** 316–328.

Desimone M, Henke A, Wagner E. 1996. Oxidative stress induces partial degradation of the large subunit of ribulose-1,5-bisphosphate carboxylase/oxygenase in isolated chloroplasts of barley. Plant Physiology **111,** 789–796.

Dhindsa RS, Plumb-Dhindsa P, Thorpe TA. 1981. Leaf senescence: correlated with increased levels of membrane permeability and lipid peroxidation, and decreased levels of superoxide dismutase and catalase. Journal of Experimental Botany **32,** 93–101.

Diaz-Mendoza M, Velasco-Arroyo B, Santamaria ME, González-Melendi P, Martinez M, Diaz I. 2016. Plant senescence and proteolysis: two processes with one destiny. Genetics and Molecular Biology **39,** 329–338.

Doelling JH, Walker JM, Friedman EM, Thompson AR, Vierstra RD. 2002. The APG8/12-activating enzyme APG7 is required for proper nutrient recycling and senescence in *Arabidopsis thaliana*. The Journal of Biological Chemistry **277,** 33105–33114.

Du YY, Wang PC, Chen J, Song CP. 2008. Comprehensive functional analysis of the catalase gene family in *Arabidopsis thaliana*. Journal of Integrative Plant Biology **50,** 1318–1326.

Filipovic A, Poljak M, Skobic D. 2013. Response of chlorophyll *a*, SPAD values and chlorophyll fluorescence parameters in leaves of apricot affected some abiotic factors. Journal of Food Science and Engineering **3,** 19.

Gan S. 1995. Molecular characterization and genetic manipulation of plant senescence. Doctoral dissertation, Madison: University of Wisconsin.

Garapati P, Xue GP, Munné-Bosch S, Balazadeh S. 2015. Transcription factor ATAF1 in Arabidopsis promotes senescence by direct regulation of key chloroplast maintenance and senescence transcriptional cascades. Plant Physiology **168,** 1122–1139.

Genty B, Briantais J-M, Baker NR. 1989. The relationship between the quantum yield of photosynthetic electron transport and quenching of chlorophyll fluorescence. Biochimica et Biophysica Acta (BBA) - General Subjects **990,** 87–92.

Gombert J, Etienne P, Ourry A, Le Dily F. 2006. The expression patterns of *SAG12/Cab* genes reveal the spatial and temporal progression of leaf senescence in *Brassica napus* L. with sensitivity to the environment. Journal of Experimental Botany **57,** 1949–1956.

Green BR, Pichersky E, Kloppstech K. 1991. Chlorophyll *a*/*b*-binding proteins: an extended family. Trends in Biochemical Sciences **16,** 181–186.

Guo Y, Cai Z, Gan S. 2004. Transcriptome of Arabidopsis leaf senescence. Plant, Cell & Environment **27,** 521–549.

Guo Y, Gan S. 2006. AtNAP, a NAC family transcription factor, has an important role in leaf senescence. The Plant Journal **46,** 601–612.

Hanaoka H, Noda T, Shirano Y, Kato T, Hayashi H, Shibata D, Tabata S, Ohsumi Y. 2002. Leaf senescence and starvation-induced chlorosis are accelerated by the disruption of an Arabidopsis autophagy gene. Plant Physiology **129,** 1181–1193.

He J, Giusti MM. 2010. Anthocyanins: natural colorants with health-promoting properties. Annual Review of Food Science and Technology **1,** 163–187.

He Y, Gan S. 2002. A gene encoding an acyl hydrolase is involved in leaf senescence in Arabidopsis. The Plant Cell **14,** 805–815.

Hensel LL, Grbić V, Baumgarten DA, Bleecker AB. 1993. Developmental and age-related processes that influence the longevity and senescence of photosynthetic tissues in arabidopsis. The Plant Cell **5,** 553–564.

Hinderhofer K, Zentgraf U. 2001. Identification of a transcription factor specifically expressed at the onset of leaf senescence. Planta **213,** 469–473.

Hodges DM, DeLong JM, Forney CF, Prange RK. 1999. Improving the thiobarbituric acid-reactive-substances assay for estimating lipid peroxidation in plant tissues containing anthocyanin and other interfering compounds. Planta **207,** 604–611.

Hodges DM, Nozzolillo C. 1995. Anthocyanin and anthocyanoplast content of cruciferous seedlings subjected to mineral nutrient deficiencies. Journal of Plant Physiology **147,** 749–754.

Hoel BO, Solhaug KA. 1998. Effect of irradiance on chlorophyll estimation with the Minolta SPAD-502 leaf chlorophyll meter. Annals of Botany **82,** 389–392.

Ishida H, Yoshimoto K, Izumi M, Reisen D, Yano Y, Makino A, Ohsumi Y, Hanson MR, Mae T. 2008. Mobilization of rubisco and

stroma-localized fluorescent proteins of chloroplasts to the vacuole by an *ATG* gene-dependent autophagic process. Plant Physiology **148,** 142–155.

Ito H, Ohtsuka T, Tanaka A. 1996. Conversion of chlorophyll *b* to chlorophyll *a* via 7-hydroxymethyl chlorophyll. The Journal of Biological Chemistry **271,** 1475–1479.

Izumi M, Tsunoda H, Suzuki Y, Makino A, Ishida H. 2012. *RBCS1A* and *RBCS3B*, two major members within the Arabidopsis *RBCS* multigene family, function to yield sufficient Rubisco content for leaf photosynthetic capacity. Journal of Experimental Botany **63,** 2159–2170.

Janero DR. 1990. Malondialdehyde and thiobarbituric acid-reactivity as diagnostic indices of lipid peroxidation and peroxidative tissue injury. Free Radical Biology & Medicine **9,** 515–540.

Jansson S, Thomas H. 2008. Senescence: developmental program or timetable? New Phytologist **179,** 575–579.

Jenkins GI, Baker NR, Woolhouse HW. 1981. Changes in chlorophyll content and organization during senescence of the primary leaves of *Phaseolus vulgaris* L. in relation to photosynthetic electron transport. Journal of Experimental Botany **32,** 1009–1020.

Johansson E, Olsson O, Nyström T. 2004. Progression and specificity of protein oxidation in the life cycle of *Arabidopsis thaliana*. The Journal of Biological Chemistry **279,** 22204–22208.

Kim JH, Woo HR, Kim J, Lim PO, Lee IC, Choi SH, Hwang D, Nam HG. 2009. Trifurcate feed-forward regulation of age-dependent cell death involving miR164 in Arabidopsis. Science **323,** 1053–1057.

Koornneef M, Hanhart CJ, van der Veen JH. 1991. A genetic and physiological analysis of late flowering mutants in *Arabidopsis thaliana*. Molecular & General Genetics **229,** 57–66.

Krupinska K, Mulisch M, Hollmann J, Tokarz K, Zschiesche W, Kage H, Humbeck K, Bilger W. 2012. An alternative strategy of dismantling of the chloroplasts during leaf senescence observed in a high-yield variety of barley. Physiologia Plantarum **144,** 189–200.

Kuriyama H, Fukuda H. 2002. Developmental programmed cell death in plants. Current Opinion in Plant Biology **5,** 568–573.

Li Z, Peng J, Wen X, Guo H. 2012. Gene network analysis and functional studies of senescence-associated genes reveal novel regulators of Arabidopsis leaf senescence. Journal of Integrative Plant Biology **54,** 526–539.

Li Z, Peng J, Wen X, Guo H. 2013. ETHYLENE-INSENSITIVE3 is a senescence-associated gene that accelerates age-dependent leaf senescence by directly repressing miR164 transcription in Arabidopsis. The Plant Cell **25,** 3311–3328.

Lim PO, Kim HJ, Nam HG. 2007. Leaf senescence. Annual Review of Plant Biology **58,** 115–136.

Liu R, Xu Y-H, Jiang S-C, *et al*. 2013. Light-harvesting chlorophyll *a*/*b*-binding proteins, positively involved in abscisic acid signalling, require a transcription repressor, WRKY40, to balance their function. Journal of Experimental Botany **64,** 5443–5456.

Liu X, Li Z, Jiang Z, Zhao Y, Peng J, Jin J, Guo H, Luo J. 2010. LSD: a leaf senescence database. Nucleic Acids Research **39,** D1103–D1107.

Lohman KN, Gan S, John MC, Amasino RM. 1994. Molecular analysis of natural leaf senescence in *Arabidopsis thaliana*. Physiologia Plantarum **92,** 322–328.

Mae T, Kai N, Makino A, Ohira K. 1984. Relation between ribulose bisphosphate carboxylase content and chloroplast number in naturally senescing primary leaves of wheat. Plant and Cell Physiology **25,** 333–336.

Malagoli P, Lainé P, Le Deunff E, Rossato L, Ney B, Ourry A. 2004. Modeling nitrogen uptake in oilseed rape cv Capitol during a growth cycle using influx kinetics of root nitrate transport systems and field experimental data. Plant Physiology **134,** 388–400.

Markwell J, Osterman JC, Mitchell JL. 1995. Calibration of the Minolta SPAD-502 leaf chlorophyll meter. Photosynthesis Research **46,** 467–472.

Masclaux-Daubresse C, Daniel-Vedele F, Dechorgnat J, Chardon F, Gaufichon L, Suzuki A. 2010. Nitrogen uptake, assimilation and remobilization in plants: challenges for sustainable and productive agriculture. Annals of Botany **105,** 1141–1157.

Maunders MJ, Brown SB. 1983. The effect of light on chlorophyll loss in senescing leaves of sycamore (*Acer pseudoplatanus* L.). Planta **158,** 309–311.

Maxwell K, Johnson GN. 2000. Chlorophyll fluorescence—a practical guide. Journal of Experimental Botany **51,** 659–668.

Miao Y, Laun T, Zimmermann P, Zentgraf U. 2004. Targets of the WRKY53 transcription factor and its role during leaf senescence in Arabidopsis. Plant Molecular Biology **55,** 853–867.

Miao Y, Zentgraf U. 2010. A HECT E3 ubiquitin ligase negatively regulates Arabidopsis leaf senescence through degradation of the transcription factor WRKY53. The Plant Journal **63,** 179–188.

Miller G, Shulaev V, Mittler R. 2008. Reactive oxygen signaling and abiotic stress. Physiologia Plantarum **133,** 481–489.

Mittler R, Vanderauwera S, Gollery M, Van Breusegem F. 2004. Reactive oxygen gene network of plants. Trends in Plant Science **9,** 490–498.

Murchie EH, Lawson T. 2013. Chlorophyll fluorescence analysis: a guide to good practice and understanding some new applications. Journal of Experimental Botany **64,** 3983–3998.

Noh YS, Amasino RM. 1999. Identification of a promoter region responsible for the senescence-specific expression of SAG12. Plant Molecular Biology **41,** 181–194.

Nooden LD, Hillsberg JW, Schneider MJ. 1996. Induction of leaf senescence in *Arabidopsis thaliana* by long days through a light-dosage effect. Physiologia Plantarum **96,** 491–495.

Novichonok E, Novichonok A, Kurbatova J, Markovskaya E. 2016. Use of the atLEAF+ chlorophyll meter for a nondestructive estimate of chlorophyll content. Photosynthetica **54,** 130–137.

Ondzighi CA, Christopher DA, Cho EJ, Chang SC, Staehelin LA. 2008. Arabidopsis protein disulfide isomerase-5 inhibits cysteine proteases during trafficking to vacuoles before programmed cell death of the endothelium in developing seeds. The Plant Cell **20,** 2205–2220.

Orendi G, Zimmermann P, Baar C, Zentgraf U. 2001. Loss of stress-induced expression of *catalase3* during leaf senescence in *Arabidopsis thaliana* is restricted to oxidative stress. Plant Science **161,** 301–314.

Otegui MS, Noh YS, Martínez DE, Vila Petroff MG, Staehelin LA, Amasino RM, Guiamet JJ. 2005. Senescence-associated vacuoles with intense proteolytic activity develop in leaves of Arabidopsis and soybean. The Plant Journal **41,** 831–844.

Panchuk II, Zentgraf U, Volkov RA. 2005. Expression of the *Apx* gene family during leaf senescence of *Arabidopsis thaliana*. Planta **222,** 926–932.

Pfaffl MW. 2001. A new mathematical model for relative quantification in real-time RT-PCR. Nucleic Acids Research **29,** e45.

Pruzinská A, Tanner G, Aubry S, *et al*. 2005. Chlorophyll breakdown in senescent Arabidopsis leaves. Characterization of chlorophyll catabolites and of chlorophyll catabolic enzymes involved in the degreening reaction. Plant Physiology **139,** 52–63.

R Development Core Team. 2009. *R: a language and environment for statistical computing*. Vienna, Austria: R Foundation for Statistical Computing, www.r-project.org.

Rizhsky L, Davletova S, Liang H, Mittler R. 2004a. The zinc finger protein Zat12 is required for cytosolic ascorbate peroxidase 1 expression during oxidative stress in Arabidopsis. The Journal of Biological Chemistry **279,** 11736–11743.

Rizhsky L, Liang H, Shuman J, Shulaev V, Davletova S, Mittler R. 2004b. When defense pathways collide. The response of Arabidopsis to a combination of drought and heat stress. Plant Physiology **134,** 1683–1696.

Rolny N, Costa L, Carrión C, Guiamet JJ. 2011. Is the electrolyte leakage assay an unequivocal test of membrane deterioration during leaf senescence? Plant Physiology and Biochemistry **49,** 1220–1227.

Sakuraba Y, Balazadeh S, Tanaka R, Mueller-Roeber B, Tanaka A. 2012. Overproduction of Chl *b* retards senescence through transcriptional reprogramming in Arabidopsis. Plant & Cell Physiology **53,** 505–517.

Sakuraba Y, Lee SH, Kim YS, Park OK, Hörtensteiner S, Paek NC. 2014. Delayed degradation of chlorophylls and photosynthetic proteins in Arabidopsis autophagy mutants during stress-induced leaf yellowing. Journal of Experimental Botany **65,** 3915–3925.

Saltveit ME. 2002. The rate of ion leakage from chilling-sensitive tissue does not immediately increase upon exposure to chilling temperatures. Postharvest Biology and Technology **26,** 295–304.

Steynen QJ, Bolokoski DA, Schultz EA. 2001. Alteration in flowering time causes accelerated or decelerated progression through Arabidopsis vegetative phases. Canadian Journal of Botany **79,** 657–665.

Suzuki Y, Makino A. 2013. Translational downregulation of RBCL is operative in the coordinated expression of Rubisco genes in senescent leaves in rice. Journal of Experimental Botany **64,** 1145–1152.

Tanaka A, Tanaka R. 2006. Chlorophyll metabolism. Current Opinion in Plant Biology **9,** 248–255.

Thomas H. 2013. Senescence, ageing and death of the whole plant. New Phytologist **197,** 696–711.

Thompson AR, Vierstra RD. 2005. Autophagic recycling: lessons from yeast help define the process in plants. Current Opinion in Plant Biology **8,** 165–173.

Uddling J, Gelang-Alfredsson J, Piikki K, Pleijel H. 2007. Evaluating the relationship between leaf chlorophyll concentration and SPAD-502 chlorophyll meter readings. Photosynthesis Research **91,** 37–46.

Vasseur F, Pantin F, Vile D. 2011. Changes in light intensity reveal a major role for carbon balance in Arabidopsis responses to high temperature. Plant, Cell & Environment **34,** 1563–1576.

Vogel JT, Zarka DG, Van Buskirk HA, Fowler SG, Thomashow MF. 2005. Roles of the CBF2 and ZAT12 transcription factors in configuring the low temperature transcriptome of Arabidopsis. The Plant Journal **41,** 195–211.

Weaver LM, Gan S, Quirino B, Amasino RM. 1998. A comparison of the expression patterns of several senescence-associated genes in response to stress and hormone treatment. Plant Molecular Biology **37,** 455–469.

Wittenbach VA. 1978. Breakdown of ribulose bisphosphate carboxylase and change in proteolytic activity during dark-induced senescence of wheat seedlings. Plant Physiology **62,** 604–608.

Woo NS, Badger MR, Pogson BJ. 2008. A rapid, non-invasive procedure for quantitative assessment of drought survival using chlorophyll fluorescence. Plant Methods **4,** 27.

Wu A, Allu AD, Garapati P, *et al*. 2012. JUNGBRUNNEN1, a reactive oxygen species-responsive NAC transcription factor, regulates longevity in Arabidopsis. The Plant Cell **24,** 482–506.

Xie Y, Huhn K, Brandt R, *et al*. 2014. REVOLUTA and WRKY53 connect early and late leaf development in Arabidopsis. Development **141,** 4772–4783.

Ye Z, Rodriguez R, Tran A, Hoang H, de los Santos D, Brown S, Vellanoweth RL. 2000. The developmental transition to flowering represses ascorbate peroxidase activity and induces enzymatic lipid peroxidation in leaf tissue in *Arabidopsis thaliana*. Plant Science **158,** 115–127.

Yoshimoto K, Hanaoka H, Sato S, Kato T, Tabata S, Noda T, Ohsumi Y. 2004. Processing of ATG8s, ubiquitin-like proteins, and their deconjugation by ATG4s are essential for plant autophagy. The Plant Cell **16,** 2967–2983.

Zentgraf U, Jobst J, Kolb D, Rentsch D. 2004. Senescence-related gene expression profiles of rosette leaves of *Arabidopsis thaliana*: leaf age versus plant age. Plant Biology **6,** 178–183.

Zentgraf U, Laun T, Miao Y. 2010. The complex regulation of WRKY53 during leaf senescence of *Arabidopsis thaliana*. European Journal of Cell Biology **89,** 133–137.

Zentgraf U, Smykowski A, Zimmermann P. 2012. Role of intracellular hydrogen peroxide as signalling molecule for plant senescence. In: Nagata T, ed. Senescence. Rijeka, Croatia: INTECH, 31–50, doi:10.5772/34576.

Zimmermann P, Heinlein C, Orendi G, Zentgraf U. 2006. Senescence-specific regulation of catalases in *Arabidopsis thaliana* (L.) Heynh. Plant, Cell & Environment **29,** 1049–1060.

Zimmermann P, Zentgraf U. 2005. The correlation between oxidative stress and leaf senescence during plant development. Cellular & Molecular Biology Letters **10,** 515–534.

genes

MDPI

Article

Nitrogen Supply Drives Senescence-Related Seed Storage Protein Expression in Rapeseed Leaves

Stefan Bieker [1], Lena Riester [1], Jasmin Doll [1], Jürgen Franzaring [2], Andreas Fangmeier [2] and Ulrike Zentgraf [1,*]

[1] Centre of Molecular Biology of Plants, University of Tübingen, Auf der Morgenstelle 32, D-72076 Tübingen, Germany; stefan.bieker@zmbp.uni-tuebingen.de (S.B.); lena.riester@zmbp.uni-tuebingen.de (L.R.); jasmin.doll@zmbp.uni-tuebingen.de (J.D.)

[2] Institute of Landscape and Plant Ecology, University of Hohenheim, August-von-Hartmann-Str. 3, D-70599 Stuttgart, Germany; Juergen.Franzaring@uni-hohenheim.de (J.F.); andreas.fangmeier@uni-hohenheim.de (A.F.)

* Correspondence: ulrike.zentgraf@zmbp.uni-tuebingen.de

Received: 20 December 2018; Accepted: 17 January 2019; Published: 22 January 2019

Abstract: In general, yield and fruit quality strongly rely on efficient nutrient remobilization during plant development and senescence. Transcriptome changes associated with senescence in spring oilseed rape grown under optimal nitrogen supply or mild nitrogen deficiency revealed differences in senescence and nutrient mobilization in old lower canopy leaves and younger higher canopy leaves [1]. Having a closer look at this transcriptome analyses, we identified the major classes of seed storage proteins (SSP) to be expressed in vegetative tissue, namely leaf and stem tissue. Expression of SSPs was not only dependent on the nitrogen supply but transcripts appeared to correlate with intracellular H_2O_2 contents, which functions as well-known signaling molecule in developmental senescence. The abundance of SSPs in leaf material transiently progressed from the oldest leaves to the youngest. Moreover, stems also exhibited short-term production of SSPs, which hints at an interim storage function. In order to decipher whether hydrogen peroxide also functions as a signaling molecule in nitrogen deficiency-induced senescence, we analyzed hydrogen peroxide contents after complete nitrogen depletion in oilseed rape and Arabidopsis plants. In both cases, hydrogen peroxide contents were lower in nitrogen deficient plants, indicating that at least parts of the developmental senescence program appear to be suppressed under nitrogen deficiency.

Keywords: senescence; nitrogen remobilization; nitrogen supply; oil seed rape; seed storage proteins; hydrogen peroxide

1. Introduction

Despite being a member of the glucosinolate producing Brassicaceae family, selection and breeding of oilseed rape (OSR, *Brassica napus* L.) has made it one of the most important oilseed crops after soybean and oil palm. In addition to high oil contents, its seeds contain high amounts of protein, constituting up to 20%–25% of seed dry weight [2]. Around 60% of this protein content are composed of seed storage proteins (SSPs), which in turn are mainly comprised of two protein families: 12S globulins (Cruciferins) and 2S albumins (Napins) [3,4]. Cruciferins and napins have distinct molecular characteristics and respond differentially to the changes in pH and temperature, therefore their functionalities are most likely contrasting rather than complementary [5]. SSPs are synthesized in the endoplasmatic reticulum and then stored in protein storage vacuoles. Seed storage reserves accumulate with progression of seed growth and development and in mature oilseed rape seeds, the endosperm and the cells of embryo are packed full of protein storage vacuoles and oil bodies. The

protein content in the seeds of the Brassica species is affected by the translocation of amino-N and loading of amino acids in the phloem sap of leaves, indicating that seed filling and seed quality strongly rely on remobilization of previously acquired nutrients from the leaves. Phloem unloading in the endosperm and embryo cells by specific transporters also plays an important role. In Arabidopsis, amino acid permease 1 and 2 (AAP1/2) and the cationic amino acid transporter 6 (AtCAT6) mediate AA uptake in the embryo and have an impact on SSP accumulation [6]. QTL mapping identified a total of 67 and 38 QTLs for seed oil and protein content and provided new insights into the complex genetic mechanism of oil and protein accumulation in the seeds of OSR [7]. During germination, the seed storage reserves deposited in the protein storage vacuoles and oil bodies in the endosperm and embryo tissue are degraded for energy supply and anabolic processes of seedling development. In-depth proteomic dissection contributed to a better understanding of the mobilization of seed storage reserves and regulatory mechanisms of the germination process in *B. napus* [8].

Before anthesis, sequential leaf senescence leads to the repartitioning of nutrients from older leaves to newly developing non-reproductive organs. The bottleneck of weak nitrogen (N) remobilization associated with senescence in vegetative stages appears not to be amino acid transport from leaf to phloem but rather an incomplete hydrolysis of foliar proteins [9]. After anthesis, monocarpic leaf senescence governs the nutrient reallocation to the now developing reproductive organs and therefore, has a critical impact on yield quality and quantity. For example in wheat, leaf-derived N remobilized by senescence processes accounts for up to 90% of the total grain N-content [10]. Consistent with the importance of senescence for the plants' reproductive success, highly controlled processes are put in place to govern it. A complex interplay between hormone action, genetic reprogramming as well as biotic and abiotic factors administer initiation, progression and termination of senescence and thus influences the outcome of nutrient recycling. In Arabidopsis, differential regulation of more than 6000 genes during onset and progression of leaf senescence emphasizes the importance of this developmental program [11]. In this analysis, autophagy, transport and response to reactive oxygen species (ROS) are the first processes activated in the chronology of leaf senescence [11]. ROS, especially H_2O_2, are well known signaling molecules in senescence and we have demonstrated that developmental senescence in Arabidopsis as well as in OSR is associated with the down-regulation of central components of the anti-oxidative systems and thus associated with a transient increase in intracellular H_2O_2 contents [12,13]. If this H_2O_2 signal is suppressed in Arabidopsis, senescence is delayed [12].

Even though *B. napus'* performance regarding uptake of inorganic N is relatively high, N-remobilization during leaf senescence is believed to not be very efficient [14]. As a consequence of high demand and uptake during vegetative growth but rather low remobilization afterwards, surrounding ecosystems are often polluted by leaching of remaining soluble leaf-nitrogen (NO_3^-) into the water as well as by volatilization of N_2O and NH_3 into the atmosphere. In addition to the detrimental impacts on environment and water supply by oversaturation with nitrogenous compounds, production of inorganic nitrogen fertilizers is highly resource- and cost-intensive. Enormous progress has already been made by breeding plants with respective traits for high nutrient uptake and remobilization efficiencies, high photosynthetic rates, high sink capacities, variation of fatty acid contents etc. However, there seems to be a natural trade-off between high yield and high protein content [6,15,16]. Hence, besides new breeds, genetically modified crops seem to be one of the most viable and tangible options, not only to avoid a further increase of environmental pollution, but also to tackle upcoming bottlenecks in the global food supply.

Developmental senescence progresses sequentially from the lower to the upper leaves in which the sink leaves in young plants later turn into source leaves during pod ripening [17]. N-deficiency leads to earlier induction of senescence in older leaves, while senescence is delayed at higher leaf positions [18,19]. Transcriptome analyses of leaves in two canopy levels over development of plants grown under two N-fertilization regimes also revealed opposite effects of N-depletion on senescence in lower versus upper canopy leaves. Several transcriptional regulators and protein degradation genes were identified to be differentially expressed in N-depleted lower leaf positions [1].

Morphology and performance analyses of exactly the same plants used in this study have been previously reported by Franzaring, et al. [20] who analyzed the effect of todays and future CO_2 and its interaction with nitrogen supply. Even though the flowering window of OSR was largely extended due to elevated CO_2, plants were not able to produce more pods but strongly branched out and produced many side shoots pointing to a prevented apical switch-off by high CO_2 [20]. N-remobilization was more affected by the different N-supply than by the CO_2 enrichment. Under ambient CO_2 concentrations, the nitrogen use efficiency (NUE) of the seeds was reduced by 2%, 33% and 65% under low, optimal, and high N treatments, respectively [21]. Moreover, ^{15}N-labeled fertilizer was supplied at three different time points to follow up nitrogen recovery over time and the distribution of the nutrient between source and sink organs. ^{15}N-supplied at the beginning of plant development mainly accumulated in roots and shed senescent leaves while ^{15}N-supplied at later stages ended up in late leaves, stem and reproductive tissue [21].

In order to understand the nitrogen remobilization processes in OSR under different nitrogen regimes more precisely, we analyzed the transcriptome data, which have been produced by Safavi-Rizi and co-workers [1] for genes involved in nitrogen remobilization and metabolism. Surprisingly, we realized that a remarkable amount of SSPs or proteins related to SSP expression were also expressed in leaf tissue, which we followed up in more detail to get some clues about their function in leaves. In a new growth experiment, we confirmed that the SSP genes *CRUCIFERIN* and *NAPIN* were expressed and that the corresponding proteins are produced in leaf tissue. *CRUCIFERIN* mRNA accumulated in leaf tissue at the onset of leaf senescence under high but not under low N-supply. In contrast, *NAPIN* expression was higher in leaves fertilized with low amounts of N but lower under high N-supply. SSP production progressed from the oldest to the youngest leaves and correlated with increasing hydrogen peroxide levels. SSPs were also detected in stem tissue and pod walls pointing to a possible function as an interim N-storage during N-remobilization. *In-silico* analysis of the corresponding promoter sequences identified motifs suggesting a (redox-) stress and nutritional supply dependent expression control. Moreover, when N was completely withdrawn, N-starvation induced premature senescence, but at the same time, a reduction of intracellular H_2O_2 contents in OSR as well as in Arabidopsis was observed. This indicates that N-starvation induced senescence is driven by different signals compared to developmental senescence and that at least the hydrogen peroxide-driven parts of the developmental senescence processes appear to be suppressed in N-starvation induced senescence.

2. Material and Methods

2.1. Plant Growth Conditions

Oilseed rape plants (*Brassica napus* cv Mozart):

Nitrogen starvation and developmental OSR series on soil: Plants were grown in greenhouses at 19–22 °C, with a 16 h photoperiod. All plants were sown on *Einheitserde classic-Topferde* (Einheitserde Werkverband e.V., Sinntal-Altengronau, Germany) in 6 × 6 cm pots. Later, plants for N-starvation experiments were put on a nutrient depleted soil (*Einheitserde Typ 0*). This was combined with repotting at around 4 weeks of plant age. Here, only control plants received fertilization with *Wuxal® Super* (Wilhelm Haug GmbH & Co KG, Ammerbuch-Pfäffingen, Germany) containing 99.2g N/L. Each pot was watered with 1 L of a 0.2% fertilizer solution once a week. After 4 days of habituation, harvests were conducted as indicated. Plants for developmental senescence assays were kept on *Einheitserde classic-Topferde*. Plants were sown in a weekly rhythm for 16 weeks in the green house. Leaf positions 5, 8, 12, the leaf residing directly below the first developing pods (terminal leaf/T-Leaf), the stem between T-leaf and first pod, and the siliques were sampled on the same day at the same time point.

Field-near conditions: Climate conditions were simulated in growth chambers at the University of Hohenheim, using the seasonal changes of day length and temperature of South-Western Germany as described in Franzaring, Weller, Schmid and Fangmeier [20]. N was supplied in three different regimes, namely *low* (N_L), *optimal* (N_O) and *plus* (N_P), fertilized with 75, 150 and 225 kg ha^{-1},

respectively. Nutrient supply and atmospheric conditions were kept as described in Franzaring, Gensheimer, Weller, Schmid and Fangmeier [21]. Plants were ^{15}N-labeled with double labeled ammonium nitrate with a ^{15}N excess of 10% ($\delta^{15}N$ of 100‰) at DC 0 (first fertilization at 0 DAS, "old N"), at DC 30 (second fertilization at 72 DAS) or at DC 59 (third fertilization at 80 DAS, "new N") as described in Franzaring, Gensheimer, Weller, Schmid and Fangmeier [21].

Nitrogen starvation on hydroponics: Plants were germinated at a 16 h photoperiod, 18–22 °C and 75% relative humidity (RH) on filter paper sandwiched between sponges and PVC-plates on both sides. After seven days, the seedlings were transferred to pots with 6 liters liquid medium in a greenhouse with also 16 h photoperiod and 75% RH. After 28 days pre-culture at 2 mM N, N-starved plants received low N liquid medium (0.1 mM N), full N plants continued receiving N-rich medium (4 mM N). For more detailed composition see Supplementary Materials Table S1 (published in Koeslin-Findeklee et al. [22])

Arabidopsis thaliana Col-0 plants: Plants were grown on a modified Araponics© system (Araponics SA, Liege, Belgium) including aeration of the liquid medium. Moreover, plants were grown on sterilized mineral-wool instead of the recommended agarose. Seeds were stratified for 4 days at 4 °C, and then moved into growth chambers. Temperature was kept at 21 °C, day length was 8 h. Liquid media were exchanged every second day. During the first week after germination, tap water was used as hydroponic medium. Afterwards, plants received 0.5 mM N during the second week and 1 mM N during the third week. With the beginning of the treatment (the fourth week onwards) 0 and 4 mM were supplied to N-starved and control plants, respectively (for more detailed media composition and schedule see Supplementary Materials Table S2).

2.2. H_2O_2 Measurements

Leaf discs (1 cm diameter, *B. napus*) or whole leaves (*A. thaliana*) were sampled from the same leaf positions and then incubated in MS-Medium (pH 5.7) with 9.5 µM 5(6)-Carboxy-Di-Hydro-Di-Chloro-Fluorescein-Di-Acetate (Carboxy-H_2DCFDA). After 45 min incubation, samples were rinsed twice with distilled water and frozen in liquid nitrogen. Homogenization was conducted on ice in 500 µL 40 mM Tris-HCl pH 7. After 30 min of centrifugation at 4 °C and 14,000 rpm, fluorescence of supernatant was determined (480 nm excitation, 525 nm emission, Berthold TriStar LB941, BERTHOLD TECHNOLOGIES, Bad Wildbad, Germany). H_2DCFDA solution was prepared freshly for each harvest and calibrated by chemical de-acetylation and oxidation following Cathcart et al. [23].

2.3. Generation of Anti-SSP Antisera

Antisera were generated against VVEFEDDA (NAPIN) and VVRPLLRQ (CRUCIFERIN) peptides. Peptide synthesis and animal immunization were carried out by *BioGenes* (Berlin, Germany). Peptide sequences were chosen based on alignments of Arabidopsis and *B. napus* seed storage protein. Antisera were used directly without further purification.

2.4. Protein Extraction and Western-Blotting

Samples were homogenized on liquid nitrogen. Protein extraction buffer was added according to the sample amount (modified QB-Buffer; 100 mM KPO_4, 1 mM EDTA, 1% Triton-X100, 10% glycerol, 1 mM DTT, 150 mM NaCl), samples were then incubated for 20–30 min on ice. After subsequent centrifugation at 20.800 g and 4 °C for 20–60 min (depended on sample type: shoot material with many fibers as well as oily seed material were centrifuged longer) total protein content of the supernatant was determined. 15 µg total protein of the very same *B. napus* (cv. Mozart) seed sample as positive control and 25 µg of total protein of all other samples were then separated by SDS-DISC-PAGE (15% PAA separating, 3.5% PAA stacking gel). After transfer on PVDF-membranes by semi-dry blotting, membranes were washed twice with TBS-T, incubated for 1 h in 5% milk-powder TBS-T and after another washing with TBS-T incubated in 1.5% milk-powder TBS-T with 1:500 diluted antisera for 1–2 h. Anti-rabbit-HRP antibody (CellSignaling, #7074) was used as secondary

antibody in a 1:3,000 dilution in 1.5% milk-powder TBS-T. Blots were incubated another hour in this solution. After three times washing with TBS-T, detection was carried out with luminol detection kit (*Pierce ECL* or *BioRad Clarity*) in an *Amersham Imager 600* (GE Healthcare, Berlin, Germany).

For relative quantification, the gel analyzer plugin of *ImageJ* was used. Integrated band intensities were normalized to bands of the respective positive controls. As different antisera were used, NAPIN and CRUCIFERIN signals could not be directly compared and signal intensities were normalized to appropriate bands in whole seed extracts that served as positive controls.

2.5. RNA Extraction and qRT-PCR

Primer design for qRT-PCR was done via QuantPrime [24]. RNA extraction and cDNA synthesis were conducted with InviTrap Spin Universal RNA Mini Kit (Invitek Inc, San Francisco, CA, USA) and qScript cDNA SuperMix (Quanta Biosciences, Beverley, Massachusetts, USA) according to the manufacturer's protocols. qRT-PCR was performed with Perfect CTa SybrGreen Fast Mix (Quanta Biosciences, Beverley, MA, USA) in an iCycler IQ system (Biorad, München, Germany). Relative quantification to *ACTIN2* was calculated with $\Delta\Delta C_T$–Method [25]. Primers used for *B. napus NAPIN2 (Bna.2093)* were: 5′-TGG CAA GCT CTT AGG TGT TGA GC (FW) and 5′-CCG GCC CAT TTA GGA TTC CAA G (REV). For *CRUCIFERIN1 (Bna.2089)*: 5′-AGA CCA CTT TGA CGC ACA GCA G (FW) and 5′-AAG CCC TTA AGC ATC AGC CTT CC (REV).

2.6. Chlorophyll Measurements

Chlorophyll (Chl) contents were estimated via a *SPAD 502 (KONICA MINOLTA)* photometer or the *atLEAF + (FT Green, LLC)* device. Measurements were conducted at least three times per leaf on varying positions to avoid positional effects.

2.7. Microarray Data Evaluation

The plant material of *Brassica napus* cv. Mozart, which was used for transcriptome analyses, the design of the *B. napus* custom microarray, the identification of *Arabidopsis thaliana* homologues of the *B. napus* unigenes, and the basic data analysis workflow are described in Safavi-Rizi et al. [1]. In this experiment, oilseed rape plants were grown under two different nitrogen regimes, optimal (N_O) and low (N_L) nitrogen. The lower canopy leaf No. 4 was harvested at 78, 85, 92, and 99 days after sowing (DAS) and the upper canopy leaf No. 8 at 92 and 106 DAS (Figure 1A). Physiological analysis with respect to carbon and N-dependent effects as well as detailed description of growth conditions were published in Franzaring, Weller, Schmid and Fangmeier [20] and Franzaring, Gensheimer, Weller, Schmid and Fangmeier [21]. Briefly, expression data analysis was conducted in R [26] with the *Linear Model for Microarray and RNA-Seq Data* (LIMMA) package [27] applying the standard time-course experiment workflow. Contrast matrixes were built within one treatment with a *p*-value cut-off 0.05 (Benjamini Hochberg correction) and log2 fold-change cut-off of 1. *B. napus* genes were annotated by their most similar *A. thaliana* orthologue, identified by local BLAST+ (version 2.2.30 +, build Aug 28 2015 11:17:27, [28]) against the *TAIR*-10-Database [29]. Blast results with an e-value > 10^{-3} were excluded from further analysis. Finally, all transcripts associated with SSPs were extracted by matching *AGI* identifiers to a list of identifiers of SSP associated genes (for listings see Supplementary Materials Table S3).

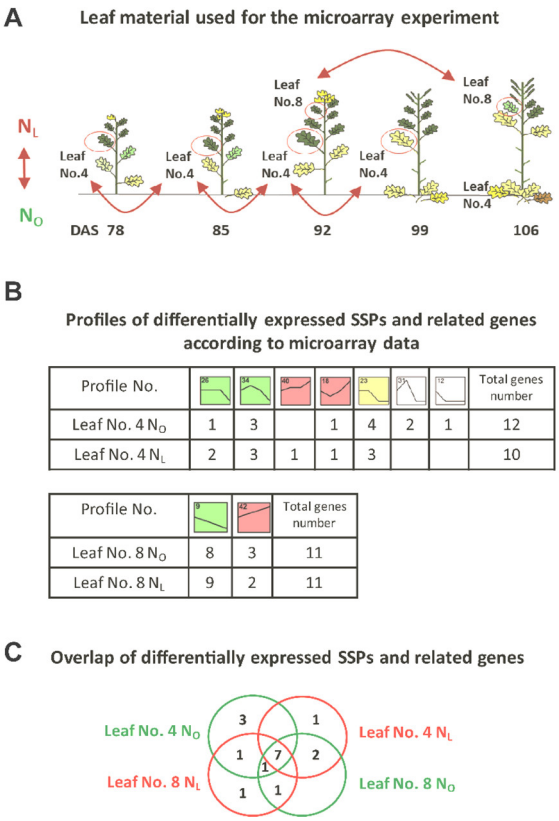

Profile No.								Total genes number
Leaf No. 4 N_O	1	3		1	4	2	1	12
Leaf No. 4 N_L	2	3	1	1	3			10

Profile No.			Total genes number
Leaf No. 8 N_O	8	3	11
Leaf No. 8 N_L	9	2	11

Figure 1. SSPs and related genes differentially expressed during development and/or N-supply assigned to 9 different expression profiles. (**A**) Illustration of the leaf material used in the microarray experiment (modified after Safavi-Rizi et al. [1]). Leaf No. 4 was analyzed at 4 different time points, leaf No.8 was analyzed at 2 different time points under N_L or N_O supply, respectively. (**B**) Number of SSPs and related genes, which were differentially expressed in leaf No. 4 and leaf No. 8 under N_L and under N_O conditions. Each box represents one of 50 pre-defined expression profiles [1]. The number of each model expression profile is shown in the top left corner of each box, all colored profiles contain a significant number of temporally and N-dependently regulated genes. Profiles with the same color are very similar and defined as one cluster in Safavi-Rizi et al. [1]. (**C**) Overlap of differentially expressed SSPs and related genes between leaf No. 4 and No. 8 and the growth conditions N_L and N_O.

2.8. Total N and δ^{15}N-Measurements

Seeds were ground in liquid nitrogen. Subsequently, the homogenized powder was lyophilized and total N-content was measured by a CN-element analyzer (Elementar Vario EL III, Elementar Analysensysteme GmbH, Langenselbold, Germany) via heat combustion at 1150 °C and thermal conductivity detection. The stable isotope ratio $^{15}N/^{14}N$ was measured as described in Franzaring, Gensheimer, Weller, Schmid and Fangmeier [20] using an isotope ratio mass spectrometer (Deltaplus XL, Thermo Finnigan, Bremen, Germany) connected by an open split device (ConFlow II, Thermo Finnigan, Bremen, Germany). The $^{14}N/^{15}N$ ratio was expressed relative to the isotopic signature of N_2 in the air as δ values (in ‰).

2.9. Catalase Zymograms

Leaf discs (1 cm diameter) were taken from approx. the same position within the respective leaf and frozen in liquid nitrogen. After homogenization on ice with extraction buffer (100 mM Tris, 20% glycerol (*v*/*v*), 30 mM DTT, pH 8.0) samples were centrifuged for 15 min at 4 °C and 14,000 rpm. Total protein concentration of the supernatant was determined and 15 µg protein were separated via native PAGE (7.5% polyacrylamide, 1.5 M Tris, pH 8.8; running buffer: 25 mM Tris, 250 mM Glycin, pH 8.3). After protein separation, gels were rinsed twice with distilled water, incubated for 2 min in 0.01% hydrogen peroxide solution and then rinsed again twice with water. Incubation in staining solution

(1% $FeCl_3$ and 1% $K_3[Fe(CN)_6]$) was carried out under constant agitation until bands became visible (4–6 min). To stop any staining reaction, the solution was removed and the gel was rinsed with water.

3. Results

3.1. Transcriptome Analysis of OSR during Induction of Senescence under Two Different N-Supplies

To investigate the process of senescence induction and N-remobilization in OSR in more detail, microarray data made available by Safavi-Rizi et al. [1] were screened for genes related to nitrogen metabolism and nitrogen storage differentially expressed under optimal (N_O) and low (N_L) nitrogen. Among the genes that we identified to be related to nitrogen metabolism, we found a substantial number of genes encoding SSPs or proteins related to them, which were initially described to be exclusively expressed in seed tissue. However, here we found a reasonable expression in leaf tissue. An AGI code list with SSP and SSP-associated transcripts was compiled (Supplementary Materials Table S3). Out of the 124 AGI identifiers, 17 *Bn* unigenes or gene clusters were differentially expressed in OSR according to development and/or N-supply. These could be assigned to 9 different expression profiles which have been defined by Safavi-Rizi and co-workers [1]; all colored profiles contain a significant number of temporally and N-dependently regulated genes [1]. Seven SSP and/or related genes were differentially expressed in leaf No. 4 and leaf No. 8 under both N-supplies, 15 under optimal N-supply (N_O) and 14 under low N-supply (N_L). A fairly high number of SSP related genes were differentially regulated in both leaves (11 out of 17), indicating that these transcripts appear to play a role during senescence progression at different canopies of the OSR plants (Figure 1B,C).

One important signaling molecule governing senescence regulation is hydrogen peroxide. Therefore, intracellular hydrogen peroxide contents of the same plant material were measured in leaf No.5 and already published in Bieker et al. [12]. Under optimal N-supply H_2O_2 reached its maximum levels at 12 weeks after sowing (85 DAS) and these high levels were maintained until week 13, while under low N the maximum was higher and was reached at week 13 (92 DAS). H_2O_2 declined at week 14 under both treatments. In order to get some hints whether H_2O_2 is involved in regulation of N-dependent senescence-associated gene expression and in the transcriptional regulation of the SSP-associated genes, we analyzed the correlation between H_2O_2 profiles and gene expression. Transcripts similar to *CRUCIFERIN3* (*CRU3*, At4G28520) and *MAIGO2* (*MAG2*, At3G47700) were induced in parallel to the H_2O_2 increase. CRU3 belongs to the SSPs of the Cruciferin superfamily whereas the MAG2 protein is involved in the ER exit of SSPs [30,31]. Interestingly, *SEED STORAGE ALBUMIN4* (*SESA4*, At4g27170) expression was reduced with rising H_2O_2 contents and induced when H_2O_2 levels declined again. This antagonistic behavior was also observed for *ECTOPIC EXPRESSION OF SSP1* (*ESSP1,* At2g19560) and several bifunctional-lipid transfer proteins (*BI-LTPs*). The same analysis was conducted for N_L data. Again, some SSPs were found to follow the H_2O_2 profile. However, instead of *CRUCIFERIN* transcripts, *NAPIN* (*SESA4*) peaked in its expression together with highest H_2O_2 levels, thus showing the exact adverse behavior compared to N_O. Moreover, under N_L conditions, *MAG2* was found to be repressed with increasing H_2O_2 contents and expression increased again with decreasing H_2O_2 levels. Disregarding H_2O_2 contents, overall up-regulated transcripts included transcripts similar to *BRAHMA* (*BRM*, At2gG46020) and SSP processing enzymes (homologues to At4g32940 e.g., *GAMMA-VPE*, γ-vacuolar processing enzyme). Interestingly, the BRM protein mediates SSP repression in vegetative tissues. Down-regulated transcripts contained multiple homologues to bifunctional-lipid transfer proteins (*BI-LTPs*), *VACUOLAR SORTING RECEPTOR HOMOLOG1* (*VSR1*, At3G52850) and *ESSP1.*

3.2. Verification of SSP Expression via qRT-PCR and Western-Blot

In order to confirm the expression patterns of the mayor seed storage proteins, the 12S globulins (Cruciferins) and 2S albumins (Napins) via qRT-PCR and to verify the production of the corresponding proteins in leaves, another series of OSR plants was grown under constant greenhouse conditions. Again, an increase in SSP gene expression upon accumulation of H_2O_2 in *B. napus* leaves was observed. Moreover, timing of induction and repression of *CRUCIFERIN* coincided with the

accumulation and decrease of intracellular H_2O_2. However, in contrast to the microarray-experiment, in this experiment both, *CRUCIFERIN* and *NAPIN* were up-regulated which might be due to different growth conditions and uncontrolled N-supply. In addition, protein levels were analyzed via Western blot and subsequent immune detection of SSPs. Here, a progressive accumulation pattern emerged, starting with SSP production in the leaves at the lower canopy level when plants were still young. Later, expression continued with a build-up in upper canopy leaves when development progressed and SSPs usually start to accumulate in siliques and seeds. In addition, accumulation of SSPs was also observed in shoot tissue (Figure 2).

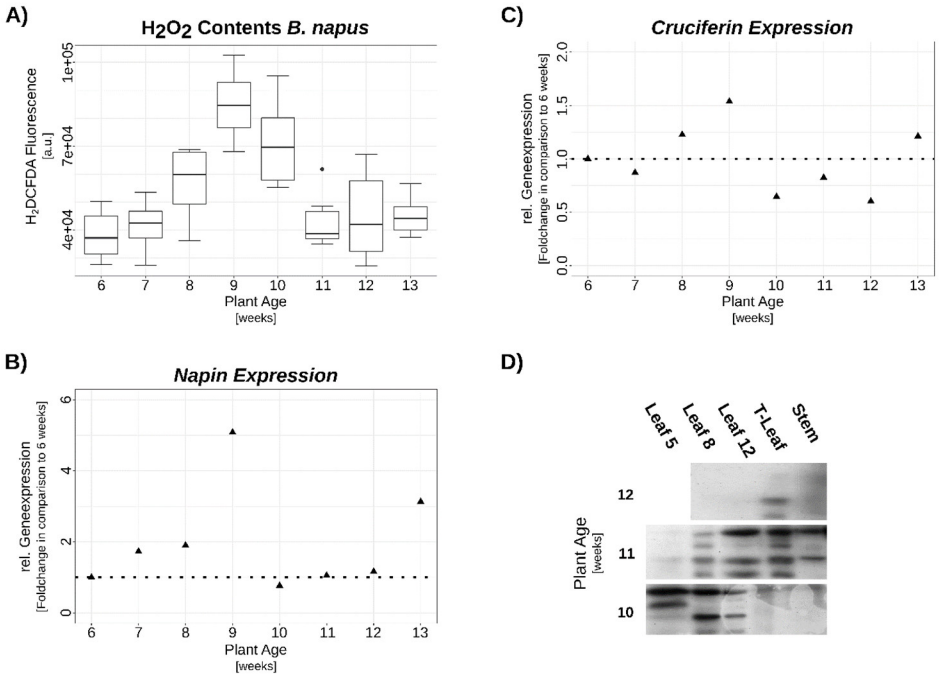

Figure 2. OSR developmental series. Exemplary plants grown in the green house under stable conditions are shown at the top, numbers indicate weeks after sowing. (**A**) H_2O_2 contents in leaf No. 8. (**B**) and (**C**) relative gene-expression of *NAPIN* and *CRUCIFERIN*, respectively, analyzed by qRT-PCR. Expression was normalized to *ACTIN2* and expressed relative to value at 6 weeks. (**D**) Western-blot of the corresponding plant material immune-detected with anti-NAPIN antiserum. Analyzed proteins are samples of 3–5 biological replicates pooled in equal amounts. Leaves are numbered according to their appearance; terminal leaf (T-leaf) is the leaf residing directly below the first developing pods. H_2O_2 data are medians +/−1.5xIQR of at least 3 biological and 2 technical replicates each. Gene expression data are means of 3 technical replicates from pools of at least 3 biological replicates.

To confirm the protein expression also under controlled N conditions as described in references [1,20], leaf positions 4, 8 and 12, the terminal leaf as well as shoot tissue and siliques were harvested of another growth series. Chlorophyll contents were measured via *atLeaf+*. Leaf No.4, the lowest leaf position analyzed, remained on the plant only until week 8 under N_O conditions, whereas under N_L conditions this leaf was shed between week 11 and 12. Longer maintenance of photosynthetic capacities, especially of lower canopy leaves, enhanced assimilate supply to the pods as well as the roots [22]. The higher canopy leaves exhibited a slightly higher Chl-content under higher N-supply.

Under N_O conditions, quantification of detected CRU proteins showed a similar pattern to the *CRU* transcripts in the microarray and the qRT-PCR experiments. A stepwise increase in CRU protein contents in the leaves was observed beginning at the lowest positions with peak levels between weeks 8 and 10 (Figure 3A). Under N_L conditions CRU production was reduced approx. 10-fold and no comparable pattern became clear. For NAPIN, the detected amount of protein was much higher

under N_L conditions than under N_O like in the microarray expression data. Accumulation patterns were similar, but expression was more pronounced in the lower leaf positions, analogous to the prolonged Chl retention observed there. However, a direct comparison between NAPIN and CRUCIFERIN contents is not possible as both proteins were detected with different antisera. Therefore, the signals were normalized to the respective signals of the controls. Nevertheless, both proteins could be detected not only in leaves but also in stems (Figure 3A,B,D). Moreover, total N-content in the seeds was approx. 25% higher under N_O than under N_L conditions (Supplementary Materials Figure S1). Gironde, et al. [32] have already indicated an interim storage function for shoot tissue upon asynchronous senescence and seed filling. Our results support this possible function. Even under N-starvation conditions, where a reduction of H_2O_2 contents and barely detectable CRU synthesis was shown in leaves, still a minimal build-up of SSPs occurred in the shoot (Supplementary Materials Figure S2).

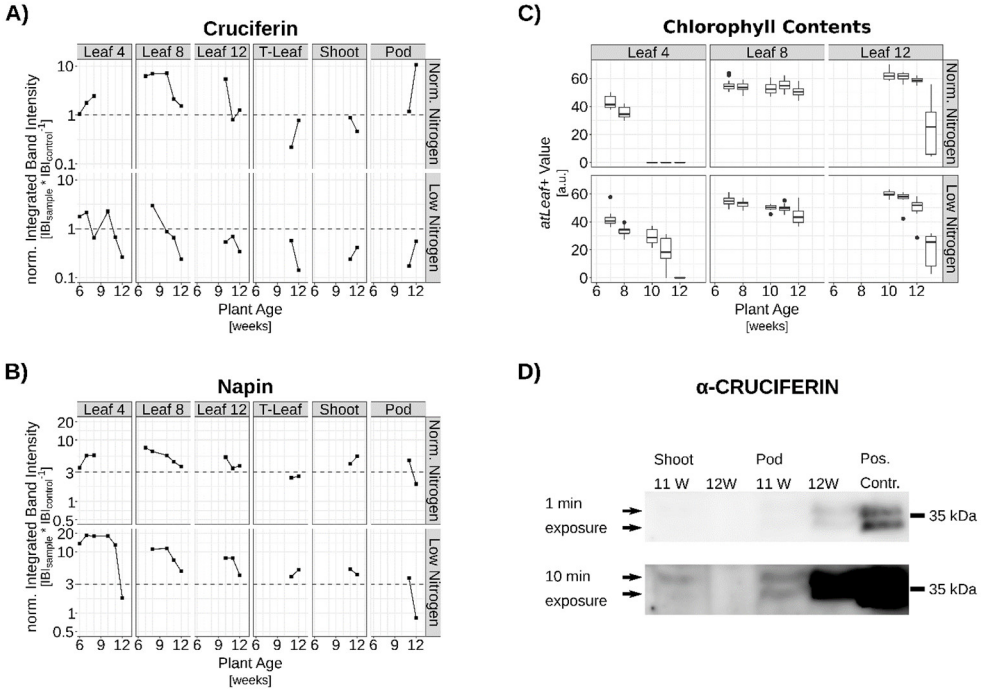

Figure 3. Seed storage protein (SSP) levels of OSR plants grown under normal and limiting nitrogen (N) supply. Quantification of (**A**) CRUCIFERIN and (**B**) NAPIN signals. Material analyzed are samples of 3–5 biological replicates pooled in equal amounts. (**C**) Corresponding chlorophyll contents (median +/−1.5xIQR of 3 biological replicates). Upper graphs normal N-supply, lower graphs N-limitation. (**D**) Exemplary signal of stem and pod material detected in a Western blot (marked by arrows, 25 µg total protein). One min exposure (top) to show non-oversaturated positive control (15 µg total protein) and 10 min exposure for the shoot and pod signals (bottom).

The idea of an interim N-storage is also supported by the follow-up of ^{15}N-labeled nitrogen over time in parallel to the expression profiling [21]. ^{15}N-labeled fertilizer was supplied at three different time points, directly after sowing (DC 0), 72 DAS (DC 30), and 80 DAS (DC 59). Nitrogen recovery and the distribution of the labeled N to different organs was measured by isotope ratio mass spectrometry [21]. Here, we present the $\delta^{15}N$ mean values for pooled green and senescent leaves as well as for the individual leaves No. 4, 5 and 8 at harvest 4 (92 DAS). Exactly the same leaf material was also used for expression profiling (No. 4 and 8; [1]) and hydrogen peroxide measurements (No. 5; [12]). At this time point, early supplied nitrogen (DC 0) appeared to be inefficiently remobilized and mainly rested in the older leaves (No. 4 and 5) while the highest proportion was shed in senescent leaves. In contrast, nitrogen originating from the second and third N gift (DC 30 and DC 59) accumulated less in shed senescent leaves but more in the younger leaf No.8. This can be observed

under both N-supplies in which the effect is most prominent under N_L and DC 30 labelling (Figure 4). This might indicate that N taken up at flowering time appears to be stored temporarily in the younger leaves most likely to be further remobilized to the developing seeds after anthesis. Possibly, also stems and pods contribute to this interim storage, as total N in stem and pods declined while total N in seeds increased (Supplementary Materials Figure S3).

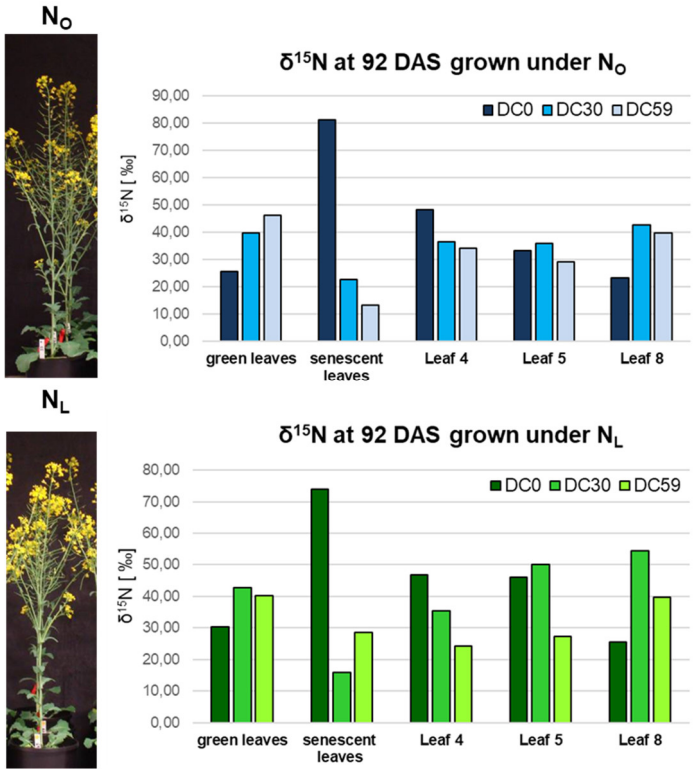

Figure 4. Nitrogen recovery and the distribution of the labeled N to different organs. $\delta^{15}N$ signatures at 92 DAS (days after sowing) in pooled green and senescent leaves as well as in leaves No. 4, No. 5 and No. 8 of plants grown under N_L (lower chart) and under N_O (upper chart) conditions are presented (DC0: fertilization at 0 DAS, "old N", DC30: fertilization at 72 DAS, DC59: fertilization at 80 DAS, "new N"). The stable isotope ratio $^{15}N/^{14}N$ was related to the isotopic signature of N_2 in the air and is reported here as "delta" δ values in ‰. Exactly the same plant material was used for the microarray analyses of Safavi-Rizi et al., [1] and physiological analyses in Franzaring et al. [20,21].

Taken together, our results indicate that a transcriptional control of SSP expression via H_2O_2 but also via the plants' N-status appears to be in place. Therefore, we wanted to identify possible regulatory elements (RE) in the promoter regions of the respective genes by in silico analyses. As *Brassica napus* was formed ~7500 years ago by hybridization between *B. rapa* and *B. oleracea*, followed by chromosome doubling, and most orthologous gene pairs in *B. rapa* and *B. oleracea* remain as homologous pairs in *B. napus* [33], we analyzed the promoter regions of both SSP gene copies, respectively. The NSITEM-PL program with RegSite PL Database of Plant Regulatory Elements (Release 14, May 03, 2014; default parameters were set) [34] tests for the presence of known REs in conjunction with positional conservation within the supplied sequence sets comprising 3kb upstream sequences of *B. oleracea* and *B. rapa* as well as of the *B. napus CRUCIFERIN* or *NAPIN* homologues. Remarkably, several binding sites for transcription factors involved in either ROS response or N-management or both were identified (Supplementary Materials Figure S4). For example, binding elements for TGACG-BINDING FACTOR2 (TGA2, a bZIP transcription factor involved in general ROS-and pathogen-response, TEOSINTE BRANCHED1/CYCLOIDEA /PROLIFERATING CELL FACTOR20 (TCP20, involved in systemic N-status signaling and leaf-senescence) and ELONGATED HYPOCOTYL5 (HY5, a ROS-responsive bZIP transcription factor involved in N management) were found (for a complete listing see Supplementary Materials Tables S4 and S5).

3.3. Hydrogen Peroxide Signaling under Complete N-Starvation

To explore a possible interplay between the plants' nitrogen status and H_2O_2 as signaling molecule during the induction of leaf senescence and SSP expression, N-starvation experiments with OSR plants grown on hydroponics were conducted. As expected, N-starvation led to the induction of premature senescence indicated by the decrease in chlorophyll contents, especially in older leaves. However, no increase in intracellular H_2O_2 contents could be measured, as would have been expected for a senescence signaling molecule, but rather a slight reduction of H_2O_2 was determined (Figure 5). Nevertheless, a reduction of catalase activity was observed (Supplementary Materials Figure S5) as was already described during developmental senescence under full N-supply [12].

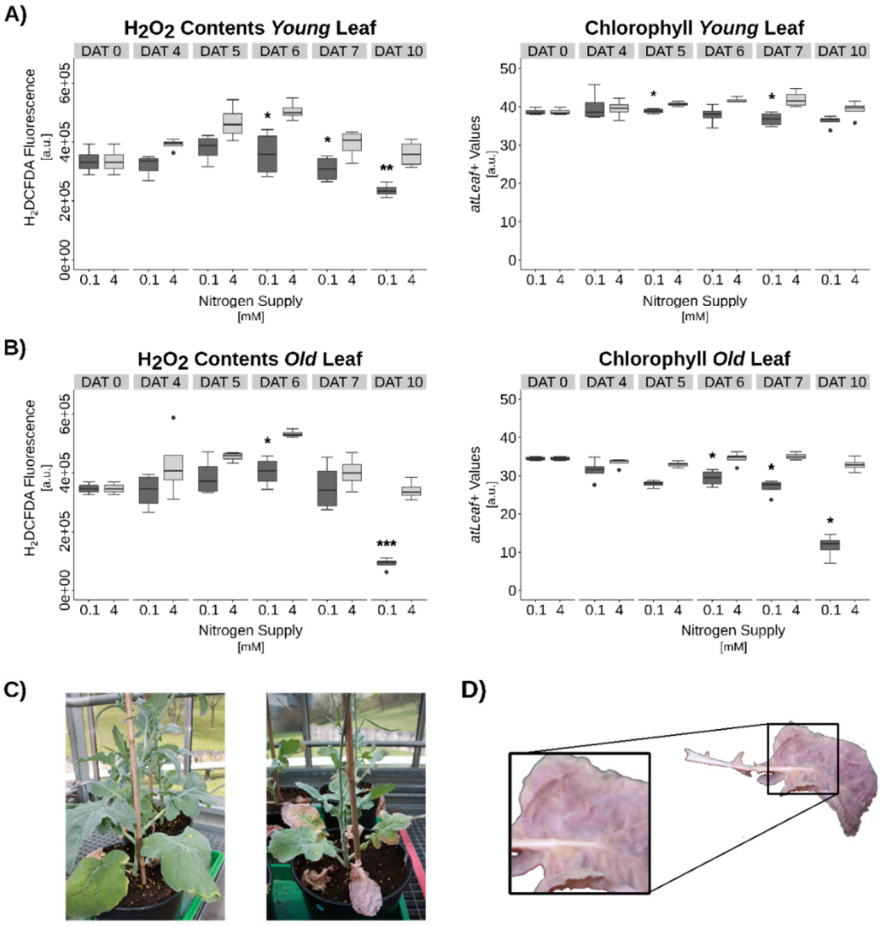

Figure 5. Nitrogen (N) starvation induced senescence in *Brassica napus*. (**A**) and (**B**) Hydrogen peroxide (H_2O_2) and chlorophyll contents in young leaves (**A**) and in old leaves (**B**). (**C**) Plant grown under full N-supply (left) and under N-starvation (right). (**D**) Exemplary anthocyanin accumulation pattern in N-starved plants. Statistics: Welch's t-test. Significance levels: $p < 0.001$ = ***; $p < 0.01$=**; $p < 0.05$ = *. Data are medians +/−1.5xIQR of at least 3 biological and 2 technical replicates each.

Arabidopsis plants subjected to N-starvation on hydroponic culture consistently exhibited similar effects. Shortly before anticipated senescence induction, hydroponic medium was switched from full nutrient supply to N-free medium. Now, an even more pronounced reduction of H_2O_2 contents was detected (Figure 6). However, in both cases, an extensive production of anthocyanins became visible. In Arabidopsis, anthocyanin production was strongest at vasculature during the early phases of N-depletion (Figure 6D). In OSR, anthocyanin accumulation was also observed after N-depletion (Figure 5C,D) but for OSR the vasculature seemed to remain with very low anthocyanin production (Figure 5D). Obviously, OSR leaf vein and leaf laminae are tissues with different regulatory mechanisms during senescence. Besides other functions, anthocyanins were discussed to act as ROS scavenging molecules. Accordingly, reduction of intracellular H_2O_2 was observed in N-

starved Arabidopsis as well as in OSR leaves (Figures 5A,B and 6A,B). For both species, Chl-contents remained constant in young leaves during the treatment, while older leaves showed a significant reduction in Chl-contents (Figures 5A,B and 6A,B). These findings tempted us to speculate that one possible role of anthocyanin production during N-starvation-induced senescence is the scavenging of the signaling molecule H_2O_2 and by that a suppression of at least part of the developmental senescence program. SSP accumulation under complete N-starvation conditions was barely detectable in leaf tissue (Supplementary Materials Figure S2).

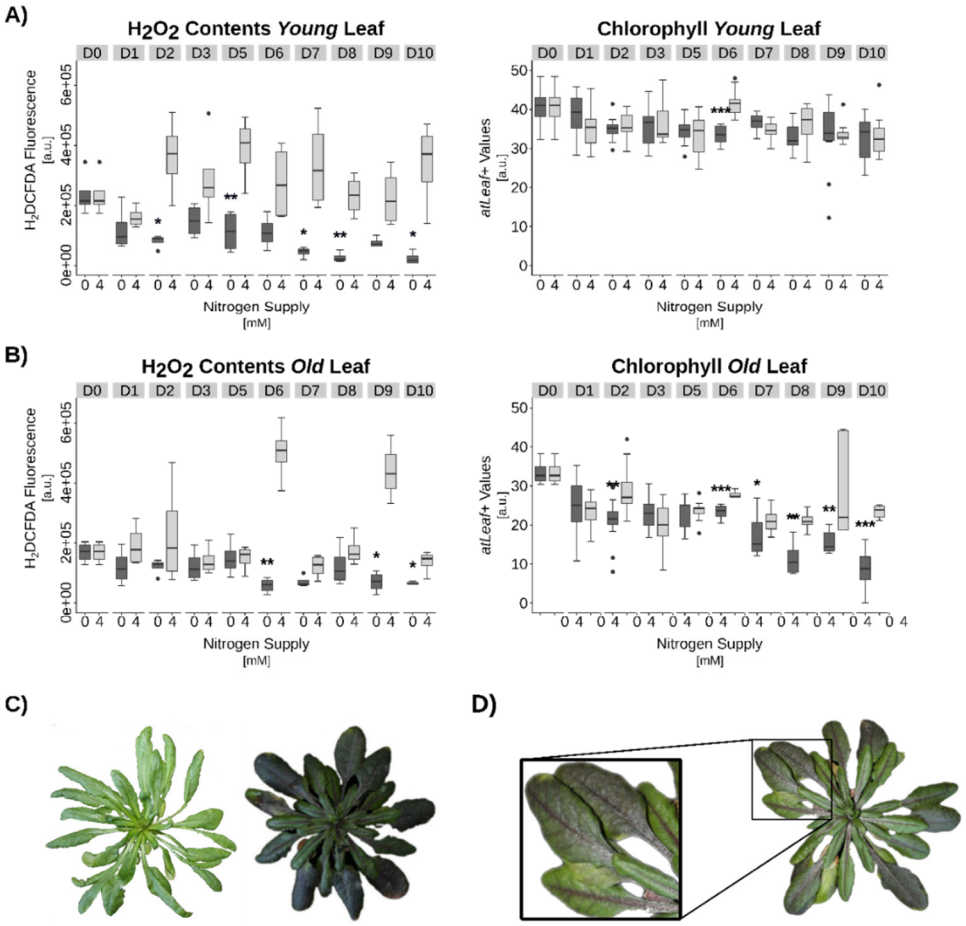

Figure 6. Nitrogen (N) starvation induced senescence in *Arabidopsis thaliana*. (**A**) Hydrogen peroxide (H_2O_2) and chlorophyll contents in young leaves, (**B**) in old leaves. (**C**) Left: plants grown under full N-supply, right under N-starvation. (**D**) Exemplary anthocyanin accumulation pattern in N-starved plants. Statistics: Welch's t-test. Significance levels: $p < 0.001$ = ***; $p < 0.01$=**; $p < 0.05$ = *. Data are medians +/−1.5xIQR of at least 3 biological and 2 technical replicates each.

4. Discussions

Genome-wide expression analyses of OSR grown under two different N-regimes revealed that, according to the gene expression profiles, long-term and mild N-deficiency provokes accelerated senescence in lower canopy leaves but delayed senescence in upper canopy leaves [1]. The most important feature of senescence is the remobilization of nutrients out of the senescing tissue into developing parts of the plants, especially to fruits and seeds. By ^{15}N-labelling at different time points in the same experiment, we could show that N taken up early during development was not efficiently remobilized and a high proportion of the labeled N was shed with senescent leaves. N taken up at flowering time appeared to be better remobilized and stored temporarily in the younger leaves. It was also most likely to be further translocated to the developing seeds after anthesis. This effect is most prominent under low N-supply (Figure 4) when N-remobilization is most likely to be more important. N-recovery in general and to the seeds was improved under low N, as 50.7% of the total

N-gift was deposited in the seeds compared to 44.5% under N_O conditions [21]. A genome-wide expression analyses via microarrays of exactly the same plant material offered the possibility to analyze the expression profiles of genes involved in N-remobilization and N-storage (Supplementary Materials Table S3). The most striking result for us in this analysis was that transcripts of seed storage protein genes or genes related to them, which were formerly thought to be restricted to seed tissue, were identified in leaves at different canopies like leaf No. 4 and No. 8 (Figure 1). Moreover, not only the transcripts but also the proteins were detected in leaf tissue (Figures 2 and 3). However, the accumulation of these storage proteins was not equally distributed across all leaves but a wave-like spreading of SSPs was observed starting in the oldest leaves when plants were still young and climbing up into younger leaves with the progression of development and declining again in later stages with a residual SSP content in the terminal leaf (Figure 2). SSP protein accumulation was also detected in shoots and pods (Figure 3). Considerable differences were observed between the two different N regimes: While *NAPINS* appeared to be more highly expressed under N_L conditions, more *CRUCIFERINS* were produced under higher N supply, creating the SSPs possible candidates for interim storage of N in leaves during N remobilization processes of senescence. As CRUCIFERINS and NAPINS have distinct molecular characteristics and functionalities [5], it makes sense that these two classes of SSPs are also expressed in contrary ways under different nitrogen regimes in leaves. SSP proteins also detected in stems and pods and total N-analyses in stems and pods additionally points to interim N-storage in these tissues as total N in stem and pods declined while total N in seeds increased (Supplementary Materials Figures S1 and S3). In maize *opaque-2* knock-out plants, storage protein synthesis significantly reduced the pool of free AAs in mature endosperm [35] and could thus enhance sink strength for further N-remobilization. A similar mechanism could possibly operate in leaf tissue as source strength of the disintegrating leaves might exceed sink strength of the newly developing organs [32]. Therefore, the pool of free AAs could be reduced by the built-up of storage proteins decreasing the source strength of the respective leaves. As such, a stepwise N remobilization from lower leaf canopies could take place, which coincides with the wave-like expression of the SSPs (Figure 2). How this is coordinated in oilseed rape plants is still an open question. However, accurate QTL mapping and potential candidates identified based on high-density linkage map and BSA analyses revealed that complex genetic mechanisms for oil and protein accumulation in the seeds of rapeseed are in place [7]. Further analyses of these candidate genes will allow for finding out whether they are also expressed in leaf tissue and contribute to storage reserves in seeds through an interim storage of N via SSPs in leaves. To function as an efficient interim storage, two main prerequisites need to be fulfilled, namely an efficient and compact storage and an easy access for remobilization [32], which both holds true for SSPs. SSPs are usually stored in higher complexes with multimeric conformation in protein storage vacuoles [6]. To achieve this conformation, extensive processing of pre-cursor proteins by VPEs (vacuolar processing enzymes) is necessary. Indeed, γ-VPE (AT4G32940) and other VPEs were differentially expressed in leaves under both N treatments (Table S3) indicating that SSP storage in a processed multimeric form is also possible in leaves. In the three plant growth series conducted under different conditions, *CRUCIFERIN* and *NAPIN* expression and accumulation correlated with intracellular hydrogen peroxide contents (Figure 2, [12]), which might be the link to the regulation of senescence processes, as hydrogen peroxide is a well-known signaling molecule in leaf senescence. Many transcriptional regulators and SAGs are up-regulated by increasing intracellular hydrogen peroxide concentrations. In silico analyses of 3 kbp upstream of the coding regions of *CRUCIFERIN* and *NAPIN* genes also supported the existence of a direct link between SSP expression and oxidative status of the cells (Supplementary Materials Figure S4, Supplementary Materials Tables S4 and S5). Spatiotemporal occurrence and distribution of SSPs and the corresponding mRNAs were shown to be tightly regulated and were so far thought to be restricted to the developing seeds [36]. In consistence, most of the *cis* elements identified by *in silco* analyses of the SSP promoter regions (Supplementary Materials Figure S4, Tables S4 and S5) are characteristic for seed-specific expression in various species. Multiple abscisic acid (ABA) responsive elements were found in *CRUCIFERIN* as well as *NAPIN* upstream regions. ABA is known to be a key factor during seed maturation by suppressing premature germination and regulating a variety of

processes during embryogenesis [37,38]. This also points to seed-specific expression. During SSP deposition, ABA contents steadily rise until they decrease again during desiccation. However, ABA is also a senescence-promoting hormone accumulating during developmental as well as N-starvation induced senescence [39,40]. For *CRUCIFERINs*, besides the known RY/G-Box and ABA responsive elements, a further motif for seed specific *GLUTELIN* expression known from *Oryza sativa* (OSMYB5 binding site) was found [41]. Additionally, an OPAQUE-2 binding site, a *cis* element identified in *Zea mays* regulating *ZEIN* expression [42], was found to be present in *CRUCIFERIN* upstream sequences.

Studies on SSPs in *A. thaliana* have shown the interplay of the bZIP transcription factors bZIP53, bZIP10 and ABI3 to be necessary for full promoter activation [43]. Simultaneous overexpression of all three factors led to most pronounced promoter activation. Although expression of one of these factors alone showed only marginal *SSP* promoter induction in transient assays, the authors have depicted the crucial role of bZIP53, since constitutive *bZIP53* overexpression *in planta* was able to induce seed-specific promoter activation in non-seed tissue [43]. Therefore, we screened the OSR microarray data for the expression of the corresponding transcription factors. None of these transcription factors (TFs) were expressed in leaves throughout development of the OSR plants and transient overexpression of *AtbZIP53* together with a *BnSSP:GUS* construct in Arabidopsis protoplasts did not change expression of the reporter gene (Data have been provided as non-published material). Accordingly, a different mechanism of leaf-specific expression has to be in place in OSR.

The overall SSP expression pattern suggests a correlation with the developmental senescence program coupled to ROS contents and N availability. In 2001, Desikan and colleagues already identified Arabidopsis seed storage proteins to be responsive to oxidative stress [44]. Here, expression of *NAPIN* and *CRUCIFERIN* coincided with the hydrogen peroxide peak in the microarray experiment and was also confirmed by qRT-PCR in a second growth experiment on soil (Figure 2). Moreover, this also concurs with our database-aided motif identification. *Cis* elements known for redox-responsiveness were found in the upstream sequences of both SSP-classes. Besides the direct ROS responsive elements of *HY5*, other motifs suggesting an indirect coupling to ROS were identified. The LS7 Box of the PATHOGENESIS RELATED GENE1 (PR-1) and the G-Box of the *VEGETATIVE STORAGE PROTEIN-A* gene (*VSP-A*) of soybean, which are both involved in pathogen responses and ROS bursts, were identified [45–47]. Furthermore, we found a TGA2 binding site. TGA2 is involved in salicylic acid and late jasmonic acid signaling pathways, and is an interaction partner of NON-EXPRESSER OF PR-GENES1 (NPR1), which acts as a central transcription activator of many defense-related genes. NPR1 is redox sensitive and cytoplasmic H_2O_2 prevents the translocation of NPR1 to the nucleus [48]. Earlier publications have reported that SSPs can be massively oxidized, especially by carbonylation [49,50]. Besides an easier access to SSP monomers after multimer destabilization upon carbonylation, a ROS scavenging function has been proposed [51]. Recently, Nguyen, et al. [52] have shown anti-oxidative functions for CRUCIFERINs in Arabidopsis seeds. Seeds generated from Arabidopsis triple *cruciferin* KO lines (*crua*/*crub*/*cruc*) displayed a much higher sensitivity to artificial ageing as well as considerably higher protein carbonylation.

More evidence for N-status dependent transcription of SSPs is given by the presence of a TCP20 binding site in *NAPIN* upstream regions. TCP20 participates in systemic N-status signaling as well as in leaf senescence [53,54]. This dependency on the plant N-status is also reflected in our analyses of the microarray expression data. When plants were grown under N_L conditions, the expression of *NAPIN* was induced whereas under N_O conditions, *CRUCIFERIN* was predominantly expressed. Thus, the type of SSP which is expressed in leaf tissue under different N availability might be selected by its capability to store N as the amount of N per protein molecule is more than 3-fold higher for CRUCIFERIN than for NAPIN. CRUCIFERIN (488 amino acids) is much larger than NAPIN (159 amino acids) and thus requires more input but also has more N storage capacity (698 N atoms vs. 228 N atoms, respectively). A similar mechanism for nutrient availability-dependent SSP expression was shown already for sulfur. Low sulfur supply increased the ratio between S-rich CRUCIFERIN and S-poor NAPIN significantly and reduced total fatty-acid contents [2]. Accordingly, SSP accumulation

under complete N-starvation conditions was barely detectable in leaf tissue, as an interim storage is not necessary under these conditions. Remarkably, also no H_2O_2 accumulation was observed (Figure 5, Supplementary Materials Figure S2). However, how differential expression of *CRUCIFERIN* under N_O and *NAPIN* under N_L is achieved and which role hydrogen peroxide exactly plays, still needs to be further investigated. Besides TCP20, HY5 is also not solely involved in ROS responses but also in N management by regulating expression of *NITRITE-REDUCTASE-1* (*NIR1*) and *AMMONIUM-TRANSPORTER-1;2* (*AMT1;2*) in dependence of N-supply [55]. Moreover, HY5 can interact with PHYTOCHROME B (PHYB) during prolonged red-light exposure and induce EDS1 (*ENHANCED DISEASE SUSCEPTIBILITY-1*), which then promotes ROS production [56]. This interaction hints at a possible link to PHYTOCHROME-INTERACTING FACTOR7 (PIF7). PIF7 binding elements are present in *NAPIN* upstream sequences and could be targeted by PHYB-recruited PIF7 as part of a HY5-PHYB response.

Another indirect mechanism might be emanating from a NAC (NAM/ATAF1/2/CUC2) recognition site (NACRS) in *NAPIN* upstream regions, which is known to be bound by ANAC019, 055 and 072 [57]. Thus, another link to the senescence program in general is given. These factors take part in the regulation of major chlorophyll catabolic genes and ANAC019 has been identified as an activator of senescence in Arabiodpsis [58,59]. More recently, a *Brassica napus* NAC factor, NAC87, which also binds the NACRS, has been characterized to regulate both, ROS generation and leaf senescence regulatory genes [60]. An additional indirect N-dependent regulation might be exerted by GNC (**G**ATA, **N**itrate-inducible, **C**arbon metabolism-involved), which controls expression of ANAC019 [61].

Complete N-starvation appeared to elicit premature senescence and most likely a stress-induced N-remobilization program. A general indicator for several stress responses is the induction of the phenylpropanoid pathway, which in turn leads to lignification, anthocyanin production and build-up of other repellents and protective secondary metabolites. Several studies in different plant species have shown the induction of the phenylpropanoid pathway or an increase in anthocyanin production provoked by N-limitation [62–64]. In our experiments, anthocyanins were present in high amounts, so that they were visible with the naked eye and most likely were able to reduce ROS contents. This might explain why despite an induction of premature senescence and reduction of catalase activity no increase of H_2O_2 was measured (Figures 5 and 6, Supplementary Materials Figure S5). In contrast, H_2O_2 levels were even reduced. The hypothesis that anthocyanins scavenge substantial amounts of H_2O_2 and thus simply mask the increment in ROS contents will be further investigated by experiments with anthocyanin synthesis mutants *transparent testa* (*tt*) in Arabidopsis. Remarkably, *tt* mutants grown under limiting nitrogen supply did not show a difference in senescence measured by chlorophyll loss and *SAG12* expression [65]. Moreover, non-enzymatic scavengers like ascorbate and tocopherol are elevated during senescence under low nitrogen in OSR in the leaf laminae as well as in the leaf veins [66]. However, *nla* (*nitrogen limitation adaptation*) mutant Arabidopsis plants grown under low N could not accumulate anthocyanins and instead produced a severe N-limitation-induced early senescence phenotype, perhaps due to the fact that the senescence-inducing H_2O_2 signal was not quenched by anthocyanins [63]. Therefore, anthocyanin production under N-starvation might also serve the repression of at least the H_2O_2-controlled part of the senescence program. While reduction of catalase activity hints at a promotion of the standard developmental senescence program (Supplementary Materials Figure S4), the apparent decrease in H_2O_2 contents contradicts this assumption (Figure 6). In accordance with these observations, comparative expression analyses have shown strong differences between stress-induced and developmental senescence programs in early stages, which then converged in later stages [67]. Taken together, a complex interplay between intracellular hydrogen peroxide contents and nitrogen availability appears to govern the senescence program and N-remobilization efficiency.

Supplemental Materials: The following are available online at www.mdpi.com/xxx/s1. Supplementary Figure S1: Total N-content in seeds under N_O and N_L conditions; Supplementary Figure S2: Quantification of immune-detection of CRU proteins from N-starved plants; Supplementary Figure S3: Total N-content in the shoots, pods and seeds over development; Supplementary Figure S4: Catalase zymogram of N-starved Arabidopsis plants;

Supplementary Figure S5: Schematic drawing of promoter regions of OSR NAPIN and OSR CRUCIFERIN; Supplementary Table S1: Hydroponic media N-starvation *A. thaliana*; Supplementary Table S2: Hydroponic media N-starvation *B. napus*; Table S3: Cis elements identified in upstream regions of OSR CRUCIFERIN; Supplementary Table S4: AGI codes and description of SSP associated transcripts in *A. thaliana*; Supplementary Table S5: Cis elements identified in upstream regions of OSR NAPIN Supplementary.

Authors Contributions: Conceptualization, U.Z. and S.B.; Methodology, S.B., J.D., J.F. and L.R.; Validation, S.B., L.R., J.D. and J.F.; Formal Analysis, S.B.; J.F.; Investigation, L.R., J.F., J.D. and S.B.; Writing—Original Draft Preparation, S.B.; Writing—Review & Editing, J.D.; A.F., J.F. and U.Z.; Visualization, S.B. and U.Z.; Supervision, U.Z.; Project Administration, S.B. and U.Z.; Funding Acquisition, A.F. and U.Z."

Funding: This research was supported by the Deutsche Forschungsgemeinschaft (FOR948 (ZE 313/8-1, ZE 313/8-2), ZE 313/9-1, CRC 1101 (B06).

Acknowledgments: We thank Daniel Werner Jeschke and Gabriele Eggers-Schumacher (ZMBP, University of Tuebingen, Germany) for their excellent technical assistance. We are grateful to Fabian Koeslin-Findeklee and Walter Horst (University of Hannover, Germany) for providing leaf material of OSR grown in hydroponics. We thank Reinhard Kunze (Free University of Berlin, Germany) for providing the transcriptome data and for critical discussion on the manuscript.

Conflicts of Interest: The authors declare no conflict of interest.

References

1. Safavi-Rizi, V.; Franzaring, J.; Fangmeier, A.; Kunze, R. Divergent N Deficiency-Dependent Senescence and Transcriptome Response in Developmentally Old and Young *Brassica napus* Leaves. *Front. Plant Sci.* **2018**, *9*, 48.
2. Brunel-Muguet, S.; D'Hooghe, P.; Bataille, M.P.; Larre, C.; Kim, T.H.; Trouverie, J.; Avice, J.C.; Etienne, P.; Durr, C. Heat stress during seed filling interferes with sulfur restriction on grain composition and seed germination in oilseed rape (*Brassica napus* L.). *Front. Plant Sci.* **2015**, *6*, 213.
3. Monsalve, R.I.; Lopez-Otin, C.; Villalba, M.; Rodriguez, R. A new distinct group of 2 S albumins from rapeseed. Amino acid sequence of two low molecular weight napins. *FEBS Lett.* **1991**, *295*, 207–210.
4. Schwenke, K.D.; Raab, B.; Linow, K.J.; Pahtz, W.; Uhlig, J. Isolation of the 12 S globulin from rapeseed *(Brassica napus* L.) and characterization as a "neutral" protein. On seed proteins. Part 13. *Die Nahrung* **1981**, *25*, 271–280.
5. Perera, S.P.; McIntosh, T.C.; Wanasundara, J.P. Structural properties of cruciferin and napin of *Brassica napus* (Canola) show distinct responses to changes in pH and temperature. *Plants* **2016**, *5*, E36.
6. Gacek, K.; Bartkowiak-Broda, I.; Batley, J. Genetic and Molecular Regulation of Seed Storage Proteins (SSPs) to Improve Protein Nutritional Value of Oilseed Rape (*Brassica napus* L.) Seeds. *Front. Plant Sci.* **2018**, *9*, 890.
7. Chao, H.; Wang, H.; Wang, X.; Guo, L.; Gu, J.; Zhao, W.; Li, B.; Chen, D.; Raboanatahiry, N.; Li, M. Genetic dissection of seed oil and protein content and identification of networks associated with oil content in Brassica napus. *Sci. Rep.* **2017**, *7*, 46295.
8. Gu, J.; Chao, H.; Gan, L.; Guo, L.; Zhang, K.; Li, Y.; Wang, H.; Raboanatahiry, N.; Li, M. Proteomic Dissection of Seed Germination and Seedling Establishment in Brassica napus. *Front. Plant Sci.* **2016**, *7*,1482.
9. Tilsner, J.; Kassner, N.; Struck, C.; Lohaus, G. Amino acid contents and transport in oilseed rape (*Brassica napus* L.) under different nitrogen conditions. *Planta* **2005**, *221*, 328–338.
10. Kichey, T.; Hirel, B.; Heumez, E.; Dubois, F.; Le Gouis, J. In winter wheat (*Triticum aestivum* L.), post-anthesis nitrogen uptake and remobilisation to the grain correlates with agronomic traits and nitrogen physiological markers. *Field Crop. Res.* **2007**, *102*, 22–32.
11. Breeze, E.; Harrison, E.; McHattie, S.; Hughes, L.; Hickman, R.; Hill, C.; Kiddle, S.; Kim, Y.S.; Penfold, C.A.; Jenkins, D.; et al. High-resolution temporal profiling of transcripts during

Arabidopsis leaf senescence reveals a distinct chronology of processes and regulation. *Plant Cell* **2011**, *23*, 873–894.
12. Bieker, S.; Riester, L.; Stahl, M.; Franzaring, J.; Zentgraf, U. Senescence-specific alteration of hydrogen peroxide levels in Arabidopsis thaliana and oilseed rape spring variety *Brassica napus* L. cv. Mozart. J. *Integr. Plant Biol.* **2012**, *54*, 540–554.
13. Zimmermann, P.; Heinlein, C.; Orendi, G.; Zentgraf, U. Senescence-specific regulation of catalases in *Arabidopsis thaliana* (L.) Heynh. *Plant Cell Environ*. **2006,** *29*, 1049–1060.
14. Rossato, L.; Lainé, P.; Ourry, A. Nitrogen storage and remobilization in *Brassica napus* L. during the growth cycle: Nitrogen fluxes within the plant and changes in soluble protein patterns. *J. Exp. Bot.* **2001**, *52*, 1655–1663.
15. Oury, F.-X.; Godin, C. Yield and grain protein concentration in bread wheat: How to use the negative relationship between the two characters to identify favourable genotypes? *Euphytica* **2007**, *157*, 45–57.
16. Bogard, M.; Jourdan, M.; Allard, V.; Martre, P.; Perretant, M.R.; Ravel, C.; Heumez, E.; Orford, S.; Snape, J.; Griffiths, S.; et al. Anthesis date mainly explained correlations between post-anthesis leaf senescence, grain yield, and grain protein concentration in a winter wheat population segregating for flowering time QTLs. *J. Exp. Bot. 2***011**, *62*, 3621–3636.
17. Avice, J.C.; Etienne, P. Leaf senescence and nitrogen remobilization efficiency in oilseed rape (*Brassica napus* L.). *J. Exp. Bot*. **2014**, *65*, 3813–3824.
18. Desclos, M.; Dubousset, L.; Etienne, P.; Le Caherec, F.; Satoh, H.; Bonnefoy, J.; Ourry, A.; Avice, J.C. A proteomic profiling approach to reveal a novel role of *Brassica napus* drought 22 kD/water-soluble chlorophyll-binding protein in young leaves during nitrogen remobilization induced by stressful conditions. *Plant Physiol.* **2008**, *147*, 1830–1844.
19. Etienne, P.; Desclos, M.; Le Gou, L.; Gombert, J.; Bonnefoy, J.; Maurel, K.; Le Dily, F.; Ourry, A.; Avice, J.-C. N-protein mobilisation associated with the leaf senescence process in oilseed rape is concomitant with the disappearance of trypsin inhibitor activity. *Funct. Plant Biol.* **2007**, *34*, 895–906.
20. Franzaring, J.; Weller, S.; Schmid, I.; Fangmeier, A. Growth, senescence and water use efficiency of spring oilseed rape (*Brassica napus* L. cv. Mozart) grown in a factorial combination of nitrogen supply and elevated CO_2. *Environ. Exp. Bot.* **2011**, *72*, 284–296.
21. Franzaring, J.; Gensheimer, G.; Weller, S.; Schmid, I.; Fangmeier, A. Allocation and remobilisation of nitrogen in spring oilseed rape (*Brassica napus* L. cv. Mozart) as affected by N supply and elevated CO_2. *Environ. Exp. Bot.* **2012**, *83*, 12–22.
22. Koeslin-Findeklee, F.; Meyer, A.; Girke, A.; Beckmann, K.; Horst, W.J. The superior nitrogen efficiency of winter oilseed rape (*Brassica napus* L.) hybrids is not related to delayed nitrogen starvation-induced leaf senescence. *Plant Soil* **2014**, *384*, 347–362.
23. Cathcart, R.; Schwiers, E.; Ames, B.N. Detection of picomole levels of hydroperoxides using a fluorescent dichlorofluorescein assay. *Anal. Biochem.* **1983**, *134*, 111–116.
24. Arvidsson, S.; Kwasniewski, M.; Riano-Pachon, D.M.; Mueller-Roeber, B. QuantPrime-a flexible tool for reliable high-throughput primer design for quantitative PCR. *BMC Bioinf.* **2008**, *9*, 465.
25. Pfaffl, M.W. A new mathematical model for relative quantification in real-time RT-PCR. *Nucl. Acids Res.* **2001**, *29*, e45.
26. R Development Core Team. *R: A Language and Environment for Statistical Computing*; R Foundation for Statistical Computing: Vienna, Austria, 2017.
27. Ritchie, M.E.; Phipson, B.; Wu, D.; Hu, Y.; Law, C.W.; Shi, W.; Smyth, G.K. Limma powers differential expression analyses for RNA-sequencing and microarray studies. *Nucl. Acids Res.* **2015**, *43*, e47–e47.
28. Camacho, C.; Coulouris, G.; Avagyan, V.; Ma, N.; Papadopoulos, J.; Bealer, K.; Madden, T.L. BLAST+: Architecture and applications. *BMC Bioinf.* **2009**, *10*, 421.
29. Lamesch, P.; Berardini, T.Z.; Li, D.; Swarbreck, D.; Wilks, C.; Sasidharan, R.; Muller, R.; Dreher, K.; Alexander, D.L.; Garcia-Hernandez, M.; et al. The Arabidopsis Information Resource (TAIR): Improved gene annotation and new tools. *Nucl. Acids Res.* **2012**, *40*, D1202–D1210..

30. Li, L.; Shimada,T.; Takahashi, H.; Ueda, H.; Fukao, Y.; Kondo, M.; Nishimura, M.; Hara-Nishimura, I. MAIGO2 is involved in exit of seed storage proteins from the endoplasmic reticulum in *Arabidopsis thaliana. Plant Cell* **2006,** *18,* 3535–3547.
31. Li, L.; Shimada, T.; Takahashi, H.; Koumoto, Y.; Shirakawa, M.; Takagi, J.; Zhao, X.; Tu, B.; Jin, H.; et al. MAG2 and three MAG2-INTERACTING PROTEINs form an ER-localized complex to facilitate storage protein transport in *Arabidopsis thaliana. Plant J.* **2013**, *76*, 781–791.
32. Gironde, A.; Etienne, P.; Trouverie, J.; Bouchereau, A.; Le Caherec, F.; Leport, L.; Orsel, M.; Niogret, M.F.; Nesi, N.; Carole, D.; et al. The contrasting N management of two oilseed rape genotypes reveals the mechanisms of proteolysis associated with leaf N remobilization and the respective contributions of leaves and stems to N storage and remobilization during seed filling. *BMC Plant Biol.* **2015**, *15*, 59.
33. Chalhoub, B.; Denoeud, F.; Liu, S.; Parkin, I.A.; Tang, H.; Wang, X.; et al. Plant genetics. Early allopolyploid evolution in the post-Neolithic *Brassica napus* oilseed genome. *Science* **2014**, *345*, 950–953.
34. Solovyev, V.V.; Shahmuradov, I.A.; Salamov, A.A. Identification of promoter regions and regulatory sites. *Methods Mol. Biol.* **2010**, *674*, 57.
35. Wang, X.; Larkins, B.A. Genetic analysis of amino acid accumulation in opaque-2 maize endosperm. *Plant Physiol.* **2001**, *125*, 1766–1777.
36. Fernandez, D.E.; Turner, F.R.; Crouch, M.L. In situ localization of storage protein mRNAs in developing meristems of *Brassica napus* embryos. *Development* **1991**, *111*, 299–313.
37. Finkelstein, R.R.; Tenbarge, K.M.; Shumway, J.E.; Crouch, M.L. Role of ABA in Maturation of Rapeseed Embryos. *Plant Physiol.* **1985**, *78*, 630–636.
38. Rajjou, L.; Duval, M.; Gallardo, K.; Catusse, J.; Bally, J.; Job, C.; Job, D. Seed germination and vigor. *Ann. Rev. Plant Biol.* **2012**, *63*, 507–533.
39. Lim, P.O.; Kim, H.J.; Nam, H.G. Leaf senescence. *Ann. Revi. Plant Biol.* **2007**, *58*, 115–136.
40. Koeslin-Findeklee, F.; Becker, M.A.; van der Graaff, E.; Roitsch, T.; Horst, W.J. Differences between winter oilseed rape (*Brassica napus* L.) cultivars in nitrogen starvation-induced leaf senescence are governed by leaf-inherent rather than root-derived signals. *J. Exp. Bot.* **2015**, *66*, 3669–3681.
41. Suzuki, A.; Wu, C.Y.; Washida, H.; Takaiwa, F. Rice MYB protein OSMYB5 specifically binds to the AACA motif conserved among promoters of genes for storage protein glutelin. *Plant Cell Physiol.* **1998**, *39*, 555–559.
42. Schmidt, R.J.; Burr, F.A.; Aukerman, M.J.; Burr, B. Maize regulatory gene opaque-2 encodes a protein with a "leucine-zipper" motif that binds to zein DNA. *Proc. Natl. Acad. Sci. USA* **1990**, *87*, 46–50.
43. Alonso, R.; Onate-Sanchez, L.; Weltmeier, F.; Ehlert, A.; Diaz, I.; Dietrich, K.; Vicente-Carbajosa, J.; Droge-Laser, W. A pivotal role of the basic leucine zipper transcription factor bZIP53 in the regulation of *Arabidopsis* seed maturation gene expression based on heterodimerization and protein complex formation. *Plant Cell* **2009**, *21*, 1747–1761.
44. Desikan, R.; S, A.H.-M.; Hancock, J.T.; Neill, S.J. Regulation of the Arabidopsis transcriptome by oxidative stress. *Plant Physiol.* **2001**, *127*, 159–172.
45. Berger, S.; Bell, E.; Sadka, A.; Mullet, J.E. *Arabidopsis thaliana* Atvsp is homologous to soybean VspA and VspB, genes encoding vegetative storage protein acid phosphatases, and is regulated similarly by methyl jasmonate, wounding, sugars, light and phosphate. *Plant Mol. Biol.* **1995**, *27*, 933–942.
46. Liu, Y.; Ahn, J.E.; Datta, S.; Salzman, R.A.; Moon, J.; Huyghues-Despointes, B.; Pittendrigh, B.; Murdock, L.L.; Koiwa, H.; Zhu-Salzman, K. *Arabidopsis* vegetative storage protein is an anti-insect acid phosphatase. *Plant Physiol.* **2005**, *139*, 1545–1556.
47. Chen, D.; Xu, G.; Tang, W.; Jing, Y.; Ji, Q.; Fei, Z.; Lin, R. Antagonistic basic helix-loop-helix/bZIP transcription factors form transcriptional modules that integrate light and reactive oxygen species signaling in *Arabidopsis*. *Plant Cell* **2013**, *25*, 1657–1673.

48. Peleg-Grossman, S.; Melamed-Book, N.; Cohen, G.; Levine, A. Cytoplasmic H_2O_2 prevents translocation of NPR1 to the nucleus and inhibits the induction of PR genes in Arabidopsis. *Plant Signal Behav.* **2010**, *5*, 1401–1406.
49. Job, C.; Rajjou, L.; Lovigny, Y.; Belghazi, M.; Job, D. Patterns of protein oxidation in *Arabidopsis* seeds and during germination. *Plant Physiol.* **2005**, *138*, 790–802.
50. Barba-Espin, G.; Diaz-Vivancos, P.; Job, D.; Belghazi, M.; Job, C.; Hernandez, J.A. Understanding the role of H_2O_2 during pea seed germination: A combined proteomic and hormone profiling approach. *Plant Cell Environ.* **2011**, *34*, 1907–1919.
51. El-Maarouf-Bouteau, H.; Meimoun, P.; Job, C.; Job, D.; Bailly, C. Role of protein and mRNA oxidation in seed dormancy and germination. *Front. Plant Sci.* **2013**, *4*, 77.
52. Nguyen, T.P.; Cueff, G.; Hegedus, D.D.; Rajjou, L.; Bentsink, L. A role for seed storage proteins in *Arabidopsis* seed longevity. *J. Exp. Bot.* **2015**, *66*, 6399–6413.
53. Guan, P.; Wang, R.; Nacry, P.; Breton, G.; Kay, S.A.; Pruneda-Paz, J.L.; Davani, A.; Crawford, N.M. Nitrate foraging by Arabidopsis roots is mediated by the transcription factor TCP20 through the systemic signaling pathway. *Proc. Natl. Acad. Sci. USA* **2014**, *111*, 15267–15272.
54. Danisman, S.; van Dijk, A.D.; Bimbo, A.; van der Wal, F.; Hennig, L.; de Folter, S.; Angenent, G.C.; Immink, R.G. Analysis of functional redundancies within the Arabidopsis TCP transcription factor family. *J. Exp. Bot.* **2013**, *64*, 5673–5685.
55. Huang, L.; Zhang, H.; Zhang, H.; Deng, X.W.; Wei, N. HY5 regulates nitrite reductase 1 (NIR1) and ammonium transporter1;2 (AMT1;2) in Arabidopsis seedlings. *Plant Sci.* **2015**, *238*, 330–339.
56. Chai, T.; Zhou, J.; Liu, J.; Xing, D. LSD1 and HY5 antagonistically regulate red light induced-programmed cell death in *Arabidopsis*. *Front. Plant Sci.* **2015**, *6*, 292.
57. Tran, L.S.; Nakashima, K.; Sakuma, Y.; Simpson, S.D.; Fujita, Y.; Maruyama, K.; Fujita, M.; Seki, M.; Shinozaki, K.; Yamaguchi-Shinozaki, K. Isolation and functional analysis of *Arabidopsis* stress-inducible NAC transcription factors that bind to a drought-responsive cis-element in the early responsive to dehydration stress 1 promoter. *Plant Cell* **2004**, *16*, 2481–2498.
58. Zhu, X.; Chen, J.; Xie, Z.; Gao, J.; Ren, G.; Gao, S.; Zhou, X.; Kuai, B. Jasmonic acid promotes degreening via MYC2/3/4- and ANAC019/055/072-mediated regulation of major chlorophyll catabolic genes. *Plant J.* **2015**, *84*, 597–610.
59. Hickman, R.; Hill, C.; Penfold, C.A.; Breeze, E.; Bowden, L.; Moore, J.D.; Zhang, P.; Jackson, A.; Cooke, E.; Bewicke-Copley, F.; et al. A local regulatory network around three NAC transcription factors in stress responses and senescence in Arabidopsis leaves. *Plant J.* **2013**, *75*, 26–39.
60. Yan, J.; Tong, T.; Li, X.; Chen, Q.; Dai, M.; Niu, F.; et al. A Novel NAC-Type Transcription Factor, NAC87, from Oilseed Rape Modulates Reactive Oxygen Species Accumulation and Cell Death. *Plant Cell Physiol.* **2018**, *59*, 290–303.
61. Bi, Y.M.; Zhang, Y.; Signorelli, T.; Zhao, R.; Zhu, T.; Rothstein, S. Genetic analysis of Arabidopsis GATA transcription factor gene family reveals a nitrate-inducible member important for chlorophyll synthesis and glucose sensitivity. *Plant J.* **2005**, *44*, 680–692.
62. Fritz, C.; Palacios-Rojas, N.; Feil, R.; Stitt, M. Regulation of secondary metabolism by the carbon-nitrogen status in tobacco: Nitrate inhibits large sectors of phenylpropanoid metabolism. *Plant J.* **2006**, *46*, 533–548.
63. Peng, M.; Hudson, D.; Schofield, A.; Tsao, R.; Yang, R.; Gu, H.; Bi, Y.M.; Rothstein, S.J. Adaptation of Arabidopsis to nitrogen limitation involves induction of anthocyanin synthesis which is controlled by the NLA gene. *J. Exp. Bot.* **2008**, *59*, 2933–2944.
64. Soubeyrand, E.; Basteau, C.; Hilbert, G.; van Leeuwen, C.; Delrot, S.; Gomes, E. Nitrogen supply affects anthocyanin biosynthetic and regulatory genes in grapevine cv. Cabernet-Sauvignon berries. *Phytochemistry* **2014**, *103*, 38–49.
65. Misyura, M.; Colasanti, J.; Rothstein, S.J. Physiological and genetic analysis of Arabidopsis thaliana anthocyanin biosynthesis mutants under chronic adverse environmental conditions. *J. Exp. Bot.* **2013**, *64*, 229–240.

66. Clément, G.; Moison, M.; Soulay, F.; Reisdorf-Cren, M.; Masclaux-Daubresse, C. Metabolomics of laminae and midvein during leaf senescence and source-sink metabolite management in *Brassica napus* L. leaves. *J. Exp. Bot.* **2018**, *69*, 891–903.
67. Guo, Y.; Gan, S.S. Convergence and divergence in gene expression profiles induced by leaf senescence and 27 senescence-promoting hormonal, pathological and environmental stress treatments. *Plant Cell Environ.* **2012**, *35*, 644–655.